

# **Expression of Arc/Arg3.1 in GABAergic neurons and in hippocampal-septal circuits, regulates Learning, memory and stress-related disorders**

Dissertation

Zur Erlangung des akademischen Grades  
des Doktors der Naturwissenschaften (Dr.rer.nat.)

des Fachbereichs Biologie,  
der Fakultät für Mathematik, Informatik und Naturwissenschaften,  
der Universität Hamburg

vorgelegt von

**Xiaoyu Yang**

aus Hebei, China

Hamburg, 2024







1<sup>st</sup> Gutachter: Prof. Dr. Dietmar Kuhl

2<sup>nd</sup> Gutachter: Prof. Dr. Christian Lohr

Die Arbeit wurde im Zeitraum von Dezember 2019 bis Juni 2024 im Institut für Molekulare und Zelluläre Kognition, das Zentrum für Molekulare Neurobiologie Hamburg (ZMNH) unter der Anleitung von Herrn Prof. Dietmar Kuhl und Frau Dr. Ora Ohana angefertigt.

Tag der Disputation: 26.09.2024

**Eidesstattliche Versicherung:**

Hiermit versichere ich an Eides statt, die vorliegende Dissertationsschrift selbst verfasst und keine anderen als die angegebenen Hilfsmittel und Quellen benutzt zu haben.

Sofern im Zuge der Erstellung der vorliegenden Dissertationsschrift generative Künstliche Intelligenz (gKI) basierte elektronische Hilfsmittel verwendet wurden, versichere ich, dass meine eigene Leistung im Vordergrund stand und dass eine vollständige Dokumentation aller verwendeten Hilfsmittel gemäß der Guten wissenschaftlichen Praxis vorliegt. Ich trage die Verantwortung für eventuell durch die gKI generierte fehlerhafte oder verzerrte Inhalte, fehlerhafte Referenzen, Verstöße gegen das Datenschutz- und Urheberrecht oder Plagiate.

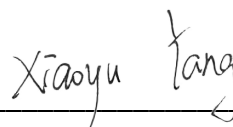
**Affidavit:**

I hereby declare and affirm that this doctoral dissertation is my own work and that I have not used any aids and sources other than those indicated.

If electronic resources based on generative artificial intelligence (gAI) were used in the course of writing this dissertation, I confirm that my own work was the main and value-adding contribution and that complete documentation of all resources used is available in accordance with good scientific practice. I am responsible for any erroneous or distorted content, incorrect references, violations of data protection and copyright law or plagiarism that may have been generated by the gAI.

Hamburg, den | date

27.09.2024

A handwritten signature in black ink, reading 'Xiaoyu Tang', written over a horizontal line.

Unterschrift | Signature



Ich versichere, dass dieses gebundene Exemplar der Dissertation und das in elektronischer Form eingereichte Dissertationsexemplar (über den Docata-Upload) und das bei der Fakultät (zuständiges Studienbüro bzw. Promotionsbüro Physik) zur Archivierung eingereichte gedruckte gebundene Exemplar der Dissertationsschrift identisch sind. |

I, the undersigned, declare that this bound copy of the dissertation and the dissertation submitted in electronic form (via the Docata upload) and the printed bound copy of the dissertation submitted to the faculty (responsible Academic Office or the Doctoral Office Physics) for archiving are identical.

Hamburg, Datum | Date

---

---

Vorname und Nachname, Unterschrift |

First name and surname, signature



---

## Contents

<b>Abbreviations.....</b>	<b>1</b>
<b>Abstract .....</b>	<b>5</b>
<b>Zusammenfassung .....</b>	<b>9</b>
<b>Introduction .....</b>	<b>13</b>
<b>1. Learning and memory.....</b>	<b>15</b>
1.1. Learning .....	16
1.2. Explicit and implicit memory .....	19
<b>2. Memory consolidation .....</b>	<b>19</b>
<b>3. Memory generalization .....</b>	<b>21</b>
<b>4. Role of Arc/Arg3.1 in synaptic plasticity, memory consolidation, and memory discrimination .....</b>	<b>25</b>
4.1. Arc/Arg3.1 is essential for synaptic plasticity.....	28
4.2. Arc/Arg3.1 involved in memory consolidation.....	30
<b>5. Role of Arc/Arg3.1 in stress and major depressive disorder (MDD) .....</b>	<b>32</b>
5.1. Major depressive disorder (MDD) and sensory processing disorder .....	32
5.2. Arc/Arg3.1 in stress and major depressive disorder (MDD) .....	33
<b>Part I Role of Arc/Arg3.1-mediated plasticity in modulating hippocampal-lateral septal (HPC- LS) circuit for fear memory in mice.....</b>	<b>35</b>
<b>Introduction .....</b>	<b>37</b>
<b>Aims of the study for Part I .....</b>	<b>42</b>
<b>Results .....</b>	<b>43</b>

---

<b>1. Upregulation of Arc/Arg3.1 after fear memory acquisition and retrieval in the hippocampus (HPC) and the lateral septum (LS). .....</b>	<b>45</b>
<b>2. Anterograde and retrograde tracing of hippocampal-lateral septal (HPC-LS) circuit.....</b>	<b>49</b>
<b>3. Optogenetic suppression of the hippocampal-lateral septal (HPC-LS) circuit increased fear generalization.....</b>	<b>50</b>
3.1. Optical suppression of the dorsal hippocampal-lateral septal (dHPC-LS) circuit during memory acquisition increased fear generalization. ....	53
3.2. Acute optical suppression of the dCA1-LS circuit in the altered context test increased fear generalization. ....	55
3.3. Optical suppression of the dCA1-LS circuit during context exposure decreased neuronal activity in CA1 and Arc/Arg3.1 engrams in the LS. ....	56
<b>4. Ablation of Arc/Arg3.1 in the lateral septum (LS) increased fear generalization. ....</b>	<b>59</b>
<b>5. Arc/Arg3.1-dependent consolidation of implicit memory in the hippocampal-lateral septal circuit. ....</b>	<b>63</b>
5.1. Long-term implicit memories in hippocampal-lateral septal circuit optical inhibition mice and lateral septal Arc/Arg3.1 ablated mice.....	64
5.2. Tone fear memory in hippocampal-lateral septal circuit optical inhibition mice. ....	64
5.3. Tone fear memory after local Arc/Arg3.1 ablation in the lateral septum. ....	68
<b>6. Oscillatory network activity of the hippocampal-lateral septal (HPC-LS) circuit in Arc/Arg3.1 deficient mice. ....</b>	<b>69</b>
6.1. Local field potential (LFP) recording in vivo. ....	69
6.2. Oscillatory activity of the hippocampal-lateral septal (HPC-LS) circuit in Arc/Arg3.1 KO mice, Arc/Arg3.1 dHPC-cKO mice, and Arc/Arg3.1 LS-cKO mice.....	73
6.3. Oscillatory network communication activity between the hippocampus and the lateral septal nucleus in Arc/Arg3.1 KO mice, Arc/Arg3.1 dHPC-cKO mice, and Arc/Arg3.1 LS-cKO mice.....	79
6.4. Unit spikes in the hippocampus (HPC) and lateral septal (LS) are of Arc/Arg3.1 KO mice, Arc/Arg3.1 dHPC-cKO mice, and Arc/Arg3.1 LS-cKO mice.....	87
<b>Discussion .....</b>	<b>93</b>



---

1. Modifying activities in the dCA1-dLS circuits may affect the discrimination of fear memories through Arc/Arg3.1.....	95
2. Arc/Arg3.1 in HPC-LS circuits may suppress overstress in implicit memory during retrieval. ....	96
3. Arc/Arg3.1 mediating the oscillatory and neuronal activity modulation in the dCA1-dLS circuits.....	99
Part II Role of Arc/Arg3.1 expressing GABAergic interneurons in depression and stress-related disorders in mice.....	105
Introduction.....	107
Aims of the study for Part II .....	111
Results .....	113
1. Arc/Arg3.1 KO mice showed altered stress-related disorder. ....	115
2. Detection of Arc/Arg3.1 mRNA in GABAergic interneurons in different brain regions. ..	116
2.1. Detection of Arc/Arg3.1 mRNA in parvalbumin-positive interneurons in different brain regions. ....	116
2.2. Detection of Arc/Arg3.1 mRNA in somatostatin-positive interneurons in different brain regions. ....	120
3. Role of Arc/Arg3.1 in parvalbumin-positive interneurons for emotional behavior in mice. ....	125
4. Role of Arc/Arg3.1 in somatostatin-positive interneurons for emotional behavior in mice. ....	128
5. Upregulation of Arc/Arg3.1 after physical restraint-induced stress in mice. ....	130
Discussion .....	133
Part III Contribution of Arc/Arg3.1 in GABAergic interneurons to memory processing .....	139
Introduction.....	141
Aims of the study for Part III .....	145

---

<b>Results .....</b>	<b>147</b>
<b>1. Sensory sensitivity of Arc/Arg3.1 KO and parvalbumin-cKO mice. ....</b>	<b>149</b>
<b>2. Role of Arc/Arg3.1 in GABAergic interneurons for fear memory in mice. ....</b>	<b>150</b>
2.1. Role of Arc/Arg3.1 in parvalbumin-positive interneurons for fear memory in mice. ....	150
2.2. Role of Arc/Arg3.1 in somatostatin-positive interneurons for fear memory in mice. ....	153
2.3. Role of Arc/Arg3.1 in somatostatin- and parvalbumin-positive interneurons for tone fear memory in mice. ....	155
<b>3. Role of Arc/Arg3.1 in GABAergic interneurons for spatial learning and memory in mice in mice.....</b>	<b>157</b>
3.1. Role of Arc/Arg3.1 in parvalbumin-positive interneurons for spatial learning and memory in mice.....	157
3.2. Role of Arc/Arg3.1 in somatostatin-positive interneurons for spatial memory in mice. ...	165
<b>Discussion .....</b>	<b>173</b>
<b>Summary and outlook .....</b>	<b>177</b>
<b>Materials and methods .....</b>	<b>183</b>
<b>1. Experimental animals .....</b>	<b>185</b>
<b>2. Generation of Arc/Arg3.1 deficient mice .....</b>	<b>185</b>
<b>3. Brain perfusion .....</b>	<b>186</b>
<b>4. Immunohistochemistry.....</b>	<b>186</b>
4.1. Diaminobenzidine (DAB) staining.....	187
4.2. Tyramide-conjugated fluorescence staining .....	187
4.3. Immunofluorescence staining.....	188
<b>5. RNA scope: in situ Hybridization .....</b>	<b>188</b>
<b>6. Stereotaxical operations.....</b>	<b>190</b>
6.1. Mouse anesthesia and analgesia .....	190
6.2. Stereotaxical viral vector injection in vivo.....	191
6.3. Stereotaxical opsin injection and fiber-optic cannula implantation.....	192

---

<b>7. Behavioral tests.....</b>	<b>193</b>
7.1. Open field test (OFT) .....	193
7.2. Elevated plus maze test (EPMT) .....	194
7.3. Forced swimming test (FST) .....	195
7.4. Tail suspension test (TST) .....	195
7.5. Morris water maze test (MWMT) .....	196
7.6. Fear conditioning test (1 CS-US).....	198
7.7. Optogenetic inhibition in fear conditioning test (2 CS-US).....	199
7.8. Flinch-jump threshold test .....	200
<b>8. Restraint-induced stress model .....</b>	<b>201</b>
<b>9. Kainate-induced seizure .....</b>	<b>201</b>
<b>10. Multiple electrodes local field potential recordings in vivo.....</b>	<b>202</b>
<b>11. Data analysis of local field potential recordings in vivo .....</b>	<b>203</b>
11.1. LFP analysis .....	203
11.2. Spike sorting and cell type classification. ....	205
<b>12. Statistical analysis .....</b>	<b>207</b>
<b>Appendix.....</b>	<b>209</b>
<b>1. References.....</b>	<b>211</b>
<b>2. Statement of contribution .....</b>	<b>235</b>
<b>3. Curriculum vitae .....</b>	<b>236</b>
<b>Acknowledgment / Danksagung.....</b>	<b>237</b>

## Abbreviations

5HT3aR	Serotonin receptor 3a
ACC	Anterior cingulate cortex
ANOVA	Analysis of variance
AON	Anterior olfactory nucleus
AP	Anteroposterior
Arc	Activity-regulated cytoskeletal-associated protein
Arg3.1	Activity-regulated gene of 3.1 kb
ATN	Dorsal thalamus
b.w.	Body weight
BFCs	Basal forebrain cholinergic system
BLA	Basolateral amygdala
BNST	Bed nucleus of the stria terminalis
BSA	Bovine serum albumin
CA1	Dorsal cornus ammonis 1
CA3	Dorsal cornus ammonis 3
CaMKII $\alpha$	Calcium/calmodulin-dependent kinase 2 alpha
CaMKII $\beta$	Calcium/calmodulin-dependent protein kinase 2 beta
CeA	Central nucleus of the amygdala
CFC	Contextual fear conditioning
cKO	Conditional knock out
CREB	Cyclic AMP response element-binding protein
CS	Conditioned stimulus
DAB	3,3'-diaminobenzidine
DAPI	4',6-diamidin-2-phenylindol
DG	Dentate gyrus
dLS	Dorsal lateral septum
DV	Dorsoventral
EPMT	Elevated plus maze test
FC	Fear conditioning
FST	Forced swimming test
GABA	Gamma-aminobutyric acid
GFP	Green fluorescent protein
HFO	High-frequency oscillation
HFS	High-frequency stimulation
HPC	Hippocampus
HRP	Horseradish peroxidase
IEG	Immediate early genes
IHC	Immunohistochemistry
imLS	Intermediate lateral septum

ISH	In Situ hybridization
LA	Lateral amygdala
LEC	Lateral entorhinal cortices
LFP	Local field potential
LS	Lateral septum
LSX	Lateral septal complex
LTD	Long-term depression
LTP	Long-term potentiation
LZ	Hypothalamic lateral zone
MBO	Mammillary body
MEC	Medial entorhinal cortices
MEF2	Myocyte enhancer factor 2
ML	Mediolateral
mPFC	Medial prefrontal cortex
MPP	Medial perforant path
MS	Medial septum
MSX	Medial septal complex
MWM	Morris water maze
NMD	Nonsense-mediated decay
NR	nucleus reuniens
NS	Non-significant
ODNs	oligodeoxynucleotides
OPT	Open field test
ORF	open reading frame
PAG	periaqueductal gray
PBS	Phosphate-buffered saline
PFA	Paraformaldehyde
PL	prelimbic cortex
PTSD	Post-traumatic stress disorder
PV	Parvalbumin
PVR	periventricular region
rAAV	Recombinant adeno-associated virus
REM	Rapid eye movement
RS	Restraint stress
RSC	retrosplenial cortex
RT	Room temperature
S.E.M.	Structural equation modeling
SARE	synaptic activity response element
SRF	serum response factor
SSC	Saline sodium citrate
SST	Somatostatin
stGtACR	soma-targeted Guillardia theta anion-conducting channelrhodopsin

---

SWRs	Sharp wave ripples
SWS	Slow-wave sleep
TRN	Thalamic reticular nucleus
TSA	Tyramide signal amplification
TST	Tail suspension test
TT	Taenia tecta
US	Unconditioned stimulus
VTA	ventral tegmental area
WHO	World Health Organization
WT	Wild type



## Abstract

Excessive stress and neurodegenerative diseases are conditions in which aversive memories may become excessively strong or imprecise, resulting in a generalized feeling of fear that is no longer linked to the original environment or context of the aversive event. In extreme cases, this can lead to psychiatric disorders like post-traumatic stress disorder (PTSD) and major depression. Understanding how aversive memories are encoded and stored is thus essential for preventing and treating neuropsychological disorders. In this study, I undertook to investigate the circuits and network mechanisms underlying fear memory consolidation, stress, and depression-like behaviors. I focused on GABAergic neurons and circuits capable of expressing the activity-regulated gene *Arc/Arg3.1*, known for its vital role in memory consolidation. I traced *Arc/Arg3.1* expression to identify brain regions and neuronal subtypes participating in fear memory consolidation and stress-evoked behaviors. I also utilized genetic deletion of the gene and optogenetic suppression to manipulate specific elements in the fear memory circuit. I performed multi-electrode *in vivo* recordings to investigate the consequences of *Arc/Arg3.1* deletion on network activity in the circuit. I also employed a range of behavioral tests to assess memory, anxiety, and depression-like behaviors.

In the first part of this thesis, I investigated the role of the hippocampal-lateral septum circuitry in fear memory processing. I identified simultaneous upregulation of *Arc/Arg3.1* in the hippocampus and the lateral septum, a GABAergic nucleus, and traced a monosynaptic projection pathway from dorsal CA1 to dorsal LS (dCA1-dLS). I injected a retrograde AAV virus encoding an inhibitory channelrhodopsin (stGtACR) bilaterally into the LS and implanted optical fibers above the dorsal dCA1, where dense expression of stGtACR was observed. The mice underwent fear conditioning and were tested in the stimulus context and a novel context 7 (recent memory) and 21 (remote memory) days later. Our results demonstrate that optical suppression of the dCA1-dLS circuit during memory acquisition or retrieval did not diminish freezing in the original context but abnormally enhanced freezing in a novel context, suggesting that this specific circuit is intimately involved in preventing memory generalization and enhancing memory specificity.



To better understand the role of Arc/Arg3.1 in the dHPC-dLS circuit, an AAV-Cre virus was bilaterally injected into dHPC or dLS in Arc/Arg3.1<sup>f/f</sup> mice. Following region-specific ablation of Arc/Arg3.1 (HPC-cKO or LS-cKO), mice were subjected to fear conditioning and memory tests. As previously shown, HPC-cKO mice showed increased freezing in the novel context in the remote memory test (Xiaoyan Gao, 2016). Interestingly, the LS-cKO mice showed excessive freezing in the novel context in the recent memory test. Together, these findings demonstrate that concurrent upregulation of Arc/Arg3.1 in the HPC and dLS modulate the precision of remote and recent contextual memory.

To investigate the impact of Arc/Arg3.1 on network activity in the dCA1-dLS circuitry, I conducted *in vivo*, two-site local field potential (LFP)- and unit-recordings from Arc/Arg3.1 germline KO, HPC-cKO, and LS-cKO mice. I analyzed the firing rates of individual neural subtypes and performed power spectral analysis of the regional-LFPs and their coherence as a measure of their inter-areal communication. The studies revealed alterations in oscillatory activity associated with memory consolidation processes. Specifically, reduced theta (3-5.2 Hz) and gamma (20-90 Hz) power was observed in the dCA1 of Arc/Arg3.1 germline KO mice but not of HPC-cKO and LS-cKO mice, confirming previous findings of early-life effects of Arc/Arg3.1 on hippocampal activity and indicating that an acute ablation of Arc/Arg3.1 in the adult brain no longer affects the hippocampal LFP. In contrast, the power of gamma and high-frequency (120-180 Hz) oscillations (HFO) in the dLS was markedly diminished in germline KO, HPC-cKO, and LS-cKO mice, demonstrating that constitutive Arc/Arg3.1 expression in the HPC-LS circuitry is required to maintain network activity in the dLS. Analysis of the power coherence, phase locking value, and Granger causality revealed abnormal communication from dCA1→dLS upon deletion of Arc/Arg3.1 in the LS, highlighting its importance in maintaining an appropriate information flow between the regions. Acute ablation of Arc/Arg3.1 in the hippocampus (HPC-cKO mice) reduced the firing rates of excitatory and inhibitory units in dCA1 and dLS, whereas acute dLS ablation (LS-cKO mice) increased them. My findings demonstrate a profound regulation of neuronal and network activity in the dCA1-dLS circuitry by Arc/Arg3.1 that likely underlies its impact on memory generalization.

In the second part of the thesis, I investigated the impact of Arc/Arg3.1 expression in GABAergic neurons on stress-related behavior. The inducibility of Arc/Arg3.1 by stress was

investigated by exposing WT mice to physical constraints. Dramatic upregulation of Arc/Arg3.1 was observed in the LS but not in the hippocampus, suggesting a preferential induction in GABAergic neurons of this brain area. Using RNAscope technology, I localized Arc/Arg3.1 transcripts to parvalbumin-positive neurons exclusively in the thalamic reticular nucleus (TRN) and somatostatin-positive neurons in the lateral septum, TRN, and claustrum and less frequently in the hippocampus and cortex. Conditional KO of Arc/Arg3.1 in parvalbumin (PV) and somatostatin (SST) neurons were generated by breeding Arc/Arg3.1<sup>f/f</sup> mice with either PV-Cre or SST-Cre mice, respectively. In both cases, a comprehensive and cell-specific deletion of Arc/Arg3.1 was achieved. The mice underwent stress-related behavior tests, including the open field, elevated plus maze, forced swimming, and tail suspension. The PV-cKO mice showed normal behaviors in all tests. In contrast, the SST-cKO mice showed less center area exploration time in the open field test and more immobility in the forced swimming test.

In the third part, I investigated contextual and spatial memory in PV-cKO and SST-cKO mice. PV-cKO mice performed normally in the Morris water maze (MWM) learning and memory tests and during the flagged-platform re-learning test. In contrast, the SST-cKO showed normal learning in the MWM test's hidden-platform version but slower learning in the subsequent flagged-platform task, possibly indicating re-learning inflexibility. In addition, SST-cKO mice displayed impaired context discrimination in fear memory tests, similar to the deficit seen in part I following the acute deletion of Arc/Arg3.1 in the dLS. These findings suggest that Arc/Arg3.1 expression in PV neurons does not contribute to the stress-related behaviors or memory processes tested here. In comparison, Arc/Arg3.1 in the SST-positive neurons may contribute to depression-like or other stress-related disorders in mice and modulate precise fear memory consolidation.

In summary, my study breaks new ground by identifying a hippocampal-lateral septum circuit essential for modulating fear learning, memory consolidation, and memory precision. Moreover, my findings reveal how the expression of Arc/Arg3.1 in this circuit shapes local and inter-areal activity patterns required for memory consolidation. My findings in SST-cKO mice confirmed that the processing of fear memory and its precision relies on the expression of Arc/Arg3.1 in this GABAergic population of the LS. This study shed new light on the link between memory, stress, and depressive-like behavior.



## Zusammenfassung

Übermäßiger Stress und neurodegenerative Erkrankungen sind Faktoren, bei denen aversive Erinnerungen übermäßig stark oder ungenau werden können, was zu einem allgemeinen Gefühl der Angst führt, das nicht mehr mit der ursprünglichen Umgebung oder dem Kontext des aversiven Ereignisses verbunden ist. In extremen Fällen kann dies zu psychiatrischen Störungen wie der posttraumatischen Belastungsstörung (PTBS) und schweren Depressionen führen. Zu verstehen, wie aversive Erinnerungen kodiert und gespeichert werden, ist daher für die Vorbeugung und Behandlung neuropsychologischer Störungen von entscheidender Bedeutung. In dieser Studie untersuchte ich die Schaltkreise und Netzwerkmechanismen, die der Konsolidierung von Furchtgedächtnis, Stress und depressionsähnlichen Verhaltensweisen zugrunde liegen. Ich konzentrierte mich auf GABAerge Neuronen und Schaltkreise, die in der Lage sind, das aktivitätsregulierte Gen *Arc/Arg3.1* zu exprimieren, das für seine wichtige Rolle bei der Gedächtniskonsolidierung bekannt ist. Ich untersuchte die Expression von *Arc/Arg3.1*, um Hirnregionen und neuronale Subtypen zu identifizieren, die an der Konsolidierung des Furchtgedächtnisses und an durch Stress ausgelösten Verhaltensweisen beteiligt sind. Außerdem nutzte ich die genetische Deletion des Gens und die optogenetische Suppression, um bestimmte Komponenten des Angstgedächtnis-Schaltkreises zu manipulieren. Ich führte *in-vivo*-Ableitungen mit mehreren Elektroden durch, um die Konsequenzen der *Arc/Arg3.1*-Deletion auf die Netzwerkaktivität zu bestimmen. Außerdem setzte ich eine Reihe von Verhaltenstests ein, um Gedächtnis, Angst und depressionsähnliche Verhaltensweisen zu untersuchen.

Im ersten Teil dieser Arbeit untersuchte ich die Rolle des Schaltkreises zwischen Hippocampus und lateralem Septum bei der Verarbeitung von Angstgedächtnis. Ich stellte eine gleichzeitige Hochregulierung von *Arc/Arg3.1* im Hippocampus und im lateralen Septum, einem GABA-ergen Kern, fest und identifizierte eine monosynaptische Projektionsbahn vom dorsalen CA1 zum dorsalen LS (dCA1-dLS). Ich injizierte ein retrogrades AAV-Virus, das für ein inhibitorisches Channelrhodopsin (stGtACR) kodiert, bilateral in den LS und implantierte optische Fasern über dem dorsalen dCA1, wo eine dichte Expression von stGtACR beobachtet wurde. Die Mäuse wurden einer Furchtkonditionierung unterzogen und 7 (recent memory) und 21 (remote memory) Tage später im Konditionierungskontext und in einem neuen Kontext getestet. Meine

Ergebnisse zeigen, dass die optische Suppression des dCA1-dLS-Schaltkreises während des Gedächtniserwerbs oder -abrufs das Erstarren im ursprünglichen Kontext nicht verringerte, aber das Erstarren in einem neuen Kontext abnormal verstärkte, was darauf hindeutet, dass dieser spezifische Schaltkreis eng mit der Verhinderung der Gedächtnisgeneralisierung und der Verstärkung der Gedächtnisspezifität verbunden ist. Um die Rolle von Arc/Arg3.1 im dHPC-dLS-Schaltkreis besser zu verstehen, wurde ein AAV-Cre-Virus bilateral in dHPC oder dLS von Arc/Arg3.1f/f-Mäusen injiziert. Nach der regionsspezifischen Ablation von Arc/Arg3.1 (HPC-cKO oder LS-cKO) wurden die Mäuse einer Furchtkonditionierung- und Gedächtnistests unterzogen. Wie bereits gezeigt, zeigten HPC-cKO-Mäuse erhöhtes Erstarren im neuen Kontext beim Gedächtnistest am Tag 21 (remote memory) (Xiaoyan Gao, 2016). Interessanterweise zeigten die LS-cKO-Mäuse erhöhtes Erstarren im neuen Kontext beim Gedächtnistest am Tag 7 (recent memory). Zusammengefasst zeigen diese Ergebnisse, dass die gleichzeitige Hochregulierung von Arc/Arg3.1 im HPC und dLS die Präzision des Kontextgedächtnisses (sowohl recent als auch remote memory) moduliert.

Um die Auswirkungen von Arc/Arg3.1 auf die Netzwerkaktivität im dCA1-dLS-Schaltkreis zu untersuchen, habe ich in vivo lokale Feldpotentiale (LFP) und Unit-Recordings von Arc/Arg3.1 Keimbahn-KO-, HPC-cKO- und LS-cKO-Mäusen in zwei Gehirnarealen durchgeführt. Ich analysierte die Feuerungsraten der einzelnen neuronalen Subtypen und führte eine Power Spectral-Analyse der regionalen LFPs und ihrer Kohärenz als Maß für ihre interareale Kommunikation durch. Die Analysen ergaben Veränderungen in der oszillatorischen Aktivität, die mit Gedächtniskonsolidierungsprozessen verbunden sind. Insbesondere wurde eine verringerte Theta- (3-5,2 Hz) und Gamma-Power (20-90 Hz) im dCA1 von Arc/Arg3.1 Keimbahn-KO-Mäusen, nicht aber von HPC-cKO- und LS-cKO-Mäusen beobachtet. Dies bestätigt vorhergehende Befunde über die Auswirkungen von Arc/Arg3.1 auf die Aktivität des Hippocampus im frühen Lebensalter und deutet darauf hin, dass eine akute Ablation von Arc/Arg3.1 im erwachsenen Gehirn die Hippocampus-LFP nicht mehr beeinflusst. Im Gegensatz dazu war die Power von Gamma- und hochfrequenten (120-180 Hz) -Oszillationen (HFO) im dLS bei Keimbahn-KO-, HPC-cKO- und LS-cKO-Mäusen deutlich vermindert. Dies zeigt, dass die konstitutive Arc/Arg3.1-Expression im HPC-LS-Schaltkreis zur Aufrechterhaltung der Netzwerkaktivität im dLS erforderlich ist. Die Analyse der Power-Kohärenz, des Phase-Locking-Wertes und der Granger-Kausalität zeigte eine abnormale Kommunikation von dCA1→dLS nach Deletion von Arc/Arg3.1 im LS. Dies unterstreicht die Bedeutung der Arc/Arg3.1-Expression für

die Aufrechterhaltung eines angemessenen Informationsflusses zwischen den Regionen. Die akute Ablation von Arc/Arg3.1 im Hippocampus (HPC-cKO-Mäuse) reduzierte die Feuerungsraten von erregenden und hemmenden Einheiten in dCA1 und dLS, während die akute dLS-Ablation (LS-cKO-Mäuse) diese erhöhte. Meine Ergebnisse zeigen eine tiefgreifende Regulierung der neuronalen und Netzwerkaktivität im dCA1-dLS-Schaltkreis durch Arc/Arg3.1, die wahrscheinlich dem Einfluss von Arc/Arg3.1 auf die Gedächtnisgeneralisierung zugrunde liegt.

Im zweiten Teil der Arbeit untersuchte ich die Auswirkungen der Arc/Arg3.1-Expression in GABAergen Neuronen auf stressbedingtes Verhalten. Die Induzierbarkeit von Arc/Arg3.1 durch Stress wurde untersucht, indem WT-Mäuse einer körperlichen Belastung ausgesetzt wurden. Eine drastische Hochregulierung von Arc/Arg3.1 wurde im LS, aber nicht im Hippocampus beobachtet, was auf eine bevorzugte Induktion in den GABAergen Neuronen dieses Hirnbereichs hindeutet. Mit Hilfe der RNAscope-Technologie lokalisierte ich Arc/Arg3.1-Transkripte in Parvalbumin-positiven Neuronen ausschließlich im thalamischen retikulären Nukleus (TRN) und in Somatostatin-positiven Neuronen im lateralen Septum, TRN und Claustrum und weniger häufig im Hippocampus und Kortex. Konditionale KO von Arc/Arg3.1 in Parvalbumin- (PV) und Somatostatin- (SST) Neuronen wurden durch Verpaarung von Arc/Arg3.1f/f-Mäusen mit PV-Cre- bzw. SST-Cre-Mäusen erzeugt. In beiden Fällen wurde eine umfassende und zellspezifische Deletion von Arc/Arg3.1 erreicht. Die Mäuse wurden stressbedingten Verhaltenstests unterzogen, darunter der offene Feldtest, das erhöhte Plus-Labyrinth, erzwungenes Schwimmen und Schwanzaufhängung. Die PV-cKO-Mäuse zeigten in allen Tests normale Verhaltensweisen. Im Gegensatz dazu verbrachten die SST-cKO-Mäuse weniger Zeit bei der Erkundung des zentralen Bereichs im offenen Feldtest und zeigten größere Immobilität im forcierten Schwimmtest.

Im dritten Teil untersuchte ich das kontextuelle und räumliche Gedächtnis bei PV-cKO- und SST-cKO-Mäusen. PV-cKO-Mäuse zeigten normale Leistungen in den MWM-Lern- und Gedächtnistests und im Test zum Wiedererlernen einer sichtbaren, markierten Plattform. Die SST-cKO-Mäuse dagegen zeigten zwar ein normales Lernen in der versteckten Version des Morris-Wasserlabyrinth-Tests, allerdings lernten sie langsamer in einer anschließenden Aufgabe eine sichtbare, markierte Plattform zu finden. Dies weist möglicherweise auf eine Inflexibilität beim Wiedererlernen hin. Darüber hinaus zeigten SST-cKO-Mäuse eine beeinträchtigte Kontextunterscheidung in Furchtgedächtnistests, ähnlich dem Defizit, das in

Teil I nach akuter Deletion von Arc/Arg3.1 in der dLS beobachtet wurde. Diese Ergebnisse legen nahe, dass die Expression von Arc/Arg3.1 in PV-Neuronen nicht zu den hier getesteten stressbedingten Verhaltensweisen oder Gedächtnisprozessen beiträgt. Im Vergleich dazu könnte Arc/Arg3.1 in den SST-positiven Neuronen zu depressionsähnlichen oder anderen stressbedingten Störungen bei Mäusen beitragen und die Konsolidierung des präzisen Furchtgedächtnisses modulieren.

Zusammenfassend lässt sich sagen, dass meine Studie Neuland betritt, indem sie einen Schaltkreis zwischen Hippocampus und lateralem Septum identifiziert, der für die Modulation von Furchtlernen, Gedächtniskonsolidierung und die Präzision des Gedächtnisses wesentlich ist. Außerdem zeigen meine Ergebnisse, wie die Expression von Arc/Arg3.1 in diesem Schaltkreis lokale und interareale Aktivitätsmuster formt, die für die Gedächtniskonsolidierung erforderlich sind. Meine Ergebnisse in SST-cKO-Mäusen bestätigten, dass die Verarbeitung von Furchtgedächtnis und die Präzision des Gedächtnisses von der Expression von Arc/Arg3.1 in dieser GABAergen Population des LS abhängt. Meine Studie wirft ein neues Licht auf den Zusammenhang zwischen Gedächtnis, Stress und depressionsähnlichem Verhalten.

## Introduction





“As long as our brain is a mystery, the universe, the reflection of the structure of the brain will also be a mystery.” (Santiago Ramón y Cajal, 1852-1934). As per the renowned Spanish scientist and founder of modern neuroscience, Santiago Ramón y Cajal, the human brain holds the most challenging yet fascinating mysteries to explore. The human brain is responsible for all the emotions we feel, the senses we experience, and our ability to learn and remember. As individuals, we interact with the world around us through recognition, sensory perception, and learning. We also respond to different environments with various reactions, such as emotions, motor functions, and memory retrieval. The activities in the brain continue ceaselessly, even during sleep. We sometimes wish to forget specific unpleasant experiences but become more cautious in similar situations. This is known as once bitten, twice shy. However, where and how our experiences are stored and generalized by the brain remains a crucial concern in modern research.

## **1. Learning and memory**

Learning and memory are important components of our everyday life. Learning involves acquiring new knowledge, understanding, skills, values, attitudes, and preferences, while memory is the function of the mind that encodes, stores, and retrieves information when necessary. Memory can be categorized (Figure 1) based on the relationship between the stimuli involved (associative vs non-associative) or whether the content can be communicated through language (declarative/explicit vs procedural/implicit) (Camina & Güell, 2017). Memories are dynamic processes that are constantly evolving and fundamentally constructive (Nader, 2003). Furthermore, memories have explicit and implicit functions, comprising a sensory processor, short-term (or working) memory, and long-term memory (Baddeley, 2007).

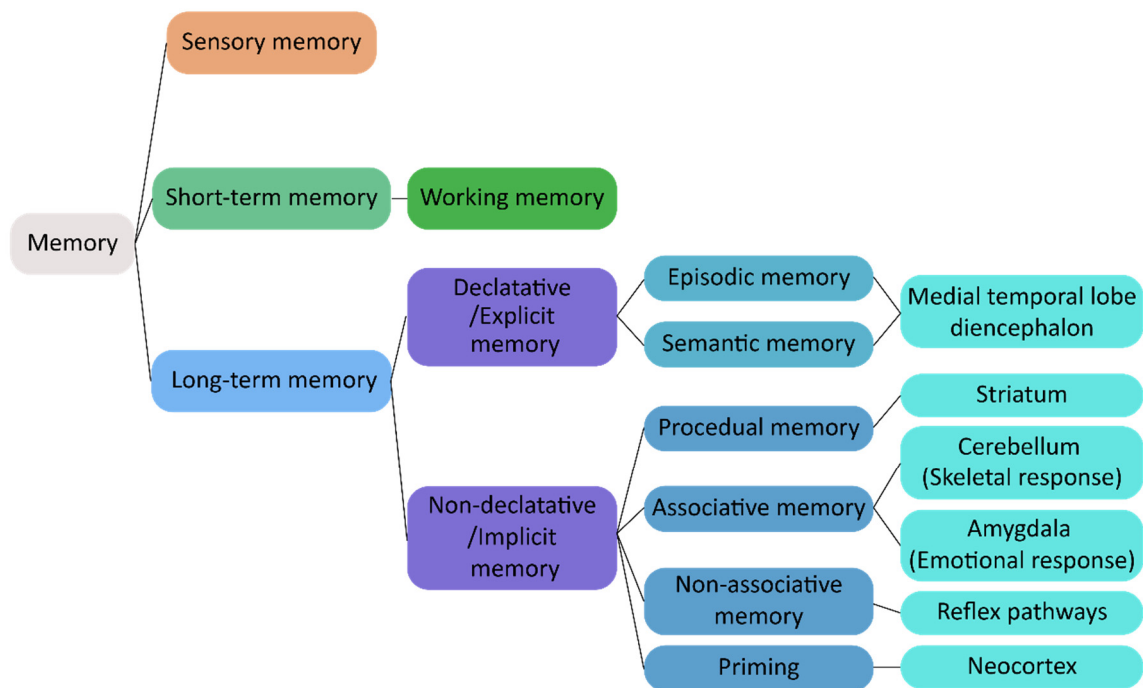


**Figure 1. Memory classification, long-term memory systems, and involved brain regions.** Adapted and modified from Squire & Dede, 2015 (Squire & Dede, 2015) and Camina & Güell, 2017 (Camina & Güell, 2017).

### 1.1. Learning

The process of learning can be divided into two classes: non-associative and associative. In non-associative learning, the strength of response to a single stimulus is permanently changed due to repeated exposure to that stimulus, which involves sensitization, habituation and imprinting (Fuentes, 2017; Goodenough, McGuire, & Jakob, 2009; Papaj & Lewis, 2012; Pearce, 2013). In associative learning, multiple stimuli or events are linked together, such as classical conditioning and operant conditioning (Plotnik, Kouyoumdjian, & Austin, 1989). In behavioral neuroscience, testing associative learning commonly involves the pairing of a conditioned stimulus (CS) with an unconditioned stimulus (US) outcome, which is typically classified as either appetitive or aversive conditioning (Cassaday et al., 2023). Food reward is typically used in appetitive conditioning, while foot shock for fear conditioning is commonly employed in aversive conditioning. While non-associative learning often occurs within relatively simple and reflex-like neural circuits, associative learning involves large and dispersed neural networks. Early studies investigated neural correlates of associative learning using electrophysiological

recordings to explore how neurons modify their activity in response to reward or threat signals (Berger, Alger, & Thompson, 1976; Segal, Disterhoft, & Olds, 1972). In well-trained animals, it has been observed that predictive stimuli (cues or stimulus used during training, which animals have learned and experienced) can potentially evoke firing responses in certain parts of the brain, for example, the hippocampus (Gilmartin & McEchron, 2005; Komorowski, Manns, & Eichenbaum, 2009; McEchron & Disterhoft, 1999), rhinal cortex (Kei M. Igarashi, Lu, Colgin, Moser, & Moser, 2014; Keene et al., 2016; Pilkiw et al., 2017), prefrontal cortex (Baeg et al., 2001; Kyriazi, Headley, & Paré, 2020; Mulder, Nordquist, Orgut, & Pennartz, 2003; Takenouchi et al., 1999), and septal nuclei (Butler, Wilson, Gunnersen, & Murphy, 2015; René Garcia & Jaffard, 2006; René Garcia, Vouimba, & Jaffard, 1997).

In this thesis, the primary associative memory test is fear conditioning, which involves quantifying freezing responses to evaluate avoidance learning (Miller, 1948; O. H. Mowrer, 1956; O. Hobart Mowrer, 1960) or inhibitory learning (J. A. Gray, 1987; Lovibond & Shanks, 2002). In fear conditioning, there is episodic learning linked with fear. In classical views, episodic memory consolidation relies on the activity of the hippocampus and related brain circuits (Scoville & Milner, 1957; Teyler & DiScenna, 1986). However, recently developed methods revealed that memories are formed and retrieved via specific neural engrams (Eichenbaum, 2016; Josselyn, Kohler, & Frankland, 2017; Tonegawa, Morrissey, & Kitamura, 2018). Researchers found that reactivating a specific group of neurons in hippocampal neurons in the dentate gyrus (Liu et al., 2012), lateral amygdala (A. Park et al., 2023; S. Park, Jung, Karimi, Jacob, & Josselyn, 2022), and cortex (Dixsaut & Graff, 2021; Kitamura et al., 2017; Stegemann et al., 2023), which were active during contextual threat conditioning (henceforth the “engram”), can retrieve the fear memory and cause freezing.

In the neurotransmitter systems (Figure 2), the dopamine, serotonin and glutamine pathways contribute to different types of learning processing in human and rodent brain systems (Banushi & Polito, 2023; Kourosh-Arabi, Komaki, & Zarrindast, 2023; Sirgy, 2019). The dopamine (DA) system also plays a crucial role in learning inhibition, as evidenced by measures of reward sensitivity in both humans and animals (Folb, Flyer-Adams, Maier, & Christianson, 2016; Migo et al., 2006; Sengupta et al., 2018; Yau & McNally, 2022), suggesting that DAergic signaling in neuronal connections is necessary for correct synaptic plasticity and cognitive functions. Speranza et al. (2021) reviewed the dopamine system in rodents as a key transmitter

involved in attention, memory and cognition (Speranza, di Porzio, Viggiano, de Donato, & Volpicelli, 2021). The glutamatergic pathways, cholinergic pathways and GABAergic pathways between the septal nucleus and hippocampus contribute to memory formation (Burjanadze et al., 2022; Givens & Olton, 1990; Khakpai, Nasehi, Haeri-Rohani, Eidi, & Zarrindast, 2013; Khakpai, Zarrindast, Nasehi, Haeri-Rohani, & Eidi, 2013; Krebs-Kraft, Wheeler, & Parent, 2007). The cholinergic pathways and GABAergic pathways between the septal nucleus and hippocampus also involve locomotion, exploration (Y. T. Chen et al., 2023) and long-term spatial memory (Dashniani et al., 2020). The medial septum (MS), part of the basal forebrain cholinergic system (BFCS), provides inputs to the hippocampus, regulating fear learning (Wilson & Fadel, 2017), spatial learning and memory (Solari & Hangya, 2018), and hippocampal theta rhythms (Gu & Yakel, 2022). The findings demonstrate that learning and memory are based on the specific patterns of simultaneous neuron activity across a network of brain regions.

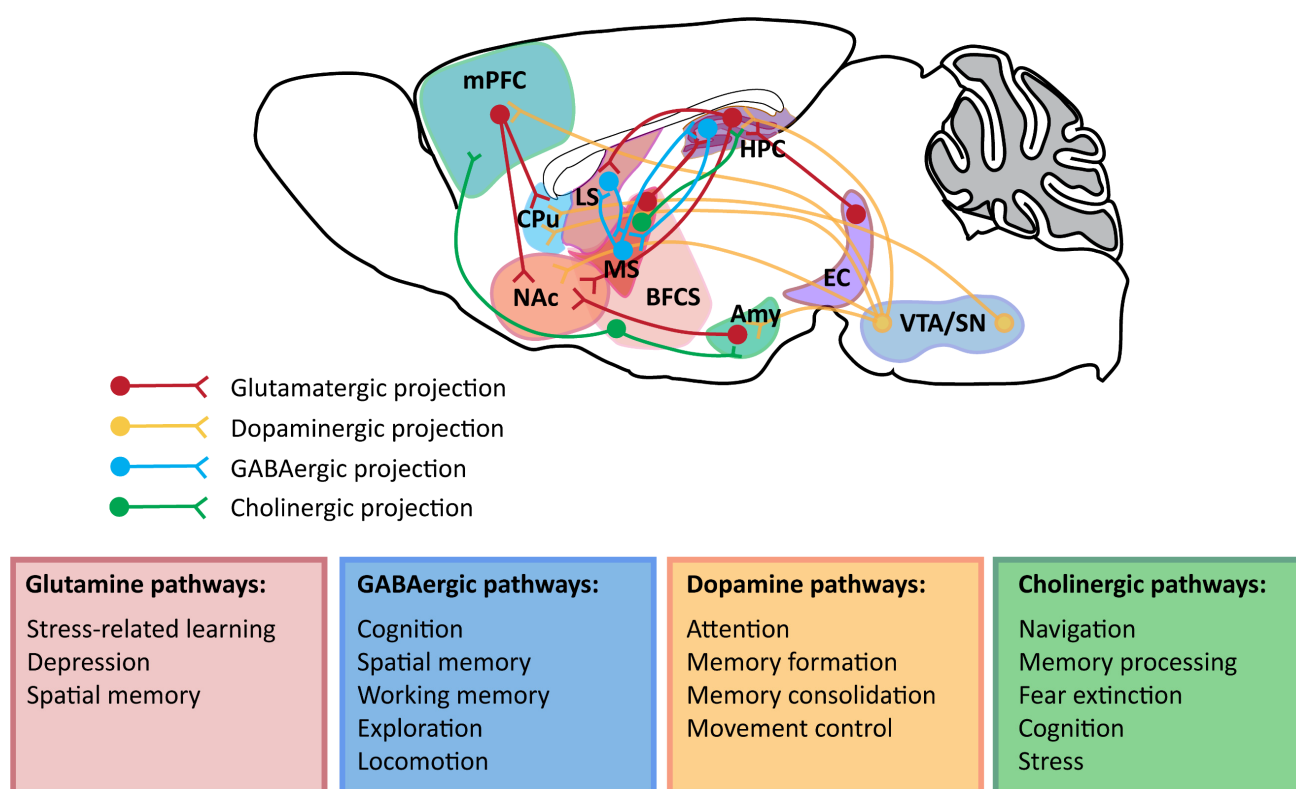


**Figure 2. Neurotransmitter pathways in rodents.** Glutamatergic transmitters mainly contribute to Stress-related learning, depression, and spatial memory. GABAergic pathways in the septo-hippocampo-septal loop involve cognition, spatial and working memory, exploration, and locomotion. Dopamine pathways are important for attention, memory formation and

consolidation, and movement control. The Cholinergic pathways related to the basal forebrain cholinergic system (BFCS) were reported to modulate navigation, memory processing, fear extinction, cognition and stress in mice. The figure was adapted and modified from Khakpai et al. (2013) and Speranza et al. (2021) (Khakpai, Zarrindast, et al., 2013; Speranza et al., 2021).

## **1.2. Explicit and implicit memory**

Memories can be classified into two categories: explicit (declarative) and implicit (non-declarative). Explicit memory is the conscious and intentional recollection of factual information, previous experiences, and concepts (Ullman, 2004). In contrast, implicit memory unconsciously influences thoughts and behaviors (Schacter, 1987). Explicit memory usually includes semantic memory and episodic memory, while implicit memory is divided into priming memory, non-associative memory, habits and skills, and simple conditioning (Hampton, Engelberg, & Brady, 2020). Explicit memory is supported by the parahippocampal gyrus (Squire & Zola-Morgan, 1991), in which the entorhinal, perirhinal, and parahippocampal cortices contribute to the encoding of objects or scenes, and the hippocampus plays a vital role in forming associations between these different structures (Davachi, 2006; Squire, Stark, & Clark, 2004; Staesina, Duncan, & Davachi, 2011). Implicit memory is more likely modulated by the activities of the striatum, neocortex, amygdala, cerebellum and reflex pathways (Squire & Dede, 2015). The explicit and implicit memory systems can operate independently by different brain networks (Eichenbaum & Cohen, 2004).

## **2. Memory consolidation**

Memory consolidation involves key processes that stabilize a memory trace after its initial acquisition (Dudai, 2004). As shown in the figure (Figure 3), synaptic consolidation is the initial process in synaptic connections and neural circuits shortly after learning, which is believed to be associated with late-phase LTP (Bramham & Messaoudi, 2005). The activation of synaptic consolidation includes the transcription of BDNF and the trafficking of mRNA (i.e., CamKII $\alpha$ ) encoded by Arc/Arg3.1 through dendrites (Bramham & Messaoudi, 2005). During the second stage of memory consolidation, systems consolidation, the function and contribution of different brain regions to memory storage and recall change. A popular theory postulates that hippocampus-dependent memories become independent of the hippocampus and reorganize

the brain network over days to years (Tonegawa et al., 2018). Researchers have recently focused on the third process, known as reconsolidation, which is reactivating previously consolidated memories to make them become unstable and undergo a protein synthesis-dependent process (Debiec & Ledoux, 2004). Memory consolidation and reconsolidation both rely on synaptic plasticity in various brain regions, including the hippocampus, cerebral cortex, cerebellum, amygdala, and striatum (P. W. Frankland & Bontempi, 2005; C. Luscher & Malenka, 2012; Tonegawa et al., 2018). Goto reviewed that maintenance of the LTP, after learning in the hippocampus and cortex, is highly related to the activity of glutamate receptors (Goto, 2022). The activation of immediate-early genes such as *Arc/Arg3.1*, *c-Fos*, and *egr-1*, which regulate LTP and synaptic plasticity, were observed in specific brain regions during memory acquisition and retrieval (Paul W. Frankland, Bontempi, Talton, Kaczmarek, & Silva, 2004; Gusev & Gubin, 2010; Jones et al., 2001; Minatohara, Akiyoshi, & Okuno, 2016; Tse et al., 2011). The processes within the brain network play an essential role in encoding and retaining memories. While there are multiple theories regarding memory consolidation, further research is needed to better understand the workings of the brain network and the types of neurons involved in memory consolidation.

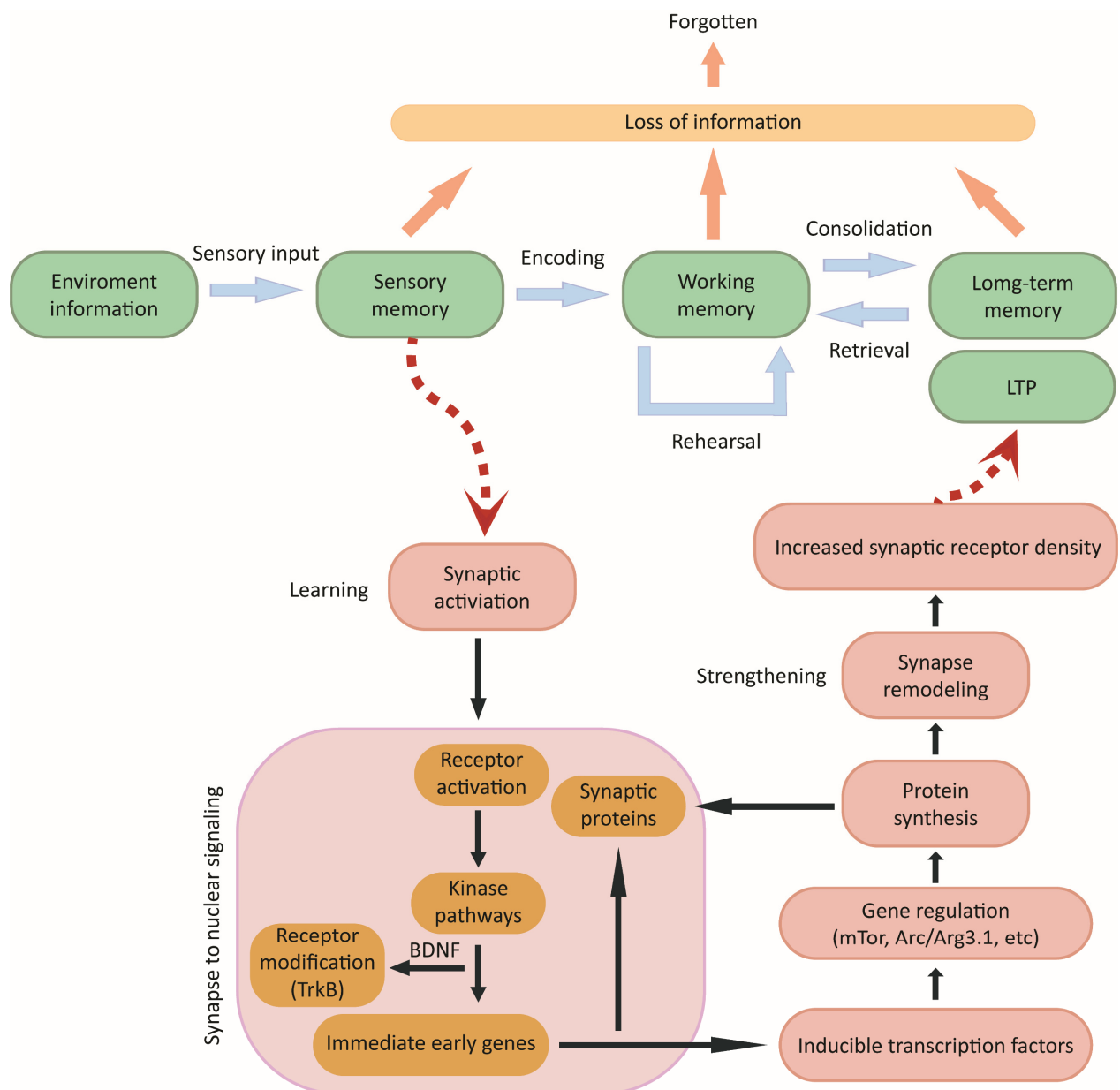


**Figure 3. Memory processes and the consolidation of synaptic plasticity mechanisms.** Memory processes include information input, sensory memory, working memory, long-term memory, and forgetting. From acquisition to memory consolidation and long-term memory, the synaptic network is active and strengthened through gene regulation and receptor modification. Adapted and modified from Kang & Bae (2021) and Spencer (2008) (Kang & Bae, 2021; Spencer, 2008).

### 3. Memory generalization

Memory discrimination is recalling relevant information while filtering out irrelevant information stored in memory (Goh & Lu, 2012; Nairne, 2005; Poirier et al., 2012; Reed Hunt,



2003). The low discrimination of relevant and irrelevant information in stored memory is memory generalization (S. H. Wang, Teixeira, Wheeler, & Frankland, 2009). Fear memory generalization allows animals to estimate and respond to potential threats in a changing environment (J. Yu, Naoi, & Sakaguchi, 2021). Over time, generalization often occurs due to a loss of precision in memory (S. H. Wang et al., 2009; Wiltgen et al., 2010). However, Overgeneralization of fear in a neutral environment is a common symptom of anxiety-related disorders, such as acute stress disorder or post-traumatic stress disorder (Abuse, 2014; Association, 2000), and can occur over a shorter time scale than the generalization that usually occurs as memories become remote (Besnard & Sahay, 2016; Jovanovic & Ressler, 2010). Rayman et al. reviewed possible reasons for discrimination failures between conditioned stimuli (CS) and similar but non-identical stimuli: an active process of inhibitory weakening, the failure to form a strong association between the conditioned stimuli (CS) and unconditioned stimulus (US) (not well-learned), and the failure of retrieval (forgetting) (Asok, Kandel, & Rayman, 2018).

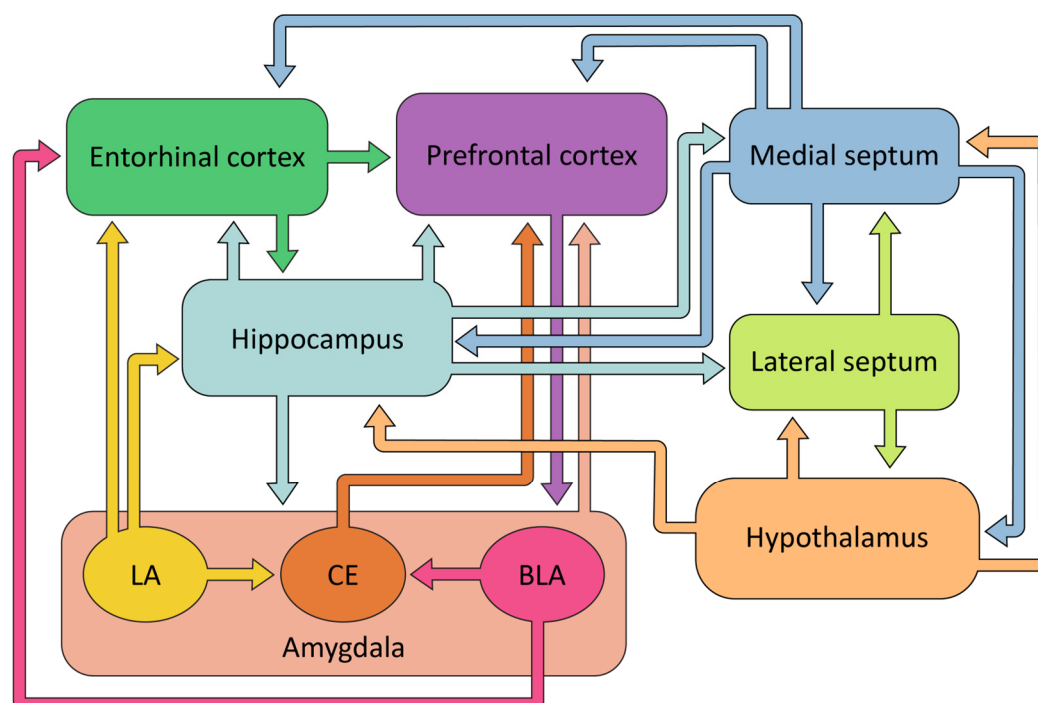


**Figure 4. Diagram representing the circuitry that interconnects the brain structures related to fear memory.** As shown in the diagram, brain circuits for fear learning and memory include the

hippocampus, lateral and medial septum, amygdala, and cortical regions. Adapted and modified from Izquierdo, Furini & Myskiw, 2016.

Fear memories rely on discrete neural circuits dependent on the type of CS-US pairing (Maren, 2001; Tovote, Fadok, & Luthi, 2015). Pavlovian fear conditioning (Maren, 2001), as a behavioral paradigm, was the most widely used fear conditioning test, including US foot shock, CS tone stimulus, and environment information (olfactory, visual, and tactile). It is important to note that fear learning depends on the interconnections between different brain regions (Izquierdo, Furini, & Myskiw, 2016) (Figure 4). A series of studies have shown that auditory fear information is transported from the auditory thalamus to the lateral nucleus of the amygdala (LA) through direct or indirect pathways via the lemniscal and extra lemniscal pathways (Ferrara, Cullen, Pullins, Rotondo, & Helmstetter, 2017; Weinberger, 2011). The lateral amygdala (LA) and the thalamus transmit information to the central nucleus of the amygdala (CeA), which modulates the behavioral (Sanford et al., 2017) and neuroendocrine aspects of fear (Ciocchi et al., 2010; Gross & Canteras, 2012; Linke, Braune, & Schwegler, 2000). Both LA and CeA then send projections to the bed nucleus of the stria terminalis (BNST), which involve anxiety-like behaviors, contextual fear, and fear generalization in mice (Asok, Draper, et al., 2018; Davis, Walker, Miles, & Grillon, 2010; H. W. Dong, Petrovich, & Swanson, 2001; Duvarci, Bauer, & Pare, 2009). During fear conditioning, the dorsal hippocampus receives projections from the medial and lateral entorhinal cortices (MEC and LEC) layers (I. Lee & Lee, 2013), and subfields are responsible for mediating fear memories and memory precision (Besnard & Sahay, 2016; Cravens, Vargas-Pinto, Christian, & Nakazawa, 2006; McHugh et al., 2007; Rolls, 2013; Roy et al., 2017). Furthermore, the ventral hippocampus is known to have distinct functions compared to the dorsal hippocampus in the consolidation of contextual fear memory (Fanselow & Dong, 2010; H. Zhu et al., 2014). The ventral hippocampus, along with its connections such as the medial prefrontal cortex (mPFC), the BLA, the retrosplenial cortex, the insular cortices, and the nucleus reuniens (NR) (Cenquizca & Swanson, 2007; Pitkanen, Pikkarainen, Nurminen, & Ylinen, 2000; Ramanathan, Ressler, Jin, & Maren, 2018; Rozeske, Valerio, Chaudun, & Herry, 2015; Xu & Sudhof, 2013), play an important role in maintaining the precision of memory (Ciocchi, Passecker, Malagon-Vina, Mikus, & Klausberger, 2015; Cullen, Gilman, Winiecki, Riccio, & Jasnow, 2015; Jimenez et al., 2018). In human studies, the striatum,

insula, and periaqueductal gray (PAG) are implicated in generalizing recent fear memories (Dunsmoor, Prince, Murty, Kragel, & LaBar, 2011). In recent studies, the hippocampus and its projections to the lateral septum (LS) have been shown to play a critical role in memory acquisition, consolidation and discrimination (Besnard, Miller, & Sahay, 2020; Decarie-Spain et al., 2022; Mondragón-Rodríguez, Gu, Fasano, Peña-Ortega, & Williams, 2019; Opalka & Wang, 2020). The review highlighted the crucial role of the medial prefrontal cortex (mPFC) and its connections with the amygdala, hippocampus, and entorhinal cortex in fear memory reconsolidation and extinction (Baldi & Bucherelli, 2015) (Figure 5). It was reported that the amygdala microcircuits, along with the auditory cortex, the PAG, and the ventral tegmental area (VTA), contribute to the discrimination of fear memories (Yan et al., 2023). The fear memory discrimination heavily relies on contextual and sensory information, making the hippocampal circuits a crucial area for further investigation. Therefore, understanding the brain network of fear memory generalization may be important for controlling symptoms associated with recurrent memory retrieval.

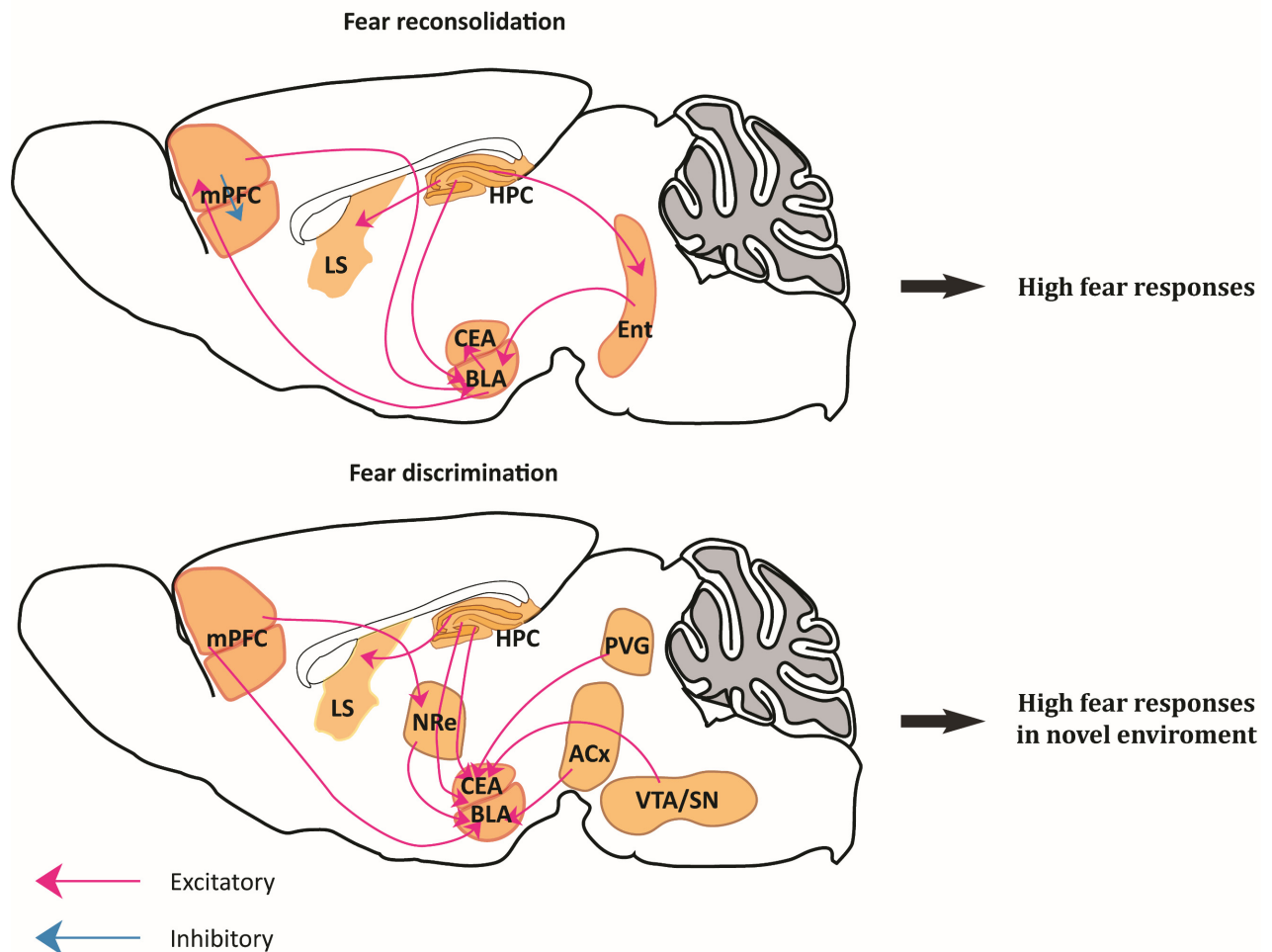


**Figure 5. Proposed neural circuits in fear memory reconsolidation and discrimination.** Different brain circuits modify fear memory consolidation and fear memory discrimination. The figure was adapted and modified from Baldi & Bucherelli (2015) and Yan et al. (2023).

#### 4. Role of Arc/Arg3.1 in synaptic plasticity, memory consolidation, and memory discrimination

The activity-regulated cytoskeletal gene Arg3.1, also known as Arc, was first identified in 1995 (Link et al., 1995; Lyford et al., 1995) and has since been found to be located on chromosome 7, 8, and 15 in rat, human, and mouse (Lyford et al., 1995). The Arc/Arg3.1 gene is a conserved gene with low homology to the  $\alpha$ -spectrin sequence (Lyford et al., 1995). The genetic sequence is composed of three exons and two introns. Following transcription, a 3.1 kb mRNA is generated that contains a 3' untranslated region (3' UTR) harboring a dendritic targeting element (Kobayashi, Yamamoto, Maruo, & Murakami, 2005). The presence of two exon

junction complexes (EJCs) in the 3' untranslated region (UTR) makes Arc/Arg3.1 a viable target for nonsense-mediated decay (NMD) (Giorgi et al., 2007). The open reading frame (ORF) of Arc/Arg3.1 can be found in the first exon and is responsible for translating 396 amino acids, which have a predicted molecular weight of 55 kDa (Link et al., 1995; Lyford et al., 1995).

The expression of Arc/Arg3.1 is regulated by plasticity-related stimuli (Chotiner et al., 2010; Link et al., 1995; J. J. Rodriguez et al., 2005; Steward, Wallace, Lyford, & Worley, 1998; Waltereit et al., 2001; Ying et al., 2002), memory acquisition (Chau, Prakapenka, Fleming, Davis, & Galvez, 2013; Gusev & Gubin, 2010; Lonergan, Gafford, Jarome, & Helmstetter, 2010; Lv, Xu, Han, & Cui, 2011), stress (Boulle et al., 2014; Leem & Chang, 2017; Muzio et al., 2016) and novelty stimulus (Inberg, Elkobi, Edri, & Rosenblum, 2013; Inberg et al., 2016; Jakkamsetti et al., 2013; Santini et al., 2011). To regulate activity-dependent transcription, several regions have been identified in the promoter region of the Arc/Arg3.1 gene. It is noteworthy that these regions include a synaptic activity response element (SARE) that contains binding sites for three major transcription factors: cyclic AMP response element-binding protein (CREB), myocyte enhancer factor 2 (MEF2), and serum response factor (SRF) (Kawashima et al., 2009). It has been observed that the promoter region contains two serum response elements (SRE) and one "Zeste-like" element (Pintchovski, Peebles, Kim, Verdin, & Finkbeiner, 2009; Wall & Correa, 2018). These elements can potentially be recruited by synaptic activity, thereby enhancing Arc/Arg3.1 induction in activated synapses within several minutes (Moga et al., 2004; Steward et al., 1998). Previous studies reported that Arc/Arg3.1 has over 30 interaction partners and is believed to serve as a protein interaction hub at the molecular level (Nikolaienko, Patil, Eriksen, & Bramham, 2018). When synapses are activated, Arc/Arg3.1 is known to interact with a number of important proteins, including clathrin adaptor protein AP2, dynamin 2, and endophilin, facilitating the process of clathrin-mediated endocytosis of AMPA-type glutamate receptors and promote a decrease in synaptic strength during LTD and synaptic scaling (S. Chowdhury et al., 2006; DaSilva et al., 2016; Wall & Correa, 2018; Waung, Pfeiffer, Nosyreva, Ronesi, & Huber, 2008). In the inactive synapses, several evidences reported that Arc/Arg3.1 can facilitate the targeting of synapses by binding to inactive calcium/calmodulin-dependent protein kinase- $\beta$  (CaMKII $\beta$ ), which can result in a selective weakening of such synapses (Okuno et al., 2012; Okuno, Minatohara, & Bito, 2018). The synthesis of Arc/Arg3.1 is essential for stabilizing nascent actin filaments and consolidating LTP (Fukazawa et al., 2003; Messaoudi et

al., 2007), as it binds to the actin cross-linking protein drebrin A (Nair et al., 2017) and regulates the activity of the actin-severing protein cofilin (Messaoudi et al., 2007). Arc/Arg3.1 has been found to enter the nucleus and interact with histone acetylases, including TI60 and CREB binding protein (Korb, Wilkinson, Delgado, Lovero, & Finkbeiner, 2013; Wee et al., 2014). The interaction of nuclear Arc/Arg3.1 affects the transcription of AMPA receptor GluA1 subunits, which is reported to support dendrite-wide synaptic downscaling (Korb et al., 2013). Additionally, recent research has suggested that Arc/Arg3.1 may also be involved in regulating chromatin state (Leung, Foo, & VanDongen, 2022; Salery et al., 2017; Wee et al., 2014). The findings of recent studies indicate that self-assembly of retrovirus-like capsid structures may occur in Arc/Arg3.1 proteins from mammals and *Drosophila*. These capsids have been observed to contain Arc/Arg3.1 mRNA and are released from neurons in extracellular vesicles (EVs), which subsequently transmit the capsid, delivering RNA into neighboring cells (Ashley et al., 2018; Pastuzyn et al., 2018). A variety of evidence suggests that Arc/Arg3.1-dependent synaptic plasticity (Figure 1) is a significant contributor to the neural dynamics and information processing involved in learning and memory.

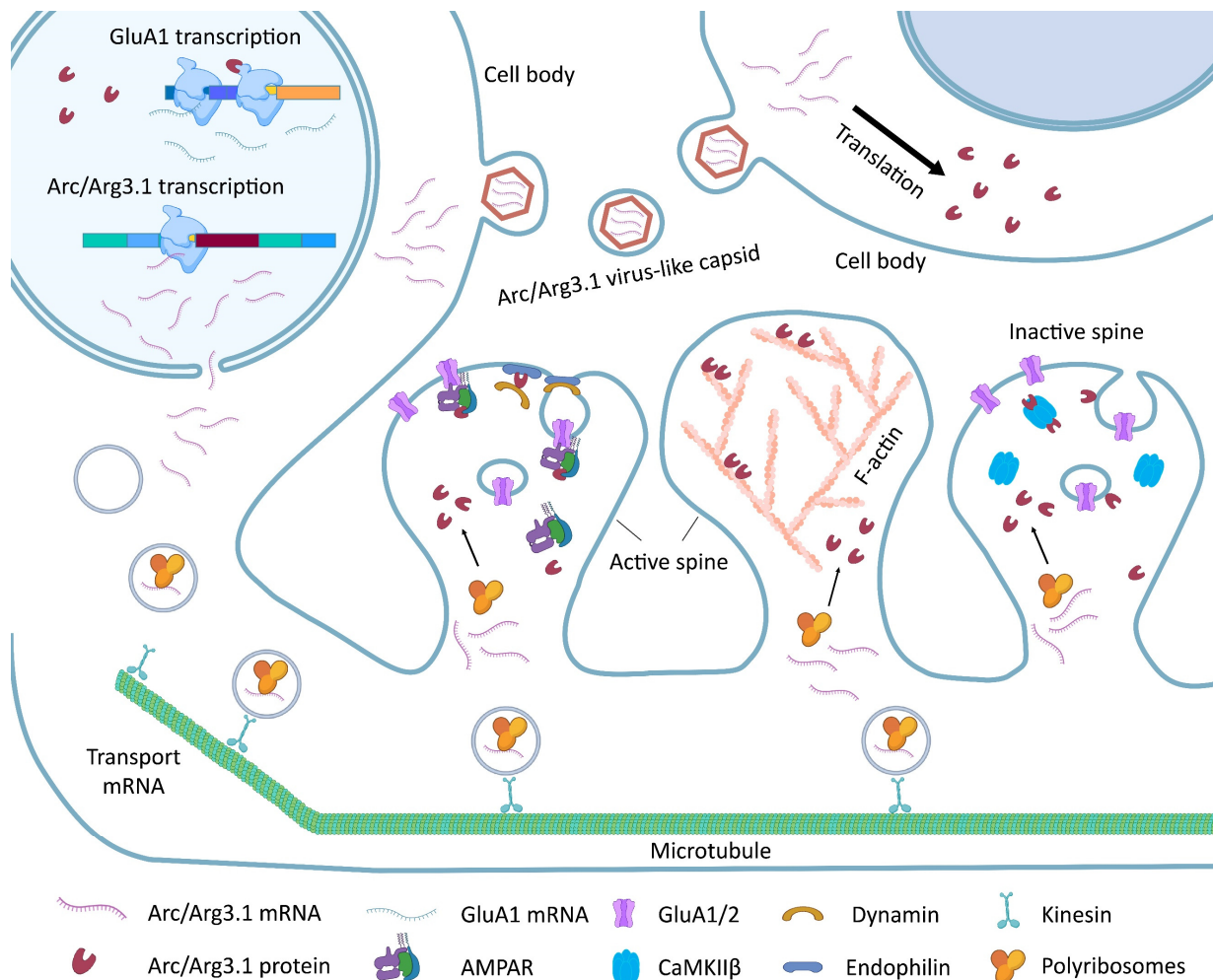


**Figure 6. The Arc/Arg3.1 protein in neuronal function.** The illustration depicts the various functions of Arc/Arg3.1 in post-synaptic glutamatergic neurons during long-term synaptic plasticity. Arc/Arg3.1 enters the nucleus of the postsynaptic neuron, where it interacts with histone acetylases and inhibits transcription of AMPAR GluA1 subunits. This indicates its role in dendrite-wide homeostatic scaling. Additionally, Arc/Arg3.1 forms virus-like capsid structures that enclose mRNA, which are then released in vesicles and taken up by neighboring cells. This suggests its function in intercellular signaling. Arc/Arg3.1 is critical for synaptic activity and plays a significant role in synaptic plasticity. Specifically, Arc/Arg3.1 interacts with endocytic machinery proteins, facilitating clathrin-mediated endocytosis of AMPA-type glutamate receptors and decreasing synaptic strength (LTD). Arc/Arg3.1 also interacts with F-actin-binding proteins, stabilizing newly polymerized actin filaments in post-synaptic spines, resulting in stable synaptic strengthening and long-term potentiation (LTP).

#### 4.1. Arc/Arg3.1 is essential for synaptic plasticity.

In the field of neuroscience, synaptic plasticity refers to the remarkable ability of synapses to adjust their strength based on activity. Synaptic plasticity is widely considered essential for information storage in neural networks (Abraham, Jones, & Glanzman, 2019; Josselyn & Tonegawa, 2020; Sossin, 2018). This crucial process is supported by three well-established forms of synaptic plasticity: long-term potentiation (LTP), long-term depression (LTD), and homeostatic plasticity. Arc/Arg3.1 is a dynamic regulator of intracellular mechanisms involved in synaptic plasticity, and it is widely believed to have cell-autonomous functions, whether they are related to synaptic or nuclear mechanisms.

Long-term potentiation (LTP) is a cellular mechanism that plays a critical role in learning and memory, which is defined as a sustained increase in synaptic strength following high-frequency stimulation or chemical induction, for example, BDNF (Ibarra et al., 2022; Plath et al., 2006; Tzingounis & Nicoll, 2006). According to previous findings, a robust upregulation of Arc/Arg3.1 in the dentate granule cells has been observed following high-frequency stimulation (HFS) of the medial perforant path (MPP) input to the dentate gyrus (Link et al., 1995; Lyford et al., 1995; Messaoudi et al., 2007; Steward et al., 1998). A recent study suggested that newly synthesized Arc/Arg3.1 undergoes rapid turnover, potentially contributing to a time window for long-term potentiation (LTP) consolidation at the perforant input to the dentate gyrus (H. Zhang & Bramham, 2021). To consolidate long-term potentiation (LTP) in the hippocampus, it is necessary to infuse Arc/Arg3.1 antisense oligodeoxynucleotides (ODNs) (Guzowski et al., 2000). However, during the LTP maintenance phase, local infusion of Arc/Arg3.1 antisense oligodeoxynucleotides results in the reversion of LTP to baseline within 30 minutes, along with significant inhibition of Arc protein synthesis (Messaoudi et al., 2007). Our colleagues reported LTP was enhanced during the first hour after high-frequency stimulation (HFS), and the LTP maintenance was impaired in the Arc/Arg3.1 knock-out mice, which indicated that Arc/Arg3.1 is essential for synaptic consolidation (Plath et al., 2006). During long-term potentiation (LTP), the synthesis of Arc/Arg3.1 is necessary to stabilize newly formed F-actin filaments in the perforant path termination zone on granule cell dendrites (Messaoudi et al., 2007). Although Arc/Arg3.1 does not bind with F-actin directly, this process is associated with the F-actin-binding protein, drebrin A (Nair et al., 2017; Walczyk-Mooradally et al., 2021). When the Arc/Arg3.1 is over-expressed, it increases the density of spines, particularly the plastic spines, in cultured neurons (Peebles et al., 2010). It has been observed that ERK has the potential to assist in the



maintenance of LTP by promoting the dendritic accumulation of Arc/Arg3.1 mRNA at stimulated perforant path synapses (Huang, Chotiner, & Steward, 2007; Steward et al., 1998) and regulates Arc/Arg3.1 translation in the synaptic compartment (Panja et al., 2014).

Long-term depression (LTD) is a type of synaptic plasticity in motor learning processes induced by low-frequency stimulation over a prolonged period. The role of Arc/Arg3.1 in the expression of long-term depression (LTD) was first reported in our lab. This demonstrated that low-frequency stimulation (LFS) induced LTD was significantly impaired in Arc/Arg3.1 knock-out mice *in vitro* (Plath et al., 2006). During LTD, Arc/Arg3.1 works in collaboration with specific components of the endocytic machinery (AP2, dynamin 2, and endophilin 3) to enhance the internalization of AMPARs (DaSilva et al., 2016). An *in vitro* study revealed that recombinant Arc/Arg3.1 has the ability to increase dynamin 2 polymerization and stimulate its GTPase activity (Byers et al., 2015). In cultured Purkinje neurons of the cerebellum, the transcription of Arc/Arg3.1 and the involvement of transcription factors such as serum response factor (SRF) are essential for the late phase of mGluR-LTD, which occurs more than an hour after stimulation (Smith-Hicks et al., 2010). Similarly, in the CA1 region of acute hippocampal slices, a rapid Arc translation rather than transcription is necessary for mGluR-LTD (Wilkerson, Albanesi, & Huber, 2018). Additionally, the acute suppression of Arc/Arg3.1 expression by using antisense ODNs prevents mGluR-LTD from occurring (Waung et al., 2008).

In mature cortical neuronal cultures, Arc/Arg3.1 also plays a role in homeostatic upscaling at the level of single synapses (Beique, Na, Kuhl, Worley, & Huganir, 2011). Arc/Arg3.1 protein in *Drosophila* forms capsid-like structures loaded into extracellular vesicles. In *Drosophila*, which harbors an Arc homologous gene (dArc), extracellular vesicles pass from motor neurons to muscles, disrupting the transfer and blocking synaptic plasticity (Ashley et al., 2018). The ability of rodent/human Arc/Arg3.1 to assemble into multimers and possibly form capsid-like structures was shown *in vitro*, yet proof for their natural occurrence in the intact brain, or for an intercellular communication were not yet obtained.

#### **4.2. Arc/Arg3.1 involved in memory consolidation**

The important role of Arc/Arg3.1 in memory consolidation has been the subject of extensive research by a number of respected neuroscientists. Infusion antisense oligodeoxynucleotides

(ODNs) of Arc/Arg3.1 in the hippocampus impairs LTP maintenance and spatial learning (Guzowski et al., 2000). The important role of Arc/Arg3.1 in memory consolidation has been further validated through experiments conducted with Arc/Arg3.1 knockout mice. These experiments showed significant impairments in long-term novel object recognition memory, spatial memory, fear memory, and conditioned taste aversion memory in these mice. However, it was observed that these mice did not exhibit any deficit in short-term novel object recognition memory or fear memory (Plath et al., 2006; Yamada et al., 2011). The results from research in our group indicate that the absence of Arc/Arg3.1 during both early (before P21) and late (after P21) postnatal periods or in the forebrain has been observed to have an impact on the long-term spatial and contextual memory of adult mice (Xiaoyan Gao, 2016; Xiaoyan Gao et al., 2018; Gómez, 2016). Arc/Arg3.1 expression is detected in the anterior cingulate and medial prefrontal cortex during inhibitory avoidance memory formation (Pontrello et al., 2012; Y. Zhang, Fukushima, & Kida, 2011). The Arc/Arg3.1 protein is required for memory retrieval (Ploski et al., 2008), reconsolidation (Maddox & Schafe, 2011), and extinction (Onoue, Nakayama, Ikegaya, Matsuki, & Nomura, 2014; L. Zhu, Zhu, Huang, Shi, & Yu, 2018) of the auditory fear memory in the lateral nucleus of the amygdala (LA). The mice showed spatial memory deficit and memory generalization when ablated Arc/Arg3.1, specifically in the hippocampus (Xiaoyan Gao, 2016; Xiaoyan Gao et al., 2018). In a pain-related emotional memory test, inhibiting the expression of the Arc/Arg3.1 gene either immediately or six hours after inhibitory avoidance training impaired long-term fear memory, while inhibiting Arc/Arg3.1 expression three hours before the memory test did not affect memory retrieval (Holloway & McIntyre, 2011).

The evidence presented above illustrates that Arc/Arg3.1 plays a crucial role in various forms of memory consolidation and reconsolidation. It also suggests that the expression of Arc/Arg3.1 in different regions of the brain may contribute to the formation of specific memories.

In summary, Arc/Arg3.1 plays a crucial role in regulating synaptic and structural plasticity, is essential for learning and memory and can modify memory-linked oscillatory activity in the brain. With these properties, Arc/Arg3.1 is posed to regulate memory by linking the molecular, cellular and system levels.

## **5. Role of Arc/Arg3.1 in stress and major depressive disorder (MDD)**

Stress is an inevitable part of our daily lives. Normal physiological stress can have beneficial effects, while chronic stress can pose a significant risk factor for psychiatric illnesses, including major depressive disorder (de Kloet, Joels, & Holsboer, 2005; Nestler et al., 2002). Major depressive disorder (MDD) is a widespread mental health issue affecting a significant number of individuals worldwide (Collins et al., 2011). World Health Organization (WHO) reported around 280 million people are experiencing depression (Institute of Health Metrics and Evaluation 2023). Depression is a condition that can have a significant impact on various aspects of life, including relationships with loved ones, academic or professional pursuits, and overall well-being. It's important to recognize the signs and symptoms of depression to seek appropriate support and care. During a depressive episode, a person usually experiences several unpleasant symptoms, such as poor concentration (Bains & Abdijadid, 2024; Eid, Gobinath, & Galea, 2019), hopelessness (Cannon et al., 1999), tiredness (Eid et al., 2019), suicidal tendencies (Harris & Barraclough, 1997; Kessler, Berglund, Borges, Nock, & Wang, 2005), sleep disorder (R. F. Chen et al., 2022; S. Chen, Cheng, Zhao, & Zhang, 2023), and unbearable pain (Ferro, 2016; Mee et al., 2011). However, further studies are necessary to gain a better understanding of the specific location and mechanisms involved in depressive disorder development within the brain.

### **5.1. Major depressive disorder (MDD) and sensory processing disorder**

A clinical study revealed that MDD patients had higher sensory sensitivity and sensation avoidance but lower sensation-seeking activities and awareness of the environment (Paquet, Calvet, Lacroix, & Girard, 2022). Most depressive people have suicidal tendencies, and a common phrase mentioned in notes is "I can't stand the (mental) pain any longer" (Harris & Barraclough, 1997; Pompili, Lester, Leenaars, Tatarelli, & Girardi, 2008; Shneidman, 1993), which indicates individuals may be seeking death to escape from the pain (Goldsmith, Pellmar, Kleinman, & Bunney, 2002). Thus, hypersensitive pain and depression frequently coexist in patients with depressive disorder (Bair, Robinson, Katon, & Kroenke, 2003; Ritov & Richter-Levin, 2014). Moreover, depression may lead to a higher intensity of pain symptoms (de Kloet et al., 2005; Torta & Munari, 2010).

Patients diagnosed with major depressive disorder (MDD) demonstrate a decreased level of response to sensory stimuli and a diminished inclination to engage in exploratory behavior (Brand & Schaal, 2017; Heckmann & Lang, 2006; Negoias et al., 2010; Paquet et al., 2022). Several pieces of evidence revealed that visual processing (Bubl, Kern, Ebert, Bach, & Tebartz van Elst, 2010) and sensory modalities, such as hearing (Schwenzer, Zattarin, Grozinger, & Mathiak, 2012) and touch (Adler & Gattaz, 1993; Freedman, 1994), may also be altered by major depression. Therefore, Major Depressive Disorder (MDD) can cause alterations in sensory perception (Fitzgerald, 2013; Pardhan et al., 2021) and result in cognitive impairment (Rock, Roiser, Riedel, & Blackwell, 2014). Thus, major depressive disorder (MDD) is always related to sensory disorders in patients.

## **5.2. Arc/Arg3.1 in stress and major depressive disorder (MDD)**

Patients with Major Depressive Disorder (MDD) can experience a reduction of hippocampal volume (Maller, Daskalakis, & Fitzgerald, 2007; Nifosi et al., 2010; Saylam, Ucerler, Kitis, Ozand, & Gonul, 2006), which is associated with longer illness duration (McKinnon, Yucel, Nazarov, & MacQueen, 2009; Travis et al., 2015) and poor clinical outcomes (Frodl et al., 2008; MacQueen, Yucel, Taylor, Macdonald, & Joffe, 2008). Successful antidepressant treatment, on the other hand, is linked to an increase in hippocampal volume (Frodl et al., 2008; Schermuly, Wolf, Lieb, Stoeter, & Fellgiebel, 2011; Tendolkar et al., 2013). A recent meta-analysis has confirmed that MDD patients have reduced volumes of the prefrontal cortex, orbitofrontal cortex, and cingulate cortex (Arnone, McIntosh, Ebmeier, Munafo, & Anderson, 2012), but increased volume of the amygdala (Saleh et al., 2012). Interestingly, stress induces reductions in dendritic spine density and synapse number in the hippocampus (Hajszan et al., 2009; Sandi et al., 2003; Tata, Marciano, & Anderson, 2006; Vestergaard-Poulsen et al., 2011) and frontal cortex (Hains et al., 2009; Radley, Anderson, Hamilton, Alcock, & Romig-Martin, 2013) of animal models.

Arc/Arg3.1 is a crucial hub for various forms of synaptic plasticity, including LTP, LTD, homeostatic plasticity, and the remodeling of dendritic spines (Y. Li et al., 2015). Consistent evidence suggests that high levels of stress increase the risk of developing MDD (Melchior et al., 2007; Sheets & Craighead, 2014; Wurtman, 2005). Studies have shown that acute stress leads to increased expression of the Arc/Arg3.1 gene or protein in the frontal cortex (Drouet et al., 2015; Mikkelsen & Larsen, 2006; Molteni et al., 2010), including the prelimbic, infralimbic, and

anterior cingulate prefrontal cortex (Ons, Marti, & Armario, 2004; Ons, Rotllant, Marin-Blasco, & Armario, 2010; Trneckova, Rotllant, Klenerova, Hynie, & Armario, 2007). Animals under repeated chronic stress exposures display up-regulation of Arc/Arg3.1 in the amygdala (Monsey et al., 2014; Ons et al., 2010; Trneckova et al., 2007) and lateral septum (Ons et al., 2004; Ons et al., 2010), but down-regulation in hippocampal CA1 (Elizalde et al., 2010; Leem & Chang, 2017; Ons et al., 2010) and frontal cortex (Ons et al., 2010). In addition, it has been observed that the chronic administration of monoamine-centered antidepressants can lead to an increase in the expression of Arc/Arg3.1 in several regions of the brain in mice, such as the hippocampus, frontal and parietal cortex, striatum, and cingulate gyrus (Y. Li et al., 2015). Specific treatments that have rapid-acting antidepressant effects, such as ketamine administration and electroconvulsive therapy, have been observed to acutely increase Arc/Arg3.1 expression (de Bartolomeis et al., 2013; Dyrvig et al., 2012; Larsen et al., 2005). Arc/Arg3.1 is a molecular target of interest for studying Major Depressive Disorder (MDD) and stress-associated disorders. In our recent research, Arc/Arg3.1 has strong colocalization with CamKII and GAD in the lateral septum (LS) (Kuku, 2020) (Figure 7). However, very little research has been done to investigate which types of neurons, such as GABAergic interneurons, express Arc/Arg3.1 and how they affect stress-associated disorders.

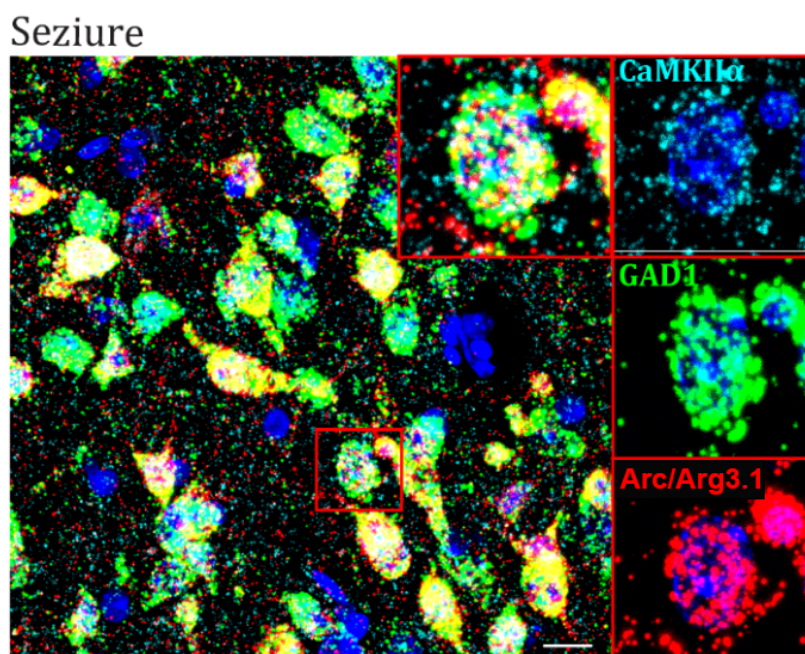


**Figure 7.** Colocalization of CaMKII $\alpha$ , GAD and Arc/Arg3.1 in LS after seizures 45 min. Taken from Kuku (2020) with permission.

## **Part I**

### **Role of Arc/Arg3.1-mediated plasticity in modulating hippocampal-lateral septal (HPC-LS) circuit for fear memory in mice**



## **Introduction**





In a natural environment, animals develop fear responses to dangerous situations and can predict danger from generalized experiences when encountering similar situations. However, overgeneralization of fear is a phenomenon of stress- and anxiety-related disorder (Shmuel Lissek & Grillon, 2010; Shmuel Lissek et al., 2005), such as posttraumatic stress disorder, panic disorder, and generalized anxiety disorder (Grillon & Morgan, 1999; Shmuel Lissek & Grillon, 2010; S. Lissek et al., 2014; Morey et al., 2015). Indeed, Anxiety-related disorders can be identified by the inability to differentiate between safe situations and those that pose a threat (Dunsmoor, Otto, & Phelps, 2017).

In the past few years, multiple theories have been developed to explain memory generalization. The hippocampus is a critical component involved in learning, cognition, memory consolidation and discrimination (Bian et al., 2019; W. B. Kim & Cho, 2020; J. Lisman et al., 2017; Rosenbaum, Gilboa, & Moscovitch, 2014; Squire, Genzel, Wixted, & Morris, 2015; Squire & Wixted, 2011). Studies have shown that the reactivation of the corresponding engrams in the hippocampus (Liu et al., 2012; Ramirez et al., 2013), as well as in connected regions such as the anterior cingulate cortex (ACC) (Bian et al., 2019), prelimbic cortex (PL) (Sotres-Bayon, Sierra-Mercado, Pardilla-Delgado, & Quirk, 2012), the retrosplenial cortex (RSC) (Ren et al., 2022), and amygdala (W. B. Kim & Cho, 2020), has been found to induce the recall of fear memory in mice and drive an active fear response. Additionally, inhibiting the hippocampus to the medial entorhinal cortex (MEC) circuit can impair auditory-related fear discrimination in mice (Yi et al., 2022). The lateral septum (LS), a forebrain structure, is implicated in regulating fear responses and fear memory (Bludau, Neumann, & Menon, 2023; Y. H. Chen et al., 2021; Hashimoto et al., 2022; Melleu, de Oliveira, Grego, Blanchard, & Canteras, 2022; Rizzi-Wise & Wang, 2021). Various studies illustrated that different structures in the hippocampus send unique projections to particular subregions within the lateral septum (LS) (Leranth, Deller, & Buzsáki, 1992; Risold & Swanson, 1997b; Rizzi-Wise & Wang, 2021; Sheehan, Chambers, & Russell, 2004). In addition, the hippocampal-lateral septal circuit has a distinct role in various brain functions within the neural network. Increasing the activity of either the dCA3-dLS or vCA3-vLS pathway can reduce the fear-associated freezing response in a fearful context (Besnard et al., 2019; Besnard et al., 2020). On the other hand, the inhibition of the dCA1-dLS pathway decreases freezing responses during exposure in the fearful context (Opalka & Wang, 2020). Moreover, studies have shown that the dCA1-dLS and dCA3-dLS pathways are involved in the acquisition of fear

memories and the discrimination process (Besnard et al., 2020; Opalka & Wang, 2020). Decarie-Spain et al. reported that a circuit between the ventral hippocampus and lateral septum selectively promotes spatial memory based on appetitive but not aversive reinforcement (Decarie-Spain et al., 2022). In a transgenic mouse model of Alzheimer's disease, the functional connectivity between the hippocampal CA1 and the lateral septum is impaired (Mondragón-Rodríguez et al., 2019). Thus, accumulating evidence indicates that close communication between the hippocampus and LS is required for proper encoding and retrieval of context memory. It remains unknown whether this circuitry also participates in the process of consolidation. While the contribution of the hippocampus to long-term remote memory remains debated, it is widely accepted that hippocampal plasticity is required for the successful consolidation of fear memory within or outside the hippocampus. In contrast, nearly nothing is known about the role of the LS in the consolidation of memory and what are the underlying plasticity mechanisms.

Arc/Arg3.1 plays an essential role in synaptic plasticity, learning, cognition, memory consolidation and memory discrimination (Eriksen & Bramham, 2022; Xiaoyan Gao et al., 2018; Penrod et al., 2019; Plath et al., 2006; Tzingounis & Nicoll, 2006). We have previously found that specific ablation of Arc/Arg3.1 in the hippocampus impaired spatial memory in mice (Xiaoyan Gao et al., 2018) but did not alter contextual fear memory (Xiaoyan Gao, 2016). However, it did reduce memory discrimination (Xiaoyan Gao, 2016). The mechanisms by which Arc/Arg3.1 could mediate memory consolidation include maintenance of long-term synaptic plasticity (LTP and LTD), stabilization of synaptic structures (Eriksen & Bramham, 2022; H. Zhang & Bramham, 2021) and modification of network oscillatory activity in the theta and gamma frequency bands (Xiaoyan Gao et al., 2018; X. Gao et al., 2019; Malkki et al., 2016). A large volume of the literature demonstrated the importance of theta and gamma oscillations in the hippocampus for recognition, discrimination, and memory (Malkov, Shevkova, Latyshkova, & Kitchigina, 2022; Neves et al., 2022; Nyhus & Curran, 2010; Vivekananda et al., 2021; Wynn, Townsend, & Nyhus, 2023). A major attribute of theta and gamma oscillations in the hippocampus is their ability to foster communication with connected brain regions, notably the prefrontal (Benchenane et al., 2010; Ramirez-Gordillo, Bayer, & Restrepo, 2022; Tamura, Spellman, Rosen, Gogos, & Gordon, 2017) and the entorhinal cortices (Buzsaki & Moser, 2013; Fernandez-Ruiz et al., 2021). This interareal communication fosters memory encoding by

optimizing information transfer and plasticity (K. M. Igarashi, 2015; Vu, Gugustea, & Leung, 2020). In addition to these regions, the hippocampus also sends profuse axonal projections to the LS, which regulates the feedback input from the MS. While septal nuclei have long been known for their role in memory, context and fear processing, the role of hippocampal-septal communication in memory encoding is only beginning to unravel. Moreover, whether the lateral septum participates in memory consolidation remains unknown.

Previous studies from our group revealed that Arc/Arg3.1 expression could be upregulated in GABAergic neurons of the LS (Kuku 2020), including in somatostatin-positive neurons, after seizures or following acute stress stimulus (Beba, 2023; Kuku, 2020). These findings raise the possibility that other natural stimuli and behaviors may induce Arc/Arg3.1 expression in the LS.

Here, I hypothesized that Arc/Arg3.1 expression in the LS might be regulated by context fear memory acquisition. I further postulated that the LS could participate in memory consolidation through activation of Arc/Arg3.1-dependent plasticity and by influencing hippocampal-septal communication. To address this hypothesis, I mapped Arc/Arg3.1 protein expression in the hippocampus and LS following acquisition and retrieval of context fear memory, revealing a strong upregulation in the LS. I utilized retrograde and anterograde rAAVs to trace the connections between the dorsal hippocampus and the lateral septum and identified projection and target cell types in each region. Using optogenetic tools I specifically inhibited the dCA1-dLS pathway and studied its influence on fear memory acquisition and retrieval. I then investigated the role of Arc/Arg3.1 in this pathway by performing locus-specific rAAV-mediated deletions of Arc/Arg3.1 in either hippocampus or LS of conditional KO mice, revealing that both regions have a key role in memory consolidation. Finally, I investigated the impact of Arc/Arg3.1 deletion in either the dCA1 or dLS on their communication. For that, I performed *in vivo* LFP and multi-channel recordings from the dCA1 and dLS, simultaneously.

## Aims of the study for Part I

Previous studies demonstrated that Arc/Arg3.1 is important for synaptic plasticity and memory consolidation. However, when Arc/Arg3.1 was ablated in the HPC in adult mice, the mice showed no deficit in memory consolidation but showed fear memory generalization in a novelty context. Moreover, Arc/Arg3.1 in the lateral septum nucleus can be evoked by a novel environment and stress. Furthermore, it was reported that the hippocampo-septo-hippocampal loop is essential for memory formation. Therefore, the aim of this part of the study is to investigate whether Arc/Arg3.1 in the HPC-LS circuits modulates circuitry activities and memory discrimination.

### **Specific goals:**

- To investigate if Arc/Arg3.1 in dHPC and LS is involved in memory processes.
- To explore whether the activities of the dCA1-dLS circuits modulate fear memory discrimination and if Arc/Arg3.1 mediates this process in mice.
- To study the role of Arc/Arg3.1 in the dHPC-LS circuits modulates fear memory discrimination.
- To understand how Arc/Arg3.1 mediates circuitry and neuronal activities in dCA1-dLS circuits.

## Results



## **1. Upregulation of Arc/Arg3.1 after fear memory acquisition and retrieval in the hippocampus (HPC) and the lateral septum (LS).**

The activity-regulated cytoskeletal-associated protein (Arc/Arg3.1) (Link et al., 1995; Lyford et al., 1995) is rapidly upregulated by novel experience, learning and memory and is, in turn, crucial for the consolidation of memory and synaptic plasticity. (El-Boustani et al., 2018; Xiaoyan Gao et al., 2018; Guzowski et al., 2000; Jakkamsetti et al., 2013; Messaoudi et al., 2007; Plath et al., 2006; X. Yang et al., 2020). In the hippocampus, Arc/Arg3.1 is specifically upregulated by synchronous high frequency activity patterns, known to induce synaptic potentiation (Link et al., 1995; Mizunuma et al., 2014). These characteristics had made Arc/Arg3.1 a prime molecular marker of memory engrams in the brain (Xiaoyan Gao et al., 2018; Gómez, 2016; Lv et al., 2011; Maddox & Schafe, 2011; Onoue et al., 2014; L. Zhu et al., 2018). These studies revealed spatial and temporal patterns of Arc/Arg3.1 regulation that are specific to the learning and memory task involved and recapitulate the network involved in processing of different memory forms (Chau et al., 2013; Gusev & Gubin, 2010; Lonergan et al., 2010; Onoue et al., 2014; Santini et al., 2011; X. Yang et al., 2020). The hippocampus is crucial for spatial perception, memory processing, and context discrimination (Scoville and Milner 1957, Morris, Garrud et al. 1982, Buzsaki and Moser 2013, Lisman, Buzsaki et al. 2017). The lateral septum is a major target of hippocampal afferents and part of a septo-hippocampal circuit (Rizzi-Wise & Wang, 2021) important for spatial learning and emotional control. The identity of the hippocampal-septal circuits that participate in memory acquisition, consolidation and recall remains largely unknown. Here we chose to address this question by investigating the role of Arc/Arg3.1 in context fear memory processing, a form of hippocampus-dependent episodic memory.

We started by asking whether Arc/Arg3.1 expression is regulated in the hippocampus and lateral septum after fear conditioning (memory acquisition) or memory retrieval. We subjected 4 groups of wild-type mice to context fear conditioning and sacrificed each group at a different time point: the first group was sacrificed 5 min and the second 90 min after conditioning. Due to the delayed increase in Arc/Arg3.1 protein expression (Plath et al., 2006), the first group represents a “baseline” level while the second reflects conditioning-dependent induction and was termed “conditioning”. The third and fourth groups were subjected to conditioning and to



memory recall 7 days later. Group 3 was sacrificed 5 min and the fourth group 90 min after recall and reflect the “no-retrieval” and “retrieval” conditions, respectively. For comparison, we also quantified the expression of cFos, an IEG whose expression is linked to a broad range of neural activity patterns (Link et al., 1995).

The numbers of Arc/Arg3.1- and cFos-positive neurons were similar in the dentate gyrus (DG) under baseline conditions. However, both following fear acquisition and memory retrieval, there was a significant increase in the number of Arc/Arg3.1 positive neurons in the dentate gyrus (DG) (Figure I. 1. A, C, E, G). On the other hand, the number of cFos-positive neurons in the dentate gyrus (DG) significantly increased only after fear acquisition, but not after memory retrieval (Figure I. 1. B, D, F, H).

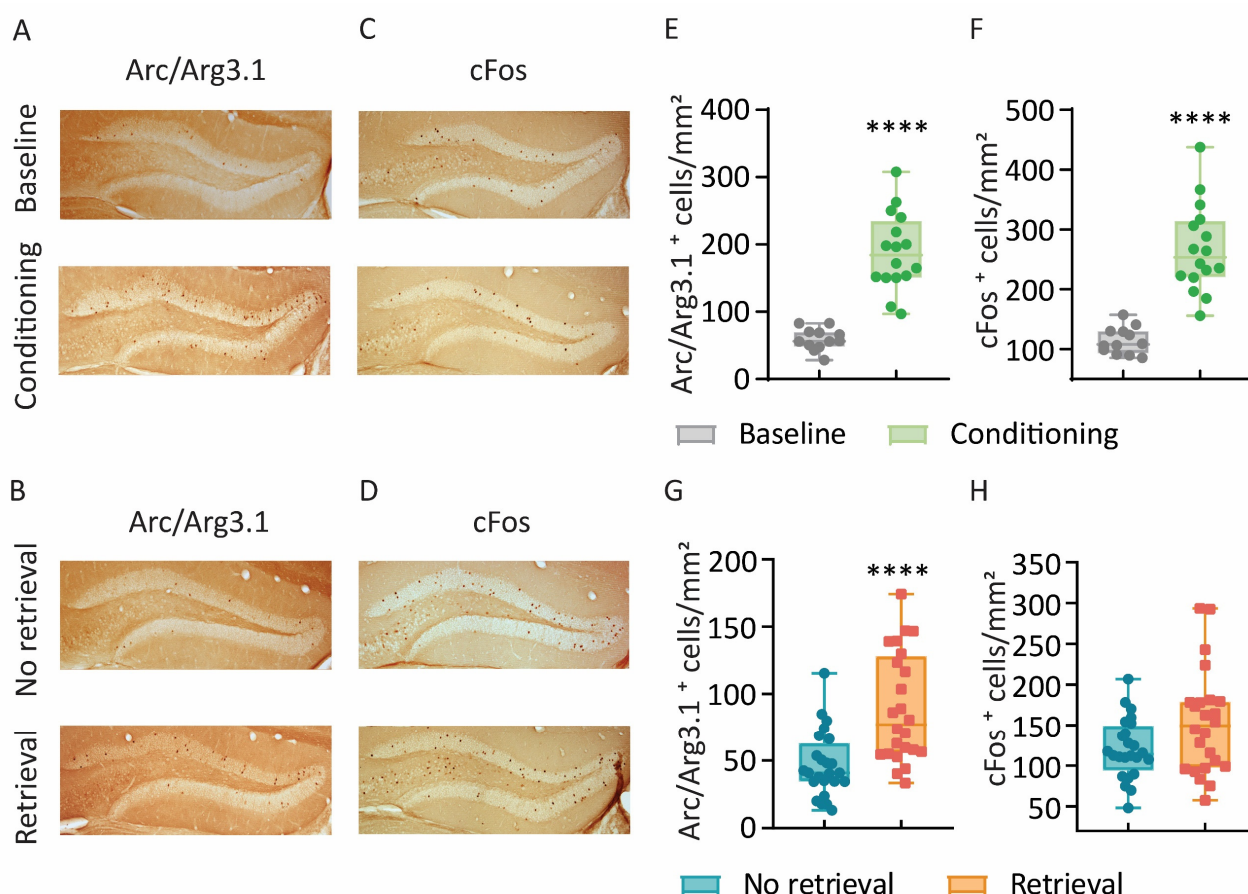


**Figure I. 1. Arc/Arg3.1 and cFos expression in the hippocampus during fear memory processing.** Arc/Arg3.1 expression in the dentate gyrus (DG) upregulated after (A, E) memory acquisition (Median: Baseline, 56.19 cells/mm<sup>2</sup>; n = 12; Condition, 184.1 cells/mm<sup>2</sup>; n = 16;

\*\*\*\* $p < 0.0001$ ) and (B, G) memory retrieval (Median: No retrieval, 40.87 cells/mm<sup>2</sup>;  $n = 24$ ; Retrieval, 77.11 cells/mm<sup>2</sup>;  $n = 24$ ; \*\*\*\* $p < 0.0001$ ). The expression of cFos in the dentate gyrus (DG) significantly upregulated after (C, F) fear acquisition (Median: Baseline, 107.8 cells/mm<sup>2</sup>;  $n = 12$ ; Condition, 253.6 cells/mm<sup>2</sup>;  $n = 16$ ; \*\*\*\* $p < 0.0001$ ) but not after (D, H) memory retrieval (Median: No retrieval, 114.0 cells/mm<sup>2</sup>;  $n = 24$ ; Retrieval, 149.4 cells/mm<sup>2</sup>;  $n = 24$ ;  $p = 0.093$ , NS). Significance was assessed with the Mann-Whitney test. The box plots showed the median (-), whiskers showed min to max, and all data points.

In fear conditioning memory the hippocampus is known to play a critical role, but the role of the lateral septum remains unclear. Whether Arc/Arg3.1 is upregulated in the LS after acquisition or retrieval is still not certain. After 90 min of fear acquisition and memory retrieval, the number of Arc/Arg3.1 positive neurons significantly increased in the lateral septum (LS) (Figure I. 2. A, C, E, G). The number of cFos-positive neurons in the lateral septum (LS) significantly increased after fear acquisition but was not affected after memory retrieval (Figure I. 2. B, D, F, H). Note that the number of Arc/Arg3.1 positive neurons in the LS was much lower than the number of cFos positive neuron, suggesting that cFos is more readily induced by sensory or behavioral stimuli and by a broader range of neural activity patterns while Arc/Arg3.1 is predominantly induced by novel experience, learning and memory retrieval as well as high frequency plasticity-inducing stimuli.

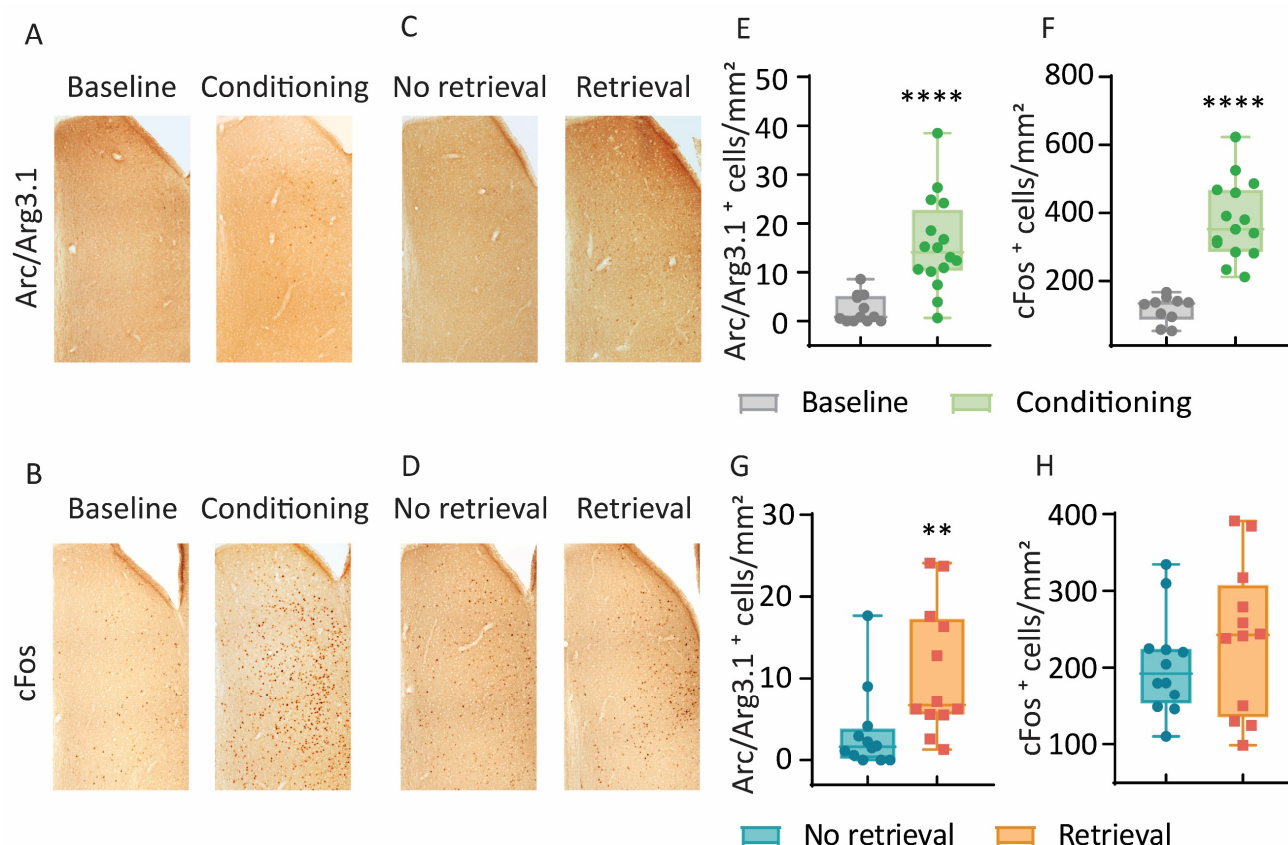


**Figure I. 2. Arc/Arg3.1 and cFos expression in lateral septum during fear memory processing.**

Arc/Arg3.1 expression in the lateral septum (LS) was upregulated after (A, E) memory acquisition (Median: Baseline, 0.857 cells/mm²; n = 12; Conditioning, 14.08 cells/mm²; n = 16; \*\*\*\*p < 0.0001) and following (C, G) memory retrieval (Median: No retrieval, 1.59 cells/mm²; n = 12; Retrieval, 6.63 cells/mm²; n = 12; \*\*p < 0.01). The expression of cFos in the lateral septum (LS) was significantly upregulated after (B, F) fear acquisition (Median: Baseline, 133.8 cells/mm²; n = 10; Condition, 351.9 cells/mm²; n = 15; \*\*\*\*p < 0.0001) but not after (D, H) memory retrieval (Median: No retrieval, 192.3 cells/mm²; n = 12; Retrieval, 242.6 cells/mm²; n = 12; p = 0.319, NS). Significance was assessed with the Mann-Whitney test. The box plots show the median (-), whiskers showed min to max, and all data points.

These findings show that both the hippocampus and the LS are involved in the processing of context fear memory. Moreover, they suggest that Arc/Arg3.1 plays a role in the acquisition and recall of memory, in both structures. The smaller size of Arc/Arg3.1 engrams in the LS, compared to cFos engrams, might reflect the differences in activity-patterns required for the induction of Immediate early genes (IEG).

## 2. Anterograde and retrograde tracing of hippocampal-lateral septal (HPC-LS) circuit.

A number of studies reported that the dorsal hippocampus (dHPC) directly projects to cortical regions and to the lateral septum (LS) (R. Garcia & Jaffard, 1992; Qiu et al., 2024; Rizzi-Wise & Wang, 2021; Takata et al., 2015; van Groen & Wyss, 1990). Additionally, different subregions of dorsal hippocampus projecting to specific regions in LS (Rizzi-Wise & Wang, 2021). Opalka et al. indicated that the photoinhibition of the dHPC-LS pathway caused memory deficits in mice (Opalka & Wang, 2020). Besnard et al. reported the activities in the dCA3-LS pathway are essential for memory consolidation and discrimination (Besnard et al., 2019; Besnard et al., 2020). However, there has been no study reported on whether the dCA1-LS pathway modulates memory consolidation or discrimination. Dorsal CA1 was reported to send and receive strong connections between intrahippocampal subregions and other regions (Besnard et al., 2020; Deng et al., 2019; Jimenez et al., 2018; Rizzi-Wise & Wang, 2021; Roy et al., 2017; Takata et al., 2015; Tao et al., 2021; van Groen & Wyss, 1990). To investigate the direct connection between the dorsal CA1 and the lateral septum, I employed anterograde and retrograde viral vectors and injected them separately into WT mice. In the first group, the anterograde viral vector, in which GFP expression is driven by CaMKII $\alpha$  promoter (rAAV-CaMKII-GFP), was unilaterally injected into the right dorsal hippocampus (Figure I. 3. A. Left). Hippocampal axons projecting to the lateral septum nucleus (LS) were labeled with GFP (Figure I. 3. A. middle and right). The highest density of GFP-fibers was observed in the dorso-medial lateral septum. In the second group, the retrograde viral vector, in which FusionRed expression is driven by CaMKII $\alpha$  promoter (rAAVrg-CaMKII-FusionRed) (Tervo et al., 2016), was bilaterally injected into the lateral septum (Figure I. 3. B. Left). Lateral septum projecting neurons in the hippocampus were labeled with FusionRed (Figure I. 3. B. Middle). The axons of neurons projecting to the LS were found in the cortex and hippocampus, in line with previous reports. Within the hippocampus, LS-projecting neurons were mostly located in the pyramidal cell layers of CA1 and CA3 (Figure I. 3. B. Middle and right). This experiment identifies pyramidal neurons in dCA1 as major projection source to the dorso-medial LS.

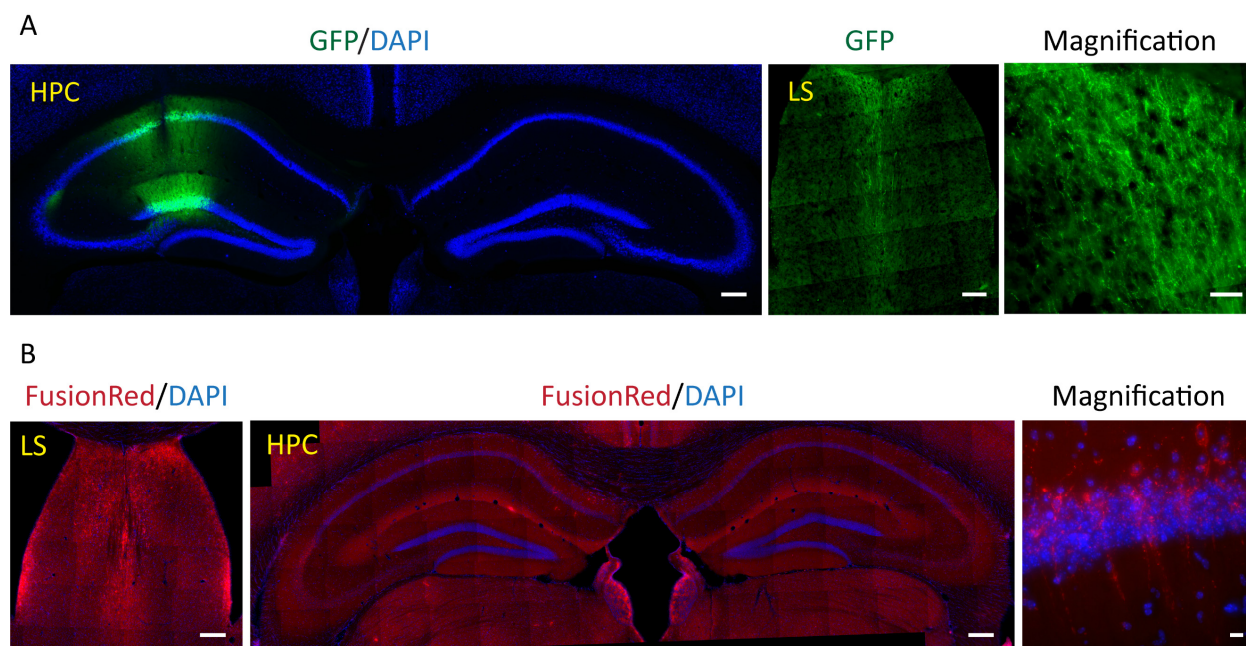


**Figure 1. 3. Anterograde and retrograde tracing of hippocampal-lateral septal (HPC-LS) circuit.** (A) rAAV-CaMKII-GFP was unilaterally injected in the dorsal CA1 (scale bar: 200  $\mu$ m), and the axons were labeled by green fluorescence (GFP) in LS (scale bar: 200  $\mu$ m). The high magnification showed dorsal CA1 projected axons in dorsal LS (scale bar: 40  $\mu$ m) (B) rAAVrg-CaMKII- FusionRed was bilaterally injected into the LS (scale bar: 200  $\mu$ m), and the projected neurons in HPC (scale bar: 200  $\mu$ m) were labeled by red fluorescence (FusionRed). The high magnification showed HPC projected neurons in the dorsal LS (scale bar: 20  $\mu$ m).

### 3. Optogenetic suppression of the hippocampal-lateral septal (HPC-LS) circuit increased fear generalization.

The hippocampal-lateral septal (HPC-LS) circuit plays an important role during encoding of spatial and context information (van der Veldt, Etter, Mosser, Manseau, & Williams, 2021), processing of contextual memories (Besnard et al., 2019; Opalka & Wang, 2020), and modulating fear discrimination (Besnard et al., 2020). Different studies illustrated that dorsal CA1 is essential for memory consolidation (A. Chowdhury et al., 2022; Montgomery & Buzsaki, 2007; Sans-Dublanc et al., 2020; J. Y. Yu et al., 2018) and discrimination (Griffin, Owens, Peters, Adelman, & Cline, 2012; Neves et al., 2022; Ramirez-Gordillo et al., 2022). Opalka et al. reported that dHPC-LS pathway modulates memory for experienced context (Opalka & Wang, 2020). Besnard et al. found that the dCA3-dCA1 and dCA3-dLS pathways have different roles in discriminating between a neutral context and a training context following consolidation

(Besnard et al., 2020). However, it remains unclear how the dCA1-LS circuit contributes to discrimination between stored and novel contexts.

To investigate this question, we designed experiments to manipulate the dCA1-LS projection pathway during context discrimination, using optogenetic tools. We injected bilaterally, a retrograde virus expressing an inhibitory opsin (rAAVrg-CaMKII-stGtACR-FusionRed) into the dorsal-intermediate LS of WT mice (Figure I. 4. B. left). Simultaneously, we implanted two optical fibers over the right and left dorsal dCA1 (Figure I. 4. A, D). The tips of the fibers were placed 100  $\mu\text{m}$  above the pyramidal layer (Figure I. 4. B. right). Four weeks after the surgery, one group of mice received optical suppression of the dCA1-to-LS projection neurons during the acquisition of contextual fear memory on day 0 (stGtACR-Conditioning) (Figure I. 4. C) and the second group received optical suppression of the dCA1-to-LS projection neurons during the memory specificity test on day 7 and day 21 (stGtACR-Novel) (Figure I. 4. D). The third group was injected with the inhibitory opsin and implanted with fiber optic canula, identical to groups 1 and 2, but did not receive any light stimuli throughout the experiment.



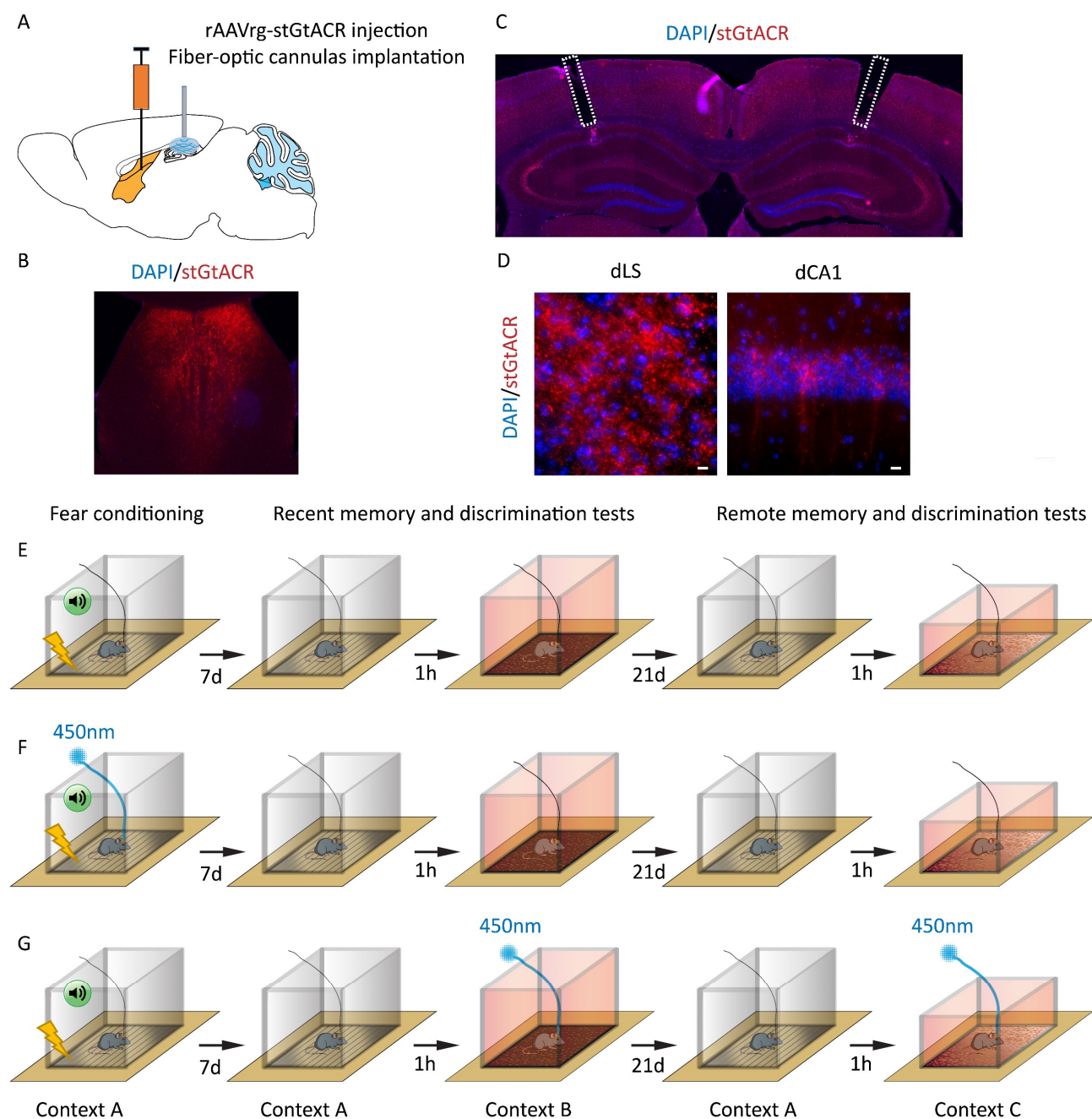


**Figure I. 4. Optical suppression of the dCA1-lateral septum (dCA1-LS) circuit in mice.** (A) Schematic of retrograde virus injection and two fiber-optic cannulas implantation. (B) AAVrg-CaMKII-stGtACR-FusionRed was injected bilaterally into the lateral septum (LS) (scale bar: 200  $\mu$ m). (C) Two fiber-optic cannulas (shown in white dashed lines) were implanted into bilateral HPC (scale bar: 200  $\mu$ m). (D) The magnification of virus expression in the dLS and dCA1 were shown (scale bar: 10  $\mu$ m). (E, F, G) Schematic of fear conditioning paradigm and protocol. After four weeks, mice were conditioned by applying a mild foot shock (0.5 mA) with a neutral tone (10k Hz, 70 dB). (E) The Control group did not receive any light stimulation. (F) The stGtACR-Conditioning group received optical suppression only during the fear condition. (G) The

stGtACR-Novel group received light stimulation in the novel context only and Contextual memory and memory specificity were tested at 7 days and 21 days delay after conditioning.

To evaluate the specificity of context memory, mice were introduced to an altered context that differed from the conditioning context in its geometrical, olfactory, auditory, and visual characteristics. We expected that mice with intact memory would recognize the original context and distinguish it from the altered context, by displaying enhanced freezing in the first, and low freezing in the latter (Figure I. 4. C, D).

### **3.1. Optical suppression of the dorsal hippocampal-lateral septal (dHPC-LS) circuit during memory acquisition increased fear generalization.**

Since we rely on freezing percentage as a readout of memory strength and specificity, we first tested whether light by itself might limit mobility or increase freezing percentage. To do so, we compared baseline freezing in the context (prior to conditioning) between mice receiving continuous light stimulation (stGtACR-Conditioning) and mice not receiving any light stimulation (control and stGtACR-Novel). The results indicated that the light stimulation may have increased freezing for some mice during baseline context exposure, but there were no significant differences between the control groups (Figure I. 6. A). Moreover, light stimulation did not prohibit successful fear induction, as evidenced by similarly strong freezing immediately after foot shocks (Figure I. 6. B) in all groups. In both the recent and remote memory tests, the mice exhibited strong freezing in the conditioning environment (Figure I. 5. A-C). These findings suggest that virus injection and optical suppression of the dCA1-LS pathway during memory acquisition did not affect the recall of contextual memory.



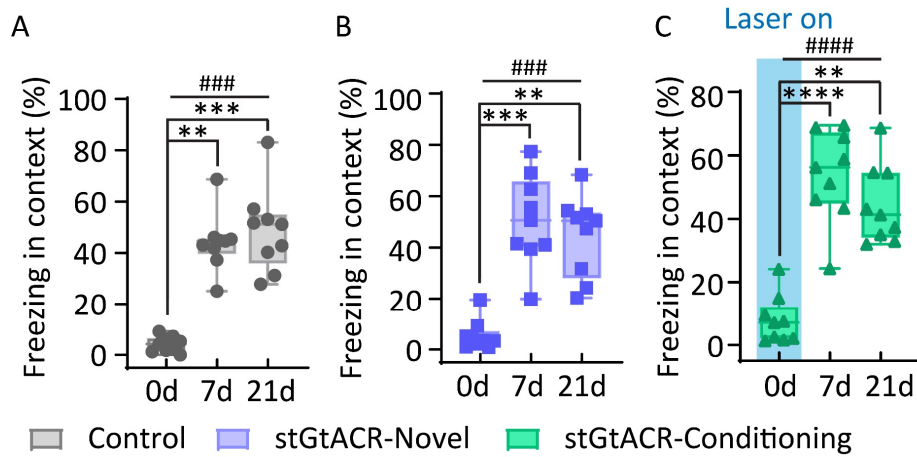


**Figure I. 5. Virus injection and optical suppression did not affect contextual fear memory in mice.** (A) Averaged percentage freezing during fear acquisition (day 0) and fear memory retrieval (day 7 and 21) in Control group phase (Median: day 0, 4.25%; day 7, 44.72%; and day 21, 51.19%; ###p < 0.001). (B) Averaged percentage freezing during fear acquisition (day 0) and fear memory retrieval (day 7 and 21) in stGtACR-Novel group (Median: day 0, 3.58%; day 7, 50.69%; and day 21, 50.50%; ###p < 0.001). (C) Averaged percentage freezing during fear acquisition (day 0) and fear memory retrieval (day 7 and 21) in stGtACR-Conditioning group (Median: day 0, 7.08%; day 7, 56.22%; and day 21, 41.33%; ####p < 0.0001). Control n = 9, stGtACR-Novel, n = 9 and stGtACR-Conditioning, n = 9. Differences between all groups were assessed with the Kruskal-Wallis test (#p < 0.05, ##p < 0.01, ###p < 0.001). Dunn's multiple comparison was performed to compare between day 0, day 7 and day 21 (\*\*p < 0.01, \*\*\*p < 0.001, \*\*\*\*p < 0.0001). The box plots showed the median (-), whiskers showed min to max, and all data points.

During the recent memory test, the stGtACR-Conditioning group displayed increased freezing in the novel context (Figure I. 6. D) and a decreased discrimination index (Figure I. 6. E) compared to the control group; however, these differences did not reach statistical significance. In contrast, in the remote memory test, stGtACR-Conditioning mice exhibited a significantly high freezing percentage in the altered context and a low discrimination index (Figure I. 6. G, H).

These results suggest that optogenetic inactivation of the dCA1-dLS pathway during memory acquisition does not prohibit context memory formation but leads to memory generalization and consequential degradation of memory specificity.

### 3.2. Acute optical suppression of the dCA1-LS circuit in the altered context test increased fear generalization.

In the stGtACR-Novel group, mice exhibited strong freezing immediately after foot shocks, but not before (Figure I. 6. A), indicating successful fear induction (Figure I. 6. B). During both recent and remote memory tests, mice in this group displayed a high freezing percentage in the conditioning context (Figure I. 6. C, F) similar to the control mice, and indicating successful retrieval of the conditioning memory.

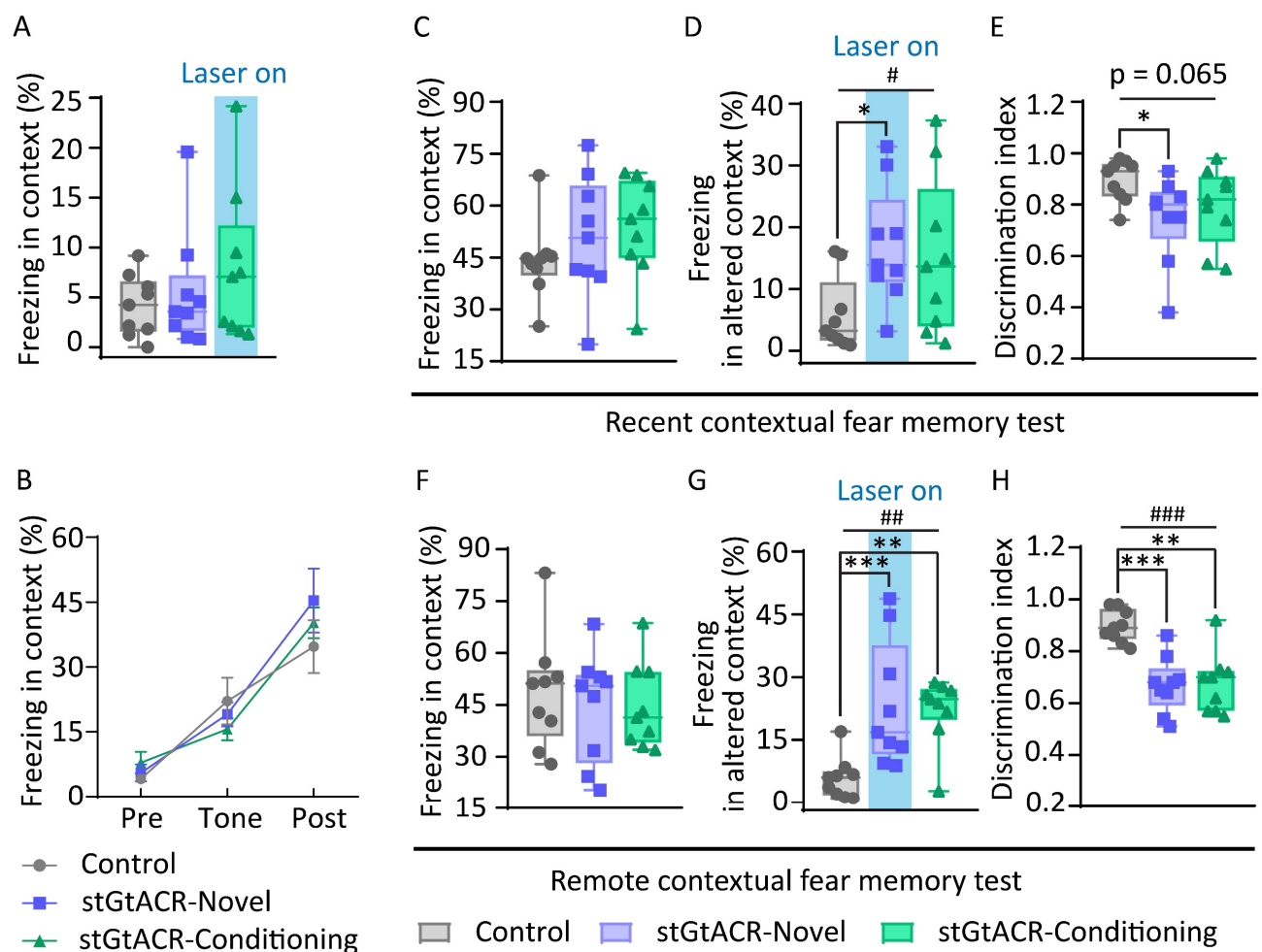


**Figure I. 6. Optical suppression of the dCA1-LS circuit increased fear generalization in mice.** (A) Averaged percentage freezing during fear acquisition phase (A, Median: Control, 4.25%; stGtACR-Novel, 3.58%; and stGtACR-Condition, 7.08%;  $p = 0.546$ , NS). The optical suppression in dCA1 did not affect the baseline freezing level of the mice. (B) All groups of mice displayed similar freezing percentage before, during and immediately after conditioning (Phase  $F(2,24) = 0.35$ ,  $p = 0.71$ , NS; group  $F(1.43,34.36) = 17.96$ ,  $p < 0.001$ ; interaction  $F(4,48) = 1.06$ ,  $p = 0.39$ ,

NS). Significance was assessed with a two-way ANOVA with a mixed-effects model and a post hoc Bonferroni test. Data represents the mean  $\pm$  S.E.M. (C-E) Recent memory test. Both stGtACR-Conditioning and stGtACR-Novel groups displayed strong freezing in the conditioning context similar to the Control group (C, Median: Control, 44.72%; stGtACR-Novel, 50.69%; and stGtACR-Condition, 56.22%;  $p = 0.239$ , NS). (D) Only the stGtACR-Novel group showed a significantly higher percentage freezing in the novel context (D, Median: Control, 3.25%; stGtACR-Novel, 13.92%; and stGtACR-Condition, 13.67%;  $\#p < 0.05$ ) and (E) lower discrimination index (E, Median: Control, 0.93; stGtACR-Novel, 0.80; and stGtACR-Conditioning, 0.82;  $p = 0.065$ , NS) compared (F-H) Remote memory test. (F) Similar percentage freezing in Both the stGtACR-Condition group and stGtACR-Novel group indicated normal freezing percentage in the contextual memory test compared to the Control group (F, Median: Control, 51.19%; stGtACR-Novel, 50.50%; and stGtACR-Condition, 41.33%;  $p = 0.916$ , NS). The stGtACR-Condition group and the stGtACR-Novel group showed a higher level of freezing in altered context (G, Median: Control, 6.00%; stGtACR-Novel, 16.83%; and stGtACR-Condition, 24.75%;  $\#\#p < 0.01$ ) and lower discrimination index (H, Median: Control, 0.89; stGtACR-Novel, 0.68; and stGtACR-Condition, 0.70;  $\#\#\#p < 0.001$ ) in comparison with control group 21 days after conditioning. Control  $n = 9$ , stGtACR-Novel,  $n = 9$  and stGtACR-Conditioning,  $n = 9$ . Differences between all groups were assessed with the Kruskal-Wallis test ( $\#p < 0.05$ ,  $\#\#p < 0.01$ ,  $\#\#\#p < 0.001$ ). Dunn's multiple comparison was performed to compare stGtACR-Novel and stGtACR-Conditioning to the Control group ( $*p < 0.05$ ,  $**p < 0.01$ ,  $***p < 0.001$ ). The box plots showed the median (-), whiskers showed min to max, and all data points.

In summary, the optogenetic manipulations show that: 1. Optical suppression of dCA1-LS during conditioning or novel context exposure does not interfere with subsequent recall of the conditioning context memory. 2. Optical suppression of the dCA1-dLS circuit during memory acquisition leads to a gradual degradation in context discrimination, becoming prominent at remote memory recall. 3. Optical suppression of the dCA1-LS circuit increases freezing responses to novel context exposure at recent and remote time points. We conclude that activation of the dCA1-LS circuitry promotes context discrimination by suppressing inappropriate freezing in unconditioned environments.

### **3.3. Optical suppression of the dCA1-LS circuit during context exposure decreased neuronal activity in CA1 and Arc/Arg3.1 engrams in the LS.**

To investigate the impact of optical suppression in the dHPC-dLS pathway on local neuronal activity and engram cell reactivation in dCA1 and dLS, we sacrificed mice 90 minutes after the remote memory specificity test. The brains were fixed with paraformaldehyde (PFA), sliced and immunostained for Arc/Arg3.1 and cFos. With the mean intensity of Arc/Arg3.1 and the number of cFos positive neurons were quantified with QuPath (<https://qupath.github.io/>) and normalized to the area of each measured region.

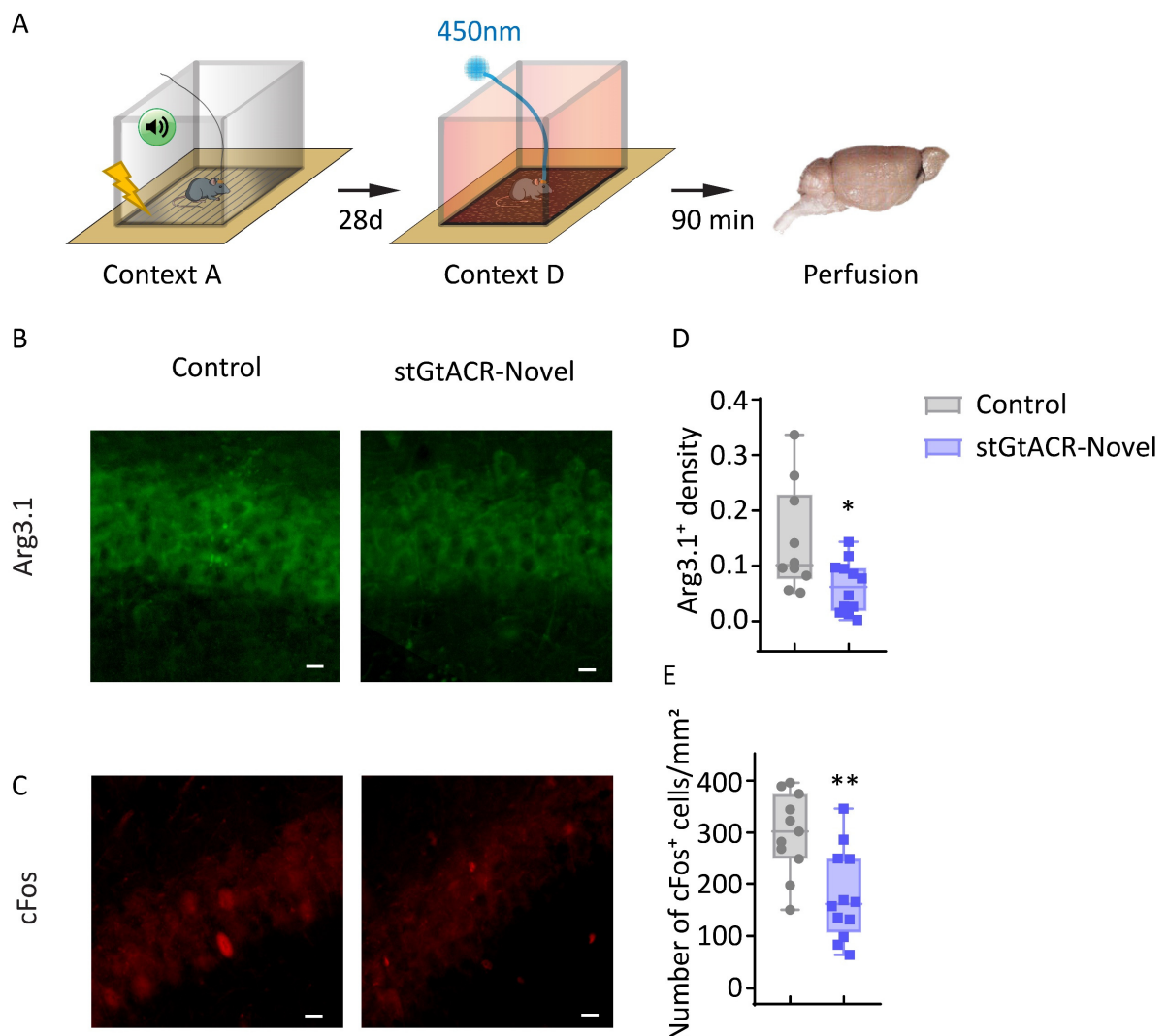


**Figure I. 7. Optical suppression decreases memory discrimination-induced expression of Arc/Arg3.1 and cFos in CA1** (A) Schematic of memory discrimination test and perfusion. (B, D) Following the context discrimination test, Arc/Arg3.1 expression in the CA1 was significantly downregulated by optical suppression (B: green: Arc/Arg3.1; scale bar: 10  $\mu$ m; D: median: Control, 0.104; n = 10; stGtACR-Novel, 0.065; n = 12; \*p < 0.05). (C, E) Following the context

discrimination test, cFos expression in the CA1 was significantly downregulated by optical suppression (C: red: cFos, scale bar: 10  $\mu\text{m}$ ; E: median: Control, 302.3 cells/ $\text{mm}^2$ ;  $n = 10$ ; stGtACR-Novel, 161.3 cells/ $\text{mm}^2$ ;  $n = 12$ ;  $**p < 0.01$ ). Significance was assessed with the Mann-Whitney test. The box plots showed the median (-), whiskers showed min to max, and all data points.

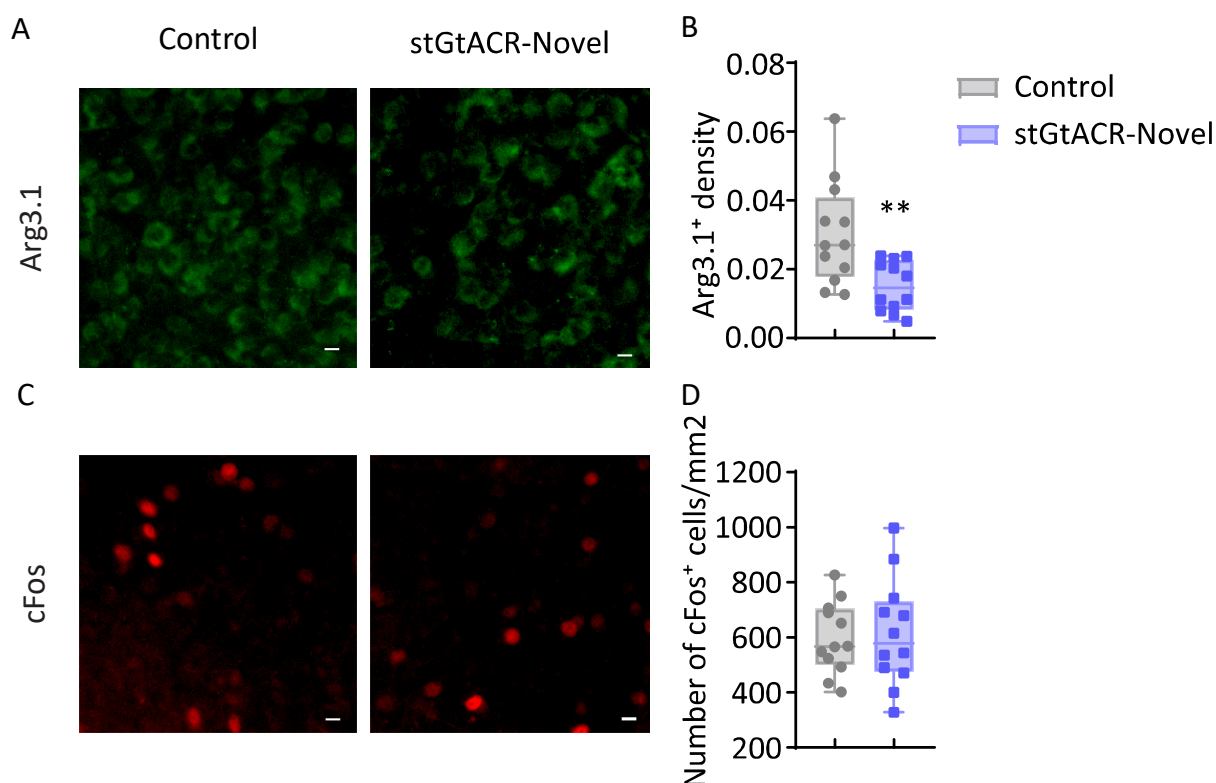


**Figure I. 8. Optical suppression decreases memory discrimination-induced expression of Arc/Arg3.1 but not cFos in LS (A, B)** Following the context discrimination test, Arc/Arg3.1 expression in the LS was significantly downregulated by optical suppression (A: green: Arc/Arg3.1, scale bar: 10  $\mu\text{m}$ ; B: Median: Control, 0.027;  $n = 12$ ; stGtACR-Novel, 0.015;  $n = 12$ ;  $**p < 0.01$ ). (C, D) Optical suppression during the context discrimination test did not alter cFos expression in the LS (C: red: cFos, scale bar: 10  $\mu\text{m}$ ; D: Median: Control, 567.5 cells/ $\text{mm}^2$ ;  $n = 12$ ; stGtACR-Novel, 579.0 cells/ $\text{mm}^2$ ;  $n = 12$ ;  $p = 0.93$ , NS). Significance was assessed with the Mann-Whitney test. The box plots showed the median (-), whiskers showed min to max, and all data points.

These findings show that the expression of Arc/Arg3.1 (Figure I. 7. A, B) and cFos in CA1 (Figure I. 7. C, D) were suppressed by optical suppression of the dCA1-LS pathway, indicating a successful inactivation of CA1 firing by the blue laser light. Interestingly, in the LS only

Arc/Arg3.1 expression was suppressed (Figure I. 8. A, B), suggesting that plasticity-inducing activity patterns were specifically abrogated by the laser stimulation. The unaltered expression of cFOS (Figure I. 8. C, D), despite reduced input from dCA1, might reflect an effect of disinhibition in the recurrent inhibitory circuit of LS and a broader range of cFOS-inducing activity patterns. These results indicate a unique role of Arc/Arg3.1 in the dCA1-LS pathway during context memory processing.

#### **4. Ablation of Arc/Arg3.1 in the lateral septum (LS) increased fear generalization.**

An independent study previously performed in our lab demonstrated that ablation of Arc/Arg3.1 in the hippocampus resulted in diminished specificity of remote context fear memory (Xiaoyan Gao, 2016). My current study verifies an upregulation of Arc/Arg3.1 in the HPC and LS following the acquisition and retrieval of context memory, which can be suppressed by optical suppression of the dCA1-LS pathway. Moreover, dCA1-LS optical suppression degrades context discrimination and reproduces the memory specificity deficit caused by hippocampal Arc/Arg3.1 ablation. Based on these findings, I hypothesized that Arc/Arg3.1 expression in the LS plays an important role in the processing of contextual memory.



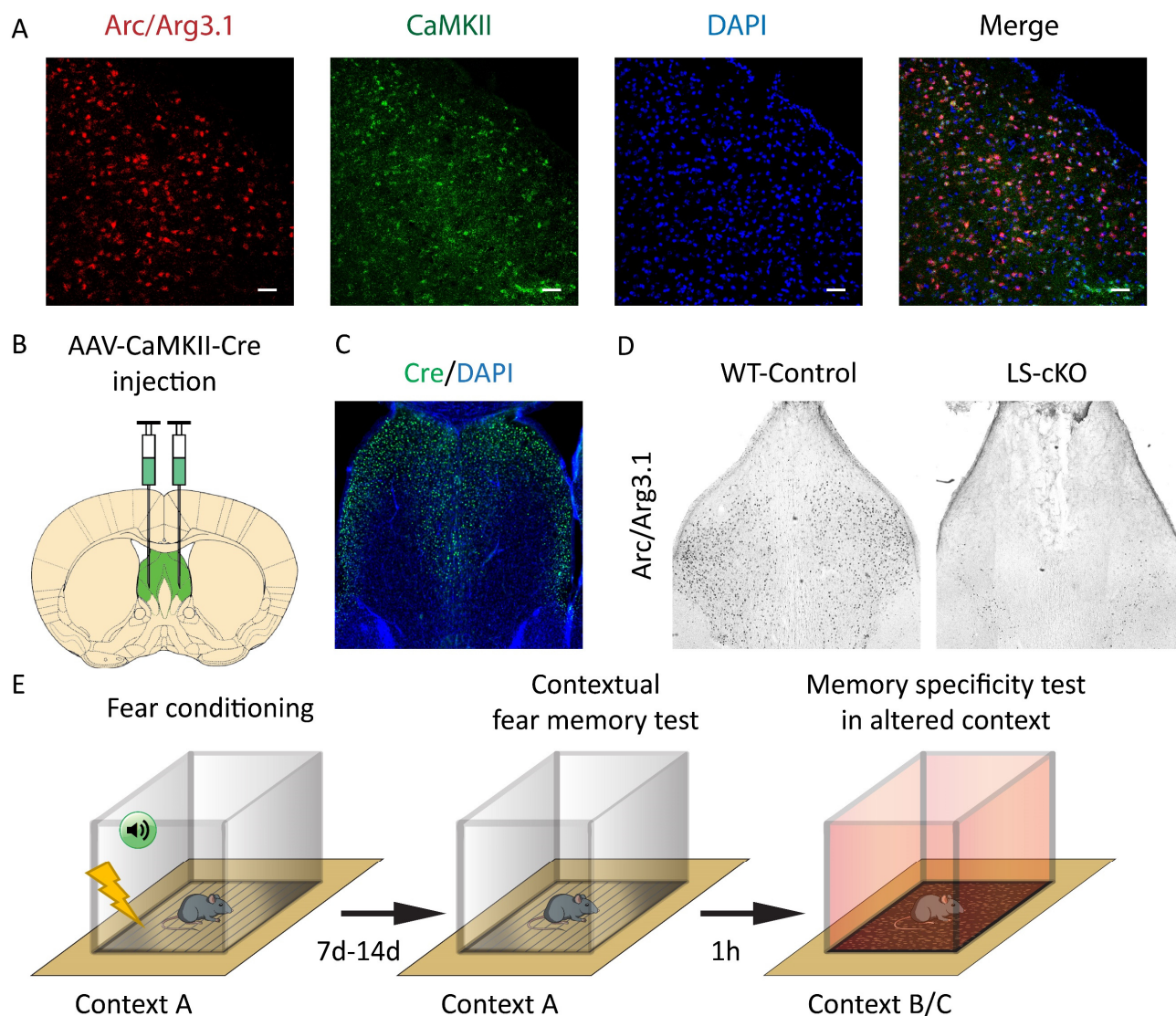


**Figure I. 9. Conditional deletion of *Arc/Arg3.1* in the lateral septum (LS) and fear conditioning memory tests in mice.** (A) The fISH (RNAscope) showed that *Arc/Arg3.1* and *CaMKII* $\alpha$  were colocalized in the dorsal lateral septum (dLS). (B, C) The rAAV-CaMKII-Cre was injected bilaterally into the lateral septum (LS) (green: Cre, blue: DAPI). (D) *Arc/Arg3.1* expression was significantly reduced after the Cre ablation. (E) Schematic of fear conditioning paradigm and protocol. The fear conditioning was performed on mice 7 days after the injection. The context memory and altered context tests were tested 7 and 14 days after the conditioning.

To address this hypothesis, I chose to conditionally delete *Arc/Arg3.1* in the LS by bilateral injection of a rAAV-CaMKII-Cre into the brains of *Arc/Arg3.1*<sup>f/f</sup> mice (Figure I. 9. B, C). The high effectiveness of this virus and the short delay to full *Arc/Arg3.1* deletion (7 days) were previously tested and confirmed in the HPC (Gao 2018). Another study in our lab (Kuku 2020)

demonstrated that, albeit inhibitory, most of the LS neurons were also positive for CaMKII $\alpha$  and expressed Arc/Arg3.1 after seizure. Thus, I expected successful deletion of Arc/Arg3.1 in the LS following rAAV-CaMKII-Cre injection. After confirming the co-expression of Arc/Arg3.1 and CaMKII $\alpha$  in the dorso-medial portion of the LS (Figure I. 9. A) I injected the virus, bilaterally into the LS of WT (Arc/Arg3.1<sup>+/+</sup>) and floxed mice (Arc/Arg3.1<sup>f/f</sup>) (Figure I. 9. B). Floxed mice in which Arc/Arg3.1 was conditionally ablated in the lateral septum (LS) (Figure I. 9. D), were named “LS-cKO”. After 7 days of recovery and 3 days of handling, the mice were subjected to the fear conditioning test (Figure I. 9. E). At the end of testing mice were sacrificed and the brains stained against Cre to evaluate the extent of deletion (Figure I. 9. C).

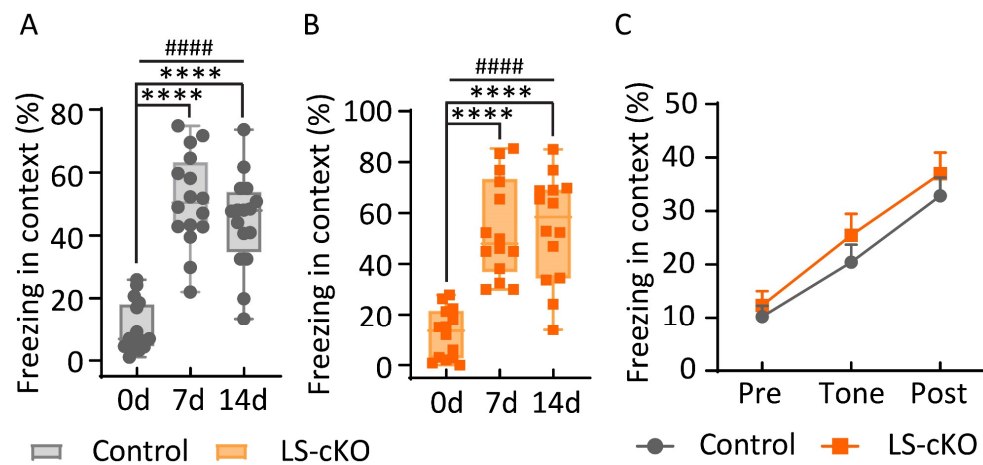


**Figure I. 10. Ablation of Arc/Arg3.1 in the lateral septum (LS) did not affect contextual fear memory and basal freezing percentages in mice.** (A) Averaged percentage freezing during fear acquisition (day 0) and fear memory retrieval (day 7 and 21) in Control group phase (Median: day 0, 6.80%; day 7, 50.43%; and day 21, 47.92%; ##### $p < 0.0001$ ). (B) Averaged percentage freezing during fear acquisition (day 0) and fear memory retrieval (day 7 and 21) in Control group phase (Median: day 0, 13.54%; day 7, 47.99%; and day 21, 58.46%; ##### $p < 0.0001$ ). Differences between all groups were assessed with the Kruskal-Wallis test (##### $p < 0.0001$ ). Dunn’s multiple comparison was performed to compare between day 0, day 7, and day 14 (\*\*\*\* $p < 0.0001$ ). The box plots showed the median (-), whiskers showed min to max, and all data points. (C) The LS-cKO mice showed similar freezing percentages compared to WT-Control mice during fear acquisition (Phase  $F_{(1,28)} = 1.26$ ,  $p = 0.27$ ; group  $F_{(1,835,51.37)} = 36.47$ ,  $p < 0.0001$ ; interaction  $F_{(2,56)} = 0.14$ ,  $p = 0.87$ , NS). Significance was assessed with a two-way ANOVA with a mixed-effects model and a post hoc Bonferroni test. Data represents the mean  $\pm$  S.E.M. Mice per group: Control,  $n = 16$ ; LS-cKO,  $n = 14$ .



The freezing percentage in the during memory acquisition (Figure I. 10. C) was not significantly different between Control and LS-cKO mice. Both groups displayed stronger freezing immediately after foot shocks (post), compared to baseline (pre) and tone stimuli (Figure I. 10. C), indicating successful fear induction. Similar post-conditioning freezing percentage of Control and LS-cKO indicates similar conditioning strength. The robust freezing response in the context tests for recent and remote memory demonstrates the establishment of a strong fear memory in all mice (Figure I. 10. A, B). Furthermore, the conditional ablation of Arc/Arg3.1 in the lateral septum (LS) did not affect the strength of recent or remote fear memory in mice (Figure I. 11. A, D). However, during recent memory tests (Figure I. 11. A-C), LS-cKO mice displayed significantly higher freezing percentages in the altered context (Figure I. 11. B) and a corresponding lower discrimination index (Figure I. 11. C), indicating memory generalization. In the remote memory tests (Figure I. 11. D-F), LS-cKO mice showed higher percentage freezing in the altered context (Figure I. 11. E) and a lower discrimination index (Figure I. 11. F), yet these differences did not reach statistical significance. These findings suggest that the conditional ablation of Arc/Arg3.1 in the lateral septum (LS) diminishes the specificity of recent contextual fear memory and to a lesser extent, the specificity of remote memory.

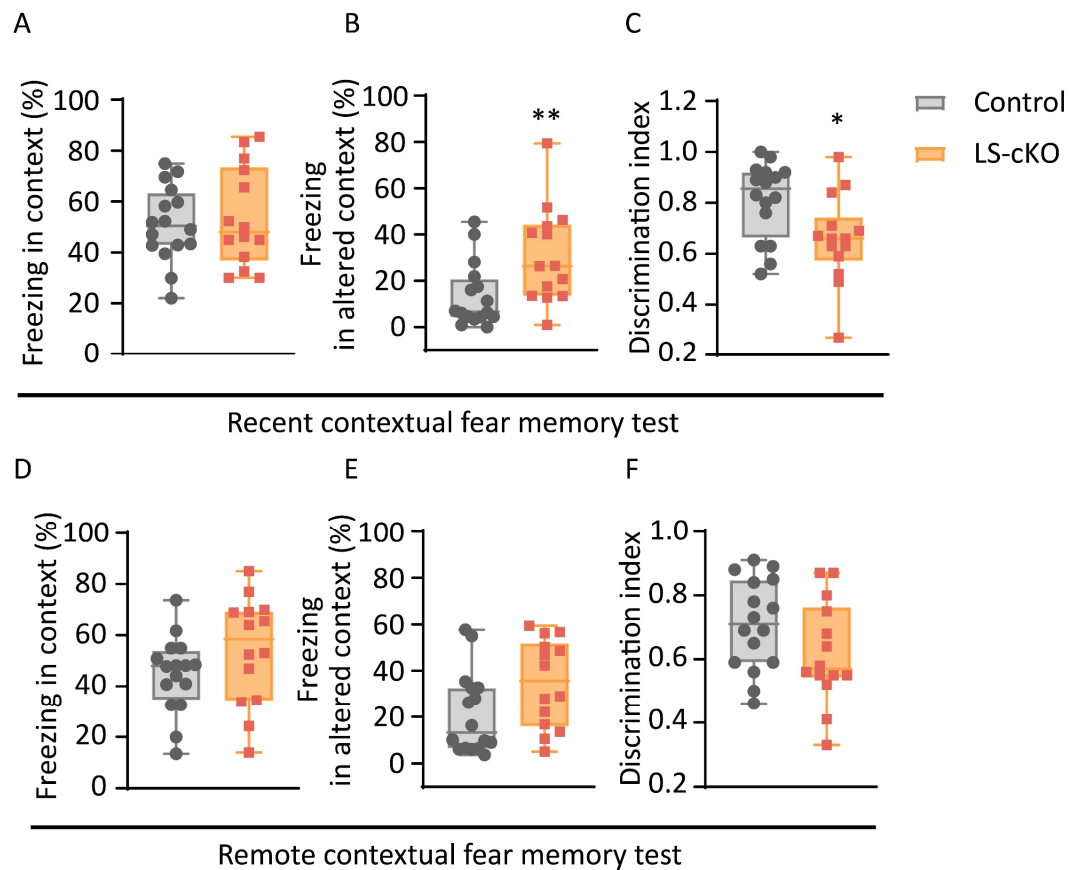


**Figure I. 11. Ablation of Arc/Arg3.1 in the lateral septum (LS) increased recent memory generalization.** (A) The LS-cKO mice showed a similar freezing level in the context memory test compared to their WT littermates (Median: Control, 50.43%; LS-cKO, 47.99%;  $p = 0.75$ , NS) 7 days after conditioning. But the LS-cKO mice showed a higher level of freezing in the (B) altered context (Median: Control, 6.59%; LS-cKO, 26.38%; \*\* $p < 0.01$ ) and lower (C) discrimination index (Median: Control, 0.86; LS-cKO, 0.66; \* $p < 0.05$ ) in comparison with the control mice 7 days after conditioning. (D) The LS-cKO mice showed similar freezing percentage in the context memory test compared to their WT littermates (Median: Control, 47.92%; LS-cKO, 58.46%;  $p = 0.13$ , NS) 14 days after conditioning. But the LS-cKO mice showed a non-significantly higher level of freezing in (E) altered context test (Median: Control, 13.17%; LS-cKO, 35.63%;  $p = 0.056$ , NS) and non-significantly lower (F) discrimination index (Median: Control, 0.71; LS-cKO, 0.57;  $p = 0.086$ , NS) in comparison with the control mice 14 days after conditioning. Mice per group: Control,  $n = 16$ ; LS-cKO,  $n = 14$ . Significance was assessed with the Mann-Whitney test. The box plots showed the median (-), whiskers showed min to max, and all data points.

## 5. Arc/Arg3.1-dependent consolidation of implicit memory in the hippocampal-lateral septal circuit.

### **5.1. Long-term implicit memories in hippocampal-lateral septal circuit optical inhibition mice and lateral septal Arc/Arg3.1 ablated mice.**

The classification of memories into working memory, short-term memory, and long-term memory has been widely accepted in the field of cognitive neuroscience. Additionally, memories can be categorized into declarative (explicit) and non-declarative (implicit) memories based on the type of information they contain (Cubelli & Della Sala, 2020; Jawabri & Cascella, 2024; Squire, 2009). Implicit memory, in particular, plays a crucial role in our daily lives as it involves the retrieval and application of learned information without conscious awareness or reference to the learning phase (Cubelli & Della Sala, 2020). Explicit and implicit memory retrieval differ in terms of conscious recollection, with the former being recalled by recognition or events (Squire, 1992). Previous research has suggested that explicit and implicit memories are modulated by different neurological systems (Dew & Cabeza, 2011; Squire & Zola-Morgan, 1991).

In the above chapters, the role of Arc/Arg3.1 in the hippocampal-lateral septal circuit in memory acquisition and consolidation of explicit memories has been investigated. The data revealed that the expression of Arc/Arg3.1 is required to maintain the regular function of the HPC-LS circuit in adult mice and is essential for memory discrimination over short and long time periods. However, the contribution of Arc/Arg3.1 in the HPC-LS circuit to implicit memory formation and the specific type of neurons it modulates remain an area of ongoing research. To address this issue, the auditory fear conditioning test has been employed.

### **5.2. Tone fear memory in hippocampal-lateral septal circuit optical inhibition mice.**

The process of auditory fear conditioning involves pairing an aversive unconditional stimulus (US), such as an electrical shock, with a neutral conditional stimulus (CS), such as a tone. Eventually, the neutral stimulus can elicit the fear state after the conditioning test. In chapter I of this thesis, I investigated contextual fear memory using an experiment design that also allows testing of tone fear memory.

To precisely control the activity of the dCA1-dLS circuit, mice received bilateral LS injections (Figure I. 12. A), targeting dorsal and intermedium LS, of AAVrg-CaMKII-stGtACR-FusionRed (stGtACR). Meanwhile, two optical fibers were implanted in the HPC (Figure I. 12. A). The tips of

the fibers were 100  $\mu\text{m}$  above the pyramidal layer. Four weeks after the surgery, one group of mice received photoinhibition of the dCA1-to-dLS projection neurons during the acquisition of tone fear memory on day 0 (stGtACR-Condition) (Figure I. 12. C), while the other group received photoinhibition of the dCA1-to-dLS projection neurons during the tone memory test on day 7 and day 21 (stGtACR-Novel) (Figure I. 12. D). The control group received no optical stimuli during the tests (Figure I. 12. B). The mice were placed in the conditioning arena and were subjected to 2 pairs of tones/foot shock stimuli. After 7 and 21 days, tone fear memory was assessed by placing mice into a novel arena with different visual, tactile, geometrical, and olfactory characteristics from the conditioning environment. The same neutral tone paired with the CS foot shocks was replayed in the altered novel environment to isolate the tone fear memory.

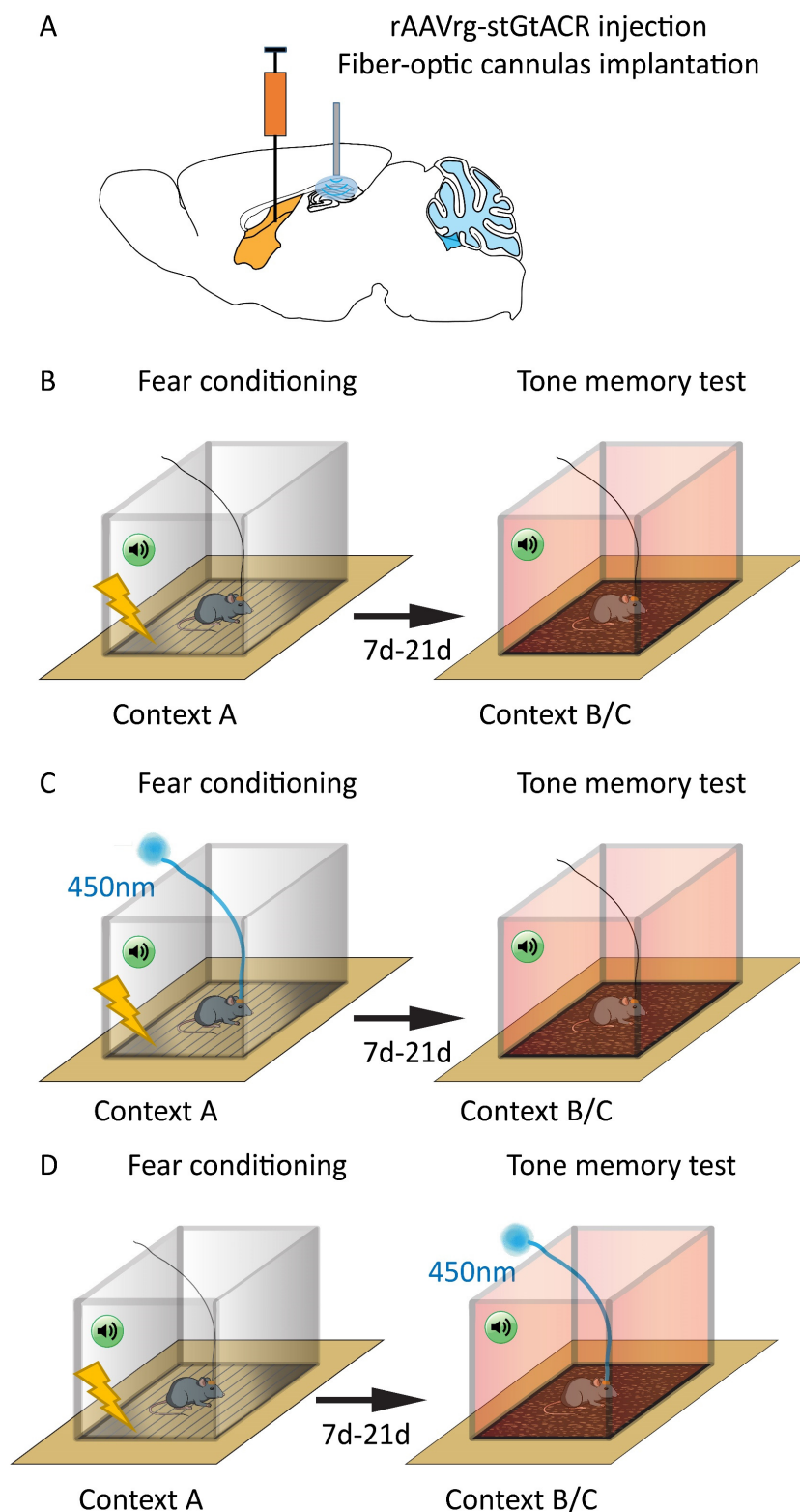


**Figure I. 12. Optical suppression of the dCA1-dLS circuit in mice.** (A, B) The retrograde virus, AAVrg-CaMKII-stGtACR-FusionRed, was injected bilaterally into the lateral septum (LS). Two fiber-optic cannulas were implanted into bilateral HPC. (C, D) Schematic of tone fear conditioning paradigm and protocol. After four weeks, the mice were introduced to the fear conditioning test. Mice were conditioned by applying a mild foot shock (0.5 mA) with a neutral

tone (10k Hz, 70 dB). The stGtACR-Condition group received photoinhibition during the tone fear condition. Tone memory was tested at 7 days and 21 days delay after conditioning. In the tone fear memory test, the stGtACR-Novel group received photoinhibition during the tone fear memory test.

During the tone conditioning, the freezing level of the stGtACR-Condition group was comparable to Control and stGtACR-Novel groups, indicating that photoinhibition did not affect the intact freezing responses to the tone stimuli in adult mice (Figure I. 13. A). However, in recent and remote tone fear memory tests, stGtACR-Condition and stGtACR-Novel groups behave significantly stronger when freezing during tone compared to the Control group (Figure I. 13. B, C). Therefore, the analysis concludes that inhibiting activities in the dCA1-dLS circuit through photoinhibition, whether during the formation or recall of tone fear memory, leads to an apparent enhancement of tone fear memory in mice.

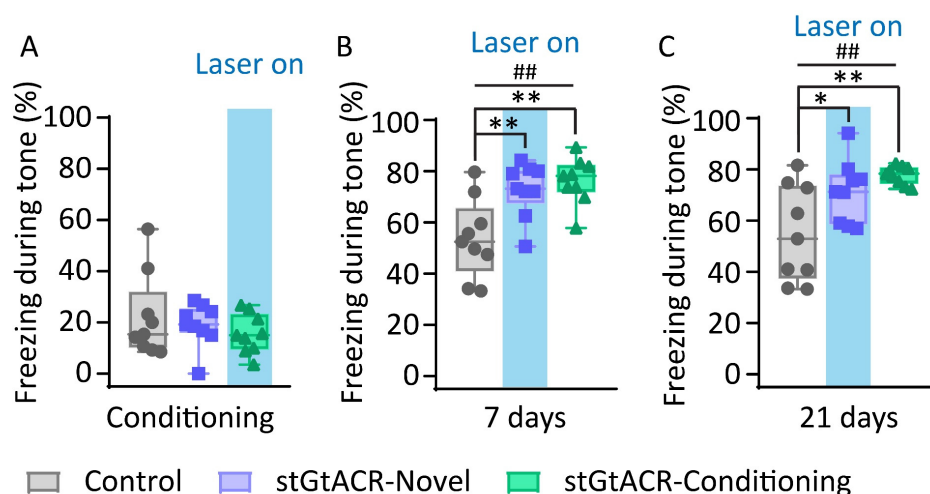


**Figure I. 13. Tone fear memory with photo-inhibited dCA1-dLS circuit in mice.** (A) The optical suppression of dCA1-LS circuits in mice increased the freezing level during tone in the conditioning test (Median: Control, 15.36%; stGtACR-Novel, 19.29%; and stGtACR-Condition, 15.00%;  $p = 0.529$ , NS). Significance was assessed with the Kruskal-Wallis test. (B, C) In the recent (B, Median: Control, 52.50%; stGtACR-Novel, 73.17%; and stGtACR-Condition, 78.17%;  $F(2,24) = 9.23$ ;  $##p < 0.01$ ) and remote (C, Median: Control, 52.92%; stGtACR-Novel, 71.52%; and stGtACR-Condition, 78.42%;  $F(2,24) = 7.435$ ;  $##p < 0.01$ ) tone fear memory test, the freezing levels were significantly higher than their WT-control group. All WT,  $n = 19$ ; LS-cKO,  $n = 18$ . Significance was assessed with the one-way ANOVA test and a post hoc Bonferroni test (\* $p < 0.05$ , \*\* $p < 0.01$ ). The box plots showed the median (-), whiskers showed min to max, and all data points.

### 5.3. Tone fear memory after local Arc/Arg3.1 ablation in the lateral septum.

In order to investigate the role of Arc/Arg3.1 mediated plasticity in the formation of tone fear memory in the lateral septum (LS), I used rAAV-CaMKII-Cre to target LS for local Arc/Arg3.1 ablation (Figure I. 14. A, B). Seven days after injection, I subjected the mice to tone fear conditioning (Figure IV. 3. C).

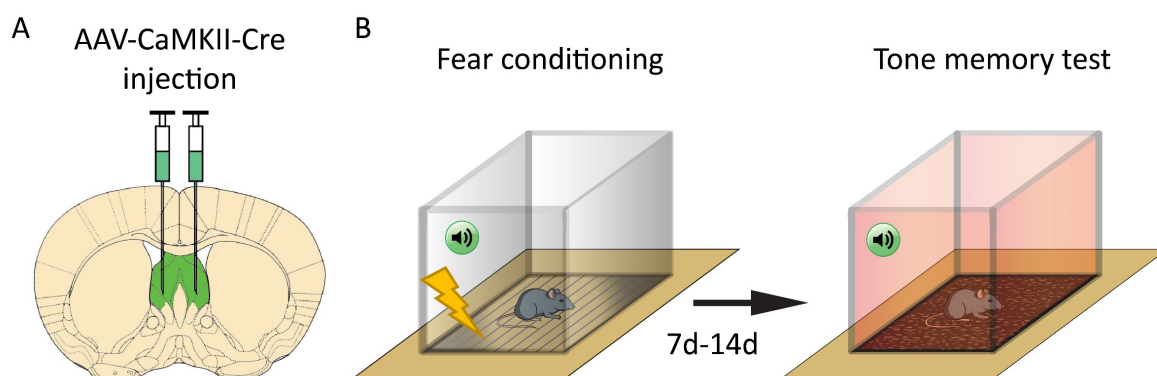


**Figure I. 14. Ablation Arc/Arg3.1 in the lateral septum (LS) and tone fear conditioning test in mice.** (A, B) The rAAV-CaMKII-Cre was injected bilaterally into the lateral septum (LS). (C) Schematic of fear conditioning paradigm and protocol. The tone fear conditioning was performed on mice 7 days after the injection. The tone fear memory was tested 7 and 14 days after the conditioning.

The LS-cKO mice exhibited normal freezing behavior in the tone fear condition test before foot shock during the tone compared to their WT littermates (Figure I. 15. A). In both recent and remote tone fear memory tests, the LS-cKO mice continued to show increased freezing during tone in the altered novel context (Figure I. 15. B, C). Therefore, I conclude that Arc/Arg3.1 ablation in the lateral septum leads to a significant enhancement in freezing percentages of tone-related fear memory in mice.

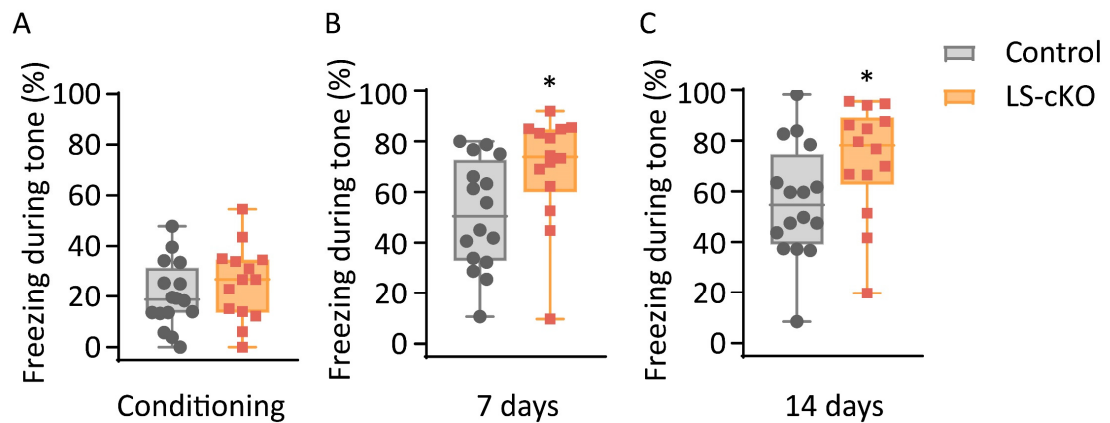


**Figure I. 15. Tone fear memory in LS-cKO mice.** (A) The ablation of Arc/Arg3.1 in the lateral septum in mice increased the freezing level during tone in the conditioning test (Median: WT, 18.75%; LS-cKO, 26.79%,  $p = 0.289$ , NS). (B, C) In the recent (B, Median: WT, 50.46%; LS-cKO, 73.92%,  $*p < 0.05$ ) and remote (C, Median: WT, 54.71%; LS-cKO, 78.21%,  $*p < 0.05$ ) tone fear memory test, the freezing levels were significantly higher than their WT-control group. All WT,  $n = 19$ ; LS-cKO,  $n = 18$ . Significance was assessed with the Mann-Whitney test. The box plots showed the median (-), whiskers showed min to max, and all data points.

## 6. Oscillatory network activity of the hippocampal-lateral septal (HPC-LS) circuit in Arc/Arg3.1 deficient mice.

### 6.1. Local field potential (LFP) recording in vivo.

Theta and gamma oscillations in the hippocampus have been found to be closely associated with learning and memory encoding and retrieval (Berry & Thompson, 1978; L. L. Colgin, 2016; Fernandez-Ruiz et al., 2021; Girardeau & Lopes-Dos-Santos, 2021; Griffin, Asaka, Darling, & Berry, 2004; Korotkova et al., 2018; Seager, Johnson, Chabot, Asaka, & Berry, 2002; Tort, Komorowski, Manns, Kopell, & Eichenbaum, 2009b). Numerous studies have shown that high-frequency oscillations, also known as sharp wave ripples, occur between 110-200 Hz in rodents (Orgy Buzs, 2015) and between 80-180 Hz in humans (Norman et al., 2019; Staresina et al., 2015), play a crucial role in memory consolidation and cognition (Buzsaki, Leung, & Vanderwolf, 1983; Dickey et al., 2022; Imbrosci et al., 2021; Julian Keil, 2023; Norman et al., 2019). The activation and silencing of hippocampal efferents in the lateral septum (LS) also changed theta oscillations in the hippocampus (Bender et al., 2015; Chee, Menard, & Dringenberg, 2015; Espinosa, Alonso, Caneo, Moran, & Fuentealba, 2022; Monmaur, Ayadi, &



Breton, 1993; Pedemonte, Barrenechea, Nunez, Gambini, & Garcia-Austt, 1998). In the current study, I show that context memory discrimination requires intact dCA1-LS activation and expression of Arc/Arg3.1 over a prolonged memory consolidation period. It remains unknown whether Arc/Arg3.1 ablation in this circuit may also modulate local oscillatory activity.

To further investigate the role of Arc/Arg3.1 in modulating the oscillatory network activities in the hippocampus and lateral septum through the dCA1-LS pathway, simultaneous multichannel depth recordings were performed in urethane-anesthetized mice. To conditionally ablated Arc/Arg3.1 in specific regions, rAAV-CaMKII-Cre was injected bilaterally into the dCA1 (Figure. I. 16. D) or LS (Figure. I. 16. F) of Arc/Arg3.1<sup>f/f</sup> mice to specifically remove Arc/Arg3.1 in the targeted brain regions. In vivo local field potential recording was performed in the hippocampus (HPC) and lateral septum (LS) in adult Arc/Arg3.1 KO mice (Figure. I. 16. A, B) or after 7 days injection in mice (Figure. I. 16. C-F).

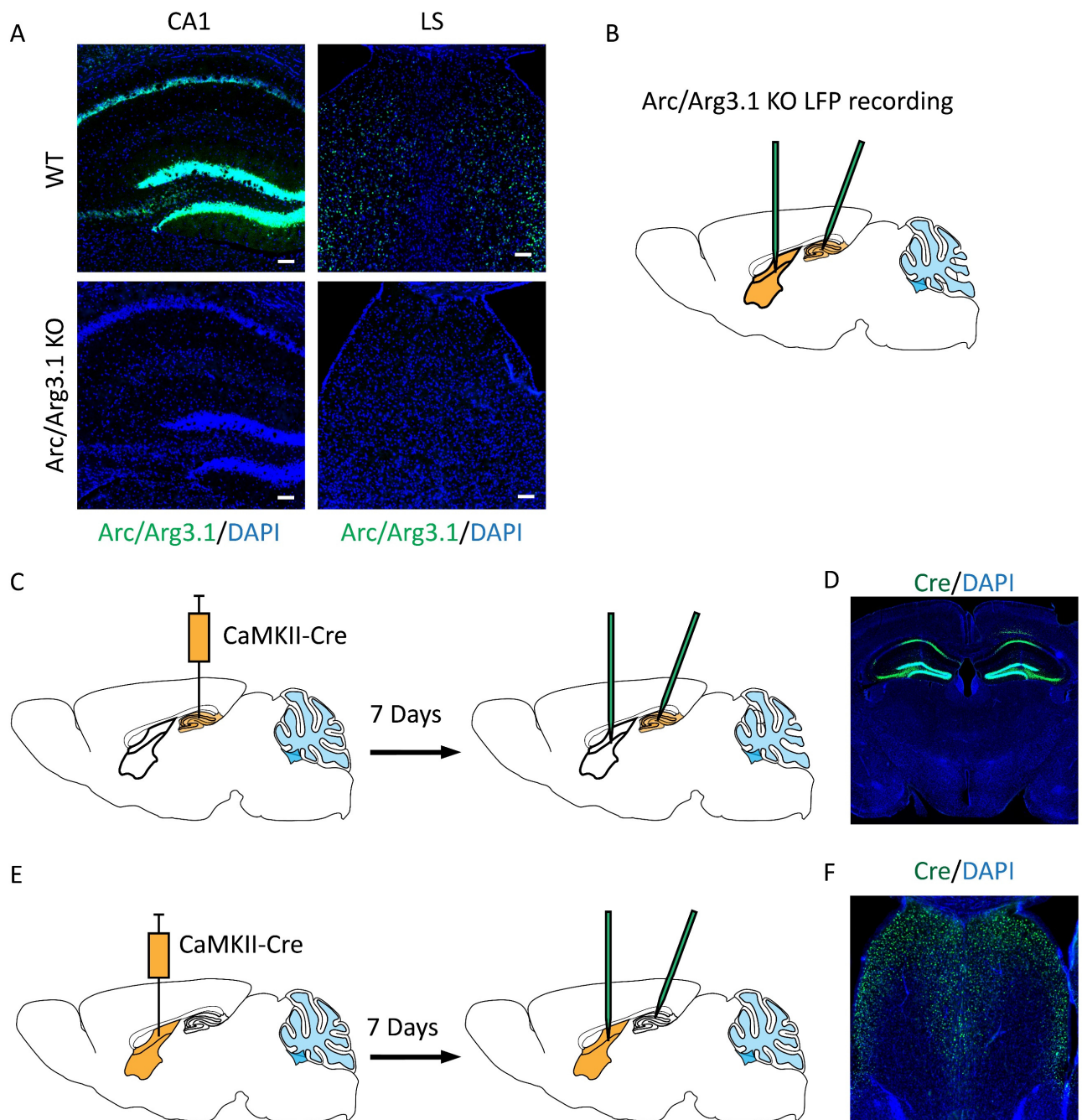


**Figure I. 16. Local field potential recording in HPC-cKO and LS-cKO mice.** (A) Arc/Arg3.1 mRNA expression in dorsal CA1 and dorsal LS 45 min after seizures (green: Arc/Arg3.1, blue: DAPI; scale bar: 100  $\mu$ m). (B) Schematic of local field potential recording (LFP) in Arc/Arg3.1 KO mice. (C) Schematic of local field potential recording (LFP) in HPC-cKO mice. (D) The rAAV-CaMKII-Cre was injected bilaterally into the hippocampus (HPC). Cre was labeled green fluorescence, and DAPI was blue. (E) Schematic of local field potential recording (LFP) in LS-cKO mice. (F) The rAAV-CaMKII-Cre was injected bilaterally into the lateral septum (LS). (D, F) Cre was labeled green fluorescence, and DAPI was blue.

Local field potentials and unit spikes were recorded from both the dorsal CA1 (Figure. I. 17. A, B) and the dorsal lateral septum (Figure. I. 17. A, C). Urethane anesthesia induces two sleep-like activity patterns: REM and SWS, which alternate spontaneously. Sleep-like phases were identified based on their characteristic rhythms with high theta/delta power ratio in REM and high delta power (ripple-rich) in the SWS epochs (Figure I. 17. D-G). The data was analyzed for each phase, separately.

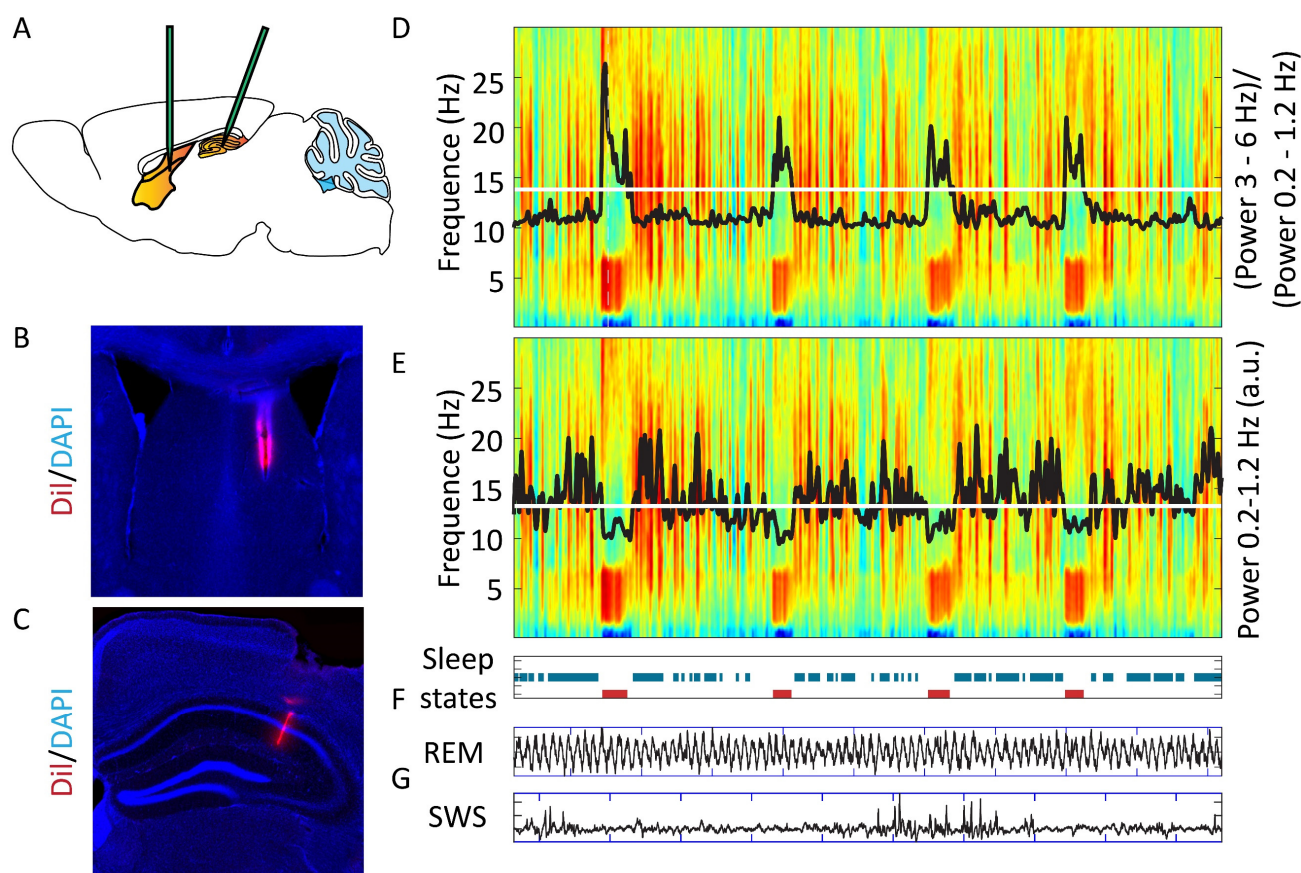


**Figure I. 17. Measurements of local field potentials.** (A) Schematic of local field potential recording (LFP). Histological verification of Dil-coated probes for (B) lateral septum (LS) and (C) hippocampal CA1 with DAPI staining is shown in blue and Dil in red. (D, E) Spectrogram excerpts from a recording show 0 – 30 Hz frequency bursts. Theta frequency (3-6 Hz) power indicates rapid eye movement sleep (REM) epochs. When the ratio (black) of theta (3-6 Hz) power and low frequency (0.2-1.2 Hz) power was greater than 1.4 times (white) than the average, the sleep epochs were defined as rapid eye movement sleep (REM) epochs. (E) Low frequency (0.2-1.2 Hz) power indicates putative slow wave sleep (SWS) epochs. When low frequency (0.2-1.2 Hz) power (black) was greater than 1.4 times (white) than the average, the

sleep epochs were defined as slow wave sleep (SWS) epochs. (F) the sleep states showed REM in red and SWS in blue. (G) Raw trace examples of REM and SWS epochs.

## **6.2. Oscillatory activity of the hippocampal-lateral septal (HPC-LS) circuit in Arc/Arg3.1 KO mice, Arc/Arg3.1 dHPC-cKO mice, and Arc/Arg3.1 LS-cKO mice.**

The current research conducted in this thesis sheds light on the detection of various activities in the pyramidal layer of hippocampal CA1 and lateral septum nucleus (LS) during REM-like sleep states or SWS sleep states in urethane-anesthetized mice. Spectral analysis shows that the power of the theta (3-5.2 Hz) oscillation was reduced in hippocampal CA1 in Arc/Arg3.1 KO mice (Figure I. 18. A), which was consistent with our previous findings (Xiaoyan Gao et al., 2018). Similarly, the power of the theta oscillation was also significantly reduced in LS in Arc/Arg3.1 KO mice (Figure I. 18. B). However, in HPC-cKO mice, the theta power was not significantly increased in either dCA1 (Figure I. 18. C) or LS (Figure I. 18. D). Similarly, LS-cKO mice exhibited unaltered theta power in CA1 (Figure I. 18. E) and LS (Figure I. 18. F) compared to their WT-controls. Our previous study (Xiaoyan Gao et al., 2018), demonstrated that deletion of Arc/Arg3.1 early during ontogenetic development reduces theta power. Whereas a late deletion of Arc/Arg3.1 has no impact on theta. In line with this report, only germline KO of Arc/Arg3.1 displayed reduced theta power. Adult local deletion of Arc/Arg3.1 in the HPC and LS had no significant effect on theta power.

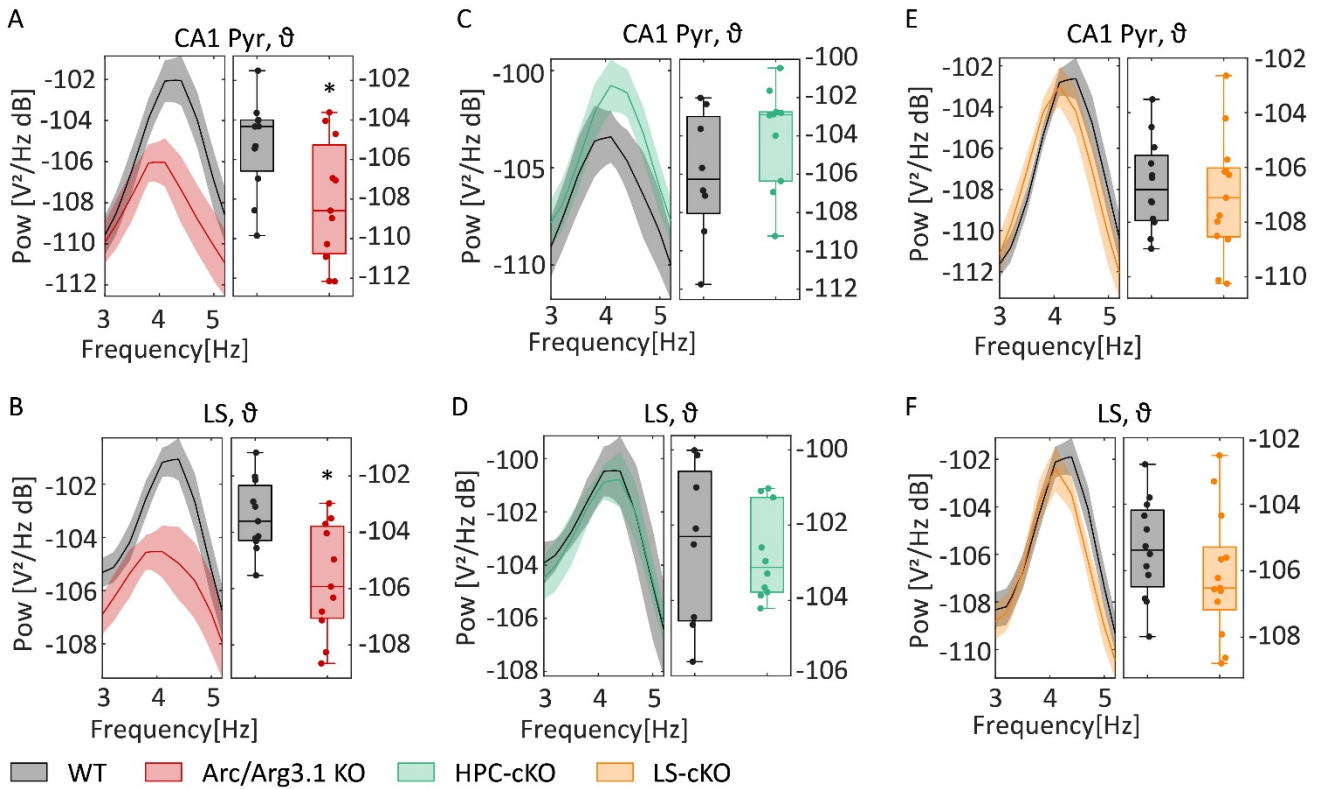


**Figure I. 18. Theta oscillation activity during REM-like sleep states in the hippocampus and lateral septum nucleus of KO, HPC-cKO, and LS-cKO mice.** Power spectra from paradoxical REM sleep for the theta band in Pyr and LS showing mean  $\pm$  S.E.M. and their corresponding box plots showing median (-), whiskers showed min to max, and all data points. Theta power was reduced in both (A) CA1 (WT, -105.27 dB,  $n = 10$ ; KO, -108.13 dB,  $n = 12$ ,  $*p < 0.05$ ) and (B) lateral septum (WT, -103.43 dB,  $n = 11$ ; KO, -105.67 dB,  $n = 11$ ,  $*p < 0.05$ ) in the Arc/Arg3.1 KO mice. In HPC-cKO mice, the theta power in (C) CA1 (WT, -106.04 dB,  $n = 8$ ; KO, -103.99 dB,  $n = 10$ ,  $p = 0.27$ , NS) was non-significantly higher than the WT mice but similar in (D) LS (WT, -102.56 dB,  $n = 8$ ; KO, -102.77 dB,  $n = 10$ ,  $p = 0.76$ , NS). In LS-cKO mice and their WT littermates, the theta power was comparable in both (E) CA1 (WT, -106.65 dB,  $n = 12$ ; KO, -107.04 dB,  $n = 13$ ,  $p = 0.76$ , NS) and (F) LS (WT, -105.35 dB,  $n = 12$ ; KO, -106.12 dB,  $n = 13$ ,  $p = 0.24$ , NS). Significance was assessed with the Mann-Whitney test.

Gamma oscillations are widely considered to be associated with perception and memory (Fell et al., 2001; Fries, Nikolic, & Singer, 2007; C. M. Gray, Konig, Engel, & Singer, 1989; Hirabayashi, Takeuchi, Tamura, & Miyashita, 2013; Montgomery & Buzsaki, 2007). Recent research by Gao et al. has found that gamma (20-50 Hz) is significantly reduced in germline Arc/Arg3.1 KO mice (Xiaoyan Gao et al., 2018). In a similar vein, I conducted analysis of the power of gamma (20-90 Hz) oscillations during REM-like sleep and found that it was significantly decreased in



hippocampal CA1 of Arc/Arg3.1 KO mice (Figure I. 19. A). However, gamma power was similar in the LS of Arc/Arg3.1 KO mice and their WT littermates (Figure I. 19. B). Interestingly, gamma power was unaltered in CA1 of HPC-cKO and LS-cKO mice compared with their respective WT-controls (Figure I. 19. C, E). However, in both groups, gamma power was significantly reduced in the LS (Figure I. 19. D, F). The results indicate that a brain-wide germline Arc/Arg3.1 deletion (KO) impairs gamma activity in CA1 but not in the LS. Interestingly, conditional deletion of Arc/Arg3.1 either in HPC or LS of adult mice, preserves gamma activity in CA1, but reduces gamma power in the LS.

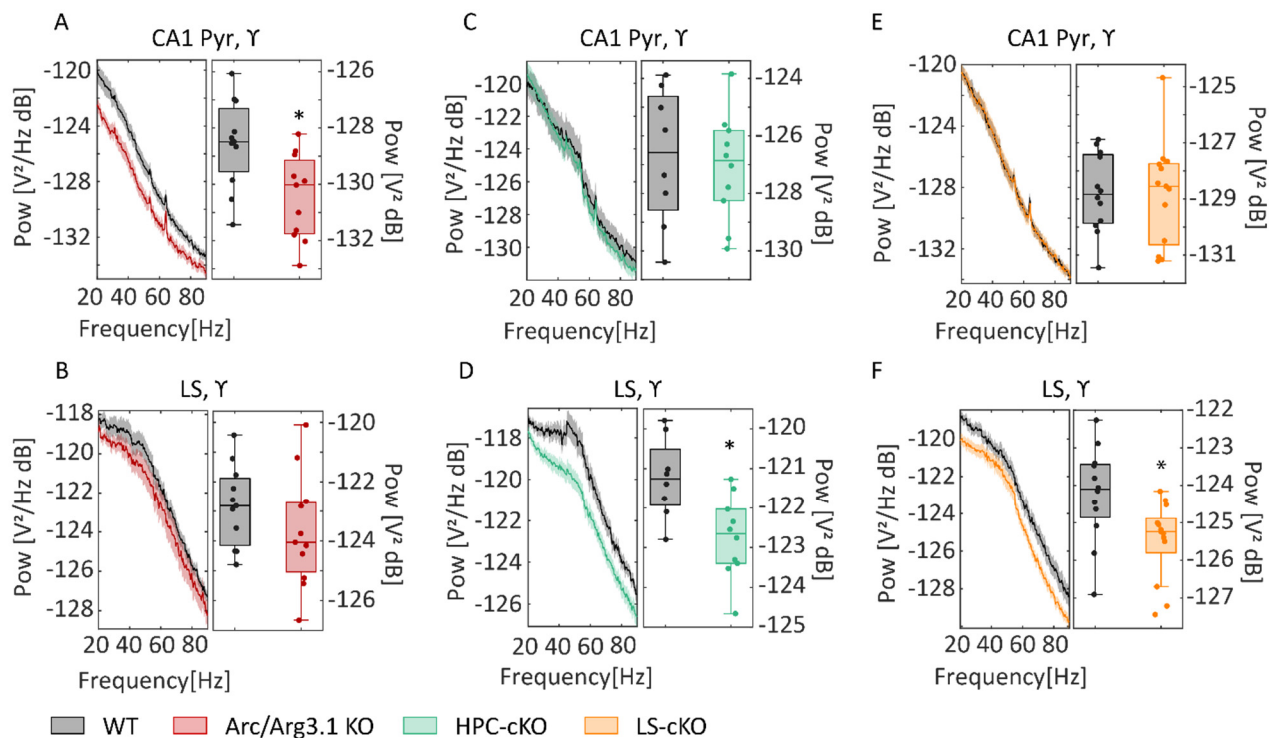


**Figure I. 19. Gamma oscillation activity during REM-like sleep states in the hippocampus and lateral septum nucleus of KO, HPC-cKO, and LS-cKO mice.** Power spectra from paradoxical REM sleep for the gamma band in Pyr and LS showing mean  $\pm$  S.E.M. and their corresponding box plots showing median (-), whiskers showed min to max, and all data points. Gamma power was significantly reduced in (A) CA1 (WT, -128.55 dB, n = 10; KO, -130.45 dB, n = 12, \*p < 0.05), but non-significantly lower in (B) lateral septum (WT, -122.83 dB, n = 11; KO, -123.68 dB, n = 11, p = 0.237, NS) in the Arc/Arg3.1 KO mice. In HPC-cKO mice and their WT littermates, the gamma power was comparable in (C) CA1 (WT, -126.73 dB, n = 8; KO, -127.08 dB, n = 10, p = 0.762, NS) but significantly reduced in (D) LS (WT, -121.25 dB, n = 8; KO, -122.74 dB, n = 10, \*p < 0.05). In LS-cKO mice and their WT littermates, the gamma power was also comparable in (E)

CA1 (WT, -128.79 dB,  $n = 12$ ; KO, -128.79 dB,  $n = 13$ ,  $p = 0.892$ , NS) but significantly reduced in (F) LS (WT, -124.25 dB,  $n = 12$ ; KO, -125.47 dB,  $n = 13$ ,  $*p < 0.05$ ). Significance was assessed with the Mann-Whitney test.

High-frequency (120-180 Hz) oscillations (HFO) are generated through recurrent inhibitory connections, such as are abundant in the LS and might also be affected by Arc/Arg3.1 deletion. Analysis of HFO during REM-like sleep revealed similar power in both CA1 and LS of Arc/Arg3.1 KO mice and their WT-littermates (Figure I. 20. A, B). In the HPC-cKO mice and the LS-cKO mice, HFO power was unchanged in CA1 (Figure I. 20. C, E), but significantly reduced in the LS (Figure I. 20. D, F). Based on these results, it can be inferred that only in the LS, high-frequency oscillations are supported by Arc/Arg3.1 presence locally, or in the HPC.

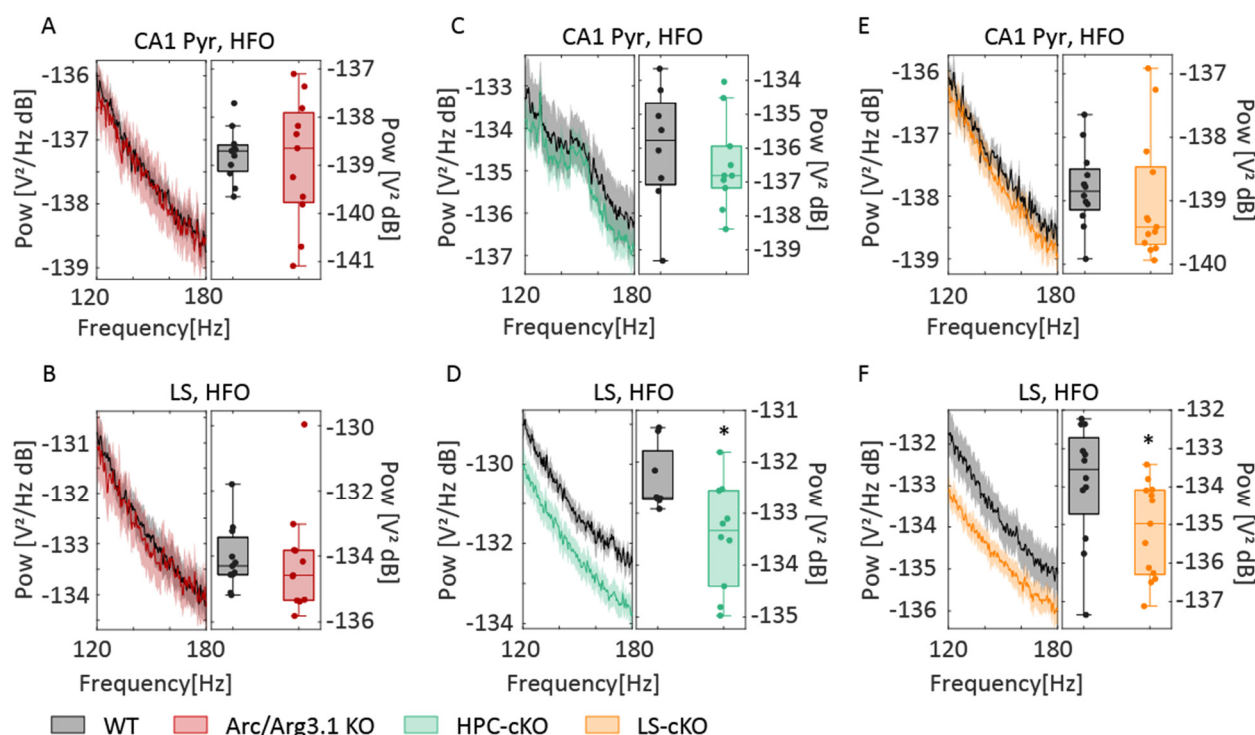


**Figure I. 20. High-frequency oscillation activity during REM-like sleep states in the hippocampus and lateral septum nucleus of KO, HPC-cKO, and LS-cKO mice.** Power spectra from paradoxical REM-like sleep for the high-frequency band in Pyr and LS showing mean  $\pm$  S.E.M. and their corresponding box plots showing median (-), whiskers showed min to max, and all data points. The high-frequency oscillation power was comparable in (A) CA1 (WT, -138.78 dB,  $n = 10$ ; KO, -138.91 dB,  $n = 12$ ,  $p = 0.99$ , NS) and (B) lateral septum (WT, -134.06 dB,  $n = 11$ ; KO, -134.17 dB,  $n = 11$ ,  $p = 0.431$ , NS) in the Arc/Arg3.1 KO mice. In HPC-cKO mice and their WT

littermates, the high-frequency oscillation was comparable in (C) CA1 (WT, -136 dB,  $n = 8$ ; KO, -136.50 dB,  $n = 10$ ,  $p = 0.46$ , NS) but significantly reduced in (D) LS (WT, -132.33 dB,  $n = 8$ ; KO, -133.44 dB,  $n = 10$ ,  $*p < 0.05$ ). In LS-cKO mice and their WT littermates, the high-frequency oscillation power was also comparable in (E) (WT, -138.80 dB,  $n = 12$ ; KO, -139 dB,  $n = 13$ ,  $p = 0.183$ , NS) but significantly reduced in (F) LS (WT, -133.90 dB,  $n = 12$ ; KO, -135.14 dB,  $n = 13$ ,  $*p < 0.05$ ). Significance was assessed with the Mann-Whitney test.

The group of Buzsáki reported that LS high-frequency oscillation events were coupled with dorsal hippocampal sharp wave ripples, during NREM sleep (Tingley & Buzsáki, 2020). I thus performed an analysis of the HFO power during SWS sleep states. I found that HFO power was not significantly decreased in CA1 and LS of Arc/Arg3.1 KO mice (Figure I. 21. A, B). In the HPC-cKO mice, the HFO power was likewise, unchanged in CA1 (Figure I. 21. C) and in the LS (Figure I. 21. D). Only in LS-cKO mice, HFO power was significantly reduced in the LS (Figure I. 21. F) but not in CA1 (Figure I. 21. E).

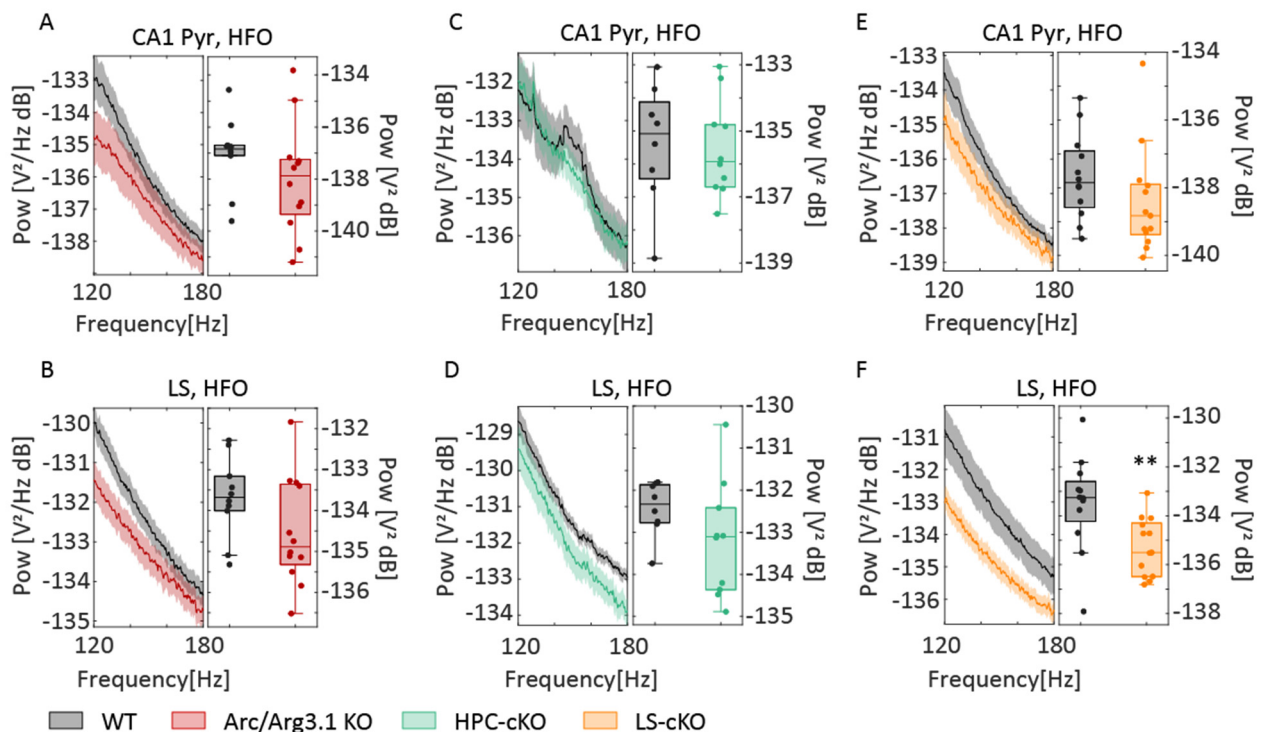


**Figure I. 21. High-frequency oscillations during SWS sleep states in the hippocampus and lateral septum nucleus of KO, HPC-cKO, and LS-cKO mice.** Power spectra from paradoxical SWS sleep for the high-frequency band in Pyr and LS showing mean  $\pm$  S.E.M. and their



corresponding box plots showing median (-), whiskers showed min to max, and all data points. The high-frequency oscillation power was non-significantly lower in (A) CA1 (WT, -137.0259 dB,  $n = 10$ ; KO, -137.99 dB,  $n = 12$ ,  $p = 0.07$ , NS) and (B) LS (WT, -133.69 dB,  $n = 10$ ; KO, -134.52 dB,  $n = 12$ ,  $p = 0.18$ , NS) in the Arc/Arg3.1 KO mice. In HPC-cKO mice and their WT littermates, the high-frequency oscillation was comparable in (C) CA1 (WT, -135.4 dB,  $n = 8$ ; KO, -135.5 dB,  $n = 10$ ,  $p = 0.70$ , NS) and (D) LS (WT, -132.4 dB,  $n = 8$ ; KO, -133.2 dB,  $n = 10$ ,  $p = 0.10$ , NS). In LS-cKO mice and their WT littermates, the high-frequency oscillation power was non-significantly lower in (E) CA1 (WT, -137.7 dB,  $n = 12$ ; KO, -138.4 dB,  $n = 13$ ,  $p = 0.09$ , NS) but significantly reduced in (F) LS (WT, -133.5 dB,  $n = 12$ ; KO, -135.3 dB,  $n = 13$ ,  $^{**}p < 0.01$ ). Significance was assessed with the Mann-Whitney test.

These results indicate that during SWS-like phases, HFO power is only sensitive to local expression of Arc/Arg3.1 in the LS only. Notably, loss of Arc/Arg3.1 in the entire HPC-LS circuit restores HFO power, both in REM and SWS phases. The latter may suggest that HFO deficits arise from an imbalance between hippocampal and LS activity.

**Table I. 1. Summary of oscillation power in dCA1 and LS.**

Sleep states	Oscillations	Arc/Arg3.1 KO		HPC-cKO		LS-cKO	
		CA1	LS	CA1	LS	CA1	LS
REM	Theta (3 – 5.2 Hz)	↓	↓	–	–	–	–
REM	Gamma (20 – 90 Hz)	↓	–	–	↓	–	↓
REM	HFO (120 – 180 Hz)	–	–	–	↓	–	↓
SWS		–	–	–	–	–	↓

↓: power reduction. –: Power did not change.

The results, summarized in Table I. 1, indicated that Arc/Arg3.1 is important for maintaining theta oscillations in the hippocampus and lateral septum and gamma oscillations in the hippocampus during development. These results are congruent with our previously published data (Xiaoyan Gao et al., 2018) and likely reflect a developmental effect on HPC wiring and synaptic transmission. In fully developed brain networks, Arc/Arg3.1 expression in the

hippocampus only impacts gamma and high frequency-gamma oscillations in the LS during REM-like sleep states. This indicates a fundamentally different mechanism of Arc/Arg3.1 action in the development of the glutamatergic network of the HPC versus a constitutive role in the maintenance of the GABAergic network of the LS. Functionally, these findings show that gamma and high-frequency oscillations in the LS are crucial for memory discrimination.

### 6.3. Inter-areal communication between the hippocampus and the lateral septum in Arc/Arg3.1 KO mice, Arc/Arg3.1 dHPC-cKO mice, and Arc/Arg3.1 LS-cKO mice.

The synchronization of oscillatory activity between brain regions, is a crucial aspect of working memory, memory recall, and cognition (Adelhofer & Beste, 2020; Chmielewski, Muckschel, Dippel, & Beste, 2016; Karakas, 2020; Sauseng, Griesmayr, Freunberger, & Klimesch, 2010). I therefore, investigated the influence of Arc/Arg3.1 on theta-, gamma- and HFO-synchronisation between dCA1 and LS. For that, I analyzed the power coherence during REM-like states in the different frequency bands between the hippocampus and lateral septum nucleus of Arc/Arg3.1 KO mice, HPC-cKO mice, LS-cKO mice, and their WT-controls. The results show that the power coherence in the theta band (3-5.2 Hz) was comparable in Arc/Arg3.1 KO mice, HPC-cKO mice, LS-cKO mice, and their WT littermates (Figure I. 22. A-C), indicating that the removal of Arc/Arg3.1 did not have an effect on the communication in the theta band (3-5.2 Hz) between the HPC and the LS in mice.

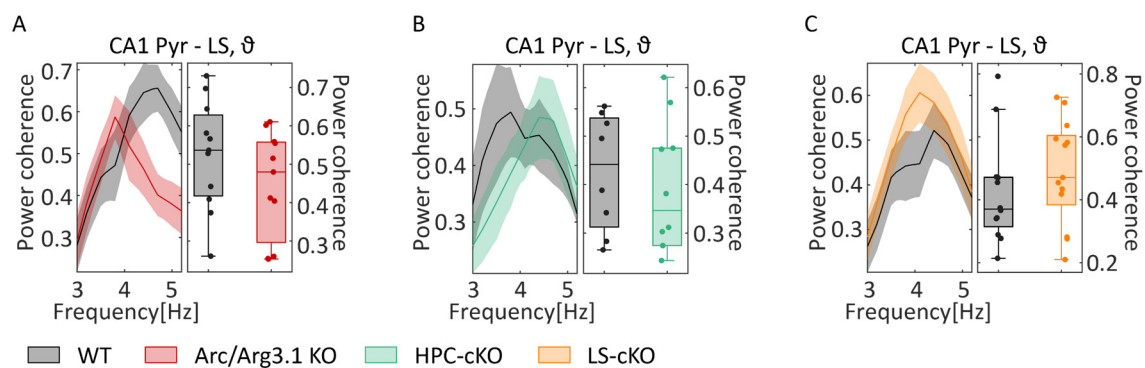


**Figure I. 22. Power coherence of theta band between the hippocampus and lateral septum nucleus of KO, HPC-cKO, and LS-cKO mice.** Power coherence spectra from paradoxical REM

sleep for the theta oscillation (3-5.2 Hz) between Pyr and LS showing mean  $\pm$  S.E.M. and their corresponding box plots showing median (-), whiskers showed min to max, and all data points. The power coherence of theta between CA1 and lateral septum was comparable in (A) the Arc/Arg3.1 KO mice (WT, 0.52, n = 10; KO, 0.45, n = 12, p = 0.21, NS), (B) HPC-cKO mice (WT, 0.43, n = 8; KO, 0.39, n = 10, p = 0.57, NS), (C) LS-cKO mice (WT, 0.42, n = 12; KO, 0.49, n = 13, p = 0.37, NS) and their WT littermates. Significance was assessed with the Mann-Whitney test.

The gamma band in neural oscillations can be divided into two distinct bands: low gamma (20-50 Hz) and high gamma (65-140 Hz) (Belluscio, Mizuseki, Schmidt, Kempter, & Buzsáki, 2012; Laura Lee Colgin et al., 2009). Low gamma oscillations are theorized to be essential for neural communication (Fries, 2009, 2015), while high gamma is traditionally considered as a proxy for ensemble spiking activity (Jia & Kohn, 2011). The strong synchronization in the low gamma range is essential for memory encoding and retrieval (Fell & Axmacher, 2011; Fell et al., 2003; Jutras, Fries, & Buffalo, 2009; J. E. Lisman & Otmakhova, 2001; Montgomery & Buzsaki, 2007; Osipova et al., 2006; Tort et al., 2009b).

Given the different functional activities of the low and high gamma bands in the brain, we separated the gamma band into two sub-bands: 20-45 Hz (low gamma) and 55-90 Hz (high gamma). Analysis of Arc/Arg3.1 KO mice revealed a substantial reduction in the power coherence between dCA1 and LS in the gamma band (20-45 Hz) (Figure I. 23. A) but not in the high-gamma frequencies (55-90 Hz) (Figure I. 23. B). Interestingly, deletion of Arc/Arg3.1 in the dorsal hippocampus did not affect the power coherence in either gamma (20-45 Hz) or high gamma (55-90 Hz) bands (Figure I. 23. C, D). Surprisingly, deletion of Arc/Arg3.1 in LS had only a small effect on the power coherence of gamma (20-45 Hz) (Figure I. 23. E). However, it strongly decreased the of high gamma oscillations (Figure I. 23. F). These findings demonstrate an important role of Arc/Arg3.1 in the communication between the hippocampus and lateral septum in gamma oscillations in mice.

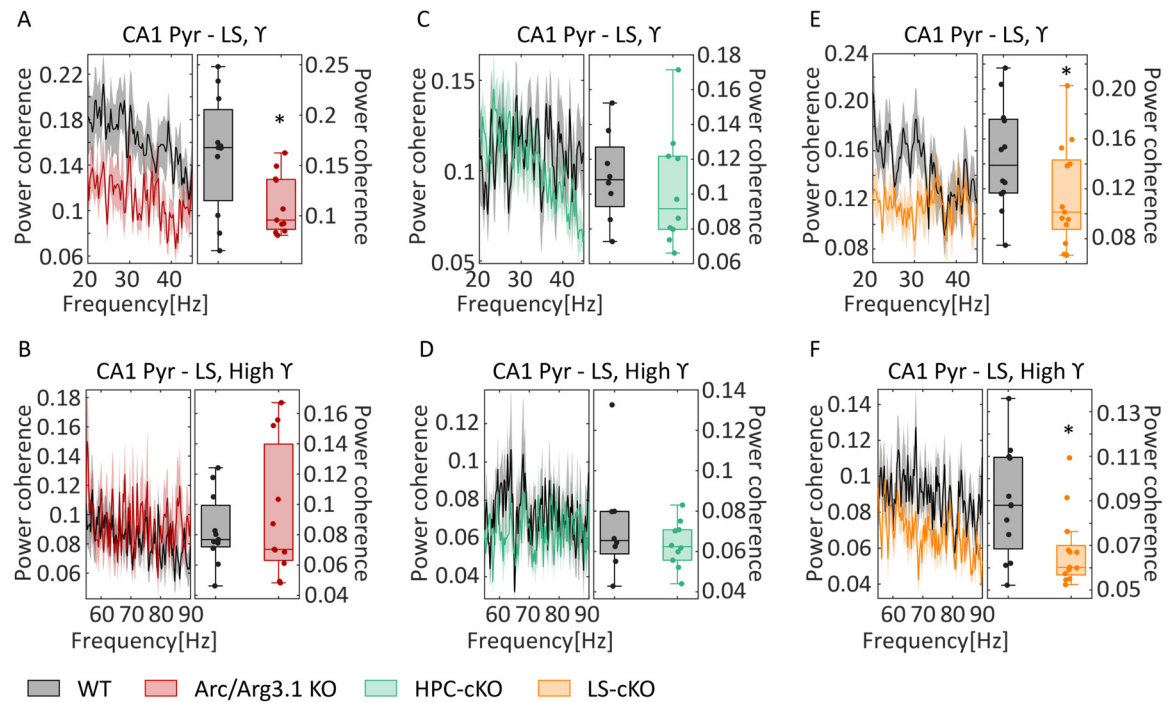


**Figure I. 23. Power coherence of gamma band between the hippocampus and lateral septum nucleus of KO, HPC-cKO, and LS-cKO mice.** Power coherence spectra from paradoxical REM sleep for the gamma (20-45 Hz) and high gamma (55-90 Hz) oscillation between Pyr and LS showing mean  $\pm$  S.E.M. and their corresponding box plots showing median (-), whiskers showed min to max, and all data points. The power coherence of (A) gamma oscillation (WT, 0.16,  $n = 10$ ; KO, 0.11,  $n = 12$ ,  $*p < 0.05$ ) between hippocampal CA1 and lateral septum was significantly reduced in the Arc/Arg3.1 KO mice compared to their WT littermates but not for (B) high gamma oscillation (WT, 0.083,  $n = 10$ ; KO, 0.094,  $n = 12$ ,  $p = 0.90$ , NS). The power coherence of neither (C) gamma (WT, 0.11,  $n = 8$ ; KO, 0.10,  $n = 10$ ,  $p = 0.57$ , NS) nor (D) high gamma (WT, 0.073,  $n = 8$ ; KO, 0.064,  $n = 10$ ,  $p = 0.57$ , NS) oscillation was affected between hippocampal CA1 and LS in HPC-cKO mice. The LS-cKO mice and their WT littermates indicated a non-significant decrease in the power coherence of the gamma band (WT, 0.145,  $n = 12$ ; KO, 0.115,  $n = 13$ ,  $*p < 0.05$ ) but a substantial reduction in the high gamma band (WT, 0.089,  $n = 12$ ; KO, 0.068,  $n = 13$ ,  $*p < 0.05$ ). Significance was assessed with the Mann-Whitney test.

During the REM-like sleep states, the power coherence of high-frequency oscillations (120-180 Hz) was observed non-significantly higher in the KO mice (Figure I. 24. A) but lower in LS-cKO mice (Figure I. 24. C). As anticipated, the ablation of Arc/Arg3.1 in the hippocampus did not affect the power coherence of HFO (Figure I. 24. B).

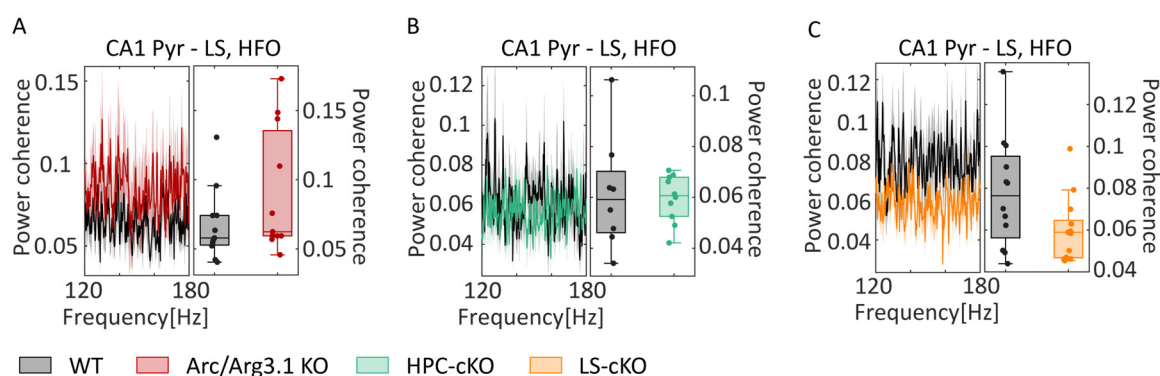


**Figure I. 24. Power coherence of high-frequency oscillation between the hippocampus and lateral septum nucleus of KO, HPC-cKO, and LS-cKO mice.** Power coherence spectra from paradoxical REM sleep for the high-frequency oscillation (120-180 Hz) between Pyr and LS showing mean  $\pm$  S.E.M. and their corresponding box plots showing median (-), whiskers showed min to max, and all data points. Arc/Arg3.1 KO mice showed non-significantly higher power coherence in (A) HFO (WT, 0.07,  $n = 10$ ; KO, 0.09,  $n = 12$ ,  $p = 0.15$ , NS). In HPC-cKO mice and their WT littermates, the power coherence of (B) HFO (WT, 0.06,  $n = 8$ ; KO, 0.06,  $n = 10$ ,  $p = 0.83$ , NS) between CA1 and lateral septum was similar. In LS-cKO mice and their WT littermates, the power coherence of (C) HFO (WT, 0.078,  $n = 12$ ; KO, 0.06,  $n = 13$ ,  $p = 0.054$ , NS) was non-significantly lower between CA1 and lateral septum. Significance was assessed with the Mann-Whitney test.

On the other hand, during the SWS sleep states, the power coherence of high-frequency oscillations (120-180 Hz) was significantly increased in the KO mice (Figure I. 25. A) but non-significantly higher in HPC-cKO mice (Figure I. 25. B) and LS-cKO mice (Figure I. 25. C).

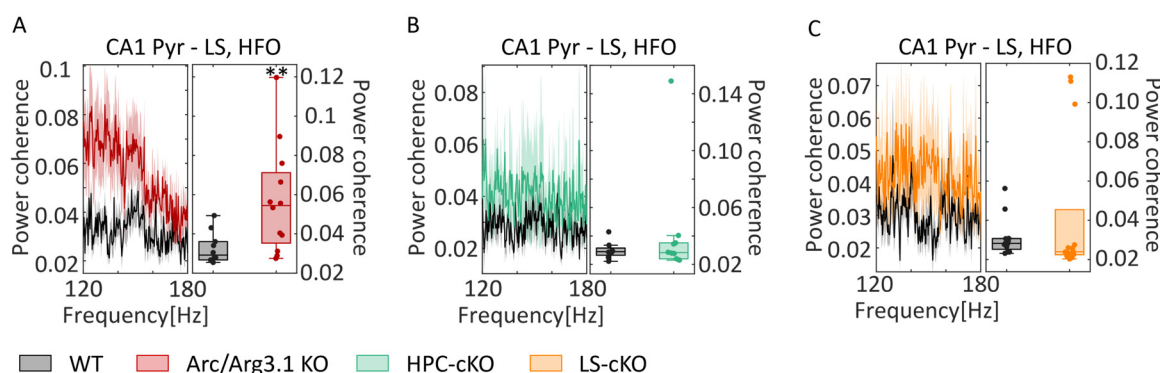


**Figure I. 25. Power coherence of high-frequency oscillation during SWS sleep states between the hippocampus and lateral septum nucleus of KO, HPC-cKO, and LS-cKO mice.** Power

coherence spectra from paradoxical SWS sleep for the high-frequency oscillation (120-180 Hz) between Pyr and LS showing mean  $\pm$  S.E.M. and their corresponding box plots showing median (-), whiskers showed min to max, and all data points. Arc/Arg3.1 KO mice showed significantly higher power coherence in (A) HFO (WT, 0.03,  $n = 10$ ; KO, 0.06,  $n = 12$ ,  $**p < 0.01$ ). In HPC-cKO mice and their WT littermates, the power coherence of (B) HFO (WT, 0.03,  $n = 8$ ; KO, 0.04,  $n = 10$ ,  $p = 0.97$ , NS) between CA1 and lateral septum was similar. In LS-cKO mice and their WT littermates, the power coherence of (C) HFO (WT, 0.031,  $n = 12$ ; KO, 0.043,  $n = 13$ ,  $p = 0.15$ , NS) was non-significantly lower between CA1 and lateral septum. Significance was assessed with the Mann-Whitney test.

Power coherence was summarized in a table (Table I. 2), germline Arc/Arg3.1 ablation decreased gamma power coherence during REM-like sleep states and increased HFO power coherence during SWS-like sleep states between dCA1 and LS. Acute ablation Arc/Arg3.1 in HPC did not change power coherence in any oscillations between dCA1 and LS. However, acute ablation of Arc/Arg3.1 in LS decreased high gamma power coherence during REM-like sleep states between dCA1 and LS. The results suggested that the deficits of high gamma power coherence may contribute to the increased memory generalization.

**Table I. 2. Summary of the effects of Arc/Arg3.1 deletion on the dCA1-LS power coherence .**

Sleep states	Power coherence	Arc/Arg3.1 KO	HPC-cKO	LS-cKO
	dCA1 - LS			
REM	Theta (3 – 5.2 Hz)	–	–	–
REM	Gamma (20 – 45 Hz)	↓	–	↓
REM	High gamma (55 – 90 Hz)	–	–	↓
REM	HFO (120 – 180 Hz)	–	–	$p = 0.054$
SWS		↑	–	–

↓: power coherence decreased. ↑: power coherence increased. –: Power coherence did not change.

To assess the phase synchronizations between dCA1 and LS, I performed phase locking value analysis (Lachaux, Rodriguez, Martinerie, & Varela, 1999). The results were summarized in a table (Table I. 3). The data suggested that knocking out Arc/Arg3.1 from the germline increased the phase synchronization in HFO (120-180 Hz) during SWS sleep states (Figure I. 26. C) but did not affect REM-like sleep states. The acute ablation of Arc/Arg3.1 in adult mice did not affect phase synchronizations in mice. However, when I acute ablated Arc/Arg3.1 in LS in adult mice, the phase locking value decreased in gamma oscillations (20-90 Hz) between dCA1 and LS (Figure I. 26. A, B).

**Table I. 3. . Summary of the effects of Arc/Arg3.1 deletion on the phase locking of dCA1 and LS oscillations.**

Sleep states	Power coherence	Arc/Arg3.1 KO	HPC-cKO	LS-cKO
	dCA1 - LS			
REM	Theta (3 – 5.2 Hz)	–	–	–
REM	Gamma (20 – 45 Hz)	–	–	p = 0.077
REM	High gamma (55 – 90 Hz)	–	–	↓
REM	HFO (120 – 180 Hz)	–	–	–
SWS		↑	–	–

↓: Phase locking value decreased. ↑: Phase locking value increased. –: Phase locking value did not change.



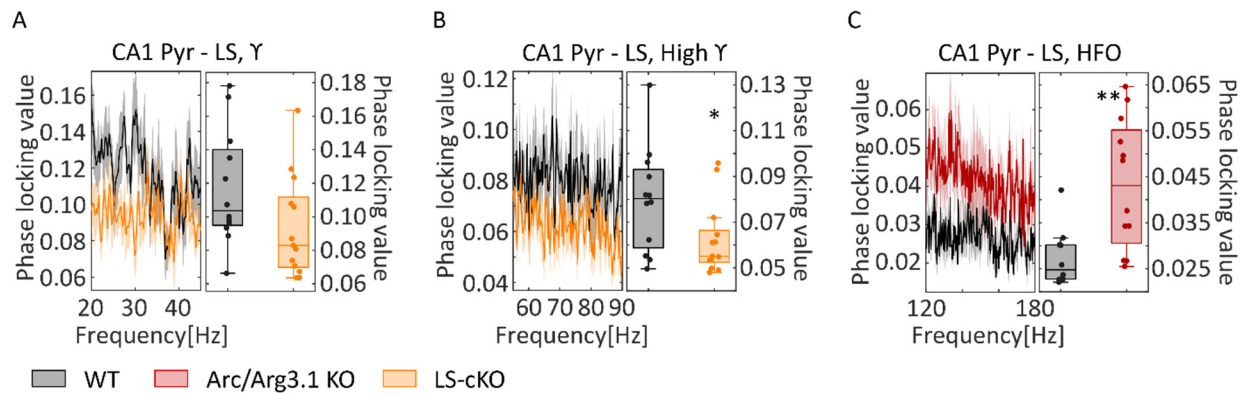


**Figure I. 26. Phase locking values between the hippocampus and lateral septum of KO, LS-cKO mice.** (A) Phase locking value from paradoxical REM sleep for the gamma oscillation (20-45 Hz) between dCA1 and LS in LS-cKO mice showed non-significant reduction (WT, 0.117,  $n = 12$ ; LS-cKO, 0.094,  $n = 13$ ,  $p = 0.077$ , NS). (B) Phase locking value from paradoxical REM sleep for the high gamma oscillation (55-90 Hz) between dCA1 and LS in LS-cKO mice showed significant reduction (WT, 0.080,  $n = 12$ ; LS-cKO, 0.062,  $n = 13$ ,  $*p < 0.05$ ). (C) Phase locking value from paradoxical SWS sleep for the high-frequency oscillation (120-180 Hz) between dCA1 and LS was significantly increased in Arc/Arg3.1 KO mice (WT, 0.027,  $n = 10$ ; KO, 0.043,  $n = 12$ ,  $**p < 0.01$ ). Spectrum showing mean  $\pm$  S.E.M. and their corresponding box plots showing median (-), whiskers showed min to max, and all data points. Significance was assessed with the Mann-Whitney test.

Granger causality is a useful tool to gain insight into the directionality of functional connectivity in brain networks (L. Gao et al., 2015; Hu, Dai, Worrell, Dai, & Liang, 2011; Stokes & Purdon, 2017). According to the analysis, I found that Arc/Arg3.1 KO and HPC-cKO did not show any effect in granger causalities between dCA1 and LS in theta (3-5.2 Hz), gamma (20-90 Hz) and high-frequency (120-180 Hz) oscillations in mice (Table I. 4). However, acute ablation of Arc/Arg3.1 in LS decreased the granger causalities from dCA1 to LS (Figure I. 27. A) in gamma oscillations (20-45 Hz). In the granger causalities of HFO (120-180 Hz), the LS-cKO mice showed decreased tendency in dCA1-LS pathway (Figure I. 27. B). Analysis of Granger causality from the LS to dCA1 did not show any significant modulations (data not shown), suggesting that in all cases the HPC predicts and possibly guides LS responses.



**Table I. 4. Summary of the effects of Arc/Arg3.1 deletion on the directional connectivity measured by granger causality between dCA1 and LS.**

Sleep states	Granger causality	Arc/Arg3.1 KO	HPC-cKO	LS-cKO
		dCA1 → LS	dCA1 → LS	dCA1 → LS
REM	Theta (3 – 5.2 Hz)	—	—	—
REM	Gamma (20 – 45 Hz)	—	—	↓
REM	High gamma (55 – 90 Hz)	—	—	—
REM	HFO (120 – 180 Hz)	—	—	p = 0.06
SWS		—	—	—

↓: Granger causality decreased. —: Granger causality did not change.

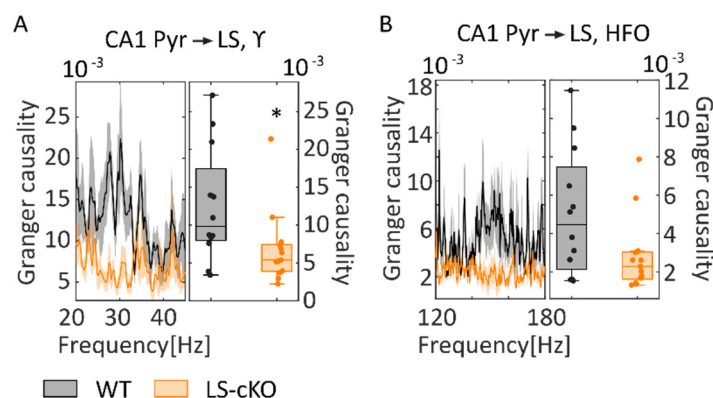


**Figure I. 27. Granger causalities between the hippocampus and lateral septum nucleus of LS-cKO mice.** Granger causality from paradoxical REM sleep for the gamma oscillation (20-45 Hz) and the high-frequency oscillation (120-180 Hz) between dCA1 and LS showing mean ± S.E.M. and their corresponding box plots showing median (-), whiskers showed min to max, and all data points. (A) LS-cKO mice showed significant reduction in the gamma oscillation (20-45 Hz) from dCA1 to LS (WT, 0.013, n = 12; LS-cKO, 0.007, n = 13, \*p < 0.05). (B) In the high-frequency oscillation (120-180 Hz), the granger causality showed non-significantly decreased from dCA1 to LS (WT, 0.005, n = 12; LS-cKO, 0.003, n = 13, p = 0.06, NS). Significance was assessed with the Mann-Whitney test.

In total, Arc/Arg3.1 is essential for maintaining the synchronization activities between dCA1 and LS in HFO (120-180 Hz) during SWS states and power coherence in gamma oscillations (20-45 Hz) during REM-like states. Interestingly, acute ablation of Arc/Arg3.1 in dCA1 in adult mice did not affect the communication between dCA1 and LS. However, acute ablation of Arc/Arg3.1 in LS in adult mice showed strong deficit of communication between dCA1 and LS in gamma and high-frequency oscillations during REM-like sleep states. The results illustrated that Arc/Arg3.1 in LS plays an important role in transmitting information in the dCA1-LS pathway, which suggested a potential neurophysiological phenotype in memory generalization in mice.

#### **6.4. Unit spikes in the hippocampus (HPC) and lateral septal (LS) of Arc/Arg3.1 KO mice, Arc/Arg3.1 dHPC-cKO mice, and Arc/Arg3.1 LS-cKO mice.**

The direct connection from the HPC to LS implies that changes in neural firing in the HPC may immediately translate to modified neural and synaptic activity in the LS. To evaluate the neural firing in both regions, we detected spikes in all recorded channels and assigned them to single units, reflecting individual neurons. Based on waveform parameters of the spikes and their autocorrelograms (Methods Figure 12), we classified hippocampal units into two types: putative excitatory and putative inhibitory neurons, following the definitions by (Sirota et al., 2008). In the LS we identified 2 clusters according to previous reports (Howe & Blair, 2021; H. G. Yamin, E. A. Stern, & D. Cohen, 2013): medium spiny neurons and fast-spiking neurons, notably, both categories are presumably inhibitory neurons which constitute the majority in the LS. Unclassified units in the LS were excluded from analysis. In the. The firing rate was calculated in REM-like and SWS-like sleep states. In CA1, mean unit firing rates of excitatory and inhibitory neurons were similar between Arc/Arg3.1 KO and WT littermates, both during REM- and SWS-like states (Figure I. 28. A, B). In contrast, excitatory neurons of HPC-cKO mice displayed significantly reduced mean firing rates, compared to their WT-control, during REM- and SWS-like states, whereas inhibitory neurons remained unchanged (Figure I. 28. C, D). Interestingly, LS-cKO mice exhibited an opposite modulation: mean firing rates of CA1 excitatory and inhibitory neurons were significantly increased during REM-like states but not in SWS-like states (Figure I. 28. E, F).

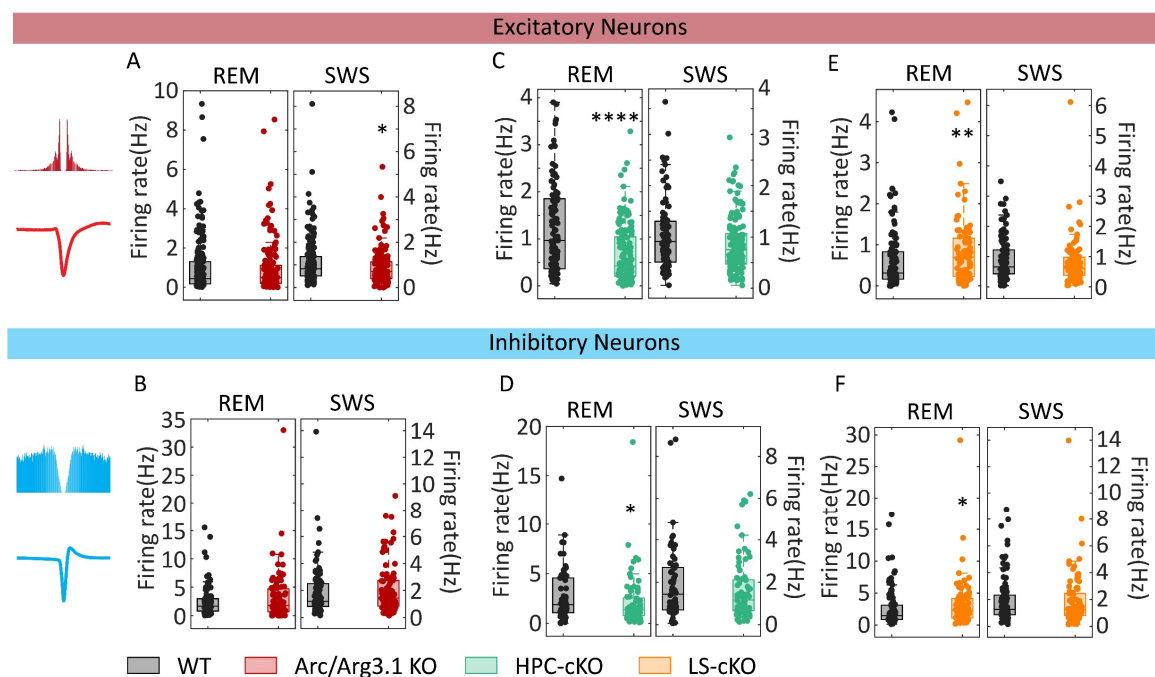


**Figure I. 28. Mean firing rates in the hippocampus of KO, HPC-cKO, and LS-cKO mice.** The autocorrelograms and waveforms of the excitatory (Red) and inhibitory (Blue) neurons are shown on the left. (A) The mean firing rate of excitatory neurons in the hippocampus was similar during REM-like states (Left: WT, 0.986 Hz,  $n = 204$ ; KO, 0.970 Hz,  $n = 155$ ;  $p = 0.923$ , NS) but decreased in Arc/Arg3.1 KO mice during SWS-like states (Right: WT, 1.089 Hz,  $n = 204$ ; KO, 0.892 Hz,  $n = 155$ ;  $*p < 0.05$ ) (B) Similar mean firing rates of inhibitory neurons during REM-like (Left: WT, 2.469 Hz,  $n = 95$ ; KO, 3.13 Hz,  $n = 96$ ;  $p = 0.698$ , NS) and SWS-like states (Right: WT, 1.883 Hz,  $n = 95$ ; KO, 2.081 Hz,  $n = 96$ ;  $p = 0.458$ , NS). (C) In HPC-cKO mice, the mean firing rates of excitatory CA1 neurons were significantly reduced during REM-like (Left: WT, 1.221 Hz,  $n = 101$ ; HPC-cKO, 0.661 Hz,  $n = 156$ ;  $****p < 0.0001$ ) but were unchanged during SWS-like states (Right: WT, 1.011 Hz,  $n = 101$ ; HPC-cKO, 0.857 Hz,  $n = 156$ ;  $p = 0.083$ , NS). (D) Firing rates of inhibitory neurons in the HPC of HPC-cKO mice also showed significant reduction during REM-like (Left: WT, 2.862 Hz,  $n = 64$ ; HPC-cKO, 2.119 Hz,  $n = 73$ ;  $*p < 0.01$ ) but not during SWS-like states (Right: WT, 1.905 Hz,  $n = 64$ ; HPC-cKO, 1.624 Hz,  $n = 73$ ;  $p = 0.27$ , NS). (E) In LS-cKO mice, the mean firing rate of excitatory neurons was significantly increased during REM-like states (Left: WT, 0.639 Hz,  $n = 106$ ; LS-cKO, 0.844 Hz,  $n = 89$ ;  $**p < 0.01$ ) but not during SWS (Right: WT, 0.906 Hz,  $n = 106$ ; LS-cKO, 0.804 Hz,  $n = 89$ ;  $p = 0.182$ , NS). (F) Hippocampal inhibitory neurons in LS-cKO mice, displayed significantly reduced firing rates in during REM-like states (Left: WT, 2.551 Hz,  $n = 104$ ; LS-cKO, 3.172 Hz,  $n = 83$ ;  $*p < 0.05$ ) but not during SWS (Right: WT, 1.883 Hz,  $n = 104$ ; LS-cKO, 1.893 Hz,  $n = 83$ ;  $p = 0.943$ , NS). Significance was assessed with the Mann-Whitney test. The box plots showed the median (-), whiskers showed min to max, and all data points.

In summary, deletion of Arc/Arg3.1 in the HPC reduced excitatory and inhibitory firings of CA1 neurons, whereas deletion in the LS increased them. Absence of Arc/Arg3.1 in both HPC and LS had no significant impact on firing rates in CA1. Modulations of hippocampal firing rates were strictly limited to REM-like states.

Next, I evaluated neuronal firing rates in the LS and found that neither medium-spiny nor fast-spiking neurons were affected in Arc/Arg3.1 KO mice (Figure I. 29. A, B). In the HPC-cKO mice and the LS-cKO mice, firing rates of medium spiny neurons remained unaffected (Figure I. 29. C, E). In contrast, deletion of Arc/Arg3.1 in the HPC decreased the firing rates of fast-spiking neurons (Figure I. 29. D), while deletion in the LS increased their firing rate (Figure I. 29. F).

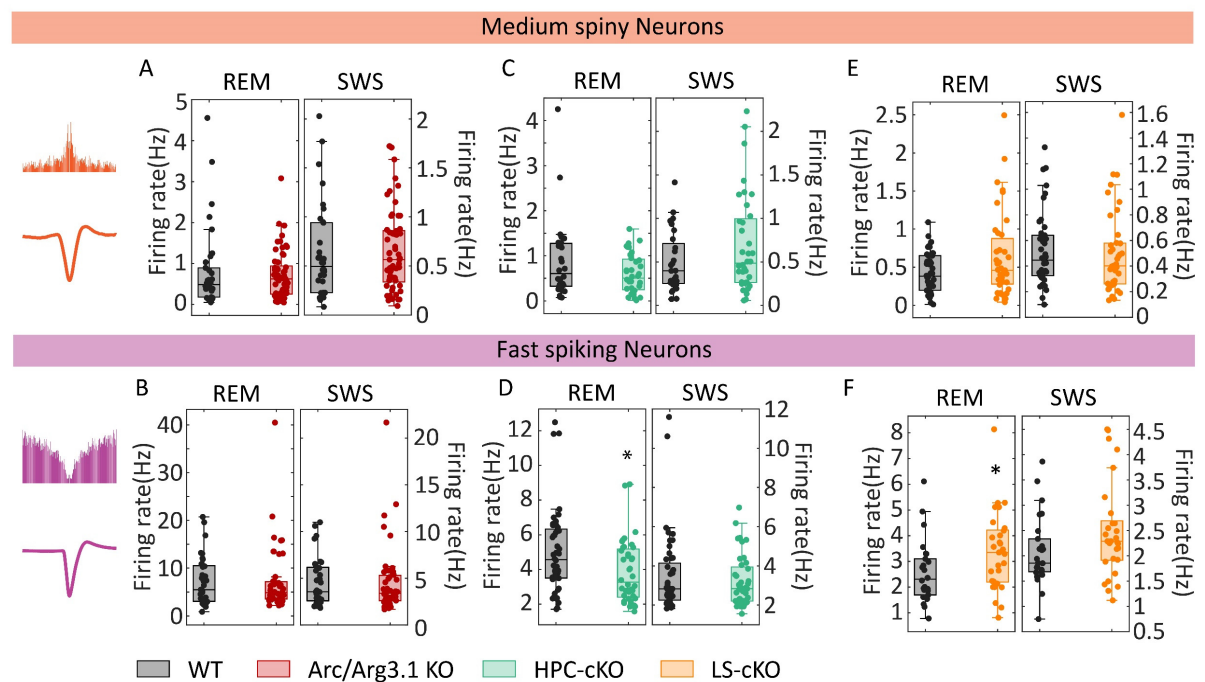


**Figure I. 29. Mean firing rates in the LS of KO, HPC-cKO, and LS-cKO mice.** The autocorrelograms and waveforms of medium-spiny (Orange) and fast-spiking (Purple) neurons are shown on the left. (A) The firing rate of medium spiny neurons in the lateral septum nucleus was comparable during REM-like sleep states (Left: WT, 0.829 Hz,  $n = 34$ ; KO, 0.721 Hz,  $n = 57$ ;  $p = 0.626$ , NS) but similarly during SWS sleep states (Right: WT, 0.630 Hz,  $n = 34$ ; KO, 0.646 Hz,  $n = 57$ ;  $p = 0.631$ , NS) in KO mice and their WT littermates. (B) The KO mice suggested a regular firing rate of fast-spiking neurons in REM-like (Left: WT, 7.344 Hz,  $n = 33$ ; KO, 7.358 Hz,  $n = 43$ ;  $p = 0.834$ , NS) and SWS sleep states (Right: WT, 4.580 Hz,  $n = 33$ ; KO, 4.639 Hz,  $n = 43$ ;  $p$

= 0.675, NS). The ablation of Arc/Arg3.1 in HPC did not change the firing rate of medium spiny neurons in REM-like (Left: WT, 0.890 Hz, n = 28; HPC-cKO, 0.602 Hz, n = 36; p = 0.253, NS) and SWS sleep states (Right: WT, 0.497 Hz, n = 28; HPC-cKO, 0.692 Hz, n = 36; p = 0.313, NS). The fast-spiking neurons in the LS of HPC-cKO mice indicated significant firing rate reduction during REM-like sleep states (Left: WT, 5.004 Hz, n = 48; HPC-cKO, 3.850 Hz, n = 40; \*p < 0.05) but a non-significantly lower firing rate in SWS sleep states (Right: WT, 3.478 Hz, n = 48; HPC-cKO, 3.219 Hz, n = 40; p = 0.937, NS). (C) In the LS-cKO mice, the firing rate of medium spiny neurons was apparently during REM-like (Left: WT, 0.435 Hz, n = 42; LS-cKO, 0.638 Hz, n = 39; p = 0.232, NS) and SWS sleep states (Right: WT, 0.527 Hz, n = 42; LS-cKO, 0.503 Hz, n = 39; p = 0.487, NS) in the LS. The ablation of Arc/Arg3.1 in LS resulted in an increased firing rate in the fast-spiking neurons in LS in REM-like sleep states (Left: WT, 2.557 Hz, n = 26; LS-cKO, 3.378 Hz, n = 29; \*p < 0.05) but non-significantly increased in the SWS sleep states (Right: WT, 2.073 Hz, n = 26; LS-cKO, 2.482 Hz, n = 29; p = 0.067, NS). Significance was assessed with the Mann-Whitney test. The box plots showed the median (-), whiskers showed min to max, and all data points.

In summary, conditional deletion of Arc/Arg3.1 modulated the firing rates of fast-spiking neurons in the LS. Whereas HPC-deletion decreased firing, rates LS-deletion increased them. Also in the LS, firing rates modulations were restricted to REM-like states.

**Table I. 5. Summary of units firing rates in dCA1 and dLS.**

Brain regions	Neuron classification	Arc/Arg3.1 KO		HPC-cKO		LS-cKO	
		REM	SWS	REM	SWS	REM	SWS
<b>dCA1</b>	Excitatory neurons	—	↓	↓	—	↑	—
	Inhibitory neurons	—	—	↓	—	↑	—
<b>dLS</b>	medium spiny neurons	—	—	—	—	—	—
	Fast-spiking neurons	—	—	↓	—	↑	—

↓: Firing rate decreased. ↑: Firing rate increased. —: Firing rate did not change.

Firing rate modulations were summarized in a table (Table I. 5), depicting only the direction of change. It becomes evident that loss of Arc/Arg3.1 in the HPC decreases CA1 and LS firing rates, while Arc/Arg3.1 loss in the LS increases them. These opposite modulations explain why a simultaneous loss of Arc/Arg3.1 in HPC and LS results in a null effect.



## **Discussion**





## **1. Modifying neural activity in the dCA1-dLS circuits may affect the discrimination of fear memories through the regulation of Arc/Arg3.1.**

In this chapter of the thesis, I focused on the role of the dCA1-LS pathway in the processing and storage of fear memory. I first demonstrated a strong upregulation of Arc/Arg3.1 in the DG and LS following fear memory conditioning and retrieval, thereby confirming previous reports on Arc/Arg3.1 expression in the HPC and expanding these with novel data on the LS (Xiaoyan Gao et al., 2018; Gómez, 2016; Lv et al., 2011; Maddox & Schafe, 2011; Onoue et al., 2014; L. Zhu et al., 2018). I used viral vectors to trace the LS-projection from the HPC to pyramidal neurons in dCA1. By specifically targeting an inhibitory opsin to LS-projecting dCA1 neurons, I found that optical suppression of their neural activity preserved behavioral responses to the conditioning context but abnormally increased the mice freezing responses to novel contexts, thereby diminishing context discrimination and memory specificity. Optical suppression of dCA1-LS neuron firings also inhibited IEG expression in the HPC and disrupted the reactivation of Arc/Arg3.1 engrams in the LS. Similarly, I discovered that removing Arc/Arg3.1 in the HPC (Gao, 2016) or LS of adult mice resulted in the loss of fear memory discrimination (Figure I. 1). In fear conditioning tests, the expression of Arc/Arg3.1 increased in DG and LS after exposure to shock in a novel environment or following fear memory retrieval. The upregulation of Arc/Arg3.1 in fear memory processes further revealed the close relationships between Arc/Arg3.1 and memory engrams (Xiaoyan Gao et al., 2018; Gómez, 2016; Lv et al., 2011; Maddox & Schafe, 2011; Onoue et al., 2014; L. Zhu et al., 2018). Suppressing dCA1-LS circuits during memory discrimination tests resulted in decreased memory precision and blunted Arc/Arg3.1 expression, suggesting that native activity patterns in the HPC optimally induce Arc/Arg3.1, whereas a general suppression of dCA1 firing prevents it. Moreover, it may suggest that the deficit in memory specificity was, in fact, caused by the failure to induce Arc/Arg3.1 in the dCA1-LS circuit and a consequential disruption of the consolidation process.

My strategy of suppressing the dCA1-LS circuits leans on injections of a retrovirus in the LS encoding for the inhibitory opsin stGtACR under the CaMKII $\alpha$ -promotor. Hence, the opsin is expressed in all projecting neurons in dCA1, including excitatory and some CaMKII $\alpha$ -positive interneurons (Sengün, 2021; Veres, Andrasi, Nagy-Pal, & Hajos, 2023). A similar promoter was used for the viral expression of Cre-recombinase to achieve hippocampus-specific deletion of

Arc/Arg3.1. However, since only 1-3% of inhibitory neurons express Arc/Arg3.1, even after seizures, in dCA1 (Sengün, 2021; Vazdarjanova et al., 2006), it is reasonable to assume that both manipulations exerted their effects on memory primarily through pyramidal neurons in dCA1. Albeit long-range CaMKII $\alpha$ -expressing GABAergic neurons might still contribute. Interestingly, similar tendencies of the results were observed in optogenetic groups and Arc/Arg3.1 conditional KO groups. HPC-cKO (Xiaoyan Gao, 2016) and only affected remote memory discrimination. LS-cKO and optical suppression of dCA1-dLS during altered context test increased memory generalization in recent memory tests.

My findings differ from those of Opalka and Wang (2020), who reported that inhibiting the dCA1-dLS circuits disrupted the consolidation of the context memory. A possible reason for this discrepancy might lie in the differences in optical suppression strategy: Opalka and Wang targeted the inhibitory opsin eNpHR3.0 to the axon terminals of hippocampal neurons and delivered light stimuli directly into the LS. The stimulation parameters used in this study were incongruent with those reported by Mahn et al. (Mahn, Prigge, Ron, Levy, & Yizhar, 2016), likely resulting in variable degrees of suppression. Other research has suggested that when the hippocampus or dCA1 are pharmacologically inactivated before the memory test, the ability to distinguish between contexts is impaired, while the retrieval of the context itself remains unaffected (de, Gaiardo, & Cerutti, 2023; Wiltgen et al., 2010). The conflicting results suggest that inhibiting the terminals of dCA1-dLS projecting neurons may be different from inhibiting the soma, and this difference could impact memory consolidation processes. For example, terminal inhibition may inhibit both spontaneous release and action potential-evoked release, whereas somatic inhibition may inhibit only the latter. Besnard et al. (2020) performed similar experiments on hippocampal CA3-CA1 and CA3-dLS circuits with the same inhibitory opsin eNpHR3.0 and demonstrated that optical suppression of dCA3-dCA1 decreased discrimination but inactivating dCA3-dLS enhanced it (Besnard et al., 2020). Taken together, the different projections in the HPC-LS circuits may govern contextual fear memory consolidation differently with different suppression strategies.

## **2. Arc/Arg3.1 in HPC-LS circuits regulates freezing to tone fear memory during retrieval.**

Here, I show that suppressing dCA1-dLS circuits or ablating Arc/Arg3.1 in the LS enhanced freezing responses during tone fear memory recall. One simple explanation could be that the tone memory was not dependent on the dCA1-LS circuit, but because it was performed in the novel context, freezing to the tone simply added up to the abnormally high responses to the novel context. Another possibility is that the dCA1-LS circuit can directly modulate responses to the tone. In line with this suggestion, Holschneider et al. reported that the LS and ventral HPC were metabolically active during tone fear memory recall (Holschneider et al., 2006), and Calandreau et al. further reported that boosting glutamatergic HPC-LS neurotransmission promoted, while antagonizing it impeded, tone fear memory recall (Calandreau, Desgranges, Jaffard, & Desmedt, 2010). The similar behavioral effects I observed with optical suppression of dCA1-LS and by Arc/Arg3.1 ablation in the LS raise the possibility that the increased freezing percentage during tone fear memory recall by the net activity in the LS was also altered by these manipulations. Optical suppression of dCA1 firing could reduce glutamate release from their axonal boutons in the LS, causing hypoactivation of target neurons. However, given that the local circuitry in the LS is made of inhibitory connections, in theory, the ultimate result of dCA1-LS suppression might still be disinhibition and an increased firing rate of some LS neurons. Immunostaining against cFos, which reflects global activity, revealed lower signals in CA1 but unchanged expression in the LS, whether some neurons increased their firing rates while others decreased cannot be determined from the cFos staining. Answering this question will require single-cell electrophysiological recordings. In contrast, Arc/Arg3.1 expression, which is sensitive to high-frequency patterned activity, was reduced in both regions. This analysis indicates that the level and pattern of neural activity might be modulated by optical suppression of dCA1-LS.

Instead of the effect in the downstream regions of LS, we may have evoked abnormal activities in other dCA1 projecting brain regions through optical suppression of dCA1 neurons. A recent study reported that single CA1 pyramidal neurons send projections into both contra- and ipsilateral target brain regions such as DG, CA fields, cortical regions, lateral septal complex (LSX), medial septal complex (MSX), NAc, diagonal band nucleus, anterior olfactory nucleus (AON), anterior group of the dorsal thalamus (ATN), basal amygdala (BA), hypothalamic lateral zone (LZ), periventricular region (PVR), and mammillary body (MBO) (Qiu et al., 2024), which suggested we altered the activities in other brain circuits as well when we suppressed dCA1 cell

bodies. The possibilities of altered activities in the amygdala (Hintiryan et al., 2021) or hypothalamus (Viellard et al., 2024) increased the freezing responses during tone fear memory retrieval. Yi et al. reported inhibiting dCA1-MEC circuits impaired auditory-related fear discrimination (Yi et al., 2022). LS was reported as a nexus between the hippocampus, amygdala, VTA, hypothalamus, entorhinal cortex, and medial septum, which are important for different aspects of stress, locomotor movement, and discrimination (Wirtshafter & Wilson, 2021). Furthermore, the amygdala, as an essential brain region for fear learning and emotional responses (Izquierdo et al., 2016), was reported to be innervated by LS afferents (Hintiryan et al., 2021). Data from our lab demonstrated that the deletion of Arc/Arg3.1 in the amygdala abolished tone fear memory in mice (Xiaoyan Gao, 2016). The connections between the lateral septum (LS) and the amygdala could be the route by which the optical suppression of dCA1-dLS circuits or loss of Arc/Arg3.1 in the LS, may increase or modulate neural activity in the amygdala, leading to an enhanced tone fear memory response. The enhanced implicit memory increased stress and anxiety emotions, then increased freezing responses.

Our research on Optical suppression and Arc/Arg3.1 ablation in LS or HPC has revealed a disturbance in brain network activity, which could potentially contribute to a discrimination deficit and enhance the freezing percentage during tone fear memory retrieval. These implications are significant and warrant further investigation.

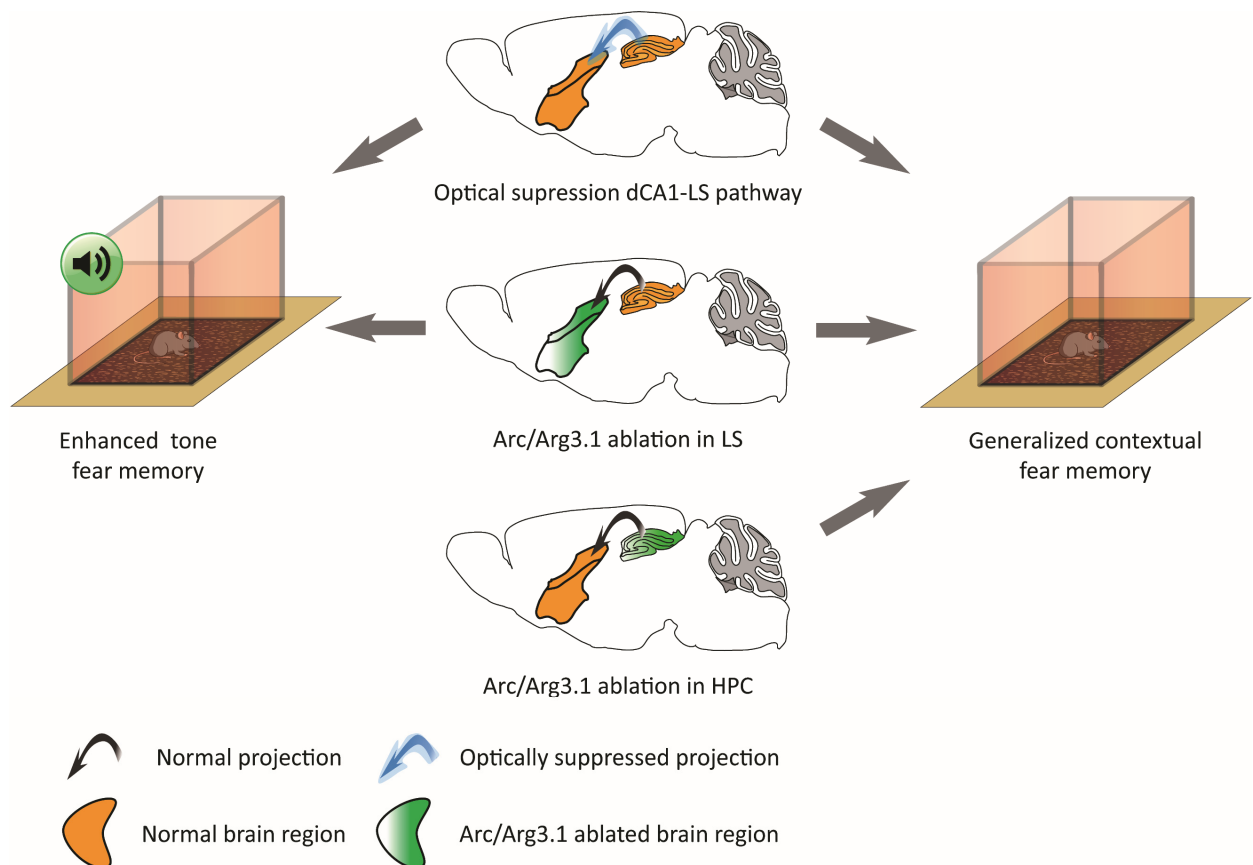


**Figure I. 1. The dCA1-LS pathway and Arc/Arg3.1 in HPC or LS modulate fear memory discrimination and tone fear memory in mice.** In contextual fear memory tests, optical suppression of the dCA1-LS pathway or acute suppression during memory discrimination tests can lead to fear memory generalization in mice. Arc/Arg3.1 deletion in the hippocampus (Xiaoyan Gao, 2016) or LS impaired fear memory generalization in mice. In the tone fear memory tests, optical suppression of the dCA1-LS pathway and ablation of Arc/Arg3.1 in LS both enhanced tone fear memory response in mice.

### 3. Arc/Arg3.1 influences oscillatory and neuronal activity in the dCA1-dLS circuits.

Arc/Arg3.1, an important protein for synaptic plasticity in hippocampal CA1 (Plath et al., 2006), was reported to alter oscillatory activities in the hippocampus (Xiaoyan Gao et al., 2018) and in the prefrontal cortex (X. Gao et al., 2019). My LFP recording in dCA1 showed similar power reductions in theta and gamma oscillations in dCA1 in Arc/Arg3.1 KO mice, in line with these reports but also revealed reduced theta in the LS. The lack of any theta reductions in HPC-cKO

and LS-cKO adult mice suggests that all effects of Arc/Arg3.1 deletions on theta oscillations are restricted to the early postnatal development period (Xiaoyan Gao et al., 2018).

The lateral septum, a GABAergic populated nucleus (Kuku, 2020), was reported to have strong oscillation coupling with sharp wave ripples in HPC (Tingley & Buzsáki, 2020). During SWS sleep states, high-frequency oscillations (HFO, also called sharp wave ripples) between dCA1 and LS increased amplitude and phase synchronization in Arc/Arg3.1 germline KO mice. The theta, gamma, and high-frequency oscillations in the hippocampus are believed to play a prime role in recognition (Neves et al., 2022), learning and memory consolidation (Xiaoyan Gao et al., 2018; Jutras et al., 2009; Malkov et al., 2022; Montgomery & Buzsaki, 2007; Nyhus & Curran, 2010; Wynn et al., 2023). Our previous studies (Xiaoyan Gao et al., 2018; Plath et al., 2006) indicated that the altered theta and gamma oscillatory activities in HPC are highly related to deficits in spatial learning (Xiaoyan Gao et al., 2018; Plath et al., 2006). My current study highlights the strong correlation between altered LFP oscillatory, neuronal activity and memory specificity.

Coordinated oscillatory activity between the hippocampus (HPC) and cortical regions is crucial for the process of learning (Khodagholy, Gelinas, & Buzsaki, 2017) and discrimination (Ruikes et al., 2024; C. Wang et al., 2021). The coordination of the theta rhythm between the hippocampus and the lateral septum is responsible for driving spatial cognition (Tingley & Buzsáki, 2018). However, we only observed altered theta oscillations in Arc/Arg3.1 germline KO mice, which is the result of developmental deficit during the early postnatal period (Xiaoyan Gao et al., 2018). In adult mice, the acute ablation of Arc/Arg3.1 in dCA1 or LS resulted in a strong reduction in gamma and high-frequency oscillation power, but only in LS and not in dCA1. Deleting Arc/Arg3.1 in adult mice impaired the coordination (including the power coherence, phase locking value and Granger causality) in gamma bands during REM-like sleep states between dCA1 and LS in LS-cKO mice but not in HPC-cKO mice. From my current data, the LFP and animal behavior test results indicated that regular gamma and HFO activities in the dCA1-LS circuits maintain the precision of contextual memory coding and retrieval in mice. It is noteworthy that the power of gamma and HFO bands plays a significant role in the consolidation of precise memories in the long term. However, the communication of gamma bands is related to maintaining precise memories.

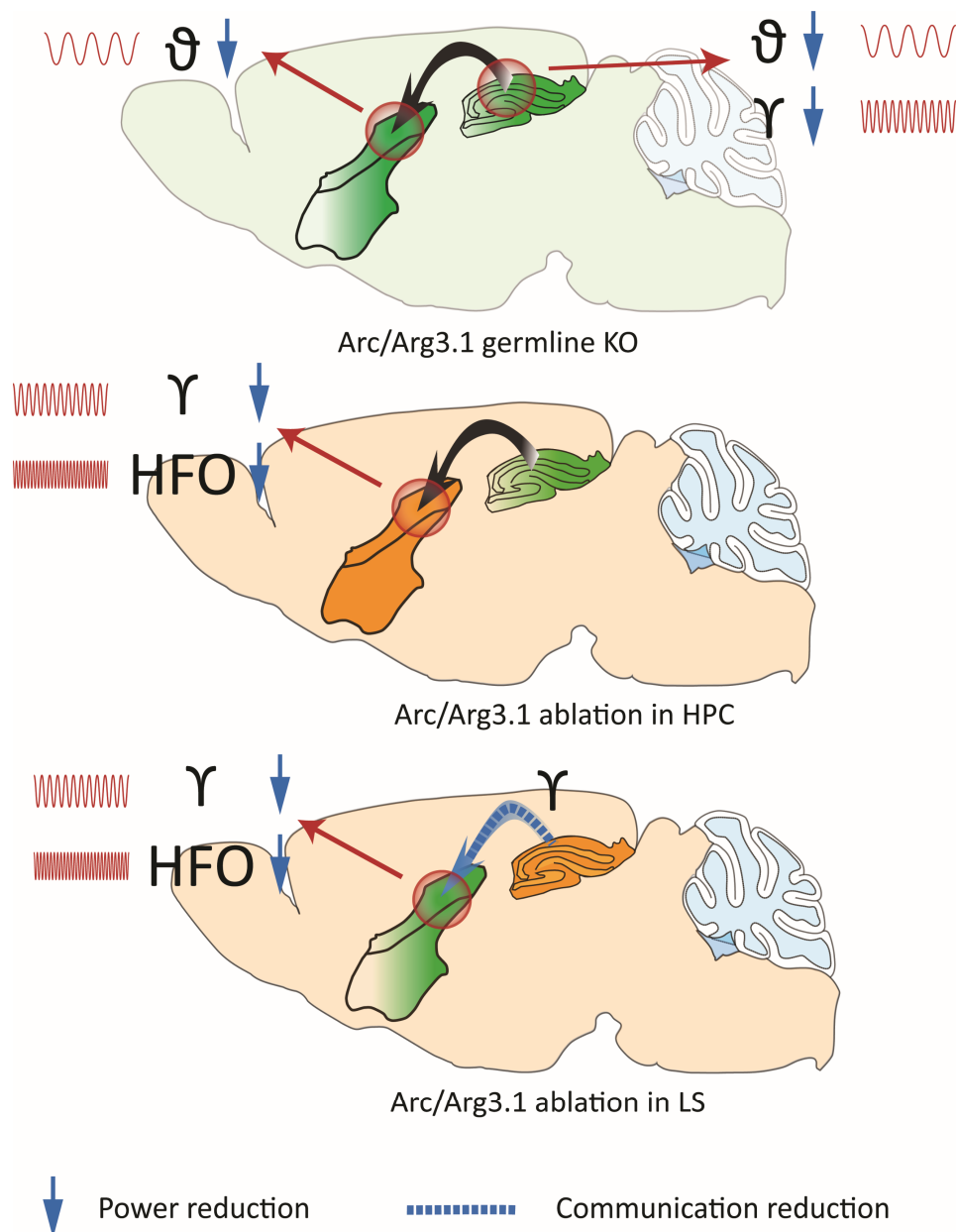


**Figure I. 2. The oscillatory activities and communication in the dCA1-LS pathway during REM-like sleep states.** When observing Arc/Arg3.1 germline KO mice during REM-like sleep states, it was found that there was a reduction in power in the theta and gamma bands in dCA1 but only a reduction in the theta bands in LS. On the other hand, when we specifically removed Arc/Arg3.1 in HPC or LS in adult mice, the reduction in oscillatory power was only observed in the gamma and HFO bands during REM-like sleep states and not in theta bands. Only when we removed Arc/Arg3.1 in LS did the communication in gamma bands between dCA1 and LS decrease.



The analysis of firing rates for different types of neurons showed a clear impact on neuronal activity in dCA1 and LS. The results indicated that the germline knockout of Arc/Arg3.1 did not affect the firing rate of any types of neurons in dCA1 or LS. However, when we specifically removed Arc/Arg3.1 in the HPC of adult mice, the firing rates of excitatory and inhibitory neurons in dCA1 showed a significant decrease during REM-like sleep states, as well as the fast-spiking neurons in LS. Interestingly, when we specifically removed Arc/arg3.1 in LS of adult mice, the firing rates of excitatory and inhibitory neurons in dCA1 and the fast-spiking neurons in LS significantly increased during REM-like sleep states. Based on the data, it is worth noting that the firing rate of excitatory and inhibitory neurons in dCA1, as well as fast-spiking neurons in LS, changed in the same direction (Figure I. 3). It was demonstrated that different types of inhibitory neurons within dCA1 modulate local circuits in CA1 (Chamberland & Topolnik, 2012; Cutsuridis & Taxidis, 2013). In my current findings, the principal neurons in dCA1 mainly drive the fast-spiking neurons in LS during REM-like sleep states and change their firing rates. Previous studies showed that interneurons in the LS project into the medial septum (MS), and then neurons in the MS directly send input into dCA1 (Tsanov, 2018). This illustrates the synaptic connection of the HPC-LS-MS-HPC circuits. Ablation of Arc/Arg3.1 in dCA1 reduced firing rates of excitatory and inhibitory neurons in dCA1 during REM-like sleep states, then decreased the activities of target fast-spiking neurons in LS. When the Arc/Arg3.1 was removed from LS, it caused an increase in the activity of fast-spiking neurons. This increase then caused a decrease in the activity of neurons in MS. As a result, the inhibition in dCA1 decreased, which led to an increase in the spike activities of both pyramidal and inhibitory neurons in dCA1. In total, removing Arc/Arg3.1 in adult HPC or LS altered neuron firing rates in opposite directions, causing abnormal activity and leading to memory precision deficits in dCA1-LS circuits.

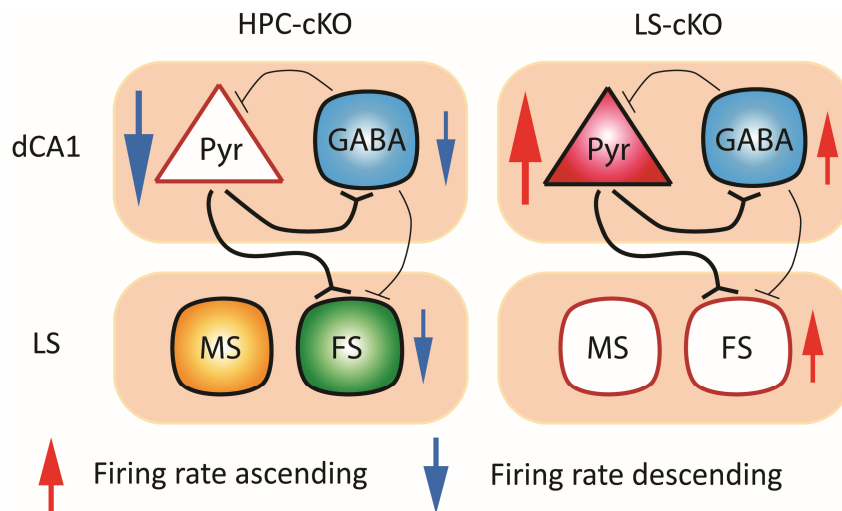


**Figure I. 3. The firing rate for different neurons in the dCA1-dLS pathway during REM-like sleep states in conditional *Arc/Arg3.1* ablated mice.** In adult conditional knockout mice, we observed a decreased firing rate of excitatory and inhibitory neurons in dCA1 and fast-spiking neurons in LS when *Arc/Arg3.1* was specifically ablated in HPC pyramidal neurons. However, in LS-specific ablation mice, we observed an increased firing rate of excitatory and inhibitory neurons in dCA1 and fast-spiking neurons in LS when *Arc/Arg3.1* was specifically ablated in LS.

In the first part of my thesis, I manipulated the dCA1-dLS circuits through optogenetic methods and the Cre-LoxP system in mice during fear memory processes. According to the data, *Arc/Arg3.1* is responsible for regulating the activities of dCA1-dLS circuits, which in turn affects memory discrimination. The local field potential recording revealed the oscillatory and neuronal activities in dCA1-dLS circuits. Although the ablation of *Arc/Arg3.1* in HPC or LS did not affect the oscillatory activities in theta bands, the balanced theta-gamma coupling was reported to play an essential role in decision-making (Amemiya & Redish, 2018), learning (Tort, Komorowski, Manns, Kopell, & Eichenbaum, 2009a), long-term memory retrieval (Vivekananda et al., 2021), and fear and safety engage (Stujenske, Likhtik, Topiwala, & Gordon, 2014). In humans and rodents, the theta-gamma coupling between the hippocampus and cortical regions was important for working memory (Borderie et al., 2024; Tamura et al., 2017). Therefore, further analysis is needed to determine whether *Arc/Arg3.1* ablation in HPC or LS affects the theta-gamma coupling or the balance between other oscillations in HPC, LS or between them. According to our data, the gamma power was reduced in LS through the ablation of *Arc/Arg3.1* in the HPC or LS but drove the firing rate of excitatory, inhibitory, and

fast-spiking neurons in opposite directions. Since there are more than two different types of GABAergic neurons in the LS (Howe & Blair, 2021; Hagar G. Yamin, Edward A. Stern, & Dana Cohen, 2013), which were difficult to separate through the parameters we utilized (Schmitzer-Torbert & Redish, 2008). Therefore, the altered firing rate in our analysis cannot completely reflect the changes in oscillatory activities. Some literature also reported that somatostatin interneurons in LS modulate the gamma oscillations during food-seeking (Carus-Cadavieco et al., 2017) and theta oscillations in dHPC (Chee et al., 2015; Espinosa et al., 2022). Further research is required to identify the types of neurons that modulate memory discrimination in dCA1-LS circuits. Another lack of analysis in our data was the phase modulation of neurons. Several studies illustrated that pyramidal neurons in HPC are selectively spiked in theta or gamma rhythms during recognition processes (Daume et al., 2024; Fujisawa & Buzsaki, 2011; Ku et al., 2024). Therefore, whether the spiking preferences for different types of neurons changed in theta or gamma rhythms still needs further analysis.

## **Part II**

### **Role of Arc/Arg3.1 expressing GABAergic interneurons in anxiety- and depressive-like behaviors in mice**



## **Introduction**



Stress and stress-related disorders can lead to severe psychiatric problems in humans, such as major depressive disorder (MDD) and anxiety disorders. Major depressive disorder (MDD) has become a worldwide problem (Institute of Health Metrics and Evaluation 2023), causing poor concentration (Bains & Abdijadid, 2024; Eid et al., 2019), hopelessness (Cannon et al., 1999), tiredness (Eid et al., 2019), suicidal tendencies (Harris & Barraclough, 1997; Kessler et al., 2005), sleep disorder (R. F. Chen et al., 2022; S. Chen et al., 2023), and unbearable pain (Ferro, 2016; Mee et al., 2011) in patients. Both neuroimaging and postmortem have revealed that subcortical brain structures were altered in patients suffering from MDD (Belleau, Treadway, & Pizzagalli, 2019; Krishnan & Nestler, 2008; Murrough et al., 2016), the volume of the dentate gyrus was reduced (MacQueen et al., 2008), and nerve growth factor levels were decreased (Wohleb, Franklin, Iwata, & Duman, 2016). Both human and animal studies showed that GABA transmission and GABA receptors are significantly reduced in MDD (Banasr et al., 2017; Duman, Sanacora, & Krystal, 2019; Jacobson, Vlachou, Slattery, Li, & Cryan, 2018; B. Luscher, Shen, & Sahir, 2011; Yin et al., 2016). Elevating GABA levels in MDD patients has been developed as a treatment for depression, using methods such as Brexanolone (SAGE-547) or transcranial stimulation (Heimrath et al., 2020; Kanes et al., 2017). According to previous studies, different interneurons in cortical regions were divided into three largely non-overlapping classes (S. Lee, Hjerling-Leffler, Zagha, Fishell, & Rudy, 2010; Rudy, Fishell, Lee, & Hjerling-Leffler, 2011): parvalbumin (PV) and somatostatin (SST) positive interneurons and serotonin receptor 3a (5HT3aR) positive interneurons. Literature reported that inhibition of GABAergic interneurons, probably somatostatin (SST) and parvalbumin (PV), in the medial prefrontal cortex (mPFC) could lead to potential antidepressant benefits (Fogaca et al., 2021). Additionally, deficits in the function of SST-positive or PV-positive interneurons in mice have been linked with behaviors resembling depression (S. Chen et al., 2022; X. Y. Yang, Ma, Storm, Cao, & Zhang, 2021). Disinhibition of SST-positive interneurons results in an anxiolytic and antidepressant-like brain state (Fuchs et al., 2017). However, the activities of PV-positive interneurons mediate depressive-like or stress-related behavioral responses (Ji et al., 2020; Perova, Delevich, & Li, 2015). Therefore, SST-positive and PV-positive interneurons may play different roles in the pathology of MDD.

Recent studies have confirmed that MDD patients have reduced volumes of the prefrontal cortex, orbitofrontal cortex, and cingulate cortex (Arnone et al., 2012) but increased amygdala



volume (Saleh et al., 2012). Interestingly, stress induces reductions in dendritic spine density and synapse number in the hippocampus (Hajszan et al., 2009; Sandi et al., 2003; Tata et al., 2006; Vestergaard-Poulsen et al., 2011) and frontal cortex (Hains et al., 2009; Radley et al., 2013) of animal models. The activity-regulated cytoskeletal gene *Arg3.1*, also known as *Arc*, plays an essential role in synaptic plasticity (Eriksen & Bramham, 2022; Lyford et al., 1995; Plath et al., 2006; H. Zhang & Bramham, 2021), stress, and depression (Leem & Chang, 2017; Y. Li et al., 2015; Mikkelsen & Larsen, 2006; Pei, Zetterstrom, Sprakes, Tordera, & Sharp, 2003). Studies have shown that acute stress leads to increased expression of the *Arc/Arg3.1* gene or protein in the frontal cortex (Drouet et al., 2015; Mikkelsen & Larsen, 2006; Molteni et al., 2010), including the prelimbic, infralimbic, and anterior cingulate prefrontal cortex (Ons et al., 2004; Ons et al., 2010; Trneckova et al., 2007). Animals under repeat chronic stress exposures are observed up-regulated *Arc/Arg3.1* expression in the amygdala (Monsey et al., 2014; Ons et al., 2010; Trneckova et al., 2007) and lateral septum (Ons et al., 2004; Ons et al., 2010), while down-regulated in hippocampal CA1 (Elizalde et al., 2010; Leem & Chang, 2017; Ons et al., 2010) and frontal cortex (Ons et al., 2010). In addition, it has been observed that the chronic administration of monoamine-centered antidepressants can lead to an increase in the expression of *Arc/Arg3.1* in several regions of the brain in mice, such as the hippocampus, frontal and parietal cortex, striatum, and cingulate gyrus (Y. Li et al., 2015). Specific treatments that have rapid-acting antidepressant effects, such as ketamine administration and electroconvulsive therapy, have been observed to acutely increase *Arc/Arg3.1* expression (de Bartolomeis et al., 2013; Dyrvig et al., 2012; Larsen et al., 2005).

Therefore, *Arc/Arg3.1* is a potential molecular target for studying Major Depressive Disorder (MDD) and stress-associated disorders. However, very little research has been done to investigate how *Arc/Arg3.1* in GABAergic interneurons affects stress-associated disorders. To better understand this question, I bred SOM-Cre and PV-Cre transgenic mice with *Arc/Arg3.1*<sup>f/f</sup> transgenic mice. This was done with the specific aim of targeting the removal of *Arc/Arg3.1* in SOM and PV interneurons. Following this, the mice were subjected to anxiety- and depressive-like behavioral tests.

## Aims of the study for Part II

Arc/Arg3.1 can be evoked by a novelty environment and a stress stimulus in GABAergic neurons such as those in the lateral septum (LS) and hippocampus. Arc/Arg3.1 germline KO mice and Arc/Arg3.1 conditional knockout in CamKII $\alpha$  positive neurons also showed altered stress-related behaviors in mice. However, the role of Arc/Arg3.1 in GABAergic neurons mediating stress-related behavior is still unknown. Therefore, the aim of this part study is to understand whether Arc/Arg3.1 in GABAergic neurons modulates anxiety- and depressive-like behaviors in mice.

### Specific goals:

- To investigate the expression of Arc/Arg3.1 in different brain regions in PV-positive and SST-positive neurons.
- To study the role of Arc/Arg3.1 in PV-positive and SST-positive neurons in anxiety-like behavior tests such as open field and elevated plus maze tests in PV-cKO and SST-cKO mice.
- To understand the role of Arc/Arg3.1 in PV-positive and SST-positive neurons in depressive-like behavior tests such as forced swimming and tail suspension tests in PV-cKO and SST-cKO mice.



## Results



## 1. Arc/Arg3.1 KO mice showed altered depressive-like behaviors.

In a previous study conducted in our laboratory, it was shown that Arc/Arg3.1 knock-out mice did not exhibit overt anxiety-like behaviors in the open field test or the elevated plus maze test (Xiaoyan Gao, 2016). Instead, mice in which Arc/Arg3.1 was removed during early postnatal development (Xiaoyan Gao, 2016; Gómez, 2016), showed anxiolytic-like behavior. Other studies reported either up- or down-regulation of Arc/Arg3.1 in the hippocampal CA1 by exposure to chronic stress (Boulle et al., 2014; Elizalde et al., 2010; Leem & Chang, 2017; Muzio et al., 2016). Stress applied chronically or transiently can induce depressive-like behavior characterized, among others, by the adoption of reduced exploratory drive and anhedonia (Pizzagalli, 2014). The expression of the Arc/Arg3.1 gene was always related to stress stimulation in the frontal cortex (Drouet et al., 2015; Mikkelsen & Larsen, 2006; Molteni et al., 2010), amygdala (Monsey et al., 2014; Ons et al., 2010; Trneckova et al., 2007), and lateral septum (Ons et al., 2004; Ons et al., 2010), and the hippocampal CA1 region (Elizalde et al., 2010; Leem & Chang, 2017; Ons et al., 2010). The knockout of Arc/Arg3.1 reduced LFP activity in the prefrontal cortex and hippocampus of mice (X. Gao et al., 2019), suggesting Arc/Arg3.1 plays a crucial role in various brain regions that are related to stress or stress-related disorders.

The forced swimming test and the tail suspension test are commonly used to screen for antidepressant activity and stress-related disorders in rodents (Commons, Cholanians, Babb, & Ehlinger, 2017; Pollak, Rey, & Monje, 2010). In the forced swimming test (Figure II. 1. A), mice were placed in the water container for 6 min. The mice were judged to be immobile when they remained floating in the water, making minimal movements to keep their heads above water. In the tail suspension test (Figure II. 1. C), mice were hung by attaching their tail to a hook using adhesive medical tape in the white box for 6 min. In both tests, immobility duration is measured and serves as a readout of depressive-like behavior. Arc/Arg3.1 KO mice showed significantly longer immobility in the FST (Figure II. 1. B) and fewer movements in the TS (Figure II. 1. D). This suggests that the Arc/Arg3.1 KO mice had less motor activity in acute inescapable conditions, indicating loss of Arc/Arg3.1 may be altered depression or other stress-related behaviors in mice.

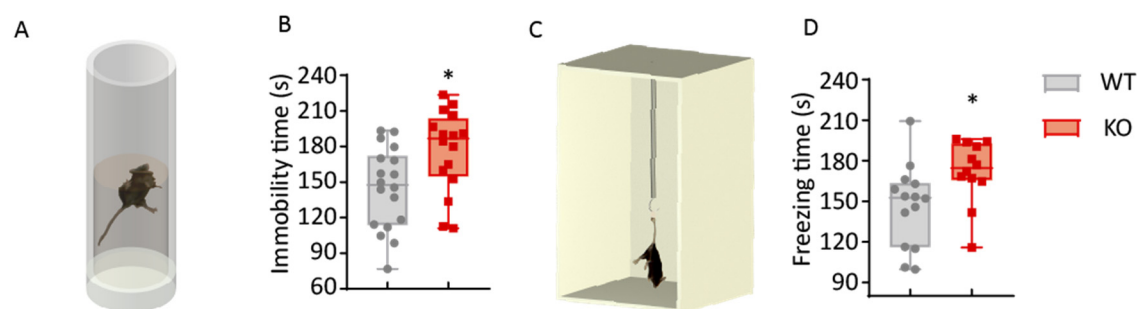


**Figure II. 1. Arc/Arg3.1 KO mice showed depressive-like behaviors.** (A) Schematic of forced swimming test. (C) Schematic of tail suspension test. (B) Arc/Arg3.1 KO mice showed increased immobility duration in the Forced swimming test (Median: WT, 147.6 s; n = 18; KO, 186.9 s; n = 16; \*p < 0.05) and (D) longer freezing times in the tail suspension test (Median: WT, 152.7 s; n = 14; KO, 174.5 s; n = 12; \*p < 0.05). Significance was assessed with the Mann-Whitney test. The box plots showed the median (-), whiskers showed min to max, and all data points.

## 2. Detection of Arc/Arg3.1 mRNA in GABAergic interneurons in different brain regions.

Arc/Arg3.1 expressed in GABAergic interneurons after stress stimulus and exploration (Vazdarjanova et al., 2006). Moreover, Arc/Arg3.1 expression is reported to be increased in two regions composed mainly of GABAergic neurons (Risold & Swanson, 1997a; Yager, Garcia, Wunsch, & Ferguson, 2015; Zhao, Eisinger, & Gammie, 2013), the lateral septum after stress stimulus (Ons et al., 2004; Ons et al., 2010) and the striatum after antidepressants (Y. Li et al., 2015). We observed loss of Arc/Arg3.1 impaired the forced swimming test and tail suspension test in mice but not for the open field test, the elevated plus maze test and the sociability test (Xiaoyan Gao, 2016; X. Gao et al., 2019). However, little literature reports whether loss of Arc/Arg3.1 in GABAergic interneurons will lead to stress-related disorders.

### 2.1. Detection of Arc/Arg3.1 mRNA in parvalbumin-positive interneurons in different brain regions.

As a first step, I asked whether Arc/Arg3.1 can be expressed in parvalbumin-positive interneurons. To maximize Arc/Arg3.1 expression in the brain, Mice were subjected to kainate-

induced seizures and subsequently perfused and prepared for fluorescent ISH. Interestingly, we observed different brain regions of mice such as ACC, RS, LS, CA1, CA3, DG, and TRN (Figure II. 2 and 3. A). However, the only region in mice that exhibits Arc/Arg3.1 and parvalbumin colocalization is the thalamic reticular nucleus (TRN) (Figure II. 3. A).



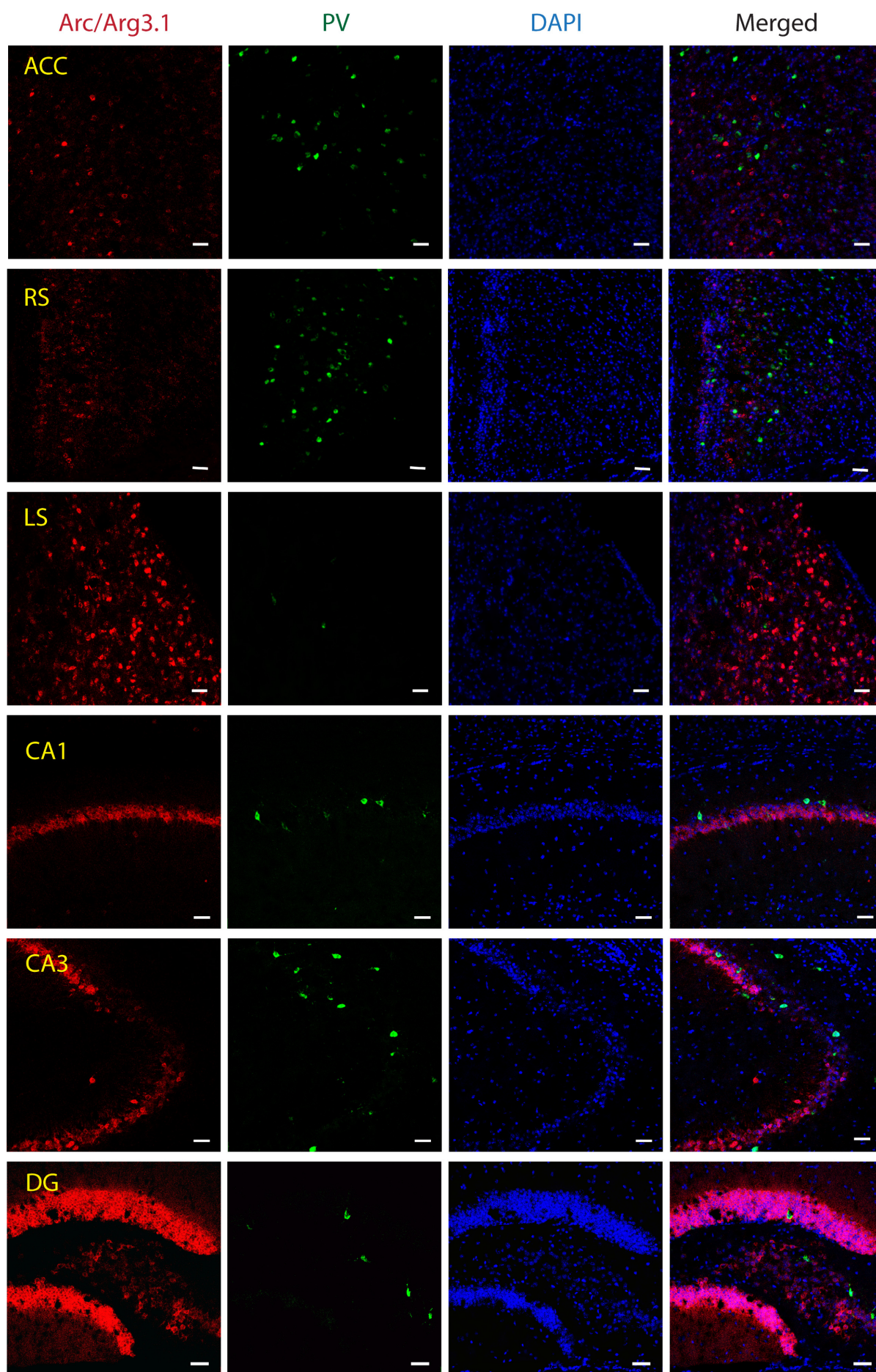


### Figure II. 2. Arc/Arg3.1 and parvalbumin (PV) expression in the different brain regions in mice.

In the ACC, RS, LS, and hippocampal regions, Arc/Arg3.1 and parvalbumin were not colocalized with the RNA in WT mice (scale bar: 50  $\mu$ m).

To explore the functional role of Arc/Arg3.1 in parvalbumin-positive interneurons, I bred Arc/Arg3.1<sup>f/f</sup> with PV-Cre mice. The offspring PV-Cre:Arc/Arg3.1<sup>f/f</sup> transgenic mice were termed “PV-cKO”. I subjected the PV-cKO mice to seizures and performed fISH using RNAscope on their brains to evaluate the extent and specificity of Arc/Arg3.1 deletion. The RNAscope staining showed a complete loss of Arc/Arg3.1 mRNA in the RTN of PV-cKO mice but an intact expression in glutamatergic hippocampal neurons. These findings demonstrate a highly efficient and specific deletion of Arc/Arg3.1 in the RTN of PV-cKO mice (Figure II. 3. B).

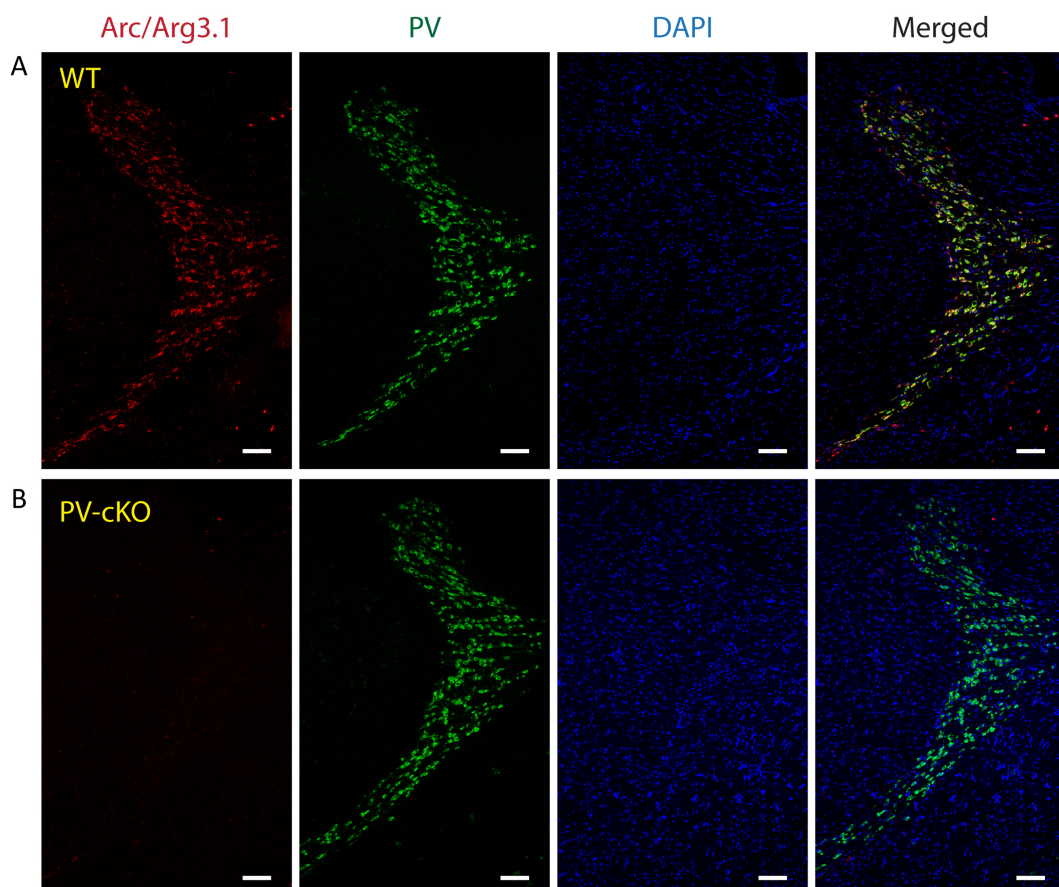


**Figure II. 3. Arc/Arg3.1 and parvalbumin (PV) expression in the thalamic reticular nucleus (TRN) in mice.** (A) In the thalamic reticular nucleus (TRN), Arc/Arg3.1 and parvalbumin were highly colocalized with the RNA in WT mice (scale bar: 100  $\mu$ m). (B) The expression of Arc/Arg3.1 was obviously knocked down in RTN in PV-cKO mice (scale bar: 100  $\mu$ m).

The thalamic reticular nucleus (TRN), a cluster of GABAergic neurons (Houser, Vaughn, Barber, & Roberts, 1980), receives nearly all its input from infragranular layers of the cortex and projects to specific thalamic nuclei, which project back to the cortex (Martins & Tavares, 2017). The TRN provides a major source of inhibition to various thalamic nuclei, thereby shaping local sensory information processing (Crick, 1984; Halassa & Acsady, 2016; Pinault, 2004). In addition, this Cortico-thalamo-cortical loop is involved in regulating cortical activity states, cognition, defensiveness, depression, and gating of sensory information (P. Dong et al., 2019; Halassa et al., 2014; P. F. Liu et al., 2022; X. Y. Wang et al., 2023; Xi et al., 2023; X. J. Yu, Xu, He, & He, 2009). Most TRN neurons express parvalbumin and were shown to be involved in establishing and modulating depression (X. Y. Wang et al., 2023). I thus hypothesized that enhanced immobility in the Arc/Arg3.1 KO mice might result from dysfunction of the TRN PV neurons.

## **2.2. Detection of Arc/Arg3.1 mRNA in somatostatin-positive interneurons in different brain regions.**

Somatostatin-positive neurons are a group of GABAergic interneurons present throughout the brain (Rudy et al., 2011). Previous studies suggested that somatostatin expression and the function of somatostatin-positive neurons are highly related to emotionality, cognitive and neuroendocrine functions (Douillard-Guilloux, Lewis, Seney, & Sibille, 2017; Guilloux et al., 2012; D. Kim et al., 2016; Lovett-Barron et al., 2014; Schmid et al., 2016; Seney, Tripp, McCune, Lewis, & Sibille, 2015; Soumier & Sibille, 2014; Tripp, Kota, Lewis, & Sibille, 2011; X. Y. Yang et al., 2021).

To investigate the expression of Arc/Arg3.1 and somatostatin in the mice brain, Kainate-induced seizures were induced in mice to maximize the expression of Arc/Arg3.1. Following seizures, mice were perfused with PBS and PFA, and RNAscope staining was employed to detect mRNA transcripts of Arc/Arg3.1 and somatostatin (SST) in the mice brain. Although the amount of transcripts or expressing neurons was not quantified here, example images show partial colocalization of Arc/Arg3.1 and somatostatin in different regions of the brain, including

the ACC, dorsal and ventral lateral septum (dLS, vLS), claustrum (CLA), CA3, polymorph layer of the dentate gyrus (PoDG), and thalamic reticular nucleus (TRN) (Figure II. 4). These data suggests that Arc/Arg3.1 can be expressed in some of the somatostatin-positive neurons, upon strong stimulation.



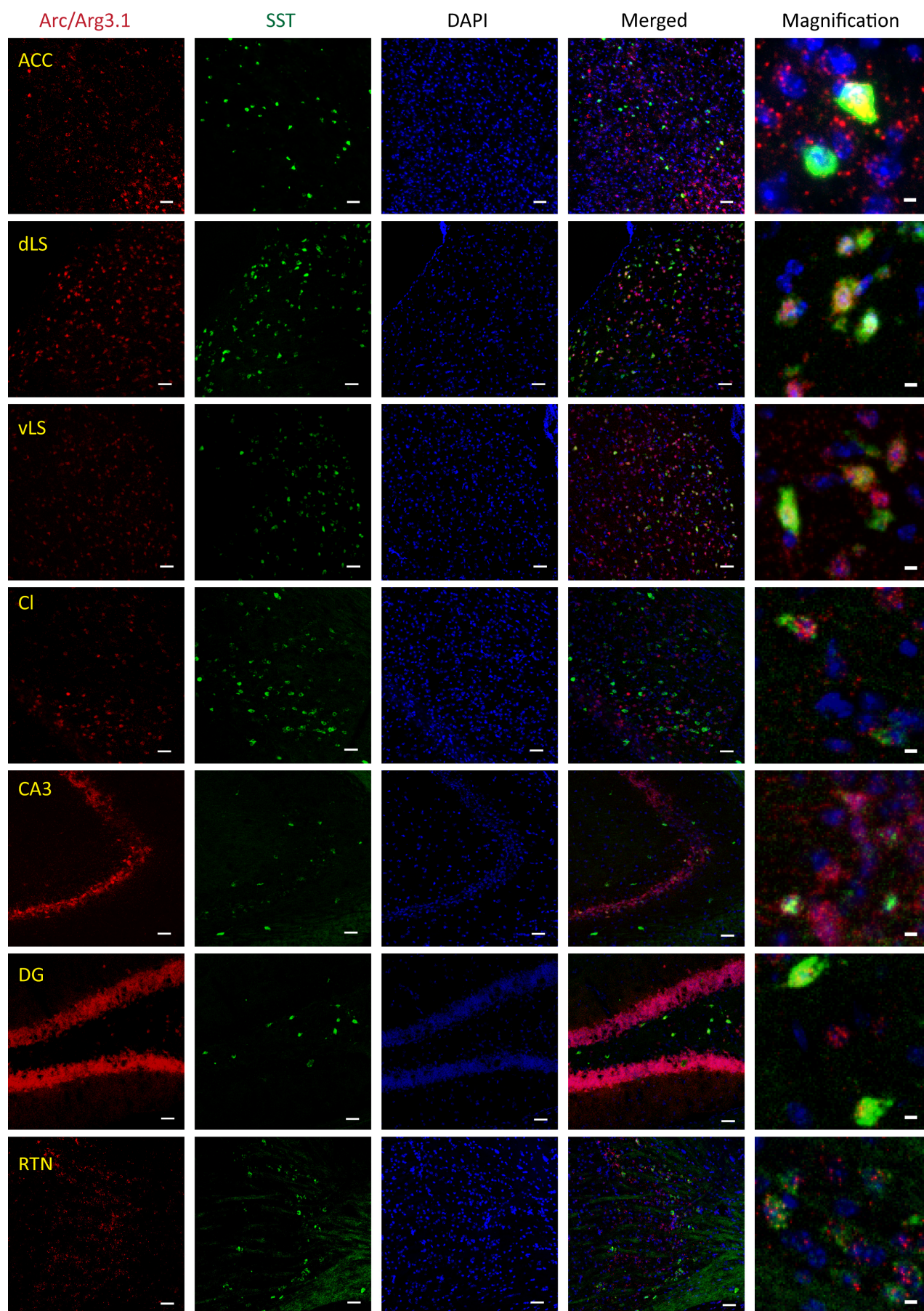


**Figure II. 4. Presence of Arc/Arg3.1 mRNA in somatostatin-positive interneurons in different brain regions in mice.** The colocalized expression of Arc/Arg3.1 and somatostatin in different brain regions (scale bar: 50  $\mu\text{m}$ ; scale bar of magnifications: 5  $\mu\text{m}$ ).

To explore the functional role of Arc/Arg3.1 in somatostatin-positive interneurons, I bred Arc/Arg3.1<sup>f/f</sup> mice with SST-Cre mice. Their SST-Cre:Arc/Arg3.1<sup>f/f</sup> offspring were termed “SST-cKO”. I examined the efficacy of Arc/Arg3.1 deletion in these mice using RNAscope, as described above. Exemplary images show that Arc/Arg3.1 mRNA was absent in the TRN but still colocalized with somatostatin mRNA in neurons of the dLS, vLS, CI and CA3 (Figure II. 5).



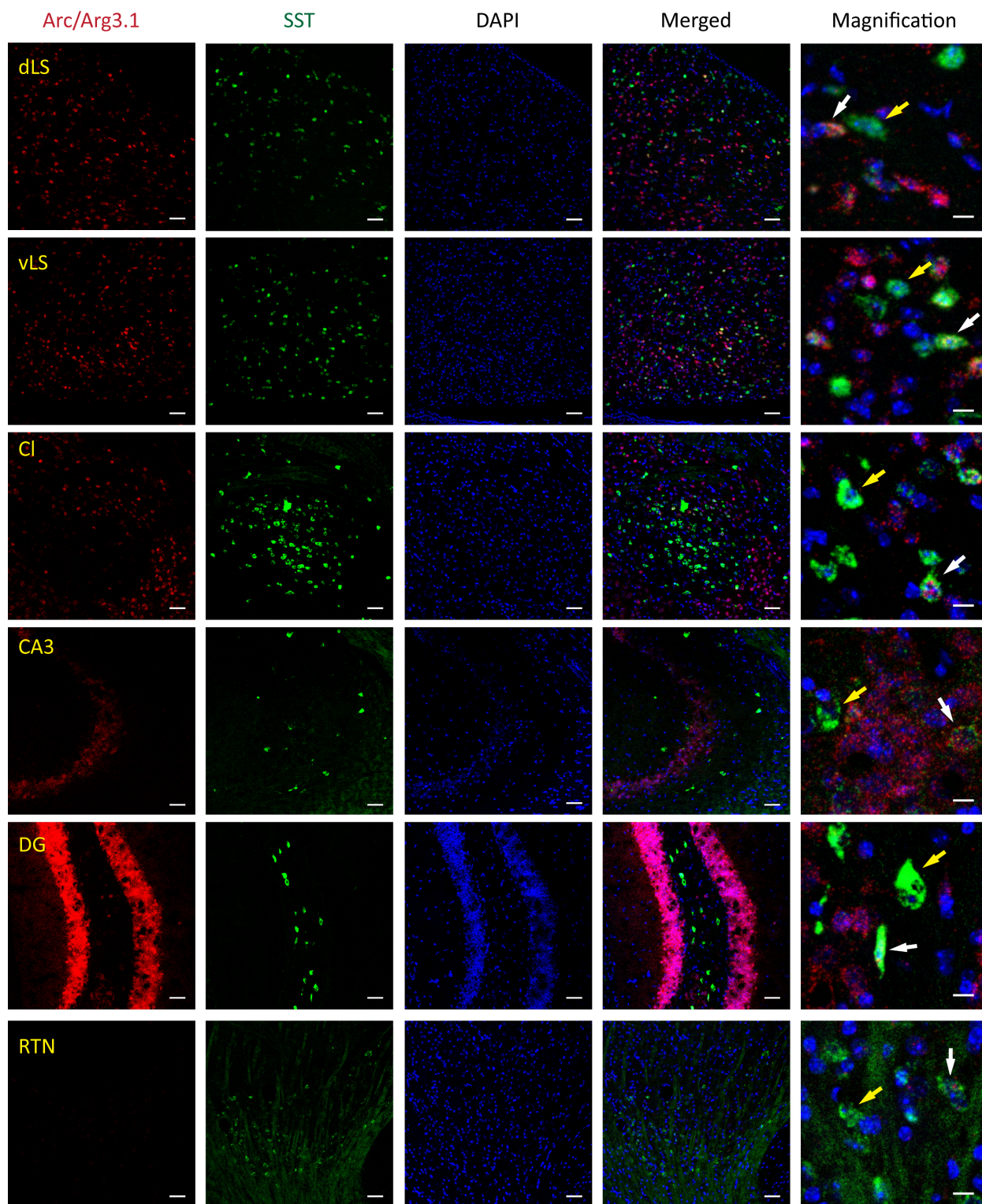


**Figure II. 5. Arc/Arg3.1 expression was knocked down in somatostatin-positive interneurons in different brain regions in mice.** The colocalized expression of Arc/Arg3.1 and somatostatin in SST-cKO mice showed Arc/Arg3.1 was knocked down in different brain regions (scale bar: 50  $\mu\text{m}$ ; scale bar of magnifications: 5  $\mu\text{m}$ ). Yellow arrows indicated that Arc/Arg3.1 mRNA fluorescence is missing in SST+ interneurons in SST-cKO mice. White arrows indicated SST-positive interneurons co-expressed Arc/Arg3.1 in SST-cKO mice.

Besides TRN, LS was also a specific brain region that has the main population of SST<sup>+</sup> neurons and Arc/Arg3.1<sup>+</sup> expression. The knockdown efficiency of Arc/Arg3.1 in SST<sup>+</sup> neurons was quantified in mice after seizures 45 min. It was observed that approximately 54% of the Arc/Arg3.1 expression in SST<sup>+</sup> neurons was reduced in the LS of SST-cKO mice, as indicated by both the overall LS morphology (Figure II. 6. A) and the percentage of SST<sup>+</sup> neurons that were also positive for Arc/Arg3.1 (Figure II. 6. B).

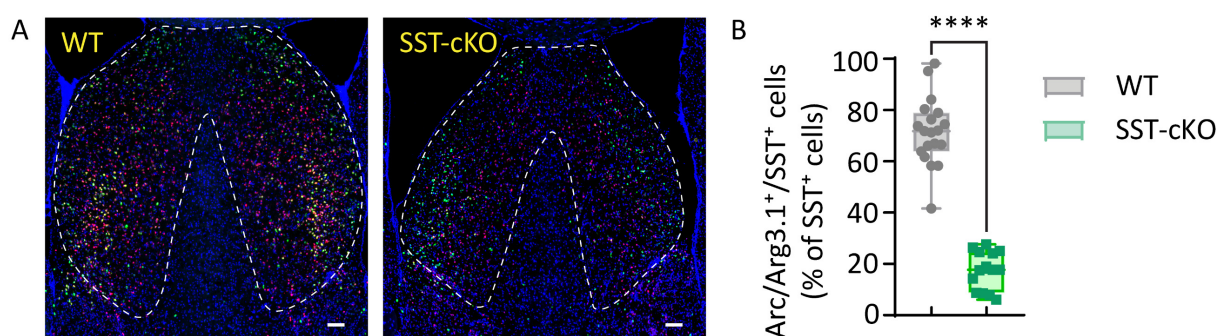


**Figure II. 6. Arc/Arg3.1 knocked down efficiency in somatostatin-positive interneurons in LS.**

(A) The colocalized expression of Arc/Arg3.1 and somatostatin in LS of WT (left) and SST-cKO (right) mice after seizures 45 min (scale bar: 100  $\mu$ m). (B) Arc/Arg3.1 was significantly knocked down in SST<sup>+</sup> neurons in SST-cKO mice compared to WT mice after seizures 45 min (Mean: WT, 71.59%,  $n = 19$ ; KO, 17.54%,  $n = 15$ . \*\*\*\* $p < 0.0001$ ). Significance was assessed with the Mann-Whitney test. The box plots showed the median (-), whiskers showed min to max, and all data points.

### 3. Role of Arc/Arg3.1 in parvalbumin-positive interneurons for emotional behavior in mice.

Next, I assessed exploratory and anxiety-driven behaviors of PV-cKO mice in the open field and elevated plus maze tests.

In the open field test (Figure II. 7. A), mice are allowed to explore an empty arena for 10 min, and a low percentage of time spent in the center is taken as a measure of anxiety. The PV-cKO



and WT littermates moved comparable distances in the arena (Figure II. 7. B), spent a similar amount of time in the center (Figure II. 7. C) and had identical movement velocities (Figure II. 7. E) during the test. Moreover, the PV-cKO mice also entered the center arena as frequently as their WT littermates (Figure II. 7. D).

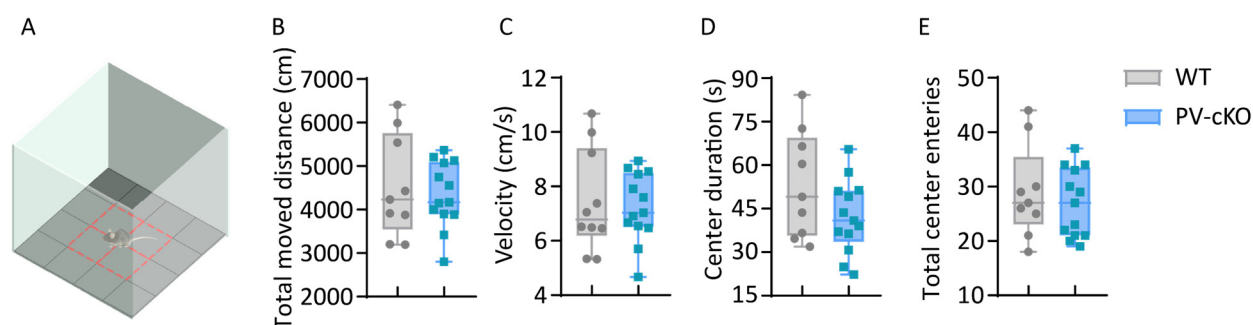


**Figure II. 7. Locomotion activity and exploratory behavior in PV-cKO mice.** (A) Schematic of open field test. (B-E) PV-cKO mice showed normal exploratory behavior (D, center area duration: median: WT, 49.08 s; PV-cKO, 40.92 s;  $p = 0.24$ , NS; E, total center entered frequency: median: WT, 27; PV-cKO, 27;  $p = 0.75$ , NS) and locomotion activity compared with their WT littermates in the open field test (B, total moved distances: median: WT, 4232 cm; PV-cKO, 4170 cm;  $p = 0.90$ , NS; C, velocity: median: WT, 6.79 cm/s; PV-cKO, 7.03 cm/s;  $p = 0.93$ , NS). All WT,  $n = 9$ ; PV-cKO,  $n = 13$ . Significance was assessed with the Mann-Whitney test. The box plots showed the median (-), whiskers showed min to max, and all data points.

The elevate plus maze test (Figure II. 8. A) is widely used in behavioral neuroscience to assess innate anxiety-like behavior. Mice behaviors in this test reflect two opposing natural instincts: one is to avoid being exposed to bright open places, and the other one is exploring the novel environment. As a result, they tend to stay in the wall-protected closed arms, which are dimly lit. The second is the natural, spontaneous exploratory instinct, driving the mice to explore the open arms. Treatments or conditions that impact on these natural drives are often considered anxiolytic or anxiogenic.

The PV-cKO mice and their WT littermates moved similar distances in the elevated plus maze test (Figure II. 8. B) and entered the open and closed arms as frequently (Figure II. 8. E). The PV-cKO mice also spent similar time in open arms (Figure II. 8. C). They had similar entry frequencies in the open arms (Figure II. 8. D) as well as their WT littermates, indicating that

deletion of Arc/Arg3.1 in parvalbumin-positive neurons did not alter innate anxiety-like behaviors.

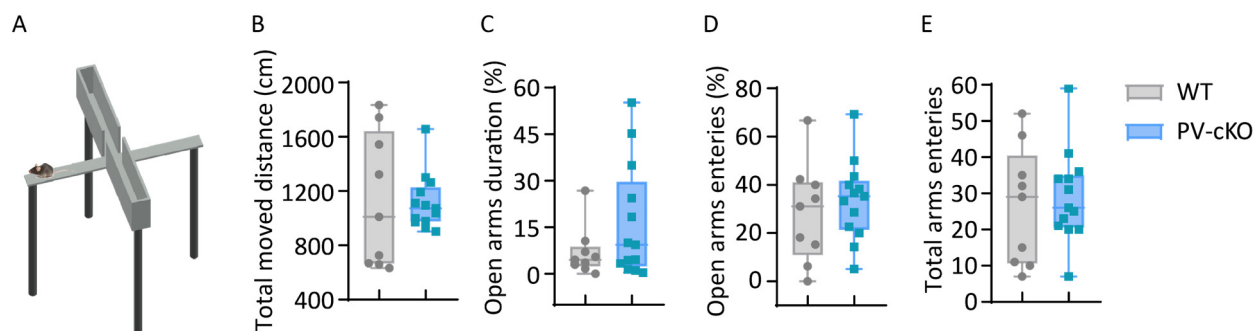


**Figure II. 8. Unaltered anxiety-like behavior in PV-cKO mice.** (A) Schematic of elevated plus maze test. (B-E) PV-cKO mice showed normal opened arms exploratory behavior compared with their WT littermates in the elevated plus maze test (B, total moved distances: median: WT, 1010 cm; PV-cKO, 1072 cm;  $p = 0.84$ , NS; C, percentage of opened arms durations: median: WT, 4.48%; PV-cKO, 9.33%;  $p = 0.39$ , NS; D, percentage of opened arms entered frequency: median: WT, 31.03%; PV-cKO, 35.29%;  $p = 0.48$ , NS; E, arms entered frequency: median: WT, 29; PV-cKO, 26;  $p = 0.71$ , NS). All WT,  $n = 9$ ; PV-cKO,  $n = 13$ . Significance was assessed with the Mann-Whitney test. The box plots showed the median (-), whiskers showed min to max, and all data points.

The PV-cKO mice exhibited similar immobility duration (Figure II. 9. B) and freezing time (Figure II. 9. D) as their WT littermates in both the forced swimming test (Figure II. 9. A) and the tail suspension test (Figure II. 9. C). These results indicate that PV-cKO mice did not display disrupted coping strategies or signs of depressive-like behaviors.

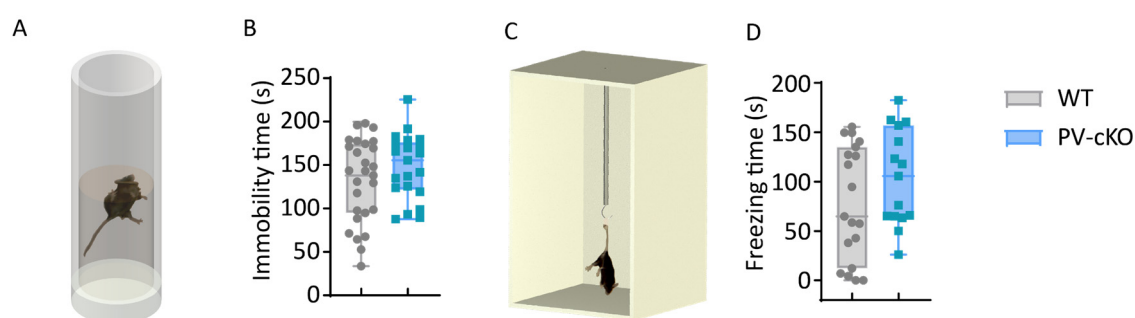


**Figure II. 9. Unaltered depressive-like behavior in PV-cKO mice.** (A) Schematic of forced swimming test. (B) PV-cKO mice showed typical immobile duration compared with their WT

littermates in the forced swimming test (Median: WT, 138.0 s; n = 31; PV-cKO, 155.6 s; n = 21; p = 0.33, NS). (C) Schematic of tail suspension test. (D) PV-cKO mice showed normal freezing time compared with their WT littermates in the tail suspension test (Median: WT, 64.73 s; n = 19; PV-cKO, 105.7 s; n = 15; p = 0.12, NS). Significance was assessed with the Mann-Whitney test. The box plots showed the median (-), whiskers showed min to max, and all data points.

#### 4. Role of Arc/Arg3.1 in somatostatin-positive interneurons for emotional behavior in mice.

To explore the functional role of Arc/Arg3.1 in somatostatin-positive interneurons in exploratory and anxiety-like behaviors in mice, the SST-cKO mice were assessed in the open field and elevated plus maze tests.

In the open field test (Figure II. 10. A), the SST-cKO mice moved similar distances (Figure II. 10. B) at the same velocity (Figure II. 10. E) as WT-littermates, indicating normal motor activity. However, the SST-cKO mice spent significantly less time in the center area (Figure II. 10. C) despite a comparable frequency of center entries (Figure II. 10. D). These findings may indicate a decrease in the exploratory drive of the center area but did not change the locomotive in the SST-cKO mice.

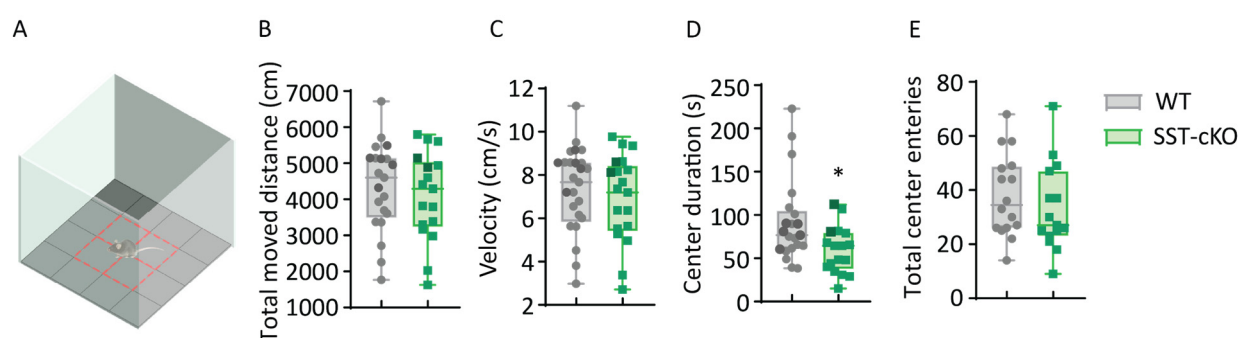


**Figure II. 10. Locomotion activity and exploratory behavior in SST-cKO mice.** (A) Schematic of open field test. (B, D, E) SST-cKO mice showed regular locomotion activity (B, total moved distances: median: WT, 4603 cm, n = 21; SST-cKO, 4292 cm, n = 17; p = 0.52, NS; E, total center entered frequency: median: WT, 34.5, n = 16; SST-cKO, 27.0, n = 15; p = 0.34, NS; C, velocity: median: WT, 7.67 cm/s, n = 21; SST-cKO, 7.19 cm/s, n = 17; p = 0.54, NS), but (D) less center area exploratory time (Median: WT, 76.76 s n = 21; SST-cKO, 64.48 s, n = 17; \*p < 0.05) compared with their WT littermates in the open field test. Significance was assessed with the

Mann-Whitney test. The box plots showed the median (-), whiskers showed min to max, and all data points. The data points with dark green color were published in the master thesis from Frederic Beba.

The performance of SST-cKO mice in the elevated plus maze test (Figure II. 11. A) was indistinguishable from their WT littermates, with similar locomotion (Figure II. 11. B) and entries to open and closed arms (Figure II. 11. C, D, E). Thus, unlike the open-field test, SST-cKO mice did not display any signs of heightened anxiety in the elevated plus-maze, indicating that ablated Arc/Arg3.1 in somatostatin-positive neurons altered the exploratory behavior but not innate anxiety-like behaviors in mice.

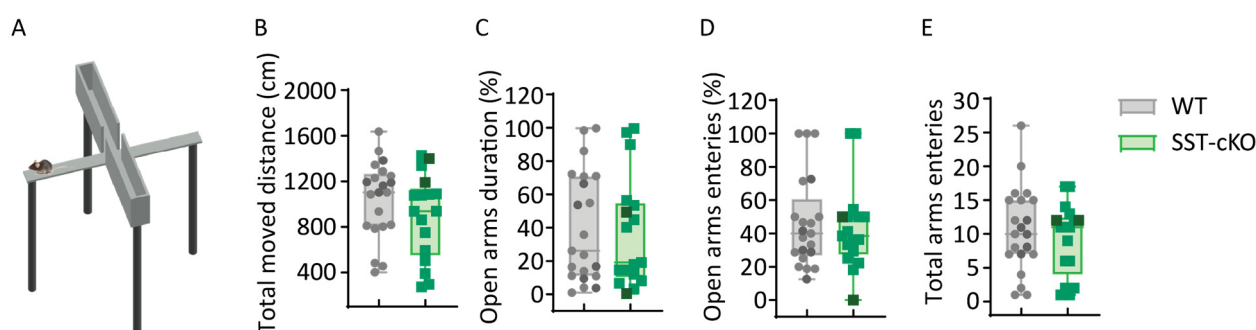


**Figure II. 11. Unaltered anxiety-like behavior in SST-cKO mice.** (A) Schematic of elevated plus maze test. (B-E) SST-cKO mice showed normal anxiety-like behavior compared with their WT littermates in the elevated plus maze test (B, total moved distances: median: WT, 1104 cm; SST-cKO, 938.5 cm;  $p = 0.19$ , NS; C, percentage of opened arms durations: median: WT, 26.17%; SST-cKO, 19.08%;  $p = 0.71$ , NS; D, percentage of opened arms entered frequency: median: WT, 40.0%; SST-cKO, 38.46%;  $p = 0.99$ , NS; E, arms entered frequency: median: WT, 10; SST-cKO, 11;  $p = 0.67$ , NS). All WT,  $n = 21$ ; SST-cKO,  $n = 17$ . Significance was assessed with the Mann-Whitney test. The box plots showed the median (-), whiskers showed min to max, and all data points. The data points with dark green color were published in the master thesis from Frederic Beba.

In the forced swimming test (Figure II. 12. A), SST-cKO mice showed significantly higher immobility duration (Figure II. 12. B) as compared to their WT littermates. However, their freezing time (Figure II. 12. D) in the tail suspension test (Figure II. 12. C) remained unaltered. Since FST and TST are good tests for antidepressants but not for depression (Commons et al.,

2017; Cryan, Mombereau, & Vassout, 2005), the increased immobile duration in the FST but not in the TST suggested the SST-cKO mice may have stress-related disorders.

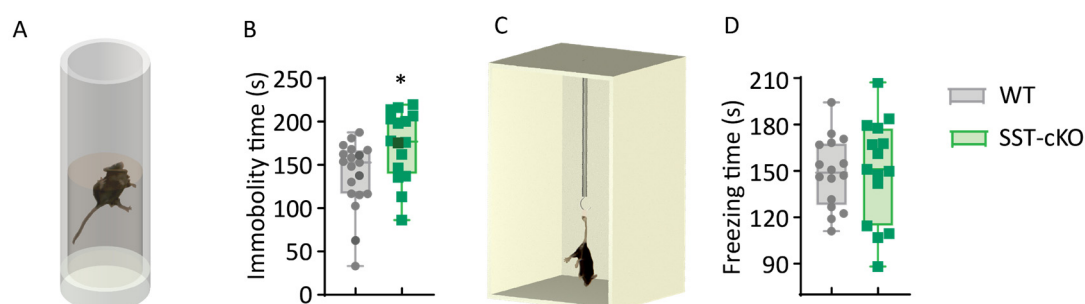


**Figure II. 12. Depressive-like behavior in SST-cKO mice.** (A) Schematic of forced swimming test. (B) Higher immobility duration in SST-cKO compared with WT littermates in the forced swimming test (Median: WT, 152.8 s; n = 19; SST-cKO, 177.0 s; n = 16; \*p < 0.05). (C) Schematic of tail suspension test. (D) SST-cKO mice showed normal freezing time compared with their WT littermates (Median: WT, 148.9 s; n = 16; SST-cKO, 151.0 s; n = 15; p = 0.80, NS). Significance was assessed with the Mann-Whitney test. The box plots showed the median (-), whiskers showed min to max, and all data points. The data points with dark green color were published in the master thesis from Frederic Beba.

## 5. Upregulation of Arc/Arg3.1 after physical restraint-induced stress in mice.

Previous studies suggest that treatment with antidepressants increases Arc/Arg3.1 expression in the hippocampus (Muzio et al., 2016), while forced swimming stress decreases its expression (Leem & Chang, 2017). Both novel environments and immobilization evoked the expression of Arc/Arg3.1 in LS (Ons et al., 2004). In the first part of this thesis, it has been shown to exhibit increased Arc/Arg3.1 and cFos expression in LS after delivery of foot shocks to induce fear conditioning (Figure I. 2). To further investigate the impact of acute stress on Arc/Arg3.1 induction in the hippocampus and lateral septum, I subjected mice to a 2-hour long physical restraint, after which the mice were sacrificed, brains were fixed and sliced. Brain sections were immunostained against Arc/Arg3.1 and cFos, and the densities of positive neurons were calculated. Expression of Arc/Arg3.1 (Figure II. 13. A, C) or cFos (Figure II. 13. B, D) in the LS was low in the baseline but dramatically increased (Figure II. 13. A, C) after physical restraint. In contrast, expression of Arc/Arg3.1 (Figure II. 13. E, G) and cFos (Figure II. 13. F, H) in the

dentate gyrus (Figure II. 13. E, G) was clearly decreased (Figure II. 13. E, G). These findings confirm that the stress induces IEG expression in the LS but suppresses it in the hippocampus. They also highlight the strong impact of restraint on IEG induction.

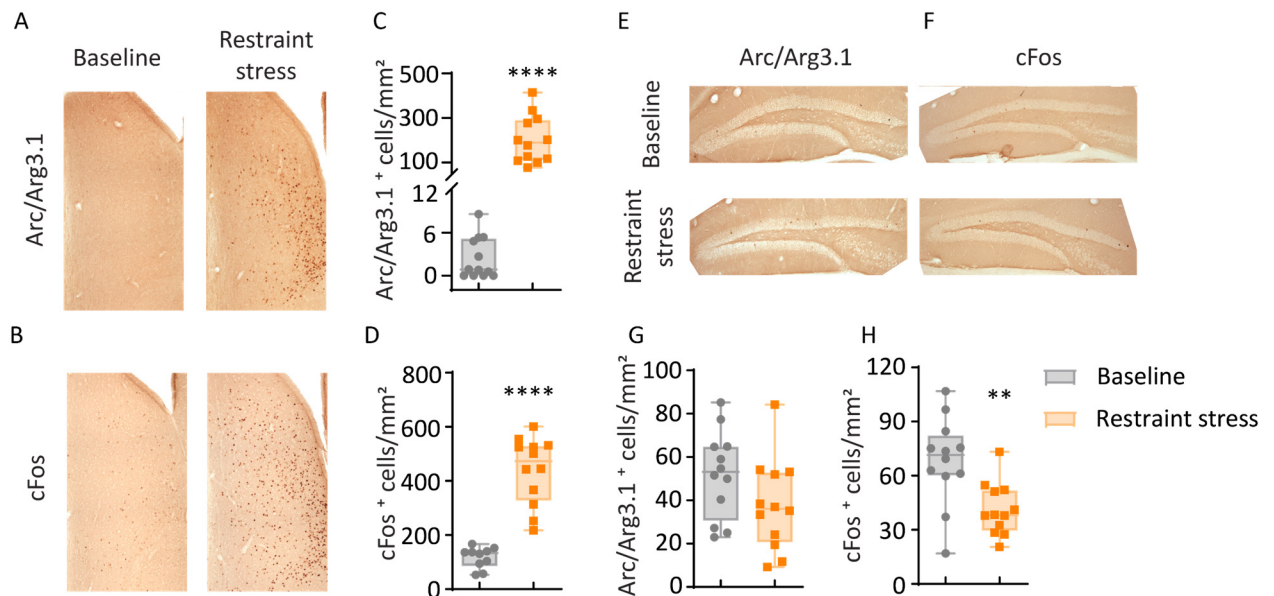


**Figure II. 13. Arc/Arg3.1 and cFos expression after physical restraint-induced stress in mice.** (A-D) The expression of Arc/Arg3.1 (Median: Baseline, 0.86 cells/mm<sup>2</sup>; n = 12; Restraint stress, 188.7 cells/mm<sup>2</sup>; n = 12; \*\*\*\*p < 0.0001) and cFos (Median: Baseline, 133.8 cells/mm<sup>2</sup>; n = 10; Restraint stress, 473.0 cells/mm<sup>2</sup>; n = 12; \*\*\*\*p < 0.0001) was significantly increased in lateral septum after restraint stress in mice. (E, G) The expression of Arc/Arg3.1 showed non-significant lower expression in the ventral hippocampal dentate gyrus after restraint stress (Median: Baseline, 53.1 cells/mm<sup>2</sup>; n = 12; Restraint stress, 36.1 cells/mm<sup>2</sup>; n = 12; p = 0.09, NS). (F, H) The expression of cFos showed a significantly decreasing in ventral hippocampal dentate gyrus after restraint stress (Median: Baseline, 71.46 cells/mm<sup>2</sup>; n = 12; Restraint stress, 38.15 cells/mm<sup>2</sup>; n = 12; \*\*p < 0.01). Significance was assessed with the Mann-Whitney test. The box plots showed the median (-), whiskers showed min to max, and all data points.



## Discussion





In this study, I investigated the contribution of Arc/Arg3.1-mediated plasticity to anxiety and coping responses to stress that are often linked with depression-like pathology. Given the dominant role of GABAergic systems in these behaviors (S. Chen et al., 2022; Fogaca et al., 2021; Fuchs et al., 2017; B. Luscher et al., 2011; D. Wang et al., 2023; Yin et al., 2016), I focused on investigating conditional Arc/Arg3.1 KO mice in specific inhibitory populations, PV-cKO and SST-cKO. I compared these to a germline KO with a complete deletion in all cells. I used the elevated-maze test to assess anxiety levels and the FST and TST to assess coping responses when escape is not possible. Decreased exploration and increased immobility in these tests are commonly interpreted as signs of elevated anxiety and depression. Yet it is important to note that other interpretations may exist and that the overall behavior is a complex outcome of different and sometimes opposing drives and traits. My findings showed Arc/Arg3.1 colocalized with PV-positive neurons only in TRN but colocalized with SST-positive neurons in different brain regions. PV-cKO mice showed intact anxiety- and depressive-like behaviors, but SST-cKO mice showed altered behaviors in OP and FST. Furthermore, Arc/Arg3.1 germline KO behaved more immobile and freezing time in FST and TST.

Previous studies from our group investigated the behavior of Arc/Arg3.1 germline knockout mice in the elevated maze, social engagement, working memory, sensorimotor gating, and native locomotor activity and did not observe any deviations from WT mice (Xiaoyan Gao, 2016; X. Gao et al., 2019; Gómez, 2016) indicating normal levels of anxiety and schizophrenia-like behaviors. Here, I tested the same KO mice in the FST and TST and revealed increased immobility. Since FST and TST are behavioral tests for antidepressants but not enough to define depression in mice (Commons et al., 2017; Cryan et al., 2005), the increased immobility suggests that loss of Arc/Arg3.1 may cause depression or anhedonia in mice. In another Arc/Arg3.1 KO mouse model, Arc/Arg3.1-deficient mice (EGFP knock-in–Arc/Arg3.1 knock-out), the mice showed anti-depressive behavioral phenotypes that are different from mine (Penrod et al., 2019). This mouse model was created by inserting a d2EGFP sequence with a stop codon and a floxed neomycin cassette into the Arc/Arg3.1 ORF, which remains in the mutant mice but not in the WT littermates (K. H. Wang et al., 2006). However, the neomycin cassette in this Arc/Arg3.1 KO model could affect the expression of neighboring genes (Pham, MacIvor, Hug, Heusel, & Ley, 1996) or cause adverse effects in mice (Scacheri et al., 2001), which could be the potential reason for the different behavioral phenotypes in different Arc/Arg3.1 KO mouse

models. In the genetic depression model rats, the transcription of Arc/Arg3.1 gene decreased in PFC and HPC (Eriksson et al., 2012), which further indicated Arc/Arg3.1 deficit could lead to depression or stress-related disorders in mice.

The RNA scope data indicated that TRN is the only brain region where Arc/Arg3.1 and parvalbumin are expressed in the same neurons. The PV-cKO mice, as TRN-specific Arc/Arg3.1 knock out, showed normal anxiety- and depressive-like behaviors, which indicated Arc/Arg3.1 in PV interneurons did not involve emotional behavior modulation in mice. The thalamic reticular nucleus (TRN) is involved in depression (Magdaleno-Madrigal et al., 2016; X. Y. Wang et al., 2023), sleep regulation (Vantomme, Osorio-Forero, Lüthi, & Fernandez, 2019), fear memory (J. H. Lee et al., 2019), and sensory (P. F. Liu et al., 2022), which indicated that Arc/Arg3.1 in TRN may contribute to a specific type of behavior instead of anxiety- or depressive-like behaviors in mice. Arc/Arg3.1 germline KO mice showed c in forced swimming and tail suspension tests. The SST-cKO mice showed less center duration in open field tests and more immobility time in forced swimming tests. The results suggested Arc/Arg3.1 in SST-positive or other neurons but not PV-positive neurons could modulate anxiety- and depressive-like behaviors in mice. Even though we observed strong Arc/Arg3.1 mRNA expression in the TRN region after seizures, there was no effect on the stress-related behavioral tests in PV-cKO mice. The function Arc/Arg3.1 in PV-positive neurons in TRN needs further investigation.

We found that the SST mRNA has colocalization with Arc/Arg3.1 in several different brain regions, such as dorsal and ventral LS (Bludau et al., 2023; Y. H. Chen et al., 2021; Hashimoto et al., 2022; M. Wang et al., 2023), claustrum (CLA) (Y. J. Wang et al., 2023), CA3 (X. Y. Li et al., 2024; Serra et al., 2018; H. Wang et al., 2021), dentate gyrus (DG) (H. H. Li et al., 2023; Ramirez et al., 2015), and thalamic reticular nucleus (TRN) (Magdaleno-Madrigal et al., 2016; X. Y. Wang et al., 2023), which relates to stress and depression in mice. The ablation of Arc/Arg3.1 in SST interneurons decreased the exploration time in the center area of the open field test and increased the immobility time in the forced swimming test. These findings suggest that Arc/Arg3.1 in SST-positive interneurons may contribute to depressive-like behavior or stress-related behavior in mice. The acute restraint stimuli strongly upregulated Arc/Arg3.1 in LS in general and also in SST-positive neurons. The increased immobilization suggested that Arc/Arg3.1 in SST-positive neurons may modulate stress-related behaviors in mice.

Previous studies reported that the expressions of Arc/Arg3.1 in HPC (Leem & Chang, 2017), cortical regions (Drouet et al., 2015), and amygdala (Y. Li et al., 2015) were highly linked to stress-related abnormalities. Our previous data indicated that loss of Arc/Arg3.1 in CaMKII $\alpha$ -positive neurons during the early postnatal period leads to anxiolytic behaviors in mice (Gómez, 2016), which suggested that Arc/Arg3.1 may modulate anxiety- and depressive-like behaviors oppositely in SST-positive neurons and CaMKII $\alpha$ -positive neurons. In the striatum, where the main neuron populations are GABAergic neurons, it was reported that dopamine 2 antagonists could raise the transcription of Arc/Arg3.1 (Fosnaugh, Bhat, Yamagata, Worley, & Baraban, 1995) and rescue Arc/Arg3.1-dependent psychomotor abnormalities (Manago et al., 2016). Furthermore, the loss of Arc/Arg3.1 increased dopamine levels in the PFC and post-synaptic D2 in the striatum (Manago et al., 2016). This part of my thesis illustrated that Arc/Arg3.1 in SST-positive neurons may modulate stress-related behaviors in mice by mediating the balance of dopamine expression and transmission in the brain.



## **Part III**

# **Contribution of Arc/Arg3.1 in GABAergic interneurons to memory processing**



## Introduction





Research in the past few decades has been centered around the function of pyramidal neurons in memory processes (Holtmaat & Caroni, 2016). Recent findings have highlighted the role of inhibitory GABAergic interneurons in learning and memory formation (Cummings, Lacagnina, & Clem, 2021; Giorgi & Marinelli, 2021; Lucas & Clem, 2018; Topolnik & Tamboli, 2022; Tzilivaki, Kastellakis, Schmitz, & Poirazi, 2022). According to previous studies, different interneurons in cortical regions were divided into three largely non-overlapping classes (S. Lee et al., 2010; Rudy et al., 2011): parvalbumin (PV) and somatostatin (SST) positive interneurons and serotonin receptor 3a (5HT3aR) positive interneurons. In the hippocampus, the Arc/Arg3.1 was reported colocalized with GAD67 in CA1 and CA3 (Vazdarjanova et al., 2006). Tzilivaki et al. summarized the essential role of GABAergic interneurons in the hippocampus, focusing on their connectivity patterns, mechanisms of plasticity induction, and regulation of oscillatory rhythms during memory processing (Tzilivaki et al., 2023). On the one hand, hippocampal GABAergic interneurons receive input from intrahippocampal regions, the entorhinal cortex (EC) (Tzilivaki et al., 2023), the septal nucleus (Freund & Antal, 1988; Sans-Dublanc et al., 2020) and the prefrontal cortex (Malik, Li, Schamiloglu, & Sohal, 2022). On the other hand, the hippocampus also sends long-range projections to the GABAergic interneurons in different brain regions, such as the medial entorhinal cortex (mEC) (Rozov et al., 2020), nucleus accumbens (NAc) (Lodge, Elam, Boley, & Donegan, 2023), the medial prefrontal cortex (mPFC) (Lodge et al., 2023), the thalamic reticular nucleus (TRN) (Cavdar et al., 2008) and lateral septum (LS) (Decarie-Spain et al., 2022; Leroy et al., 2018; Sweeney & Yang, 2015). The latest research suggests that the activities of PV and SOM interneurons in the hippocampus play a significant role in long-term synaptic plasticity and memory (Cummings & Clem, 2020; Honore, Khlaifia, Bosson, & Lacaille, 2021; Miranda, Cruz, Bessieres, & Alberini, 2022; Zicho et al., 2023). The functions of PV, SOM, and VIP interneurons in fear circuits are essential for fear memory processes (Singh & Topolnik, 2023).

The activity-regulated cytoskeletal gene Arg3.1, also known as Arc, plays an essential role in synaptic plasticity, learning, cognition, memory consolidation and memory discrimination (Eriksen & Bramham, 2022; Xiaoyan Gao et al., 2018; Penrod et al., 2019; Plath et al., 2006; Tzingounis & Nicoll, 2006). In 2020, Arc/Arg3.1 was found to colocalize with GABAergic neurons in the lateral septum after seizures (Kuku, 2020). However, the role of Arc/Arg3.1 in somatostatin and parvalbumin interneurons has yet to be fully understood. To gain further

insight into this matter, we conducted a study wherein we crossbred SOM-Cre or PV-Cre transgenic mice with Arc/Arg3.1<sup>f/f</sup> transgenic mice, striving to obtain a brain-wide ablation of Arc/Arg3.1 in either SOM or PV interneurons. We then proceeded to conduct fear conditioning and Morris water maze tests to evaluate the contextual and spatial memory behaviors of the mice involved.

## Aims of the study for Part III

Previous data indicated that Arc/Arg3.1 expressed in the GABAergic neurons after fear conditioning and exploration. Arc/Arg3.1 is a crucial protein for synaptic plasticity and memory consolidation. However, there has been no study showing whether Arc/Arg3.1 in the GABAergic neurons contributes to memory processes. Therefore, this part of the thesis aims at this question to investigate the role of Arc/Arg3.1 in PV-positive and SST-positive neurons in spatial and contextual memory processes.

### **Specific goals:**

- To investigate the role of Arc/Arg3.1 expression in PV-positive and SST-positive neurons in spatial memory processes.
- To evaluate the role of Arc/Arg3.1 in PV-positive and SST-positive neurons in contextual memory processes.



## Results



## 1. Sensory sensitivity of Arc/Arg3.1 KO and parvalbumin-cKO mice.

Pain sensitivity is a significant symptom in depression patients (S. Chen et al., 2023; Mee et al., 2011; Torta & Munari, 2010) and is higher in animal models with GABAergic deficits (Han & Pae, 2015; D. Wang et al., 2023). Aberrant plasticity is a likely mechanism underlying the comorbidity of pain and depression and expression of the IEGs cFos and Arc/Arg3.1 were observed in the spinal cord (Hossaini, Jongen, Biesheuvel, Kuhl, & Holstege, 2010) and somatosensory cortex (Bunting, Nalloor, & Vazdarjanova, 2015) following noxious sensory stimuli. Deletion of Arc/Arg3.1 in GABAergic neurons might, in theory, affect nociception and thereby depressive-like behaviors. In addition, altered nociception, would necessitate adjustments of the fear conditioning stimuli, utilized in the assessment of memory. To address this possibility, a flinch-jump test (Figure III. 1. A) was performed in the Multi-Conditioning System (TSE Systems), by applying a series of consecutive foot shocks ranging from 0.1 mA to 1.0 mA (Figure III. 1. B). The lowest shock intensity eliciting flinch and/or jump was noted as the threshold. The threshold to first flinch was around 0.175 mA for WT and Arc/Arg3.1 KO mice (Figure III. 1. C). The median value of the jump threshold was around 0.3 mA for WT and Arc/Arg3.1 knock-out mice (Figure III. 1. D). There was no significant difference between WT and Arc/Arg3.1 KO mice in any of the measures (Figure III. 1. C. D). Next, I performed the same test on the PV-cKO mice, which did not differ from their WT-littermates (Figure III. 1. E. F). These findings showed that sensitivity to electrical foot-shocks was unchanged by Arc/Arg3.1-deletion and confirmed the current-values required for reliable fear conditioning.



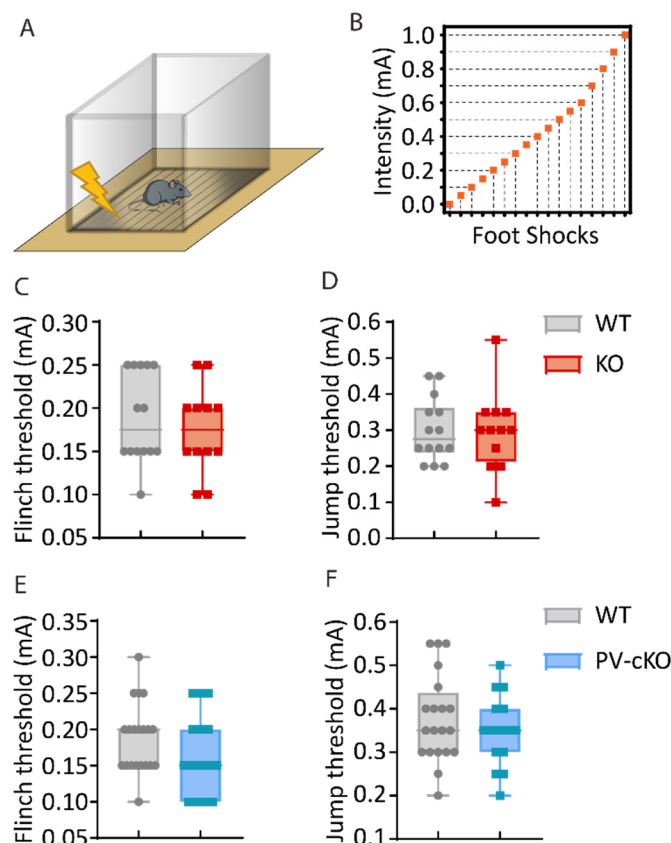


**Figure III. 1. Pain sensitivity in Arc/Arg 3.1 KO mice and PV-cKO mice.** (A) Schematic diagram of flinch-jump test and (B) electrical shock thresholds (mA) in flinch-jump test. Neither Arc/Arg3.1 KO mice have difference compare to the control group in the first flinch (C, median: WT, 0.175 mA; n = 14; KO, 0.175 mA; n = 12; p = 0.57, NS) or first jump (D, median: WT, 0.275 mA; n = 14; KO, 0.300 mA; n = 12; p > 0.99), nor PV-cKO mice have difference compare to the control group in the first flinch (E, median: WT, 0.20 mA; n = 20; PV-cKO, 0.15 mA; n = 15; p = 0.25, NS) or first jump (F, median: WT, 0.35 mA; n = 20; PV-cKO, 0.35 mA; n = 15; p = 0.53, NS). Significance was assessed with the Mann-Whitney test. The box plots showed the median (-), whiskers showed min to max, and all data points.

## 2. Role of Arc/Arg3.1 in GABAergic interneurons for fear memory in mice.

### 2.1. Role of Arc/Arg3.1 in parvalbumin-positive interneurons for fear memory in mice.

The parvalbumin-positive interneurons have been identified as playing a crucial role in learning and memory consolidation in mice (Miranda et al., 2022; Roque et al., 2023). The thalamic reticular nucleus (TRN), a brain region that houses Arc/Arg3.1, which is colocalized with parvalbumin in mice, has also been shown to be essential for cognition, learning, and memory

consolidation (Katsuki, Gerashchenko, & Brown, 2022; J. H. Lee et al., 2019; Manóach & Stickgold, 2019).

In an effort to investigate a possible contribution of Arc/Arg3.1 in PV<sup>+</sup> interneurons to fear memory in mice, a fear conditioning test was administered to PV-cKO mice. (Figure III. 2. A). PV-cKO mice exhibited strong freezing immediately after foot shocks, after 7 days and 14 days, indicating successful fear induction (Figure III. 2. B, C and D), albeit a slightly reduced tone-response (ns). Strong freezing during the context exposure in recent and remote memory tests illustrated a robust fear memory consolidation (Figure III. 2. E, H). Moreover, comparable freezing of PV-cKO and WT littermates in the altered context (Figure III. 2. F, I) and high discrimination index demonstrated an intact memory specificity (Figure III. 2. G, J). These results suggested that Arc/Arg3.1 knockout in parvalbumin-positive neurons does not significantly impact fear memory processing.

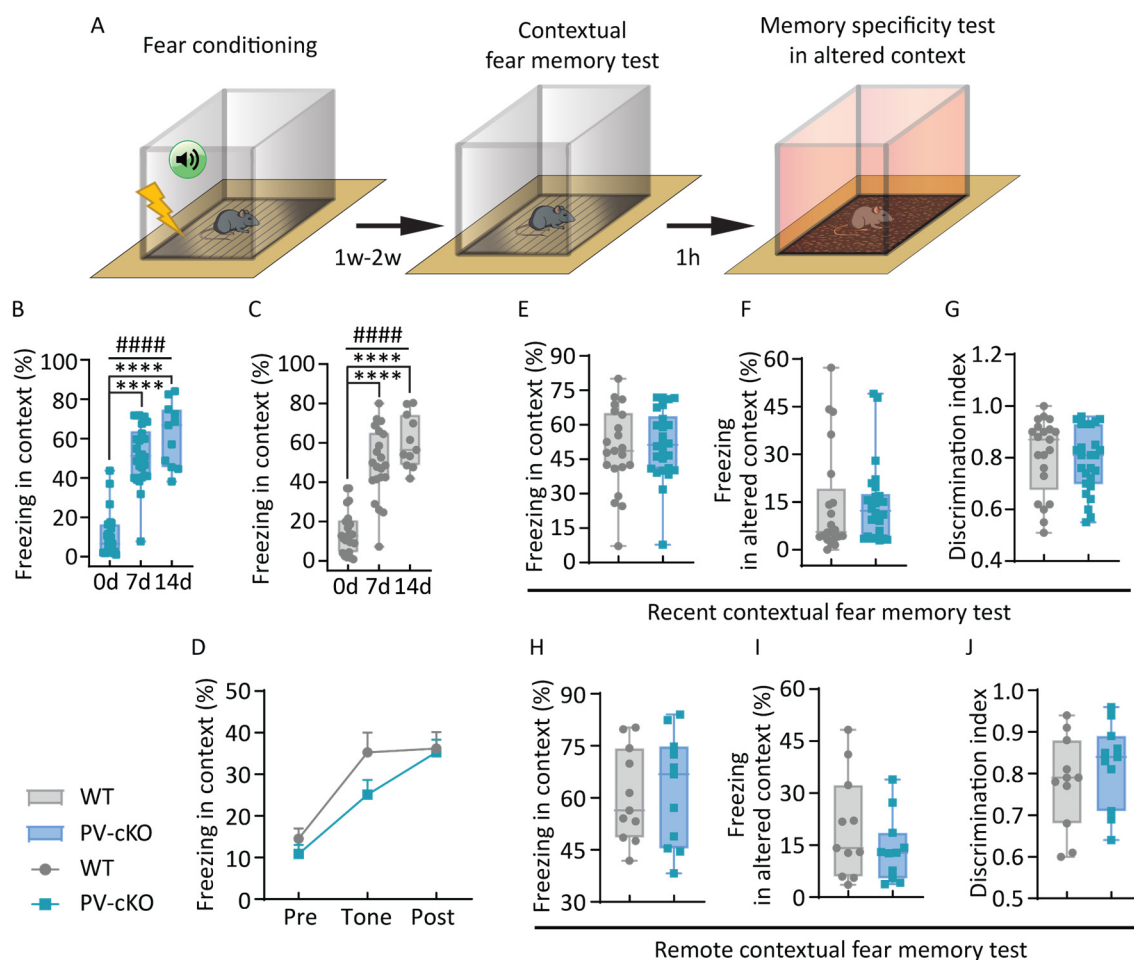


**Figure III. 2. Intact contextual fear memory retrieval and unaltered specificity of contextual fear memory in parvalbumin conditional knockdown (PV-cKO) mice.** (A) Schematic of contextual fear conditioning and memory test paradigm. (B) Averaged percentage freezing during fear acquisition (day 0) and fear memory retrieval (day 7 and 14) in WT group phase (Median: day 0, 12.75%,  $n = 21$ ; day 7, 48.61%,  $n = 21$ ; and day 14, 56.39%,  $n = 11$ ; ##### $p < 0.0001$ ). (C) Averaged percentage freezing during fear acquisition (day 0) and fear memory retrieval (day 7 and 14) in PV-cKO group phase (Median: day 0, 6.62%,  $n = 26$ ; day 7, 51.25%,  $n = 26$ ; and day 14, 66.83%,  $n = 11$ ; ##### $p < 0.0001$ ). Differences between WT and PV-cKO groups in C and D were assessed with the Kruskal-Wallis test. Dunn's multiple comparison was performed to compare between day 0, day 7, and 14 (\*\*\*\* $p < 0.0001$ ). (D) Average percent freezing during fear acquisition phases (WT,  $n = 21$ ; PV-cKO,  $n = 26$ ; Phase  $F_{(1,45)} = 1.75$ ,  $p = 0.19$ , NS; group  $F_{(1.95,87.86)} = 42.27$ ,  $p < 0.0001$ ; interaction  $F_{(2,90)} = 1.66$ ,  $p = 0.196$ , NS). Significance was assessed with a two-way ANOVA with a mixed-effects model and a post hoc Bonferroni test. Data represents the mean  $\pm$  S.E.M. In the recent memory test, the PV-cKO mice had similar freezing levels in (E) the context test (Median: WT, 48.61%,  $n = 21$ ; PV-cKO, 51.25%,  $n = 26$ ;  $p = 0.83$ , NS), (F) altered context test (Median: WT, 5.58%,  $n = 21$ ; PV-cKO, 12.25%,  $n = 26$ ;  $p = 0.32$ , NS) and similar (G) discrimination index (Median: WT, 0.87,  $n = 21$ ; PV-cKO, 0.81,  $n = 26$ ;  $p = 0.52$ , NS) 7 days after conditioning compared to their WT littermates. In the remote

memory test, the PV-cKO mice showed comparable freezing levels in the context test (H, Median: WT, 56.39%,  $n = 11$ ; PV-cKO, 66.83%,  $n = 11$ ;  $p = 0.85$ , NS), altered context test (I, Median: WT, 14.17%,  $n = 11$ ; PV-cKO, 12.83%,  $n = 11$ ;  $p = 0.37$ , NS) and similar discrimination index (J, Median: WT, 0.79,  $n = 11$ ; PV-cKO, 0.84,  $n = 11$ ;  $p = 0.26$ , NS) 14 days after conditioning compared to their WT littermates. Significance was assessed with the Mann-Whitney test. The box plots showed the median (-), whiskers showed min to max, and all data points.

## **2.2. Role of Arc/Arg3.1 in somatostatin-positive interneurons for fear memory in mice.**

Activation of somatostatin-positive neurons in the prefrontal cortex (PFC), lateral septum (LS) and the hippocampus (HPC) (Carus-Cadavieco et al., 2017; Cummings & Clem, 2020; Raven & Aton, 2021; Siwani et al., 2018; Zicho et al., 2023) plays an important role in memory encoding, recall and consolidation. To further investigate the impact of Arc/Arg3.1 in somatostatin-positive interneurons on fear memory in mice, SST-cKO mice were subjected to a fear conditioning test (Figure III. 3. A).

The results show that SST-cKO mice exhibited strong freezing immediately after foot shocks, indicating successful fear induction (Figure III. 3. B). The SST-cKO mice exhibited robust freezing in the original context during recent (Figure III. 3. C) and remote (Figure III. 3. F) memory tests. Surprisingly, they displayed significantly higher freezing (Figure III. 3. D) and concurrent lower discrimination index, in the altered context during recent (Figure III. 3. E) but not remote memory test (Figure III. 3. G. H). Overall, the data revealed that deleting Arc/Arg3.1 in somatostatin-positive neurons results in a transient increase in memory generalization at initial times but subsides as memory ages.

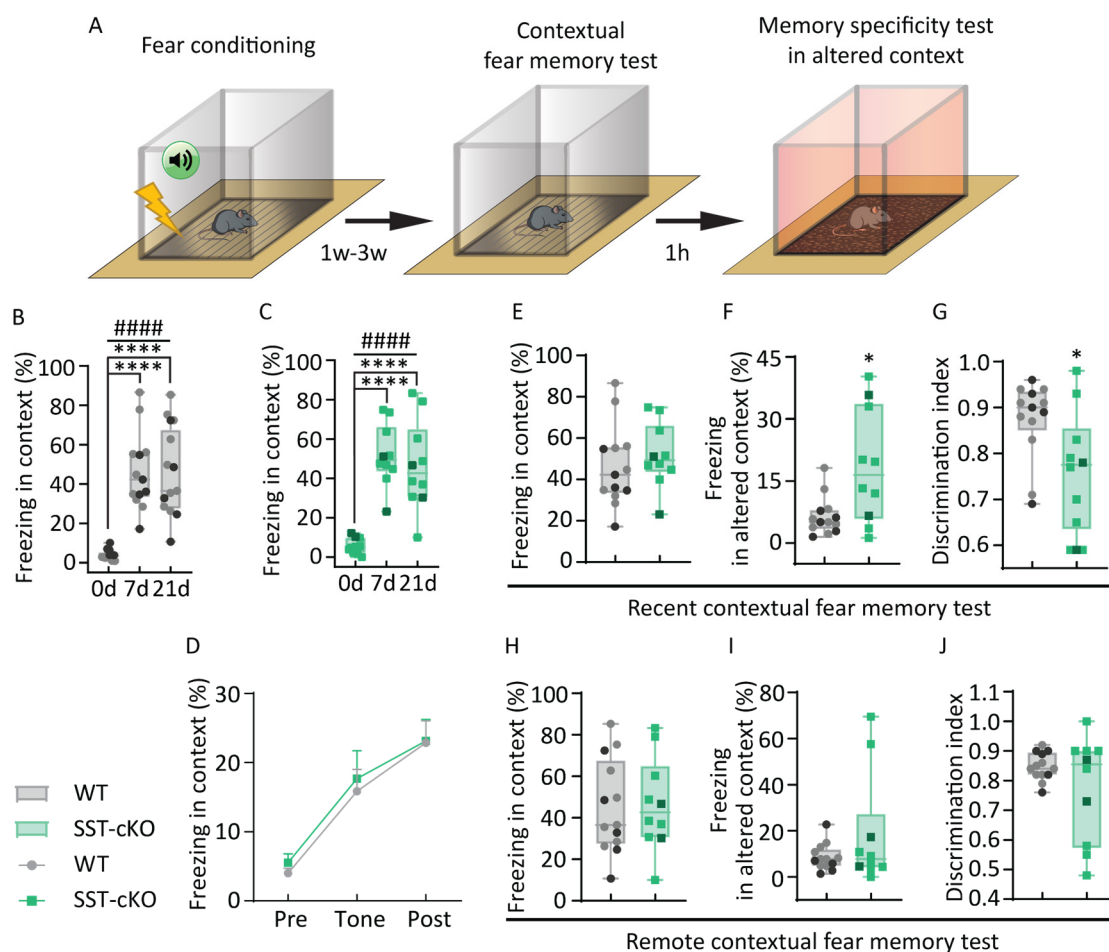


**Figure III. 3. Robust context fear memory retrieval but transient memory generalization in SST-cKO mice.** (A) Schematic of contextual fear conditioning and memory test paradigm. (B) Averaged percentage freezing during fear acquisition (day 0) and fear memory retrieval (day 7 and 21) in WT group phase (Median: day 0, 3.5%, n = 13; day 7, 42.33%, n = 13; and day 21, 36.35%, n = 13; #####p < 0.0001). (C) Averaged percentage freezing during fear acquisition (day 0) and fear memory retrieval (day 7 and 21) in SST-cKO group phase (Median: day 0, 5%, n = 10; day 7, 49.32%, n = 10; and day 21, 42.62%, n = 10; #####p < 0.0001). Differences between WT and SST-cKO groups in C and D were assessed with the Kruskal-Wallis test. Dunn's multiple comparison was performed to compare between day 0, day 7, and 21 (\*\*\*\*p < 0.0001). (D) Average percent freezing during fear acquisition phases (Phase  $F_{(1,21)} = 0.21$ ,  $p = 0.65$ , NS; group  $F_{(1,7,35.7)} = 25.99$ ,  $p < 0.0001$ ; interaction  $F_{(2,42)} = 0.053$ ,  $p = 0.949$ , NS). Significance was assessed with a two-way ANOVA with a mixed-effects model and with a post hoc Bonferroni test. Data represents the mean ± S.E.M. In the recent memory test, the SST-cKO mice had similar freezing levels in (E) the context test (Median: WT, 42.33%; SST-cKO, 49.32%;  $p = 0.38$ , NS), but a higher freezing level in the (F) altered context test (Median: WT, 5.08%; SST-cKO, 16.46%; \* $p < 0.05$ ) and lower (G) discrimination index (Median: WT, 0.90; SST-cKO, 0.78; \* $p < 0.05$ ) 7 days after conditioning compared to their WT littermates. In the remote memory test, the SST-cKO mice showed comparable freezing levels in the context test (H, Median: WT, 36.53%; SST-cKO, 42.62%;  $p = 0.78$ , NS), altered context test (I, Median: WT, 7.75%; SST-cKO, 7.75%;  $p = 0.89$ , NS)

and similar discrimination index (J, Median: WT, 0.84; SST-cKO, 0.86;  $p = 0.83$ , NS) 21s days after conditioning compared to their WT littermates. All WT,  $n = 13$ ; SST-cKO,  $n = 10$ . Significance was assessed with the Mann-Whitney test. The box plots showed the median (-), whiskers showed min to max, and all data points. The data points with dark green color were published in the master thesis from Frederic Beba.

### **2.3. Role of Arc/Arg3.1 in somatostatin- and parvalbumin-positive interneurons for tone fear memory in mice.**

The previous data in our lab also suggested an increased tendency of tone fear memory in remote memory when ablated Arc/Arg3.1 in the hippocampus (Xiaoyan Gao, 2016; Gómez, 2016). Conversely, when Arc/Arg3.1 was ablated in CaMKII positive neurons, it resulted in the extinction of tone fear memory (Xiaoyan Gao, 2016; Gómez, 2016; Plath et al., 2006). However, the role of Arc/Arg3.1 in inhibitory neurons in tone fear memory processing remained unclear. To address this research gap, we bred PV-Cre mice and SST-Cre mice with Arc/Arg3.1f/f mice to obtain PV-Cre:Arc/Arg3.1f/f mice and SST-Cre:Arc/Arg3.1f/f mice, which we named "PV-cKO" and "SST-cKO" mice, respectively. After the mice were handled for at least three days, we assessed their tone fear memory using the tone fear conditioning system (Figure III. 4. A). The results results demonstrated that ablation of Arc/Arg3.1 in parvalbumin-positive neurons or somatostatin-positive neurons did not affect the acquisition of tone fear memory (Figure III. 4. B, E) and memory recall in recent (Figure III. 4. C, F) and remote (Figure III. 4. D, G) tone fear memory tests. Therefore, it is plausible that Arc/Arg3.1 in parvalbumin-positive and somatostatin-positive neurons is not involved in the processing of tone fear memory.

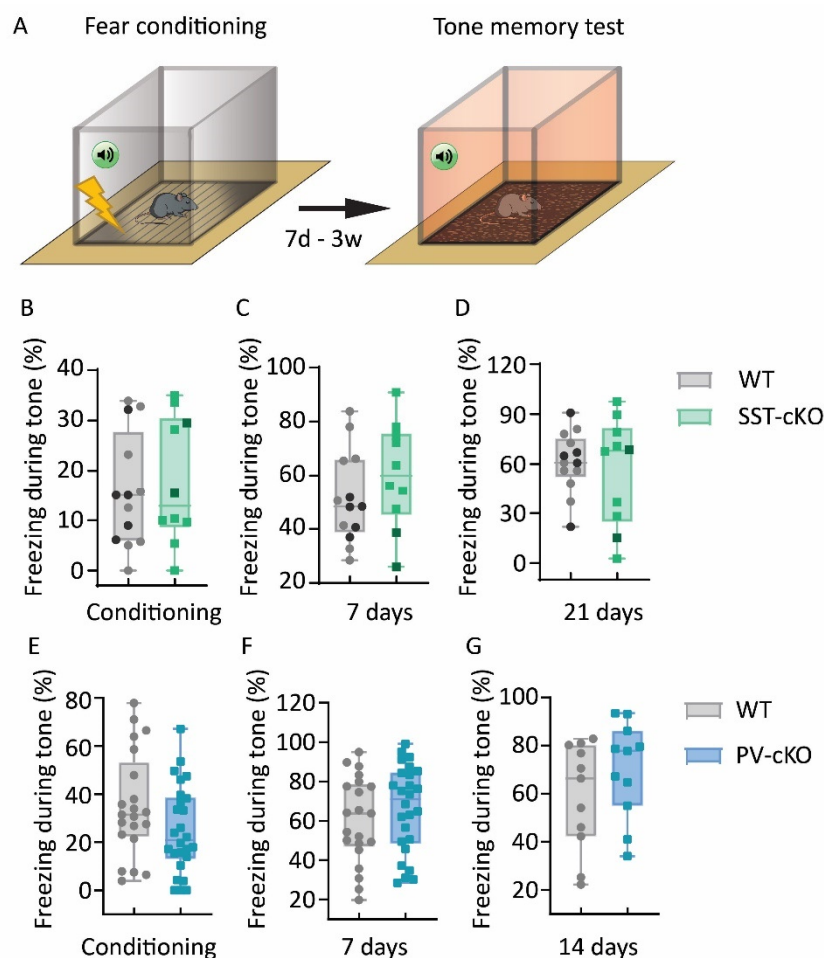


**Figure III. 4. Tone fear memory in PV-cKO mice and SST-cKO mice.** (A) Schematic of tone fear conditioning and memory test paradigm. (B) The SST-cKO mice had similar freezing levels during tone in the conditioning test (Median: WT, 15.00%; SST-cKO, 12.86%;  $p = 0.75$ , NS). (C) The SST-cKO mice had similar freezing levels in the recent fear memory test (Median: WT, 48.33%; SST-cKO, 60.00%;  $p = 0.32$ , NS) and (D) remote fear memory test (Median: WT, 60.75%; SST-cKO, 68.04%;  $p > 0.99$ , NS) 7 days and 21 days after conditioning compared to their WT littermates. All WT,  $n = 13$ ; SST-cKO,  $n = 10$ . The data points with dark green color were published in the master thesis from Frederic Beba. (E) The PV-cKO mice had similar freezing levels during tone in the conditioning test (Median: WT, 31.43%,  $n = 21$ ; PV-cKO, 20.89%,  $n = 26$ ;  $p = 0.12$ , NS). The PV-cKO mice had similar freezing levels in (F) the recent fear memory test (Median: WT, 63.75%,  $n = 21$ ; PV-cKO, 71.00%,  $n = 26$ ;  $p = 0.37$ , NS) and (G) remote fear memory test (Median: WT, 66.33%,  $n = 11$ ; PV-cKO, 77.83%,  $n = 11$ ;  $p = 0.3$ , NS) 7 days and 14 days after conditioning compared to their WT littermates. Significance was assessed with the Mann-Whitney test. The box plots showed the median (-), whiskers showed min to max, and all data points.

### **3. Assessment of the contribution of Arc/Arg3.1 in GABAergic interneurons to spatial learning and memory .**

#### **3.1. Role of Arc/Arg3.1 in parvalbumin-positive interneurons for spatial learning and memory in mice.**

In this thesis, I utilized fear conditioning and Morris water maze (MWM) tests to investigate the effects of ablation of Arc/Arg3.1 in parvalbumin (PV) positive interneurons on fear memory and spatial learning in mice. Results from fear conditioning tests showed that the fear memory and memory persistence remained unaltered in the PV-cKO mice. However, the fear conditioning test has limitations in investigating complex and protracted learning processes. Therefore, the MWM test was used to evaluate spatial learning ability in the training phases and spatial memory in the probe tests. In this test, spatial learning was evaluated in the training phases, during which the mice were trained to learn and search for a submerged, hidden platform in the opaqued water guided by the visual cues attached to the pool walls for several days. Escape latency to the platform and total distance moved were used to evaluate the spatial learning ability during the training. Spatial memory was assessed in the probe tests by removing the submerged, hidden platform in the pool.

During the training (Figure III. 5. A), PV-cKO mice and their WT littermates showed different learning curves (Figure III. 5. C, D), and similar thigmotaxis behavior (Figure III. 5. E) during the training days. A weak tendency of the PV-cKO mice to slower swimming velocities (Figure III. 5. F) compared to their WT littermates was not statistically significant. However, the WT and PV-cKO mice performed similar strategies when searching for the hidden platform (Figure III. 5. B).



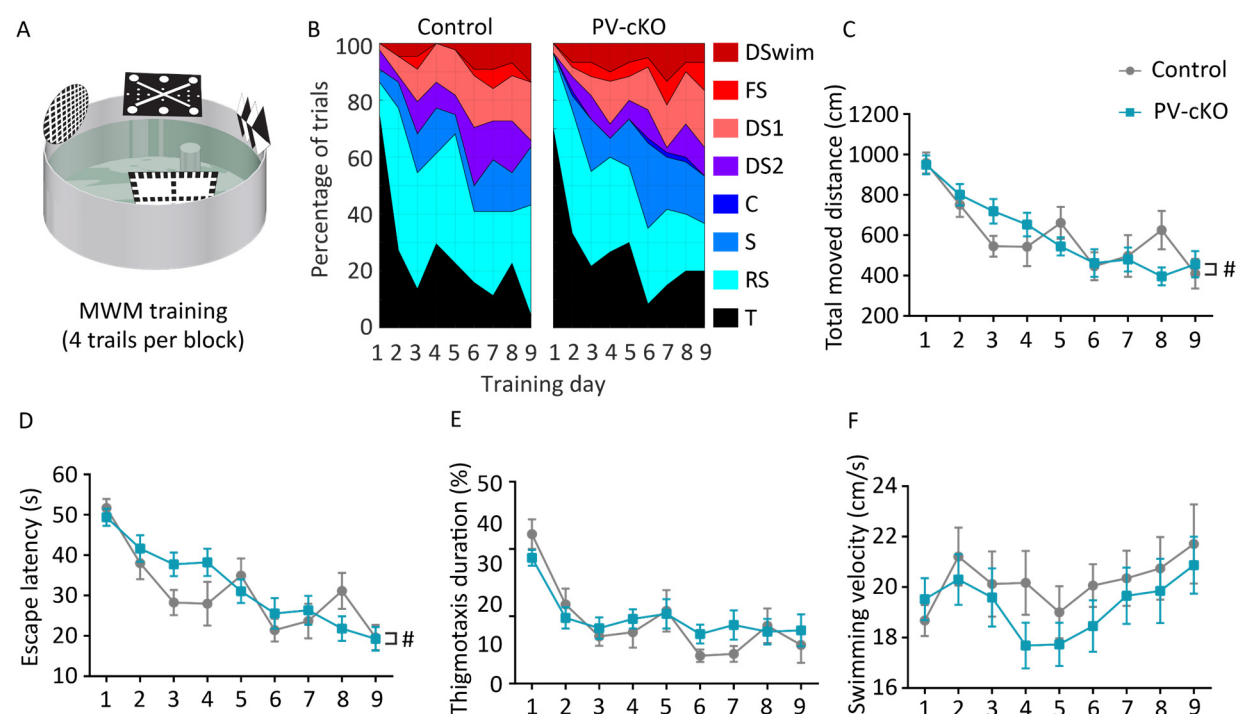


**Figure III. 5. Intact spatial learning in PV-cKO mice.** (A) Schematic of Morris water maze (MWM) training. (B) Analysis of search strategies in WT and PV-cKO mice scored as the percentage of trials for each defined strategy following 9 d of training. Similar progression of navigational strategy was observed in both groups.  $\chi^2$  test of independence for grouped strategies as color-coded ( $\chi^2_{(7)} = 5.868$ ,  $P = 0.553$ , NS). C, chaining; DS1, directional search; DS2, directed search; DSwim, direct swim; FS, focal search; RS, random search; S, scanning; T, thigmotaxis. (C, D) PV-cKO mice showed a different learning curve from their WT littermates as indicated by total moved distance (B, genotype  $F_{(1,24)} = 0.0023$ ,  $p = 0.96$ , NS; block  $F_{(5.7,136.7)} = 16.2$ ,  $p < 0.001$ ; interaction  $F_{(8,192)} = 2.03$ , # $p < 0.05$ ) and escape latency (C, genotype  $F_{(1,24)} = 0.322$ ,  $p = 0.576$ , NS; block  $F_{(5.37,128.8)} = 19.2$ ,  $p < 0.001$ ; interaction  $F_{(8,192)} = 2.12$ , # $p < 0.05$ ) to the submerged platform. (D) PV-cKO mice displayed continuously decreasing thigmotactic swimming as well as their WT littermates (Genotype  $F_{(1,24)} = 0.111$ ,  $p = 0.74$ , NS; block  $F_{(4.34,104.2)} = 17.96$ ,  $p < 0.001$ ; interaction  $F_{(8,192)} = 1.487$ ,  $p = 0.164$ , NS). (E) Slightly slower swimming of PV-cKO mice was not significantly different from WT littermates (genotype  $F_{(1,24)} = 0.5872$ ,  $p = 0.45$ , NS; block  $F_{(4.489,107.7)} = 3.207$ ,  $p < 0.05$ ; interaction  $F_{(8,192)} = 0.73$ ,  $p = 0.45$ , NS). All WT,  $n = 11$ ; PV-cKO,  $n = 15$ . Data representing the mean  $\pm$  S.E.M. Significance was assessed with a two-way ANOVA with a mixed-effects model and a post hoc Bonferroni test.

The probe test was first performed in the PV-cKO mice 1 day after the training sessions on day 10 (Figure III. 6. A). Results showed that PV-cKO mice had an intact 1-day spatial memory as their performance during the learning sessions was indistinguishable from their WT littermates. Both PV-cKO mice and their WT littermates displayed a preference for searching the submerged platform location in the target quadrant (Figure III. 6. B) or target zone (Figure III. 6. D). Furthermore, the significantly higher crossings of the target zone (Figure III. 6. C) indicated that PV-cKO mice, like their WT-littermates, formed a precise representation of the platform location and retrieved it. Averaged heatmaps exemplify the accuracy of platform search by WT and PV-cKO mice (Figure III. 6. E).

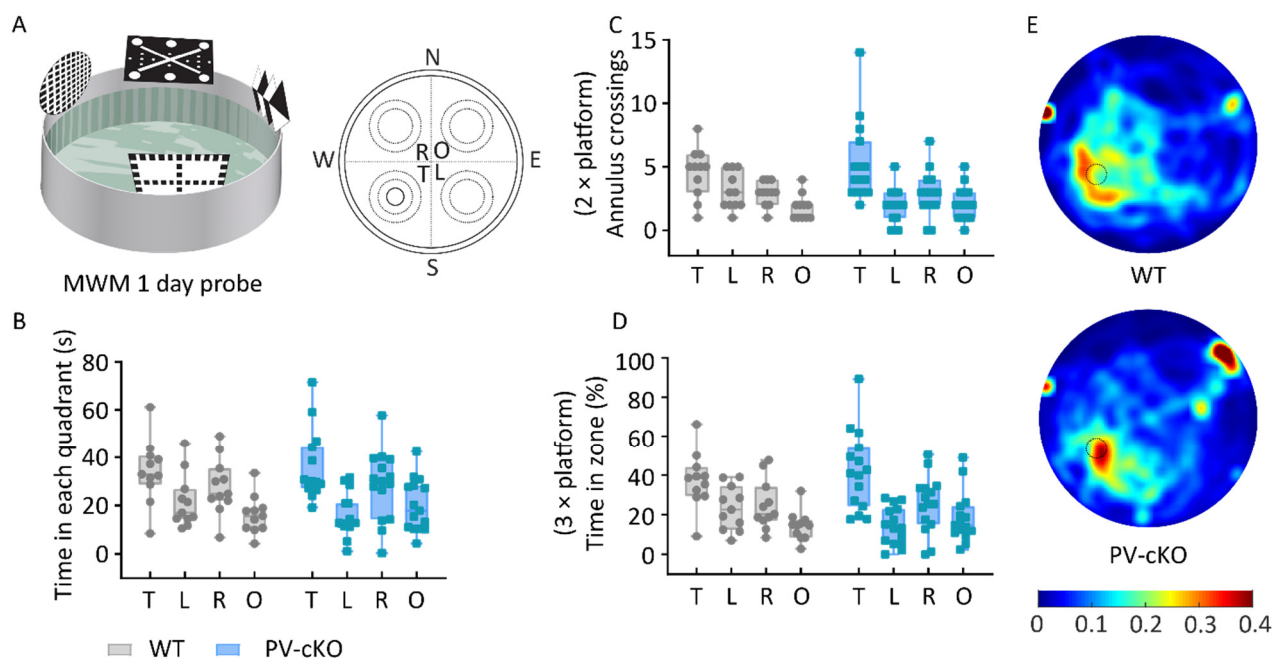


**Figure III. 6. Indistinguishable spatial memory in PV-cKO mice 1 day after training.** (A) Schematic of Morris water maze (MWM) probe test and analysis arenas. PV-cKO mice showed indistinguishable spatial memory compared with their WT littermates, which indicated by (B) spent time in each quadrant (genotype  $F_{(1,96)} = 2.45E^{-20}$ ,  $p > 0.99$ , NS; Zone  $F_{(2.15,68.73)} = 11.88$ ,  $p < 0.001$ ; interaction  $F_{(3,96)} = 0.77$ ,  $p = 0.52$ , NS), (C) annulus crossings in (2 x platform) zones (genotype  $F_{(1,96)} = 0.0262$ ,  $p = 0.87$ , NS; Zone  $F_{(1.95,62.42)} = 13.04$ ,  $p < 0.001$ ; interaction  $F_{(3,96)} = 1.388$ ,  $p = 0.25$ , NS), and (D) percent time in (3 x platform) zones (genotype  $F_{(1,96)} = 3.75E^{-21}$ ,  $p > 0.99$ , NS; Zone  $F_{(2.07,66.24)} = 15.37$ ,  $p < 0.001$ ; interaction  $F_{(3,96)} = 1.378$ ,  $p = 0.256$ , NS). (E) Occupancy plots illustrate comparable search precision of the PV-cKO mice and their WT

littermates in the vicinity of the platform zone. All WT,  $n = 11$ ; PV-cKO,  $n = 15$ . Data represents the mean  $\pm$  S.E.M. Significance was assessed with a two-way ANOVA with a mixed-effects model and with a post hoc Bonferroni test. The box plots showed the median (-), whiskers showed min to max, and all data points. Occupancy plots represent the normalized mean occupancy across the maze area. Kruska-Wallis test with Dunnett post hoc test was also performed in B, C, and D to test the preference for the target quadrant within groups (Table II. 1).

In the 7-day probe test (Figure III. 7. A), both PV-cKO mice and their WT littermates showed an intact recent spatial memory (Figure III. 7. B-E). All the mice showed a preference for crossing the target zone (Figure III. 7. C) and searching in the target quadrant (Figure III. 7. B). Both PV-cKO mice and their WT littermates preferred searching the target zone (Figure III. 7. D) instead of the entire pool, indicating that they maintained a relatively precise spatial representation of the platform location 7 days after training (Figure III. 7). Notably, the PV-cKO mice displayed more accurate memory around the platform target area than their WT littermates, as shown by the average occupancy heat maps (Figure III. 7. E).

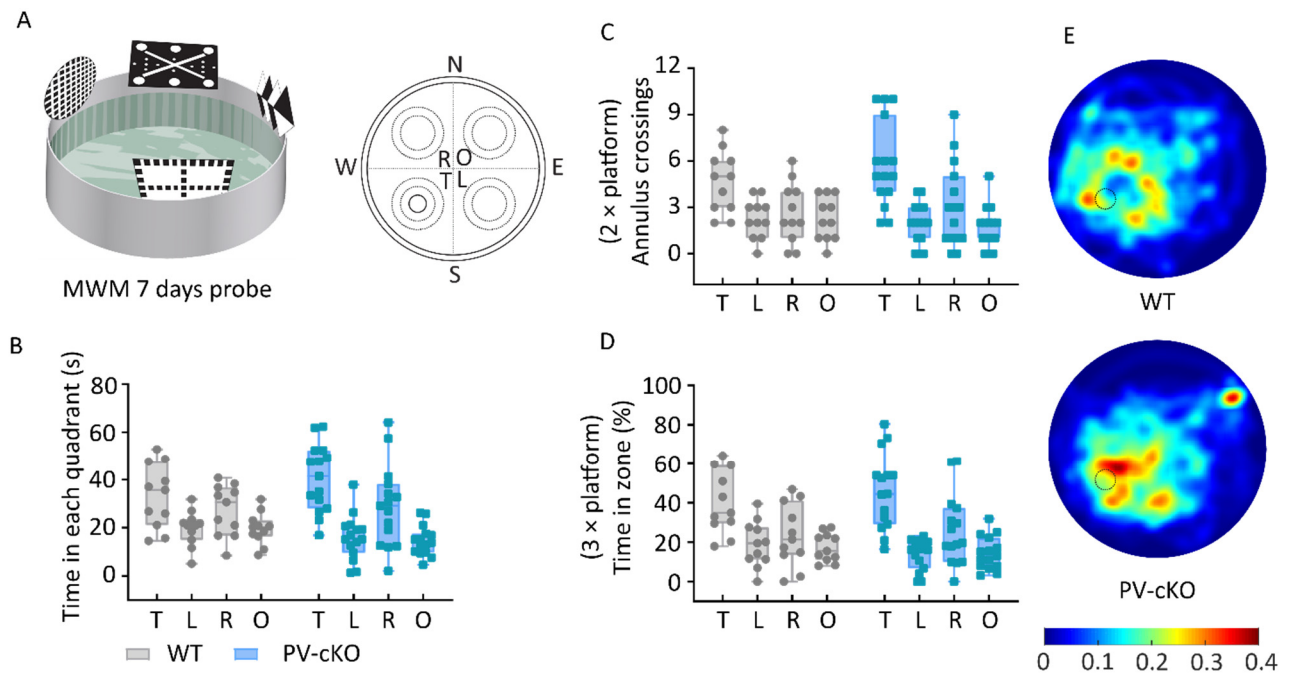


**Figure III. 7. Indistinguishable spatial memory in PV-cKO mice 7 days after training.** (A) Schematic of Morris water maze (MWM) probe test and analysis arenas. PV-cKO mice showed indistinguishable spatial memory compared with their WT littermates, which indicated by (B) time spent in each quadrant (genotype  $F_{(1,96)} = 5.42E^{-20}$ ,  $p > 0.99$ , NS; Zone  $F_{(1.68,53.74)} = 17.30$ ,  $p < 0.001$ ; interaction  $F_{(3,96)} = 1.62$ ,  $p = 0.19$ , NS), (C) annulus crossings in 2 x zones (genotype  $F_{(1,96)} = 0.17$ ,  $p = 0.68$ , NS; Zone  $F_{(1.89,60.38)} = 14.74$ ,  $p < 0.001$ ; interaction  $F_{(3,96)} = 1.04$ ,  $p = 0.38$ , NS), and (D) percent time in 3 x zones (genotype  $F_{(1,96)} = 7.65E^{-21}$ ,  $p > 0.99$ , NS; Zone  $F_{(1.76,56.32)} = 21.34$ ,  $p < 0.001$ ; interaction  $F_{(3,96)} = 0.83$ ,  $p = 0.483$ , NS). (E) Occupancy plots illustrate comparable search precision of the PV-cKO mice and their WT littermates in the vicinity of the platform zone. All WT,  $n = 11$ ; PV-cKO,  $n = 15$ . Data represents the mean  $\pm$  S.E.M. Significance was assessed with a two-way ANOVA with a mixed-effects model and with a post hoc Bonferroni test. The box plots showed the median (-), whiskers showed min to max, and all data points. Occupancy plots represent the normalized mean occupancy across the maze area. Kruska-Wallis test with Dunnett post hoc test was also performed in B, C, and D to test the preference for the target quadrant within groups (Table II. 1).

In the remote spatial memory probe test (Figure III. 8. A), both PV-cKO mice and their WT littermates still showed enduring intact spatial memory (Figure III. 8. B-E) 21 days after training. All the mice showed a preference for crossing the target zone (Figure III. 8. C) and searching in

the target quadrant (Figure III. 8. B). Both PV-cKO mice and their WT littermates preferred searching the target zone (Figure III. 8. D) instead of the entire pool, indicating the PV-cKO mice and their WT littermates maintained a relatively precise spatial representation of the platform location 21 days after training (Figure III. 8). Interestingly, the PV-cKO mice still displayed a more precise memory around the platform target area compared with their WT littermates as it showed in the average occupancy heat maps (Figure III. 8. E).

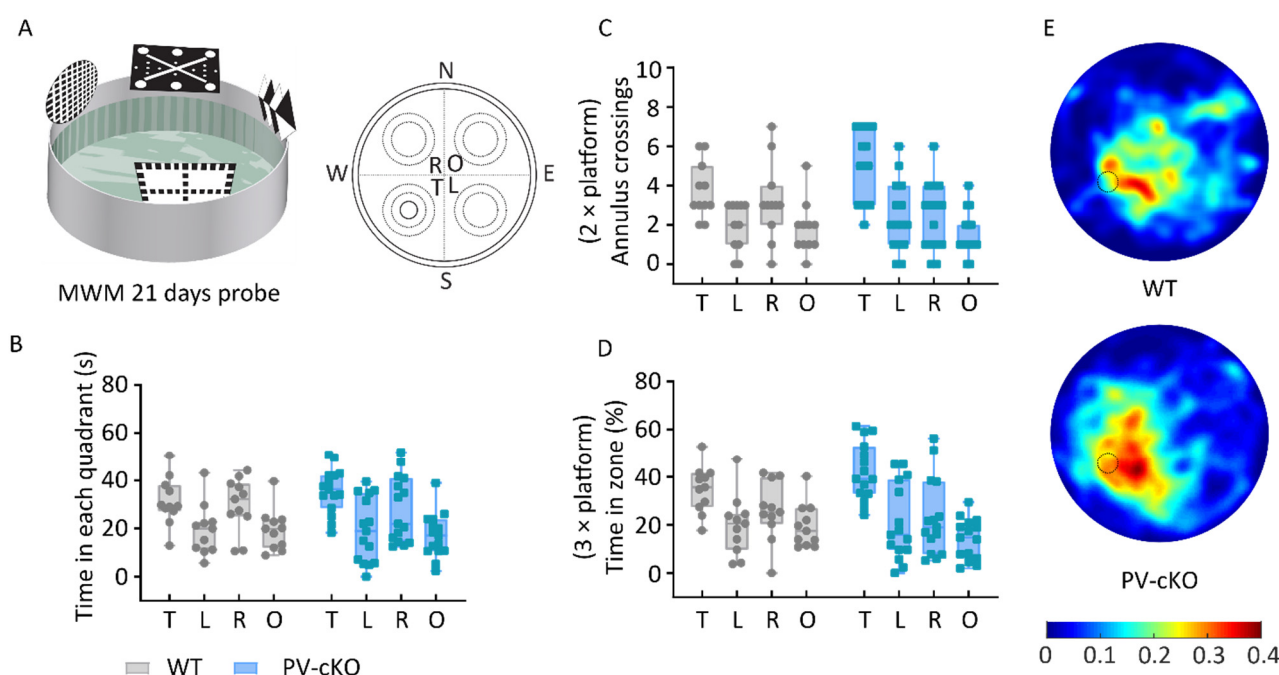


**Figure III. 8. Indistinguishable spatial memory in PV-cKO mice 21 days after training.** (A) Schematic of Morris water maze (MWM) probe test and analysis arenas. PV-cKO mice showed indistinguishable spatial memory compared with their WT littermates, which indicated by (B) spent time in each quadrant (genotype  $F_{(1,96)} = 4.67E^{-21}$ ,  $p > 0.99$ , NS; Zone  $F_{(2.05,65.72)} = 11.42$ ,  $p < 0.001$ ; interaction  $F_{(3,96)} = 0.47$ ,  $p = 0.70$ , NS), (C) annulus crossings in 2 x zones (genotype  $F_{(1,96)} = 0.37$ ,  $p = 0.55$ , NS; Zone  $F_{(2.47,79.01)} = 14.16$ ,  $p < 0.001$ ; interaction  $F_{(3,96)} = 2.16$ ,  $p = 0.097$ , NS), and (D) percent time in 3 x zones (genotype  $F_{(1,96)} = 1.21E^{-22}$ ,  $p > 0.99$ , NS; Zone  $F_{(2.21,70.86)} = 14.72$ ,  $p < 0.001$ ; interaction  $F_{(3,96)} = 1.23$ ,  $p = 0.304$ , NS). (E) Occupancy plots illustrate comparable search precision of the PV-cKO mice and their WT littermates in the vicinity of the platform zone. All WT,  $n = 11$ ; PV-cKO,  $n = 15$ . Data represents the mean  $\pm$  S.E.M. Significance was assessed with a two-way ANOVA with a mixed-effects model and with a post hoc Bonferroni test. The box plots showed the median (-), whiskers showed min to max, and all

data points. Occupancy plots represent the normalized mean occupancy across the maze area. Kruska-Wallis test with Dunnett post hoc test was also performed in B, C, and D to test the preference for the target quadrant within groups (Table II. 1).

**Table III. 1. Kruska-Wallis test within WT and PV-cKO groups.**

MWM probe trial tests for WT and PV-cKO groups				Kruskal-Wallis test with Dunn's multiple comparison			
Days	Groups	WT		Dunn's multiple comparisons p value			Figure
		p	n	T vs. O	T vs. L	T vs. R	
1 day	Time in quadrant	0.0049	11	0.003	0.060	> 0.999	Figure III. 6. B
	Time in zone	0.0044	11	0.003	0.0087	0.080	Figure III. 6. D
	Annulus crossings	0.0029	11	0.0006	0.263	0.204	Figure III. 6. C
7 day	Time in quadrant	0.0295	11	0.028	0.072	> 0.999	Figure III. 7. B
	Time in zone	0.0044	11	0.003	0.009	0.080	Figure III. 7. D
	Annulus crossings	0.0247	11	0.027	0.027	0.086	Figure III. 7. C
21 day	Time in quadrant	0.0079	11	0.029	0.028	> 0.999	Figure III. 8. B
	Time in zone	0.0062	11	0.005	0.014	0.406	Figure III. 8. D
	Annulus crossings	0.0082	11	0.008	0.034	> 0.999	Figure III. 8. C
Days	Groups	PV-cKO		Dunn's multiple comparisons p value			Figure
		p	n	T vs. O	T vs. L	T vs. R	
1 day	Time in quadrant	0.0013	15	0.019	0.002	> 0.999	Figure III. 6. B
	Time in zone	< 0.0001	15	< 0.0001	< 0.0001	0.042	Figure III. 6. D
	Annulus crossings	0.0002	15	0.0007	0.0001	0.0508	Figure III. 6. C
7 day	Time in quadrant	< 0.0001	15	< 0.0001	0.0001	0.180	Figure III. 7. B
	Time in zone	< 0.0001	15	< 0.0001	< 0.0001	0.042	Figure III. 7. D
	Annulus crossings	0.0001	15	< 0.0001	0.0007	0.020	Figure III. 7. C
21 day	Time in quadrant	0.0006	15	0.0005	0.0036	0.277	Figure III. 8. B
	Time in zone	< 0.0001	15	< 0.0001	0.002	0.006	Figure III. 8. D
	Annulus crossings	< 0.0001	15	< 0.0001	0.0001	0.0001	Figure III. 8. C

In the cued version of the Morris water maze (MWM) test (Figure III. 9. A), PV-cKO mice and their WT littermates located the flagged platform with similar latencies to the platform (Figure III. 9. C) and moved distance (Figure III. 9. B) as their WT littermates. The thigmotaxic time (Figure III. 9. D) and swimming velocity (Figure III. 9. E) were also comparable in PV-cKO mice and their WT littermates, indicating normal visual and motor functions as well as distance-based navigation (Figure III. 9).

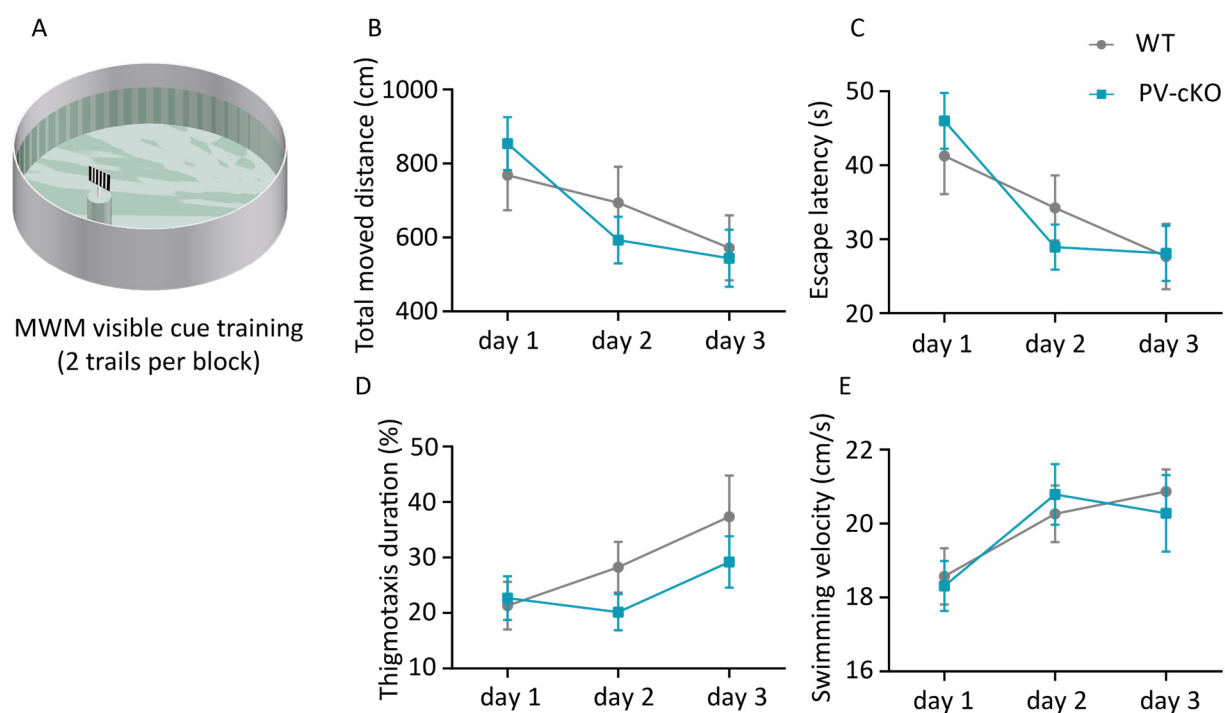


**Figure III. 9. Unaltered spatial cue learning in PV-cKO mice.** (A) Schematic of Morris water maze (MWM) cue training. Intact navigation to a cued platform in PV-cKO mice and their WT littermates is evident from comparable (B) total moved distance (genotype  $F_{(1,24)} = 0.03$ ,  $p = 0.86$ , NS; block  $F_{(1.88,45.22)} = 6.77$ ,  $p < 0.01$ ; interaction  $F_{(2,48)} = 0.89$ ,  $p = 0.41$ , NS) (C) escape latency to the platform (genotype  $F_{(1,24)} = 0.00012$ ,  $p = 0.99$ , NS; block  $F_{(1.868,44.84)} = 9.45$ ,  $p < 0.001$ ; interaction  $F_{(2,48)} = 0.88$ ,  $p = 0.42$ , NS), percentage of thigmotaxis duration (genotype  $F_{(1,24)} = 1.01$ ,  $p = 0.32$ , NS; block  $F_{(1.62,38.87)} = 4.65$ ,  $p < 0.05$ ; interaction  $F_{(2,48)} = 0.98$ ,  $p = 0.38$ , NS), and (E) swimming velocity (genotype  $F_{(1,24)} = 0.0012$ ,  $p = 0.91$ , NS; block  $F_{(1.729,41.49)} = 9.32$ ,  $p < 0.001$ ; interaction  $F_{(2,48)} = 0.52$ ,  $p = 0.60$ , NS). All WT,  $n = 11$ ; PV-cKO,  $n = 15$ . Data representing the mean  $\pm$  S.E.M. Significance was assessed with a two-way ANOVA with a mixed-effects model and a post hoc Bonferroni test.

Overall, the experiments suggested that the removal of Arc/Arg3.1 from parvalbumin-positive interneurons does not significantly affect spatial learning and memory in the Morris water maze in mice.



### 3.2. Role of Arc/Arg3.1 in somatostatin-positive interneurons for spatial memory in mice.

The results of the fear conditioning tests demonstrated that deletion of Arc/Arg3.1 in proximately 78% of SST interneurons leads to increased memory generalization (Figure II. 6). However, it remains unknown whether other forms of learning and memory might be affected. To address this question, I tested the SST-cKO mice in the Morris water maze (MWM).

During the training (Figure III. 10. A), the SST-cKO mice and their WT littermates showed comparable learning curves (Figure III. 10. C, D) but different thigmotaxis behavior (Figure III. 10. E) during the training days. However, the WT and SST-cKO mice performed similar strategies when searching for the hidden platform (Figure III. 10. B). Although the SST-cKO mice occasionally displayed higher swimming velocities (Figure III. 10. F) compared to their WT littermates, the difference was overall, not significant.

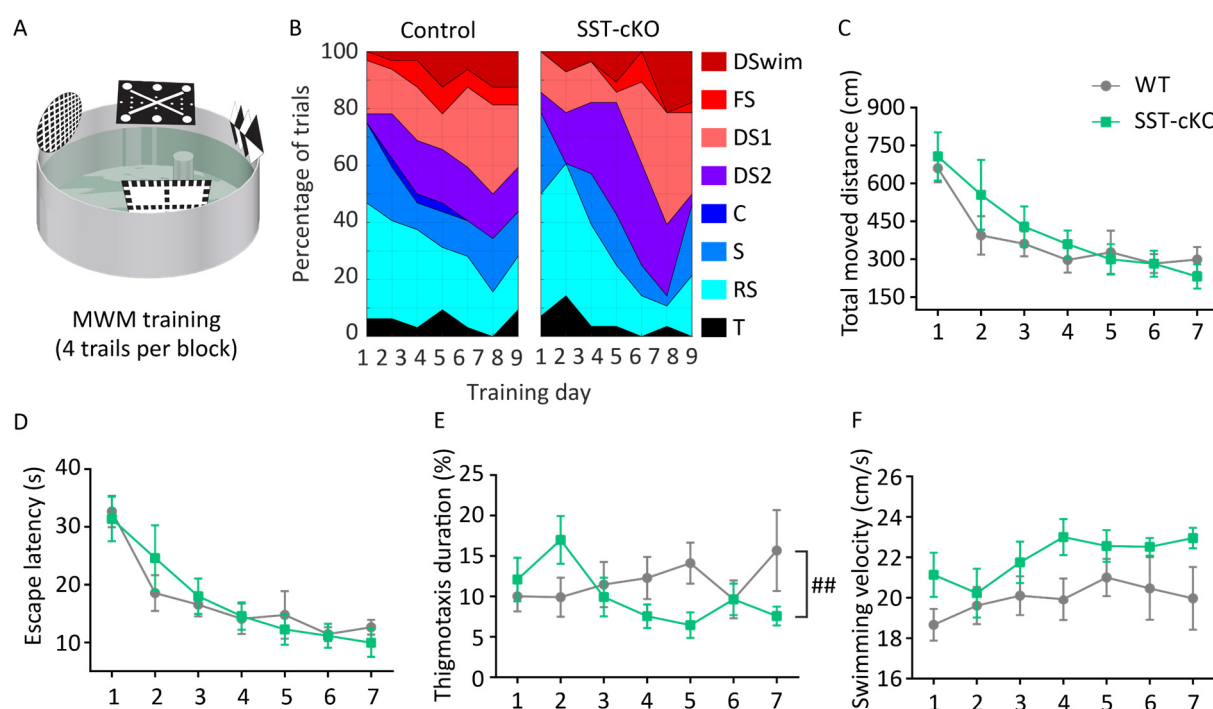


**Figure III. 10. Intact spatial learning in SST-cKO mice.** (A) Schematic of Morris water maze (MWM) training. (B) Analysis of search strategies in WT and SST-cKO mice scored as the percentage of trials for each defined strategy following 7 d of training. Similar progression of navigational strategy was observed in both groups.  $\chi^2$  test of independence for grouped strategies as color-coded ( $\chi^2_{(6)} = 6.524$ ,  $P = 0.367$ , NS). C, chaining; DS1, directional search; DS2, directed search; DSwim, direct swim; FS, focal search; RS, random search; S, scanning; T, thigmotaxis.



thigmotaxis. (C, D) SST-cKO mice showed an indistinguishable learning curve from their WT littermates as indicated by total moved distance (C, genotype  $F_{(1,13)} = 0.46$ ,  $p = 0.51$ , NS; block  $F_{(2.67,34.66)} = 10.27$ ,  $p < 0.001$ ; interaction  $F_{(6,78)} = 0.66$ ,  $p = 0.680$ , NS) and escape latency (D, genotype  $F_{(1,13)} = 0.0071$ ,  $p = 0.93$ , NS; block  $F_{(2.80,36.45)} = 14.60$ ,  $p < 0.001$ ; interaction  $F_{(6,78)} = 0.60$ ,  $p = 0.731$ , NS) to the submerged platform. (E) WT mice maintained a different thigmotactic swimming percentage over training days, while SST-cKO mice started at higher levels but subsequently decreased a 2-way ANOVA shows a significant interaction difference (genotype  $F_{(1,13)} = 0.59$ ,  $p = 0.46$ , NS; block  $F_{(3.10,40.27)} = 0.70$ ,  $p = 0.56$ ; interaction  $F_{(6,78)} = 3.14$ ,  $###p < 0.01$ ). (F) Slightly faster swimming of SST-cKO mice was not significantly different from WT littermates (genotype  $F_{(1,13)} = 3.43$ ,  $p = 0.08$ , NS; block  $F_{(1.96,52.45)} = 2.20$ ,  $p = 0.13$ ; interaction  $F_{(6,78)} = 0.68$ ,  $p = 0.66$ , NS). All WT,  $n = 8$ ; PV-cKO,  $n = 7$ . Data representing the mean  $\pm$  S.E.M. Significance was assessed with a two-way ANOVA with a mixed-effects model and a post hoc Bonferroni test.

The probe test was conducted on the SST-cKO mice 1 day after the training sessions (Figure III. 11. A). The results showed that both the SST-cKO mice and their WT littermates persistently searched for the submerged platform in the target quadrant (Figure III. 11. B) or target zone (Figure III. 11. D). Furthermore, significantly higher crossings of the target zone (Figure III. 11. C), compared to other virtual zones, indicated that both WT and SST-cKO mice were able to form an accurate representation of the platform location. Further exemplified by the similar average occupancy heat maps (Figure III. 11. E). In total, the SST-cKO mice demonstrated an intact 1-day spatial memory.

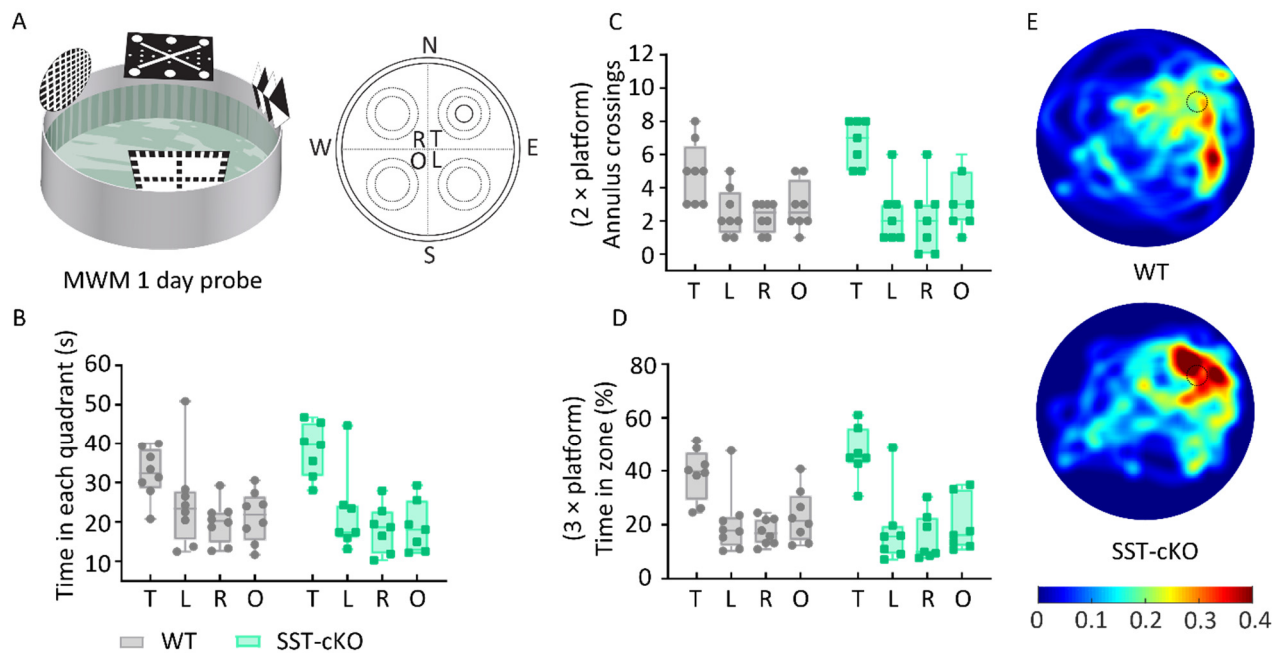


**Figure III. 11. Indistinguishable spatial memory in SST-cKO mice 1 day after training.** (A) Schematic of Morris water maze (MWM) probe test and analysis arenas. SST-cKO mice showed indistinguishable spatial memory compared with their WT littermates, which indicated by (B) spent time in each quadrant (genotype  $F_{(1,52)} = 0.012$ ,  $p = 0.91$ , NS; zone  $F_{(1.85,31.98)} = 13.42$ ,  $p < 0.001$ ; interaction  $F_{(3,52)} = 0.99$ ,  $p = 0.41$ , NS), (C) annulus crossings in  $2 \times$  zones (genotype  $F_{(1,52)} = 1.33$ ,  $p = 0.25$ , NS; zone  $F_{(2.85,49.39)} = 15.61$ ,  $p < 0.001$ ; interaction  $F_{(3,52)} = 1.21$ ,  $p = 0.99$ , NS), and (D) percent time in  $3 \times$  zones (genotype  $F_{(1,52)} = 5.16E^{-21}$ ,  $p > 0.99$ , NS; zone  $F_{(2.38,41.22)} = 21.16$ ,  $p < 0.001$ ; interaction  $F_{(3,52)} = 1.01$ ,  $p = 0.446$ , NS). (E) Occupancy plots illustrate comparable search precision of the SST-cKO mice and their WT littermates in the vicinity of the platform zone. All WT,  $n = 8$ ; SST-cKO,  $n = 7$ . Data represents the mean  $\pm$  S.E.M. Significance was assessed with a two-way ANOVA with a mixed-effects model and with a post hoc Bonferroni test. The box plots showed the median (-), whiskers showed min to max, and all data points. Occupancy plots represent the normalized mean occupancy across the maze area. Kruskal-Wallis test with Dunnett post hoc test was also performed in B, C, and D to test the preference for the target quadrant within groups (Table II. 2).

In the 7-day probe test (Figure III. 12. A), the SST-cKO mice and their WT littermates showed enduring intact recent spatial memory (Figure III. 12. B-E). All mice showed a preference for crossing the target zone (Figure III. 12. C) and searching in the target quadrant (Figure III. 12.

B). Both WT and SST-cKO mice searched preferentially in the target zone (Figure III. 12. D), indicating that the SST-cKO mice and their WT littermates maintained a relatively precise spatial representation of the platform location 7 days after training (Figure III. 12). The SST-cKO mice and their WT littermates exhibited similar searching activities around the platform target area as shown in the average occupancy heat maps (Figure III. 12. E).

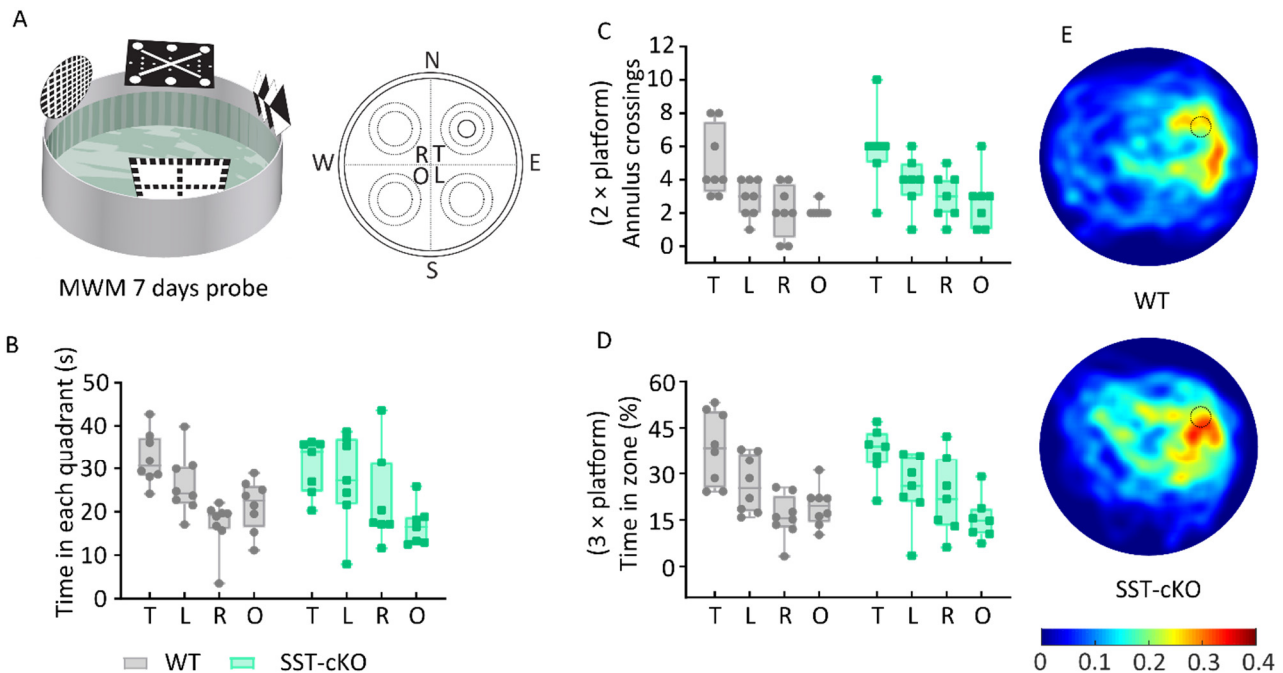


**Figure III. 12. Indistinguishable spatial memory in SST-cKO mice 7 days after training.** (A) Schematic of Morris water maze (MWM) probe test and analysis arenas. SST-cKO mice showed indistinguishable spatial memory compared with their WT littermates, which indicated by (B) spent time in each quadrant (genotype  $F_{(1,52)} = 0.0034$ ,  $p = 0.95$ , NS; zone  $F_{(1.99,34.54)} = 9.17$ ,  $p = 0.0006$ ; interaction  $F_{(3,52)} = 1.26$ ,  $p = 0.297$ , NS), (C) annulus crossings in 2 x zones (genotype  $F_{(1,52)} = 3.96$ ,  $p = 0.052$ , NS; zone  $F_{(2.50,43.33)} = 11.17$ ,  $p < 0.001$ ; interaction  $F_{(3,52)} = 0.041$ ,  $p = 0.989$ , NS), and (D) percent time in 3 x zones (genotype  $F_{(1,52)} = 4.13E^{-20}$ ,  $p > 0.99$ , NS; zone  $F_{(2.66,46.17)} = 13.93$ ,  $p < 0.001$ ; interaction  $F_{(3,52)} = 0.904$ ,  $p = 0.446$ , NS). (E) Occupancy plots illustrate comparable search precision of the SST-cKO mice and their WT littermates in the vicinity of the platform zone. All WT,  $n = 8$ ; SST-cKO,  $n = 7$ . Data represents the mean  $\pm$  S.E.M. Significance was assessed with a two-way ANOVA with mixed-effects model and with a post hoc Bonferroni test. The box plots showed the median (-), whiskers showed min to max, and all data points. Occupancy plots represent the normalized mean occupancy across the maze area.

Kruska-Wallis test with Dunnett post hoc test was also performed in B, C, and D to test the preference for the target quadrant within groups (Table II. 2).

The remote spatial memory probe test was conducted 21 days after training (Figure III. 13. A), and both the SST-cKO mice and their WT littermates demonstrated enduring intact spatial memory (Figure III. 13. B-E). All the mice showed a preference for searching in the target quadrant (Figure III. 13. B) and crossing the target zones (Figure III. 13. C. D. E), indicating the SST-cKO mice and their WT littermates maintained a relatively precise spatial representation of the platform location 21 days after training (Figure III. 13).

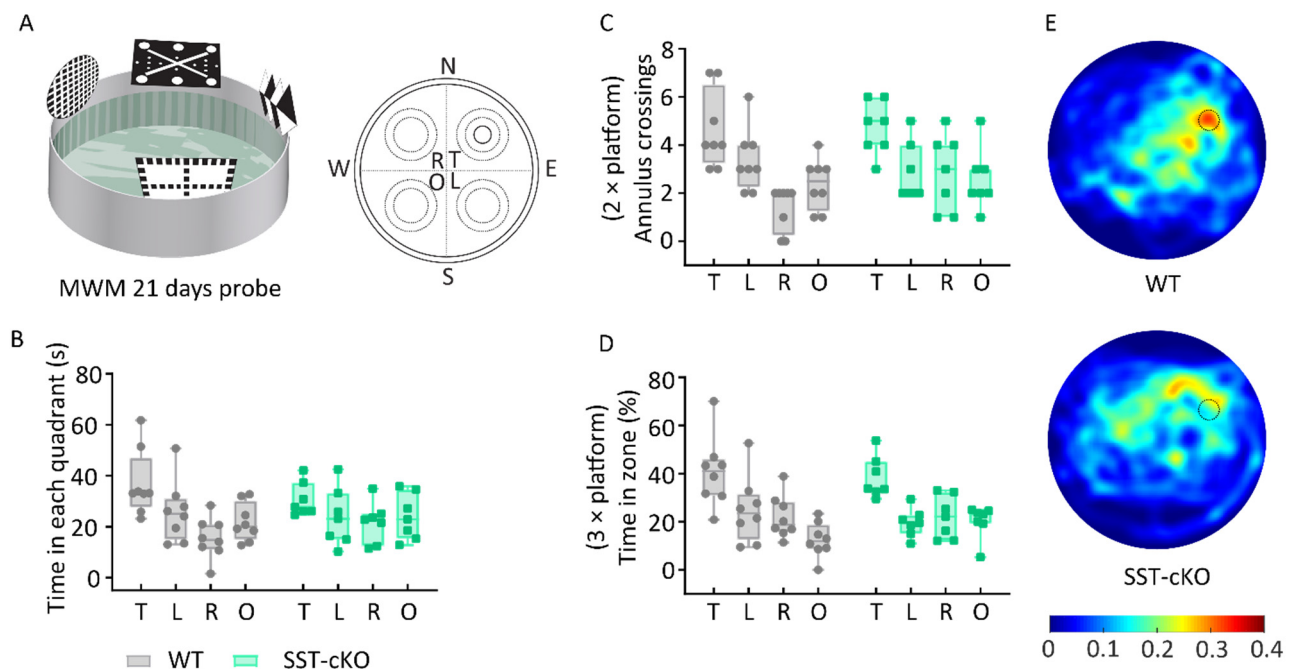


**Figure III. 13. Indistinguishable spatial memory in SST-cKO mice 21 days after training.** (A) Schematic of Morris water maze (MWM) probe test and analysis arenas. SST-cKO mice showed indistinguishable spatial memory compared with their WT littermates, which indicated by (B) spent time in each quadrant (genotype  $F_{(1,52)} = 2.44E^{-21}$ ,  $p > 0.99$ , NS; zone  $F_{(2.43,42.14)} = 6.43$ ,  $p = 0.002$ ; interaction  $F_{(3,52)} = 1.12$ ,  $p = 0.35$ , NS), (C) annulus crossings in 2 x zones (genotype  $F_{(1,13)} = 0.89$ ,  $p = 0.36$ , NS; zone  $F_{(2.60,33.78)} = 11.79$ ,  $p < 0.001$ ; interaction  $F_{(3,39)} = 1.63$ ,  $p = 0.197$ , NS), and (D) percent time in 3 x zones (genotype  $F_{(1,52)} = 8.77E^{-20}$ ,  $p > 0.99$ , NS; zone  $F_{(2.32,40.19)} = 15.33$ ,  $p < 0.001$ ; interaction  $F_{(3,52)} = 1.16$ ,  $p = 0.335$ , NS). (E) Occupancy plots illustrate comparable search precision of the SST-cKO mice and their WT littermates in the vicinity of the

platform zone. All WT,  $n = 8$ ; SST-cKO,  $n = 7$ . Data represents the mean  $\pm$  S.E.M. Significance was assessed with a two-way ANOVA with a mixed-effects model and with a post hoc Bonferroni test. The box plots showed the median (-), whiskers showed min to max, and all data points. Occupancy plots represent the normalized mean occupancy across the maze area. Kruska-Wallis test with Dunn's post hoc test was also performed in B, C, and D to test the preference for the target quadrant within groups (Table II. 2).

**Table III. 2. Kruska-Wallis test within WT and SST-cKO groups.**

MWM probe trial tests for WT and SST-cKO groups				Kruskal-Wallis test with Dunn's multiple comparison			
Days	Groups	WT		Dunn's multiple comparisons p value			Figure
		p	n	T vs. O	T vs. L	T vs. R	
1 day	Time in quadrant	0.0119	8	0.025	0.106	0.007	Figure III. 11. B
	Time in zone	0.0038	8	0.061	0.008	0.003	Figure III. 11. D
	Annulus crossings	0.0182	8	0.1006	0.024	0.016	Figure III. 11. C
7 day	Time in quadrant	0.0008	8	0.022	0.462	0.0003	Figure III. 12. B
	Time in zone	0.0019	8	0.009	0.330	0.001	Figure III. 12. D
	Annulus crossings	0.0038	8	0.002	0.148	0.0104	Figure III. 12. C
21 day	Time in quadrant	0.0033	8	0.032	0.155	0.001	Figure III. 13. B
	Time in zone	0.0015	8	0.0003	0.155	0.076	Figure III. 13. D
	Annulus crossings	0.0004	8	0.026	0.545	0.0002	Figure III. 13. C
Days	Groups	SST-cKO		Dunn's multiple comparisons p value			Figure
		p	n	T vs. O	T vs. L	T vs. R	
1 day	Time in quadrant	0.0041	7	0.008	0.031	0.004	Figure III. 11. B
	Time in zone	0.0041	7	0.049	0.0104	0.003	Figure III. 11. D
	Annulus crossings	0.0048	7	0.054	0.009	0.004	Figure III. 11. C
7 day	Time in quadrant	0.0313	7	0.021	> 0.999	0.273	Figure III. 12. B
	Time in zone	0.0113	7	0.003	0.273	0.104	Figure III. 12. D
	Annulus crossings	0.0276	7	0.018	0.377	0.044	Figure III. 12. C
21 day	Time in quadrant	0.1508	7	0.380	0.273	0.089	Figure III. 13. B
	Time in zone	0.0023	7	0.009	0.002	0.017	Figure III. 13. D
	Annulus crossings	0.0356	7	0.028	0.072	0.075	Figure III. 13. C

In the cued version of the Morris water maze (MWM) test (Figure III. 14.A), the SST-cKO mice found the flagged platform after swimming a longer distance (Figure III. 14.B), with comparable escape latencies (Figure III. 14.C) to their WT littermates. The thigmotaxic duration of SST-cKO mice (Figure III. 14. D) was similar to WT, and the swimming velocity (Figure III. 14. E) was slightly higher but not statistically significant. Given that swimming velocity was higher for the SST-cKO and that latencies on day 1 of the test were similar, it's likely that their swimming

ability was intact. Instead, their ability to switch between allosteric (submerged platform) and cued navigation (flagged platform) strategies was blunted.

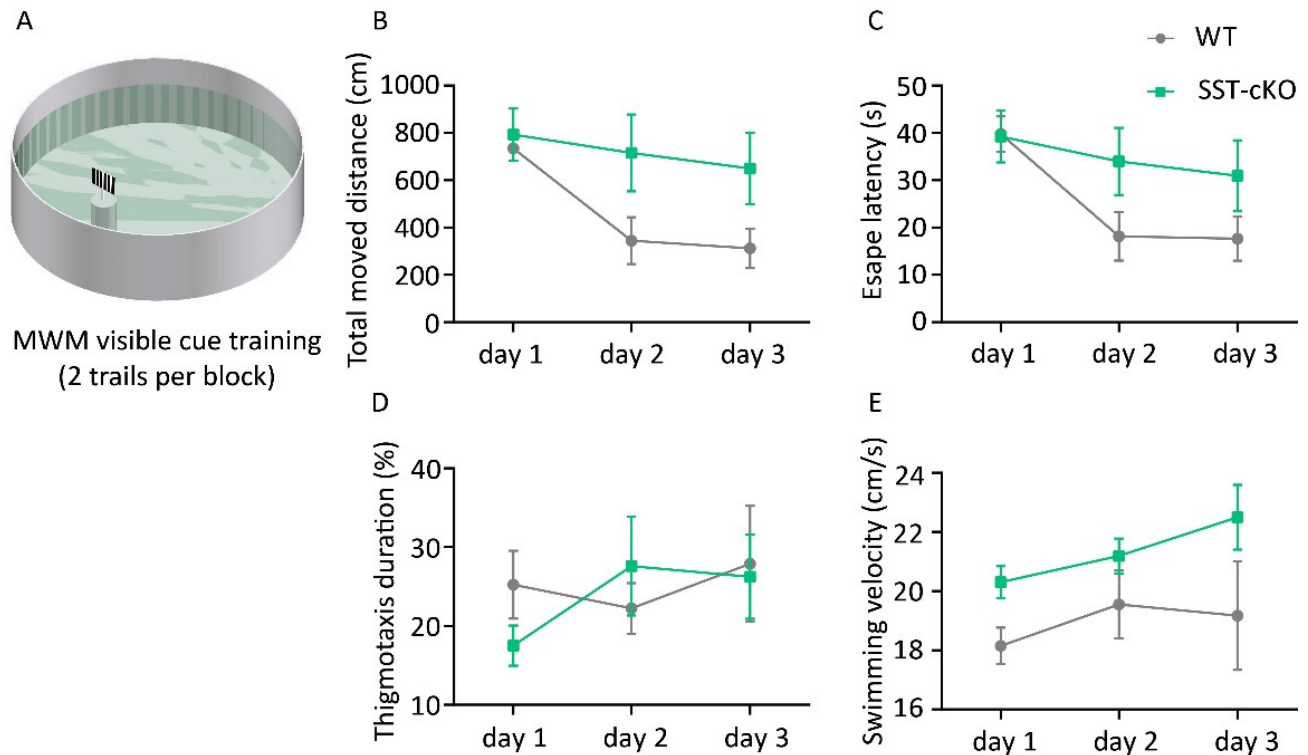


**Figure III. 14. Unaltered spatial cue learning in SST-cKO mice.** (A) Schematic of Morris water maze (MWM) cue training. Altered navigation to a cued platform in SST-cKO mice and their WT littermates is evident from (B) total distance moved (genotype  $F_{(1,13)} = 5.16$ ,  $p < 0.05$ ; block  $F_{(1.97,25.67)} = 4.87$ ,  $p < 0.05$ ; interaction  $F_{(2,26)} = 1.57$ ,  $p = 0.23$ , NS), but intact (C) escape latency to the platform (genotype  $F_{(1,13)} = 2.64$ ,  $p = 0.13$ ; block  $F_{(1.99,25.80)} = 6.38$ ,  $p < 0.01$ ; interaction  $F_{(2,26)} = 1.80$ ,  $p = 0.19$ , NS), (D) percentage of thigmotaxis duration (genotype  $F_{(1,13)} = 0.69$ ,  $p = 0.80$ ; block  $F_{(1.62,21.01)} = 0.81$ ,  $p = 0.43$ ; interaction  $F_{(2,26)} = 1.05$ ,  $p = 0.36$ , NS), and (E) swimming velocity (genotype  $F_{(1,13)} = 3.50$ ,  $p = 0.084$ ; block  $F_{(1.33,17.32)} = 2.09$ ,  $p = 0.164$ ; interaction  $F_{(2,26)} = 0.57$ ,  $p = 0.57$ , NS) were showed between SST-cKO mice and their WT littermates. All WT,  $n = 8$ ; SST-cKO,  $n = 7$ . Data representing the mean  $\pm$  S.E.M. Significance was assessed with a two-way ANOVA with a mixed-effects model and a post hoc Bonferroni test.

In summary, the experiments suggested that the removal of Arc/Arg3.1 from somatostatin-positive interneurons does not significantly affect spatial learning and memory in the Morris

water maze in mice, but may decrease cognitive flexibility upon changing from reference to cued navigation.

## Discussion





Our previous study revealed that deleting Arc/Arg3.1 in the germline or in CaMKII $\alpha$ -positive cells during the first 7 postnatal days but not after P21 specifically impaired spatial learning and oscillatory activity in adult mice (Xiaoyan Gao et al., 2018). These results were interpreted to indicate a critical period in the development of hippocampus-dependent learning functions. The same study revealed that long-term spatial and contextual memories were impaired in all KO lines, demonstrating the constant requirement of Arc/Arg3.1 consolidation for declarative memories. In the current study I asked whether Arc/Arg3.1 expression in specific inhibitory populations, the PV- and SST neurons, is required for learning and memory. I generated PV-cKO mice, and using RNAScope technology, I revealed Arc/Arg3.1 expression exclusive to PV neurons of the TRN. Somatostatin neurons displayed Arc/Arg3.1 expression in a couple of brain regions, most abundantly in the LS and least in the HPC. The PV-cKO mice displayed a near complete deletion of Arc/Arg3.1 in TRN PV neurons and SST-cKO mice lost Arc/Arg3.1 in most of LS SST neurons. Despite the extensive ablation of Arc/Arg3.1 in PV-cKO and SST-cKO mice, they showed normal spatial learning and memory in the Morris water maze. The slower learning of SST-cKO after switching to the cued-platform test could indicate cognitive inflexibility. In episodic memory tests, PV-cKO and SST-cKO mice exhibited normal contextual memory. However, SST-cKO mice had impaired memory discrimination in recent but not remote context tests. It has been observed that SST is expressed in various regions of the brain, including the LS where it is found to be colocalized with CaMKII $\alpha$  (Kuku, 2020). Additionally, the first part of this thesis indicated that acute ablation of Arc/Arg3.1 in SST/CaMKII $\alpha$  positive interneurons in the LS leads to a deficit in recent memory discrimination. This suggests that Arc/Arg3.1 in SST-positive interneurons might be involved in modulating recent memory discrimination in mice.

SST and PV neurons constitute the majority of GABAergic neurons in the forebrain. However, the expression of Arc/Arg3.1 in other GABAergic subtypes was not excluded in this study. Other inhibitory subtypes include calretinin, calbindin, and NYP, and the effects of Arc/Arg3.1 on learning and memory via these might be possible.

It has been reported that hippocampal SST-positive neurons are dysfunctional and modulate memory deficits in Alzheimer's disease model mice. (Schmid et al., 2016). Optical inactivating CA1 dendrite-targeting SST-positive neurons impaired fear learning (Lovett-Barron et al., 2014). Optogenetic (Zicho et al., 2023) or pharmacogenetic (Delorme et al., 2021) inhibition of the

SST-positive neurons in the DG both impaired the consolidation of fear memory. However, this part of my thesis demonstrated that Arc/Arg3.1 in SST-positive neurons mainly contributed to fear memory discrimination instead of other memory processes or spatial memory in mice. The second part of the thesis indicated that Arc/Arg3.1 colocalized with SST-positive neurons in the cortical regions and SST-positive neurons in the prefrontal cortex (PFC). However, a previous study indicated that acute ablation Arc/Arg3.1 in the anterior cingulate cortex (ACC) or PFC did not affect fear memory discrimination in mice (Xiaoyan Gao, 2016). A detailed study from our group (Kuku, 2020) and my results demonstrated that the lateral septum (LS) is another memory-relevant brain region rich in SST neurons. The activation of hippocampal-lateral septum circuitry was reported to play a crucial part in memory discrimination (Besnard et al., 2020; Besnard & Sahay, 2021). In contextual and spatial memory learning tasks, optical inhibition of DG SST-positive neurons disrupted the discrimination of similar memories (Morales et al., 2021). Furthermore, it is important to note that dysfunction of the plasticity of GABAergic interneurons contributes to cognitive impairments and memory deficits (Honore et al., 2021; Morales et al., 2021). Arc/Arg3.1, as a key protein for synaptic plasticity (Link et al., 1995; Plath et al., 2006; Tzingounis & Nicoll, 2006), could mediate the plasticity in SST-positive neurons or modulate the activity of other neurons that receive SST-positive neuronal projection in the brain. In the first part of the thesis, the specific ablation of Arc/Arg3.1 in LS in adult mice leads to a deficit of fear memory discrimination as well. Thus, the results suggest that Arc/Arg3.1 in SST-positive neurons in LS may modulate fear memory discrimination in mice.

## **Summary and outlook**



Since its discovery in 1995, Arc/Arg3.1 had become a prime benchmark for probing learning and memory in the brain. The ability of Arc/Arg3.1 to mediate and modulate a diverse range of plasticity processes provides a wide basis for understanding molecular, cellular, structural and network mechanisms underlying learning memory. The specificity of Arc/Arg3.1 to learning and memory processes also provides a unique opportunity to interfere with these via genetic manipulations of the gene without disrupting fundamental neural or synaptic function. The predominance of Arc/Arg3.1 expression in glutamatergic neurons in the forebrain placed this subtype at the forefront of Arc/Arg3.1 research. Indeed, deletions of the gene in CaMKII-expressing neurons, the majority of which are glutamatergic, revealed profound loss of learning and memory of all types: procedural, implicit and explicit. However, alongside glutamatergic neurons, a rarer expression of Arc/Arg3.1 was observed in GABAergic neurons. Recently, our group has mapped this expression to unique nuclei in the brain, where GABAergic cell types, including somatostatin and parvalbumin neurons, can express Arc/Arg3.1 under baseline conditions and greatly upregulate this expression after strong stimuli. The role of these Arc/Arg3.1 expressing GABAergic neurons in behavior remained entirely unknown. In this thesis, I undertook to explore this question. I first mapped Arc/Arg3.1 expression in the mouse brain following memory acquisition and recall and identified a major upregulation of the gene and protein in the lateral septum, a GABAergic nucleus involved in emotional regulation. Next, I traced a major pathway linking the dCA1 of the hippocampus, a key hub of explicit memories, with GABAergic neurons in the lateral septum. I manipulated neural activity and Arc/Arg3.1 expression in each region and investigated explicit and implicit fear memory. Finally, I studied neural activity in the circuit as the basis for the memory effects. The results showed that optical inhibition of neural activity in the dCA1-LS circuit diminishes context discrimination and downregulates Arc/Arg3.1 while exacerbating implicit fear memory. In turn, the deletion of Arc/Arg3.1 in this circuit resulted in the identical loss of context discrimination combined with excessive implicit fear memory and blunted IEG expression. In-vivo electrophysiological recordings demonstrated that Arc/Arg3.1 deletion modulated neuronal firing rates, network oscillations and inter-areal communication, reflecting disturbed GABAergic function. These findings reveal that the specificity of explicit memory relies on the dCA1-LS circuit and is guaranteed by the formation of two Arc/Arg3.1-expressing engrams: a glutamatergic one in the hippocampus and a GABAergic in the LS. The role of activity in dCA1 is to upregulate Arc/Arg3.1 locally, and via the monosynaptic projection, also in the LS. Arc/Arg3.1 expression provokes

long-lasting changes in neural activity in both engrams that enable a precise recollection of the memory. These findings uncover a new mechanism in the consolidation of memory and a novel role of Arc/Arg3.1 in GABAergic neurons. The molecular underpinnings of Arc/Arg3.1 regulation of neural firing rates in glutamatergic and GABAergic neurons remain to be discovered. The LS hosts a plethora of GABA- and neuropeptide-expressing neurons, which may have a differential impact on neural activity, local networks and memory. In the third part of this thesis, I investigated the role of two Arc/Arg3.1 expressing GABAergic neurons in learning and memory. Conditional knockout mice in somatostatin neurons (SST-cKO) displayed deficits in memory specificity similar to those observed following the inactivation of the dCA-LS circuit. Using the high-sensitivity *in situ* hybridization method, I revealed that the majority of these Arc/Arg3.1-expressing SST neurons were located in the LS, thereby identifying one of the LS neural subtypes involved in memory specificity. In other behavioral tests, SST-cKO mice displayed enhanced levels of anxiety and more immobility during stress-inducing situations that might have contributed to their memory specificity deficit. Stress enhances fear learning through the processes in the basolateral amygdala (BLA), which was revealed to modulate hippocampal plasticity and dendritic growth (Giachero, Calfa, & Molina, 2013, 2015; Maroun et al., 2013). However, excessive stress may lead to post-traumatic stress disorder (PTSD) and other memory disorders, which are characterized by symptoms like re-experiencing trauma memories and negative emotions (Ressler et al., 2022). On the one hand, the brain circuits involved in PTSD include the amygdala, prefrontal cortex (PFC), anterior cingulate cortex (ACC), and hippocampus (Ressler et al., 2022). On the other hand, the amygdala (L. A. Rodriguez et al., 2023), prefrontal cortex (de Leon Reyes et al., 2023) and hippocampus (Y. Liu et al., 2022) were reported to send direct projection into the lateral septum and modulate social novelty recognition in mice. In stressful situations, for example, restraint stress (Part II), elevated plus maze test, and tail suspension test (Kosugi et al., 2021), the neurons in vCA1-LS were activated. The brain circuits responsible for novelty discrimination also trigger aversive and anxiogenic responses in mice. This could explain how optical suppression, presumably affecting LS SST neurons or the specific ablation of Arc/Arg3.1 in these neurons affects both fear memory discrimination and stress-related behaviors in mice.

Arc/Arg3.1 is known as an important protein for synaptic plasticity (Eriksen & Bramham, 2022; Link et al., 1995; Lyford et al., 1995; Plath et al., 2006; H. Zhang & Bramham, 2021). In the LFP

recording Arc/Arg3.1 KO mice, I observed a decrease in theta and low gamma power in dCA1, reflecting the impact of Arc/Arg3.1 loss during early postnatal development (Xiaoyan Gao et al., 2018). The acute ablation of Arc/Arg3.1 in LS or HPC in the adult brain led to a decrease in the power of gamma and HFO oscillations only in the dLS, sparing the dCA1, suggesting that Arc/Arg3.1 continuously regulates gamma and HFO oscillations in dLS. Gamma oscillations in cortical regions are important for working memory (Yamamoto, Suh, Takeuchi, & Tonegawa, 2014), learning (Kei M. Igarashi et al., 2014), attention (H. Kim, Ahrlund-Richter, Wang, Deisseroth, & Carlen, 2016), cognitive (Cho et al., 2015) and sensory response (Cardin et al., 2009) processes. The gamma oscillations in the LS and its top-down pathways (mPFC-LS-LH) were reported to regulate exploration and learning in mice (Carus-Cadavieco et al., 2017) and may help maintain a precise information transfer between the cortex, hippocampus and LS and thereby support memory discrimination in mice. Deletion of Arc/Arg3.1, restricted to the lateral septum, affected not only local network activity but also the communication in the gamma frequency bands between the dorsal CA1 and dorsal lateral septum. This suggests that the typical coordination of gamma oscillations in the dorsal CA1-dorsal lateral septum circuits may play a role in encoding specific memories. Furthermore, it demonstrates that the Arc/Arg3.1 gene in the hippocampus is responsible for long-term memory discrimination in mice. Gamma oscillations are known to be generated through the activity of fast-spiking GABAergic inhibitory neurons (Bartos, Vida, & Jonas, 2007; Cardin et al., 2009; Whittington, Traub, & Jefferys, 1995). Ablation of Arc/Arg3.1 either in HPC or LS, altered the activity of fast-spiking units in the LS. In the HPC-LS-MS-HPC circuitry, hippocampal neurons send axonal projections to GABAergic neurons in the LS and MS, the LS interacts with MS through GABAergic neurons, and MS GABAergic, cholinergic, glutamatergic neurons project back to hippocampal GABAergic and glutamatergic neurons (Khakpai, Zarrindast, et al., 2013; Muller & Remy, 2018). The loss of Arc/Arg3.1 in the HPC leads to a firing rate reduction in the hippocampal pyramidal and GABAergic neurons and lateral septal fast-spiking neurons, but the loss of Arc/Arg3.1 in the LS leads to a firing rate increase in the hippocampal pyramidal and GABAergic neurons and lateral septal fast-spiking neurons. The ablation of Arc/Arg3.1 in the HPC or LS was driven by neuronal firing rate into opposite directions during REM-like sleep states. The data suggests that the Arc/Arg3.1 ablation in the LS may disinhibit the activities in the MS and further activate the neuronal activities in HPC. Although the ablation of Arc/Arg3.1 in HPC or LS showed opposite firing rate driving in parts of the neurons in the dCA1-dLS circuits,



it showed both impaired gamma and HFO oscillations in general. I hypothesized that pyramidal neurons send stronger driving activities to hippocampal GABAergic neurons and lateral septal fast-spiking neurons in dCA1-dLS circuits.

Parvalbumin neurons were implicated in sensory perception and learning memory, and their dysfunction was linked to synaptic and network pathologies of neurodevelopmental and neurodegenerative diseases. In a mapping study, I also identified parvalbumin neurons that co-express Arc/Arg3.1. These were restricted to the TRN nucleus, while PV-neurons, abundant in other brain regions, lacked Arc/Arg3.1 expression. Conditional deletion of the gene in all parvalbumin neurons (PV-cKO) had no impact on spatial learning, explicit memory, anxiety or immobility during stress-inducing conditions, suggesting that Arc/Arg3.1 expression in the TRN neurons does not partake in these behaviors, however, is likely to influence other brain functions.

My study breaks new ground by identifying a hippocampal-lateral septum circuit essential for modulating fear learning, memory consolidation and discrimination in mice. Moreover, my findings reveal how the expression of Arc/Arg3.1 in this circuit shapes local and inter-areal activity patterns required for memory consolidation. My findings in SST-cKO mice confirmed that the processing of fear memory and its precision relies on the expression of Arc/Arg3.1 in this GABAergic population of the LS. In a broader scope, expression of Arc/Arg3.1 in the lateral septum, a nucleus rich in neuropeptide-containing GABAergic neurons, could provide a mechanism for storing information on emotional states encoded by these neurons and conveying these to executive regions such as the hypothalamus, with which it is profusely connected. Through the strong and influential input from the hippocampus, the LS is in the position to link the emotional states to context information. This suggestion was bolstered by my findings of a wide range of stress-response modulations in mice lacking Arc/Arg3.1 in LS GABAergic neurons, suggesting a potential link between Arc/Arg3.1 in the LS and stress-related memory or psychiatric disorders. The ubiquitous expression of Arc/Arg3.1 in GABAergic LS neurons contrasts with its predominant expression in glutamatergic neurons in the forebrain, hinting towards possibly novel mechanisms of Arc/Arg3.1 function in plasticity and memory, which are yet to be discovered. This study is the first to report the function of Arc/Arg3.1 in GABAergic systems and provides a first work frame for future investigation of its involvement in normal and pathological conditions.

## **Materials and methods**



## 1. Experimental animals

C57BL/6J genetic background mice aged 24 to 32 weeks were group-housed (3-6 per cage) in a vivarium with an inverted 12-hour dark/light cycle (8:00 - 20:00 is dark period) under standard housing conditions ( $23 \pm 1^\circ\text{C}$ , 40-50% humidity, food, and water *ad libitum*). The animals were housed individually 1 week prior to behavioral and electrophysiological experiments but 4 weeks before optogenetic behavioral experiments. All the experiments were performed in accordance with German legislation (§ 8 des Tierschutzgesetzes vom 18. Mai 2006 BGBl. IS. 1207,1313) and approved by the local authorities of the City of Hamburg. All experimental procedures were designed to minimize pain or discomfort to the animals, and experimenters were blind to genotype when performing the behavioral tests.

## 2. Generation of Arc/Arg3.1 deficient mice

The Arc/Arg3.1 knock-out mice were generated and described in detail by Plath et al (Plath et al., 2006).

Arc/Arg3.1 ablation in different types of interneurons was accomplished by breeding the LoxP-flanked Arc/Arg3.1 mouse line (Arc/Arg3.1<sup>flox/flox</sup>), generated and characterized previously in our group ((Xiaoyan Gao et al., 2018; Plath et al., 2006) with Cre recombinase transgenic mice: parvalbumin-Cre (PV-Cre) mice B6;129P2Pvalbtm1(cre)Arbr/J (Jax008069) (Hippenmeyer et al., 2005) and somatostatin-Cre (SST-Cre) mice B6;Ssttm2.1(cre)Zjh/J (JAX013044) (Taniguchi et al., 2011). After 2 generations of cross breeding, the genotype scheme of the F3 mice became Arc/Arg3.1<sup>f/f</sup>:PV-Cre (Figure 1. A) and Arc/Arg3.1<sup>f/f</sup>:SST-Cre (Figure 1. B). The Arc/Arg3.1 gene was conditionally deleted in parvalbumin-positive or somatostatin-positive interneurons.

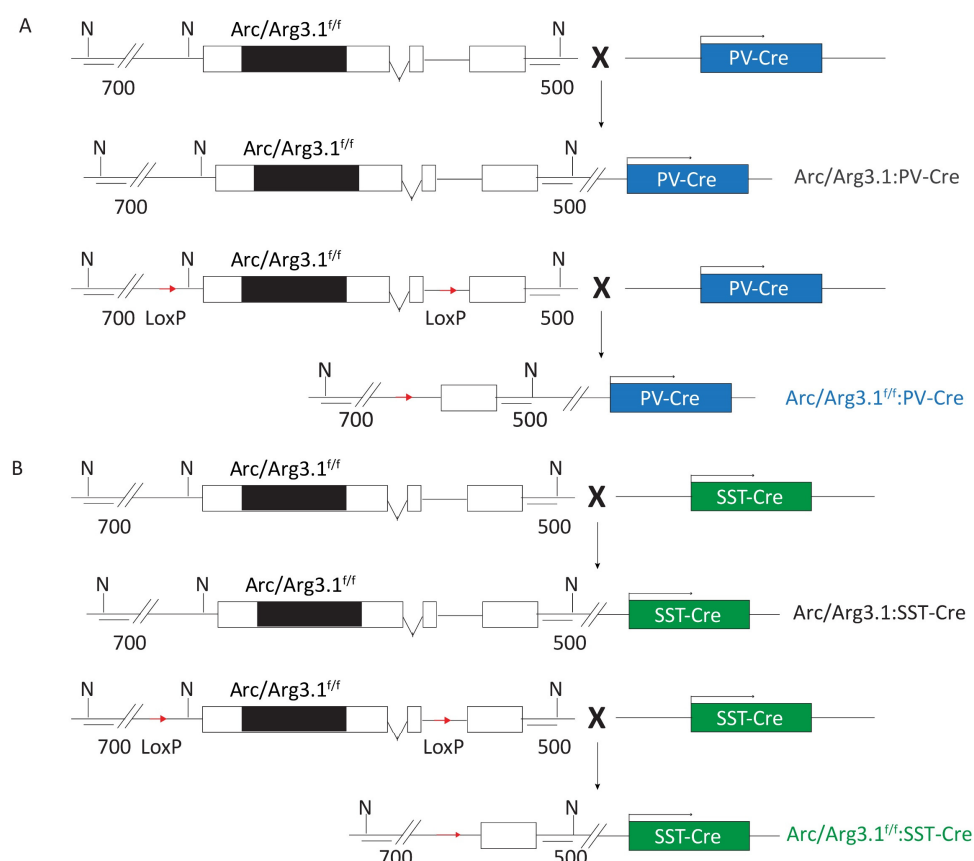


**Figure 1. Generation scheme of Arc/Arg3.1 deficient mice.** Expressing Cre recombinase in different types of interneurons enables a cell-specific ablation of Arc/Arg3.1 in (A) parvalbumin (PV) interneurons and (B) somatostatin (SST) interneurons. (A, B) The schemes on the top showed the genetic schemes of their WT littermates.

### 3. Brain perfusion

Mice were anesthetized with intraperitoneal injection of 15% urethane (1.5 mg/g b.w., Sigma) dissolved in 0.9% saline. Anesthesia depth was confirmed by loss of paw and tail reflexes in response to mechanical stimulation and loss of eyelid closure reflex in response to air puffs. Mice were intracardially perfused with 37°C 1× PBS (8g NaCl, 0.2g KCl, 1.44g Na<sub>2</sub>HPO<sub>4</sub>, 0.24g KH<sub>2</sub>PO<sub>4</sub> in 1L H<sub>2</sub>O, PH7.4) followed by 4°C 4% paraformaldehyde (PFA). Brains were collected and post-fixed in 4°C 4% PFA for at least 3 days before use.

### 4. Immunohistochemistry

Primary antibodies used in this study are: anti-Arc/Arg3.1 rabbit polyclonal antiserum (1:1000, Kuhl lab, 5904) (Xiaoyan Gao et al., 2018), anti-cFos chicken polyclonal antibody (1:1000, Sigma, GW21144), anti-cFos rat monoclonal antibody (1:1000, Synaptic Systems, 226017), anti-Cre recombinase mouse monoclonal antibody (1:2000, Millipore, MAB3120).

Secondary antibodies were: Biotinylated HRP-complex conjugated goat anti-rabbit antibody (1:1000, Vector Labs, BA-1000), poly-HRP-conjugated goat anti-rabbit secondary antibody (Thermo Fisher Science, B40925), Alexa Fluor® 488 conjugated goat anti-rabbit (1:500, Invitrogen, A-11008), Alexa Fluor® 488 conjugated goat anti-mouse (1:500, Invitrogen, A-11001), Alexa Fluor® 555 conjugated goat anti-rabbit (1:500, Invitrogen, A-21428), Alexa Fluor® 633 conjugated goat anti-rat (1:500, Invitrogen, A-21094) and Alexa Fluor® 555 conjugated goat anti-mouse secondary antibody (1:1000, Invitrogen, A-21422).

#### **4.1. Diaminobenzidine (DAB) staining**

After post-fixation, brains were sliced with a Vibratome (Leica VT1200s) on a coronal plane and 40 µm free-floating sections, were collected. Brain sections were first incubated in 0.3% H<sub>2</sub>O<sub>2</sub> (Sigma) for 30 min. Then, they were incubated in blocking solution (10% goat serum (Jackson), 0.2% Bovine serum albumin (BSA, Sigma), and 0.3% Triton X-100 (Sigma) in 1× PBS) for 60 min at room temperature (RT). After the blocking step, sections were incubated with the primary antibody in a carrier solution (1% goat serum (Jackson), 0.2% Bovine serum albumin (BSA, Sigma), and 0.3% Triton X-100 (Sigma) in 1× PBS) at 4°C overnight. On the second day, sections were washed with 1× PBS and then incubated with biotinylated HRP-complex conjugated secondary antibody (Vector Labs) in carrier solution for 120 min at RT. Immunoreactivities were detected using Vectastain ABC Kit (A, B solution 1:500 in PBS, Vector Labs) and 3, 3'-diaminobenzidine (Sigma-Aldrich) as chromogen. Sections were dried and mounted with microscopy mounting medium (Entellan - Merck Millipore).

#### **4.2. Tyramide-conjugated fluorescence staining**

The Tyramide-conjugated fluorescence staining was performed with the Tyramide SuperBoost™ Kit (Thermo Fisher Science) using Goat anti-rabbit Alexa Fluor™ 594. Free-floating coronal sections (40 µm) were prepared on a Vibratome (Leica VT1200s). Sections were first incubated in 0.3% H<sub>2</sub>O<sub>2</sub> (Tyramide SuperBoost™ Kit) for 60 min and subsequently incubated in blocking solution (Tyramide SuperBoost™ Kit) for 60 min at RT. After the blocking step, the sections were incubated with the primary antibody in carrier solution (1% goat serum (Jackson), 0.2% BSA, and 0.3% TritonX (Sigma) in 1× PBS) at 4°C overnight. On the second day, the sections were washed with 1× PBS and then incubated with poly-HRP-conjugated goat anti-rabbit secondary antibody (Tyramide SuperBoost™ Kit) for 60 min at RT. The sections were washed with 1× PBS and incubated in Tyramide working solution (100x Tyramide stock solution: 100x H<sub>2</sub>O<sub>2</sub> solution: 1x Reaction buffer = 1: 1: 100) for 8 min at RT. The reaction should be stopped immediately by adding the same volume of Reaction Stop Reagent Working solution (Reaction Stop Reagent Stop Stock solution 1:11 in 1× PBS) and incubated at room temperature for 5 min. After 1× PBS washing, the nuclear staining was obtained by incubating in NucBlue™ Fixed Cell Stain ReadyProbes™ reagent (Thermo Fisher Science) for 15 min at RT. Slices were dried, mounted with Prolong™ Gold antifade reagent (Thermo Fisher Science), and stored at 4°C until imaging.

#### **4.3. Immunofluorescence staining**

Free-floating coronal sections (40 µm) were incubated in blocking solution for 60 min at RT, followed by 4°C overnight incubation with the primary antibody in the carrier solution. On the second day, the sections were washed with 1× PBS and then incubated with secondary antibody in carrier solution for 120 min at RT. The slices were dried, mounted with Prolong™ Gold antifade reagent (Thermo Fisher Science), and stored at 4°C until imaging.

### **5. RNA scope: in situ Hybridization**

The RNA scope was performed according to the manufacture protocol (Document number 323100-USM) and the Kit from ACD-Biotechnie (Figure 2. A).

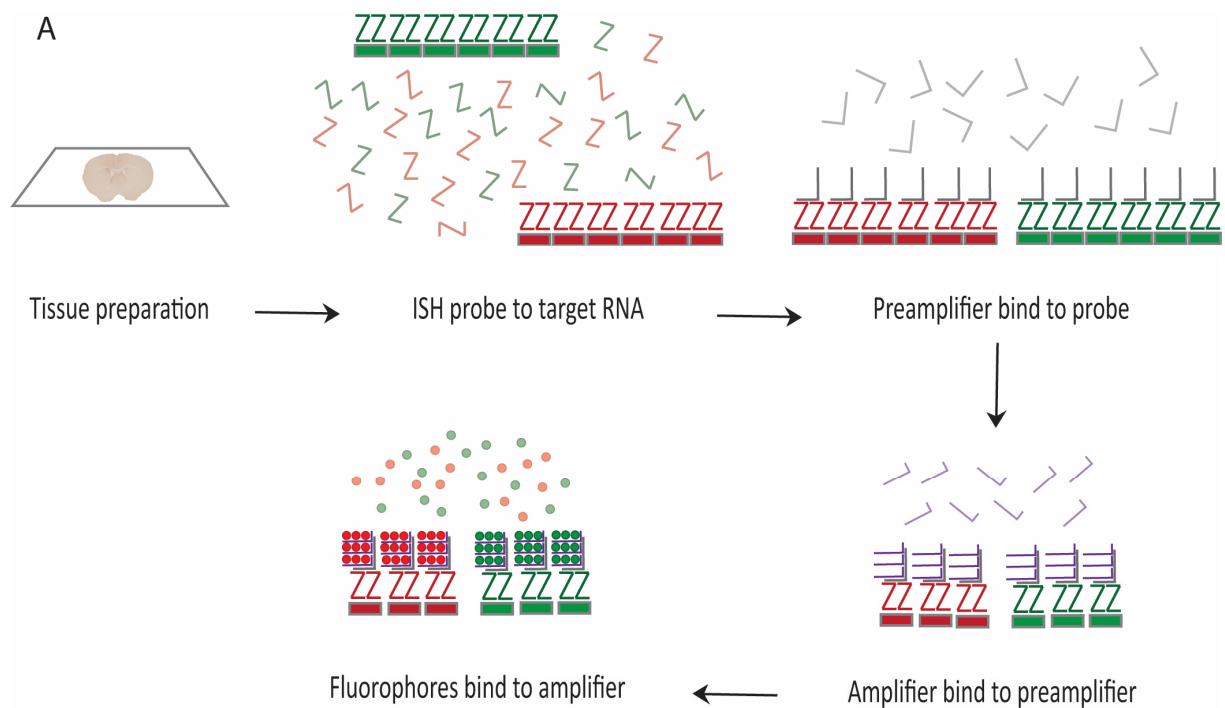


**Figure 2. RNAscope workflow.** The different target genes hybridized with ZZ pairs on 20 bases. Two adjacent Zs created a binding motif for a preamplifier, and the amplifier bonded to the preamplifier. The high specific detection confirmed by the preamplifier cannot bind to only one 'Z'. Different RNA genes were dye-labeled by different fluorophores (Hildyard, Rawson, Wells, & Piercy, 2020; F. Wang et al., 2012).

After post-fixation, the brains were subsequently placed in 10% sucrose (Sigma), 20% sucrose, and 30% sucrose solutions dissolved in 1 mol/L PB (2g KCl, 14.4g Na<sub>2</sub>HPO<sub>4</sub>, 2.4g KH<sub>2</sub>PO<sub>4</sub> in 1L H<sub>2</sub>O) at 4°C until the brains sunk to the bottom and kept in -20°C until slicing. Coronal brains sections (14µm) were prepared on a cryostat (Leica, Cryo Star HM 560) at approximately -20°C and mounted on Superfrost plus slides (Thermo Scientific). All slides were stored at -80°C until use.

Sections were first washed in 1× PBS to remove cryo-embedding media (Tissue Tek), followed by baking for 30 min at 60°C in the HybEZ™ II OVEN. After that, sections are post-fixed in ice-cold 4% PFA for 30 min, passed through an ethanol series (50% and 70% ethanol) at RT, washed with 1× PBS, followed by quenching endogenous peroxidase activity in hydrogen peroxide for 10 min at RT. To maximally expose low-abundance RNA transcripts in the tissue,



sections were treated with the target retrieval method by immersing in 99°C 1× PBS for 10 s and followed with immersing in the 1× Target Retrieval Reagent at 99°C for 5 min. After the target retrieval step, sections were placed in 1× PBS for 2 min at RT, followed by 3 min in absolute ethanol at RT. After drying in the air for 5 min at RT, a waterproof barrier was drawn around the sections with an ImmEdge hydrophobic barrier pen. We used Protease III from the Kit and incubated sections in the oven for 30 min at 40°C. After the protease treatment step, we treated the sections with rewarmed (water bath, 40°C, 10 min) mRNA conjugated hybridization probes: Arc/Arg3.1 (2924-2342-C1, custom designed, 1× solution) and Somatostatin (404631-C2, 50× stock solution). The sections were incubated in a probe mixture in the oven for 120 min at 40°C. The sections were washed with 1× Wash Buffer, prepared by diluting the rewarmed 50× RNA scope wash buffer in distilled water and stored in 5× saline sodium citrate buffer (SSC) at RT overnight. Pre-amplifiers specific to each target mRNA were added for 30 min at 40°C in the oven. Next, HRP-conjugated amplifiers were added and incubated for 15 minutes at 40°C in the oven. Opal dyes (1:1500, ACD), combined with tyramide amplification technology, were then added to bind with the amplifiers and incubated for 30 minutes at 40°C in the oven. Redundant HRP sites were covered by HRP-Blocker solution for 15 minutes at 40°C in the oven. After each hybridization step, the sections were washed with 1× Wash Buffer at room temperature. The nuclears were stained by incubating with DAPI for 5 min at RT. The sections were dried and mounted with Prolong™ Gold antifade reagent (Thermo Fisher Science). The slides were stored at 4°C until use.

## **6. Stereotaxical operations**

### **6.1. Mouse anesthesia and analgesia**

A complete anesthesia system for small animals with a stereotaxic anesthesia mask (Harvard Apparatus, Holliston) was used for mice anesthesia during the operation. Mice were anesthetized with 5% isoflurane (Abbot, Illinois) mixed with 99.8% oxygen flowing at 0.5 L/min in a transparent induction chamber. While under anesthesia, mice were subcutaneously injected with buprenorphine (0.05 mg/kg, prepared in 0.9% saline), for analgesia during the surgery. Mice were then placed in a stereotaxic apparatus (DAVID KOPF INSTRUMENTS) and

anesthesia was continuously administered via a mouth mask with ~1.5% isoflurane mixed with oxygen during the entire surgery. Body temperature was maintained at 37.5°C with a homeothermic heating pad (WPI), controlled by a feedback temperature controller system (DC Temperature controller, FHC), located under the mouse body. Following surgery, carprofen (IDT Biologika, Dessau-Roßlau) with a dose of 5 mg/kg, prepared in 0.9% saline, was administered subcutaneously for postoperative analgesia and hydration. Additional doses of Carprofen were administered every 24 hours for up to 3 days post-surgery.

## 6.2. Stereotaxical viral vector injection in vivo

Viral vectors (AAV-CaMKII-Cre, AAV1/2 titer:  $4 \times 10^{12}$  vg/ml, Addgene plasmid: 27227) (Dittgen et al., 2004) were produced and purified by the HEXT vector facility at the University Medical Center Hamburg-Eppendorf (UKE). After fixing the mouse head in the stereotaxic frame, the hair was shaved with an electric shaver, and the skin was disinfected with iodophor, followed by 70% ethanol. A midline skin incision was made with a medical scalpel. To expose the bregma and lambda, the skull was cleaned with 0.9% saline and dried by blowing air with the rubber ear washer. Small craniotomies were drilled under the stereomicroscope (Olympus) above the hippocampus (AP: -2.0 mm, ML:  $\pm 1.5$  mm, DV: -1.8 mm and -1.4 mm from the brain surface; relative to bregma; AP, ML and DV denote anteroposterior, mediolateral and dorsoventral distance from the bregma, respectively) or the lateral septum (AP: +0.6 mm, ML:  $\pm 0.25$  mm, DV: -3.2 mm and -2.7 mm from the brain surface; relative to bregma) unilaterally or bilaterally with a micro drill (Fine Science Tools). The viral vectors were delivered with a Neuros Syringe (Hamilton) controlled by an injection robot (Neurostar). Each injected region received 1  $\mu$ L of viral vector solution with the speed set as 0.1  $\mu$ L/min. The injection of 1  $\mu$ L viral vector solution was separated into two steps, 0.4  $\mu$ L at the DG and 0.6  $\mu$ L at the CA1 for the hippocampus, and with two boli of 0.5  $\mu$ L each in the ventral lateral septum and dorsal lateral septum, respectively. To facilitate the virus spread in the tissue, the syringe needle was left stationary for 3 min after the first volume and 9 min after the second volume. The skin was closed by sewing with fine suture needles and threads (Nylon monofilament). Finally, the wound was disinfected with Iodophor. The mice were administrated with carprofen and placed in their

home cage on a warm mat until fully recovered and resumed motor and feeding activity. Soft food was provided in the days following surgery.

To identify the connection between hippocampus (HPC) and lateral septum (LS), the anterograde viral vector (rAAV-CaMKII-GFP, AAV1/2 titer:  $3 \times 10^{12}$  vg/ml, Addgene plasmid: 27227) was injected into the HPC, and the retrograde viral vector (AAVrg-CaMKII-FusionRed, AAV retrograde, titer:  $4.6 \times 10^{12}$  vg/ml, Addgene plasmid: 105669) was injected into the LS. The stereotaxical coordinates are the same as above. After a 7-day expression of the viral tracers, the direct projection from the dorsal hippocampal CA1 to the lateral septum (LS) was observed after perfusion and brain slicing.

### **6.3. Stereotaxical opsin injection and fiber-optic cannula implantation**

Injection of a retrograde virus expressing the inhibitory opsin (AAVrg-CaMKII-stGtACR-FusionRed, AAV retrograde, titer:  $6 \times 10^{12}$  vg/ml, Addgene: 105669-AAVrg) in the lateral septum and the implantation of fiber-optic cannula in the hippocampus were performed in one surgery. Mice were anesthetized, fixed in the stereotaxic apparatus and the skull was exposed, as described above (6.2). Two small craniotomies were drilled above the left and right lateral septum (AP: +0.6 mm, ML:  $\pm 0.25$  mm, DV: -3.2 mm and -2.7 mm from the brain surface; relative to bregma). The Neuros Syringe needle was lowered into the left intermediate LS (imLS, DV: -3.2 mm) and 0.4  $\mu$ L retrovirus solution was injected at a speed of 0.1  $\mu$ L/min. Following 3 min pause, the syringe was elevated to the dorsal LS (dLS, DV: -2.7 mm) and 0.6  $\mu$ L virus were delivered at 0.1  $\mu$ L/min followed by a 9 min stationary pause of the needle. The syringe was retracted, and the injection was repeated, identically, on the right hemisphere.

Next, small craniotomies were drilled above the right and left dorsal hippocampus (AP: -2.0 mm, ML:  $\pm 2.0$  mm, DV: -1.1 mm from the brain surface; relative to bregma, angle: 20° to mid-line). A cannula holder was mounted on the stereotaxic arm and the optic-fiber was lowered above CA1 (DV: -1.1 mm from the brain surface) with an angle of 20° to mid-line. The fiber-optic cannula was secured to the skull with a self-curing dental adhesive resin cement (Universal Kit, Super-Bond) based on acrylic resin (4 META-TBB) technology. After the dental cement dried completely, the cannula was released from the holder. The mice received a carprofen dose and

were placed on the warm mat until they fully recovered from anesthesia. Soft food was applied in the following recovery days.

## 7. Behavioral tests

Mice were handled by experimenters for 3-4 days before behavioral tests and were habituated to the experimental laboratory for 30-60 minutes before handling or testing.

### 7.1. Open field test (OFT)

Spontaneous exploration and locomotor activity were evaluated in a white box (50 cm × 50 cm × 50 cm) constructed from opaque white plates. Testing was performed under indirect illumination (~15 Lux in the corner, ~20 Lux in the central arena) and mouse behavior was recorded by a video-tracking system (Ethovision XT v16.0, Noldus Information Technology), also used for on- and off-line analyses. The test began when the mice were put in the center of the box. After free movement for 10 min, mice were returned to their home cage. For analysis, the floor of the box was divided into 16 virtual squares of equal area (Figure 3), and the arena's center zone was defined by the area of the four center squares. The distance traveled and time spent in each zone were calculated. The box was cleaned with 70% ethanol and dried for 2 min before each test.

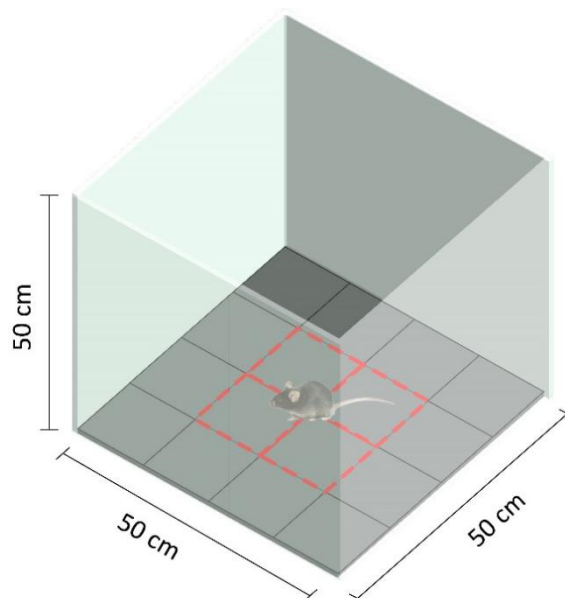


**Figure 3. Open field schematic representation.** The Gray lines represent the 16 virtual squares defined in the tracking system, and the 4 virtual squares with the red dashed lines represent the center area.

## 7.2. Elevated plus maze test (EPMT)

The elevated plus maze (Figure 4) consisted of a central platform (5 cm × 5 cm), two open arms (5 cm × 30 cm), and two closed arms (5 cm × 30 cm) with 15 cm high protective walls. The maze was elevated 70 cm above the ground and placed in a room with indirect illumination (~15 Lux in closed arms, ~20 Lux in opened arms). Mice were placed on the central plate facing the open arm and allowed to explore the maze freely for 5 min. Mouse behavior was recorded by the video-tracking system (Ethovision XT v16.0, Noldus Information Technology) also used to analyze the number of entries and time spent in each arm. The elevated plus maze was cleaned with 70% ethanol and dried for 2 min before the test for each animal.

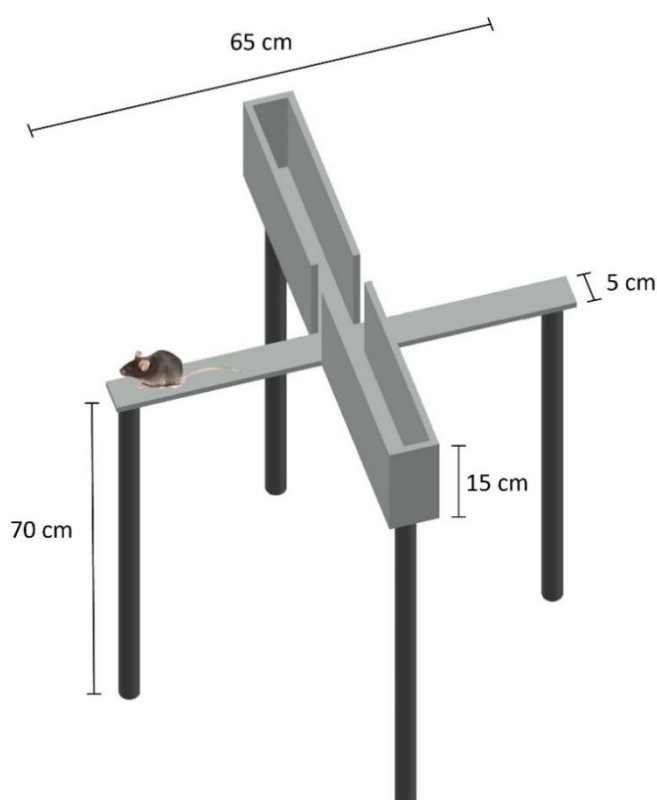


**Figure 4. Elevate plus maze schematic representation.**

### 7.3. Forced swimming test (FST)

The mice swam individually in a cylindrical glass container (Powell, Fernandes, & Schalkwyk, 2012) (diameter: 10 cm, height: 32 cm, water depth: 15 cm, Figure 5.) filled with clean water ( $22\pm 1^\circ\text{C}$ ) and placed in a room with indirect illumination ( $\sim 35$  Lux) for 6 min. Mouse activity was recorded by a video-tracking system (Ethovision XT v16.0, Noldus Information Technology). The mice were dried with soft wipes and returned to their home cages immediately after testing. Immobility time was defined as lack of any active movements except for minimum movements necessary to keep the head and nose above the water (for example, single limb paddling) (Cui et al., 2018; Powell et al., 2012; Yankelevitch-Yahav, Franko, Huly, & Doron, 2015). The total immobility time was calculated as the sum of all immobile epochs during the last 4 min of the test.

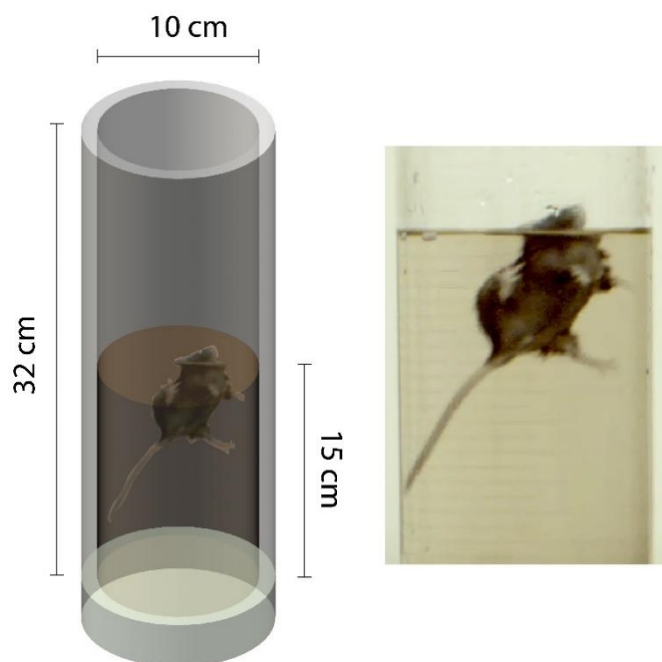


**Figure 5. Forced swimming schematic representation and apparatus.**

### 7.4. Tail suspension test (TST)

The apparatus for the tail suspension test (Powell et al., 2012) (Ramirez et al., 2015; Steru, Chermat, Thierry, & Simon, 1985; Zhou et al., 2019) was a PVC box (50 cm × 30 cm × 30 cm) covered with white paper and equipped with a hook attached to the ceiling (Figure 6). The box was placed in a room with indirect illumination (~35 Lux). Mice were suspended 15 cm above the floor with medical tape safely secured to the tail tip. The video-tracking system recorded the 6 min suspension test session (Ethovision XT v16.0, Noldus Information Technology). The freezing time was scored for the last 4 min of the session (Ramirez et al., 2015; Zhou et al., 2019). Mice were returned to their home cages after the test. The box was cleaned with 70% ethanol and dried for 2 min before each test.

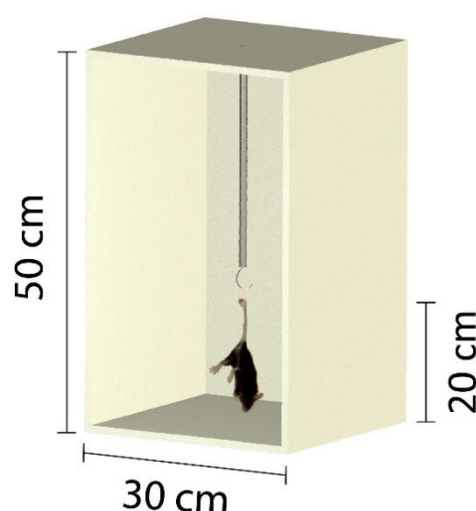


**Figure 6. Tail suspension schematic representation.**

### **7.5. Morris water maze test (MWMT)**

Spatial learning and memory were tested by the Morris water maze test (MWMT) (da Silva, Bast, & Morris, 2013; Morris, Garrud, Rawlins, & O'Keefe, 1982). The maze consisted of a circular tank (diameter: 1.5 m, Figure 7. A) filled with water ( $22 \pm 1^\circ\text{C}$ ), a submerged circular platform in the fixed position and four large reference cues. To make the water opaque and hide the platform, we mixed the water with non-toxic soluble paint (Redimix COLOR & Co. Gouache, Amazon). The circular platform (diameter: 14 cm) was placed 1 cm below the water

surface in the tank. The references were attached to the wall 5 cm above the water at an unequal distance from each other. The experiment was performed under indirect illumination with white curtains placed around the maze, for isolation. Mice were trained to find the hidden platform during the acquisition phases.

We designed 4 different start positions and 4 acquisition trials for 9 consecutive days (Figure 7. D). On each trial, mice were released at a different start position chosen in a semi-random order for each day. Mice were allowed to swim and explore the tank freely until they found the hidden platform. If the mice failed to find the platform, they were guided to the platform and allowed to rest for 60 s for the first trial on the first day, 30 s for the second trial on the first day, and 15 s for the rest of the following trials. The time mice spent (Escape latency to the platform) and the total moving distance (Moving distance) in finding the hidden platform was used to generate the learning curve. The short-term and long-term spatial memory was assessed by subjecting the mice to a single probe trial (60 s) on the first day, seventh day, and 21<sup>st</sup> day after the 9-day acquisition sessions (Figure 7. D). During the probe test, the platform was removed, and mice were released in the opposite quadrant. For analysis, the maze arena was virtually separated into 4 equal quadrants (Figure 7. B, C). A virtual annulus zone (diameter: 28 cm,  $2 \times$  platform area) was defined over the previous location of the submerged platform and copied to the corresponding position for each quadrant as identical zones. The time mice spent in the annulus zone and the number of mice that crossed the annulus zone were calculated to evaluate memory precision.

Mice were tested within the same water maze with a visual cue (a flag extended 12 cm above the water surface) placed on the submerged platform. The starting position for releasing the mice and the position of the visual cue were changed for each trial (60 s) to ensure the mice were using the visual cue to locate the platform. The video-tracking system recorded the trails (Ethovision XT v16.0, Noldus Information Technology).



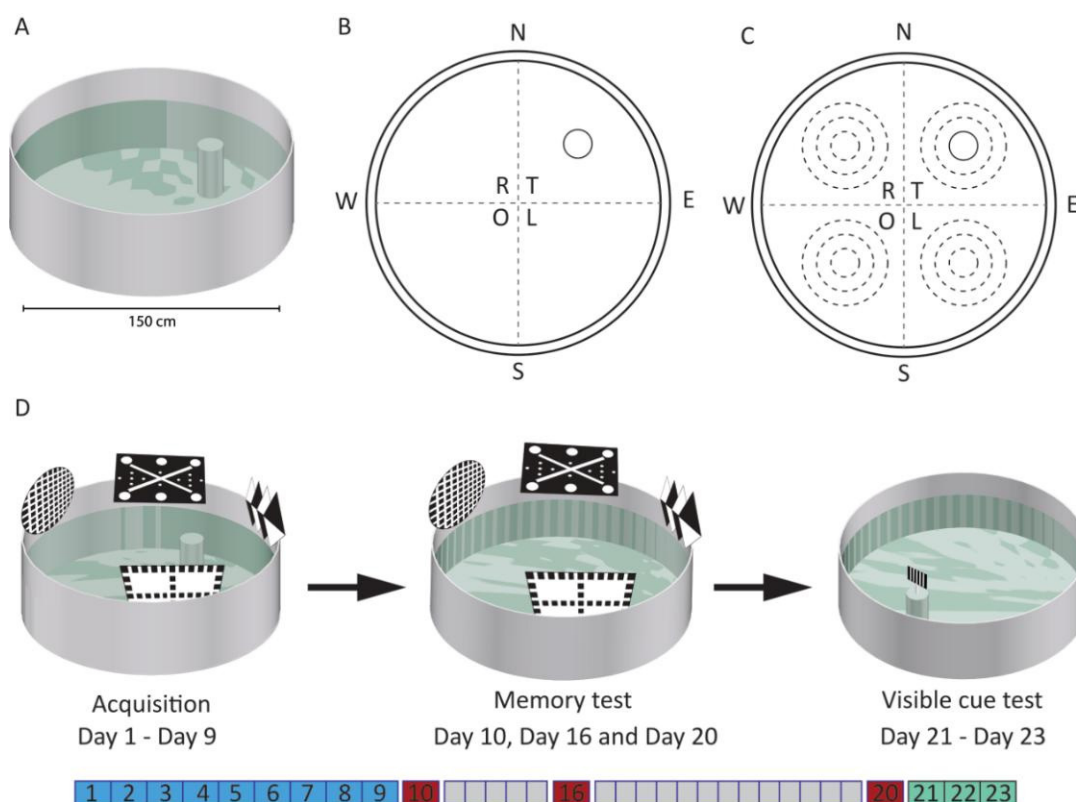


**Figure 7. Morris water maze schematic representation and experiment procedure.** (A) Schematic representation of the water maze tank. (B) The water maze was divided into 4 equal quadrants: Target quadrant (T), Opposite quadrant (O), Right quadrant (R), and Left quadrant (L). The directions were defined as North (N), South (S), East (E), and West (W). The circle shows the location of the submerged platform. (C) The schematic representation of identical zones and annulus zones for the analysis. (D) The schematic representation of the maze setting during training (blue), memory testing (red) and cued-navigation days.

## 7.6. Fear conditioning test (1 CS-US)

We designed a fear conditioning test that assesses both implicit (tone) and explicit (context) memory. The test was performed with an automated conditioning system (TSE Multi-Conditioning System). During acquisition (in Context A, Day 0), mice were placed in the conditioning chamber (Figure 8.), an acrylic transparent box (20 cm × 20 cm × 40 cm) without a floor placed over a metal grid floor and illuminated with white light (~70 Lux), and allowed to explore for 120 s. Next, a high-frequency tone (10K Hz, 70 dB) was played for 30 s and followed by an electrical foot shock (2 s, 0.5 mA) applied through the metal grids. After the shock, mice remained in the chamber for 60 s and returned to their home cages. During conditioning,

sensory cues were applied as unique identifiers of the environment: A constant background noise was emitted from an internal fan (28 dB). The box was cleaned with 70% ethanol and illuminated with dim white light (~35 Lux). Recent and remote memory were tested 7, 14 or 21 days, respectively, after conditioning. On each test day, mice were placed first in the conditioning chamber for 180 s, with all original cues present (Context A). One hour later, mice were introduced to a new chamber (Context B), an opaque box with one transparent wall (or a simulated home cage) and a plastic floor covered by fresh bedding. The background fan noise was omitted, and the box was illuminated with dim red light (~20 Lux). Distal cues were pasted on the chamber's walls and 1% acetic acid was used for cleaning and as an olfactory cue. The mice were first allowed to explore the new arena for 120 s to test the context memory specificity. Subsequently, the conditioning tone was played for 120 s. Freezing was defined as a complete lack of mobility for at least 1 s and was automatically measured based on beam-braking technology (TSE). Total freezing time was calculated for each phase of the test. Context memory specificity was evaluated based on a discrimination index (DI) calculated as follows:

$$DI = \frac{\text{Freezing time in Context A (\%)}}{\text{Freezing time in Context A (\%)} + \text{Freezing time in Context B (\%)}}$$

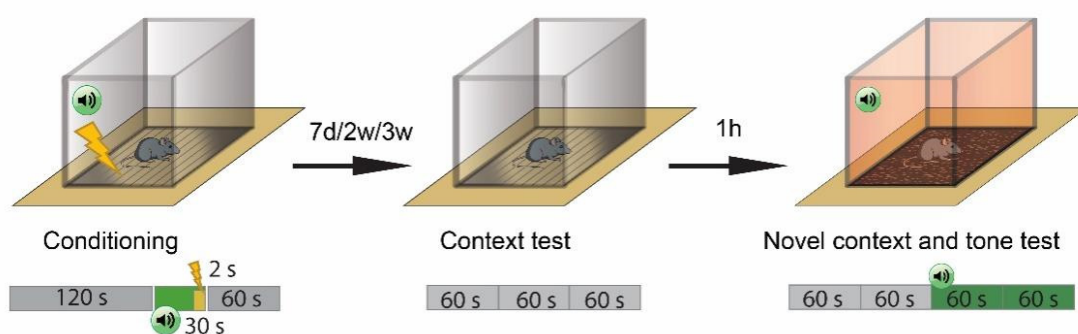


**Figure 8. Fear conditioning schematic representation.**

### 7.7. Optogenetic inhibition in fear conditioning test (2 CS-US)

For all optogenetic testing, mice implanted with optic-fibers cannula were attached to the optic cable and the laser via a patch cord with sleeves. One day prior to conditioning, mice were connected to the optic cable and placed in their home cage for 3 min to habituate to the test conditions. The test was performed with an automated conditioning system (TSE Multi-Conditioning System). The same procedure and conditions were used for optogenetical testing of fear memory as described in 7.6. One difference was using two conditioning stimuli in the optogenetic experiments instead of one. Analysis was performed as described in 7.6. The laser power emitted at the patch cord tip, was calibrated daily prior to testing with a laser power meter (Power meter Pronto-si, Doric). Depending on the experiment design, a continuous laser stimulus (450 nm, 6-9 mW) was delivered from the laser light source (Laser Diode Fiber Light Source, Doric) during the acquisition (Figure 9. B) or the discrimination test (Figure 9. A). Freezing time for each phase and DI were calculated as previously described (7.6).

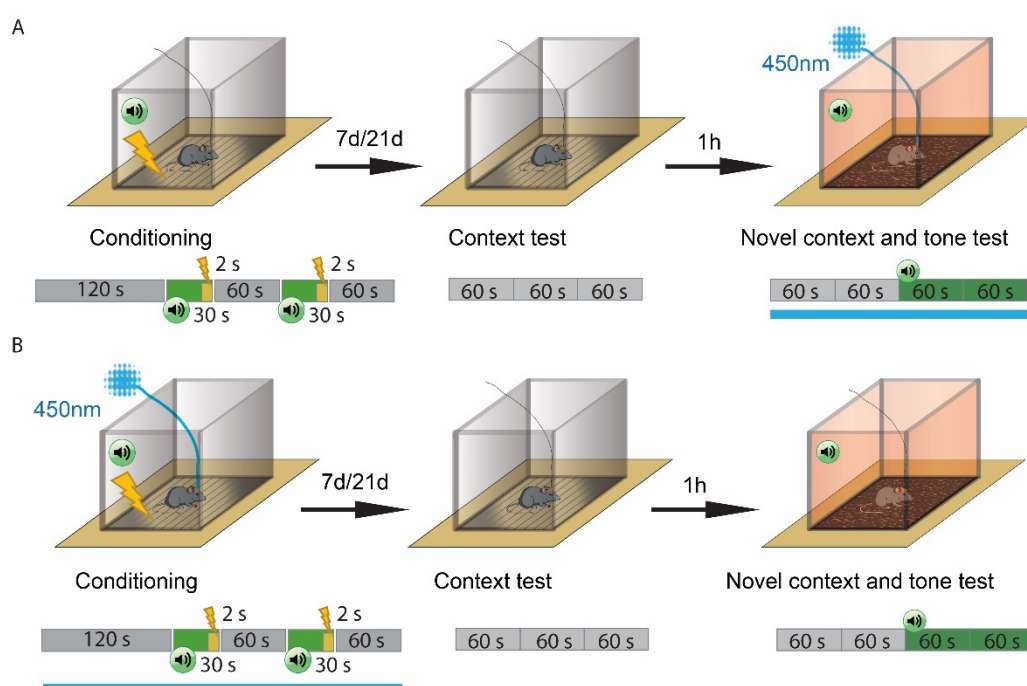


**Figure 9. Optogenetic fear conditioning schematic representation.** 450 nm light pulses were applied during (A) conditioning and (B) altered context tests.

## 7.8. Flinch-jump threshold test

The sensitivity of the mice to the electrical stimulation applied during conditioning was assessed with the flinch-jump procedure in the TSE Multi-Conditioning System. Mice were placed in a transparent box on the metal grid floor to deliver electrical currents. Mice were first habituated in the chamber illuminated with a dim white light (~70Lux) for 30 s, followed with a series of consecutive 0.5 s long foot shocks with 30 s intervals. The foot shocks were administered stepwise from 0.1 mA to 1.0 mA in steps of 0.1 mA. Behavioral responses were recorded as: no response, flinch, or jump at each intensity. The lowest current intensity eliciting a flinch or jump was considered the threshold value. This value was hitherto used in

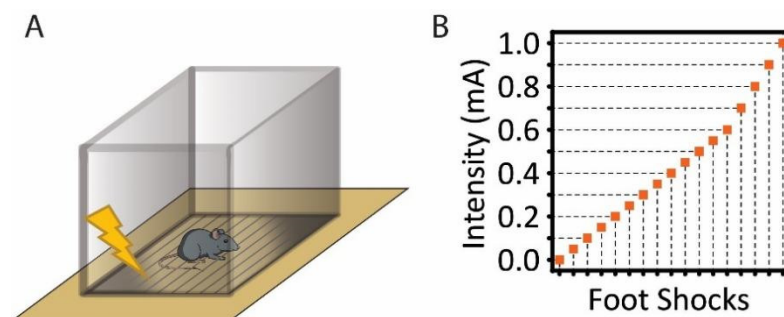


**Figure 10.** Fear conditioning schematic representation and schematic diagram of the flinch-jump threshold test.

## 8. Restraint-induced stress model

To investigate the expression of Arc/Arg3.1 by stress inducing stimulation, mice were restrained for 2 hr in a 50 ml transparent tube pierced with holes for air (diameter: 0.5 cm). Immediately afterward, mice were deeply anesthetized with 15% urethane and transcranial perfused with PFA, as described in 3.

## 9. Kainate-induced seizure

To maximize the expression of Arc/Arg3.1, mice were subjected to Kainate-induced seizures. Adult mice (20–40 g, 3–8 months of age) were intraperitoneally injected with Kainic acid (Abcam,

Cambridge, UK) (14.8 mg/kg body weight) prepared in sterile PBS. Seizures were scored based on clinical signs according to the scale table defined by Yang DD et al. (D. D. Yang et al., 1997). The process of the seizures was classified into 6 grades: 1. Arrest of motion; 2. Myoclonic jerks of the head and neck, with brief twitching movements; 3. Unilateral clonic activity; 4. Bilateral forelimb tonic and clonic activity; 5. Generalized tonic-clonic activity with loss of postural tone; 6. Death from continuous convulsions.

If the mice did not show grade 5 behavior (generalized tonic-clonic activity with loss of postural tone) within 60 min of the first injection, they were given an additional dose of Kainic acid (20  $\mu$ l). Once the mice reached score 5, they were placed in their home cages in a quiet room illuminated with dim red light ( $\sim$ 5 Lux). After 45 min or 90-120 min onset of generalization seizures, mice were deeply anesthetized with 15% urethane and transcranial perfused.

## **10. Multiple electrodes local field potential recordings in vivo**

The electrophysiology experiment was performed 7 days after the viral vector injection. Mice were initially anesthetized by 5% isoflurane mix with 99.8% oxygen, followed by an intraperitoneal injection of 1.2 mg/g *b.w.* urethane (15% w/v, Sigma) prepared in 0.9% saline. After placing the mice on the stereotaxic apparatus (Stoelting), the anesthesia was maintained with 1.0-1.5% isoflurane mixed with 99.8% oxygen during the surgery. The body temperature was maintained at 37°C using a homeothermic heating pad (WPI). The skull was exposed by making a mid-line skin incision with the medical scalpel and dried by blowing air with the rubber ear washer. Three craniotomies were drilled by a micro drill (burr tip diameter: 0.9 mm, Fine Science Tools): 1) above the right lateral septum (AP: +0.55 mm, ML: +0.25 mm, DV: -2.8 mm probe depth from the brain surface), 2) above the right dorsal hippocampus (AP: -2.45 mm, ML: +2.85 mm, DV:  $\sim$ -1.2 mm probe depth from the brain surface) and 3) above the cerebellum all coordinates are given relative to bregma. We inserted a ground wire-connected stainless-steel screw in the cerebellum as the common ground and reference electrode. In the right lateral septum, a linear 32-site silicon probe with a 25  $\mu$ m inter-site distance and 177  $\mu$ m<sup>2</sup> electrode surface (A1 $\times$ 32-5mm-25-177, NeuroNexus) was vertically lowered into the tissue. In the right dorsal hippocampus, a staggered (3 columns of sites) 32-site silicon probe with a 25

$\mu\text{m}$  inter-site distance and  $177 \mu\text{m}^2$  electrode surface (A1 $\times$ 32-poly3-5mm-25s-177, NeuroNexus) was lowered into CA1 with an angle of  $20^\circ$  to mid-line. Before insertion, probes were dipped in a Dil-solution (Vybrant®, ThermoFisher Scientific) for the postmortem probe position verification. Each probe was connected to a 1 $\times$  preamplifier (Neuralynx) mounted on the stereotaxic instrument. When the silicon probes and the sensor were in place, isoflurane anesthesia was discontinued. To remove the effects of isoflurane, recording started 10 min and lasted for  $\sim 1$  hour. Data from both probes and sensor were digitally filtered (0.5-9000 Hz bandpass) and digitized as 16-bit integers with a sampling rate of 30k Hz using a SmartBox data acquisition system (NeuroNexus). During the recording, anesthesia depth was monitored from breathing rates, twitching and electrophysiological properties. If required, an additional urethane dose (0.2 g/kg b.w.) was given. After the experiment, mice were deeply anesthetized with an intraperitoneal injection of 15% urethane (1.5 mg/g b.w., Sigma) dissolved in 0.9% saline before quick decapitation and excision of the brain. The brains were put into 4% PFA for fixation until use.

## **11. Data analysis of local field potential recordings in vivo**

### **11.1. LFP analysis**

The in vivo data was analyzed and visualized using MATLAB (MathWorks) routines. The local field potential (LFP) signals were created by lowpass filtering (Butterworth, 10<sup>th</sup> order, cutoff frequency 600 Hz) the raw traces and down sampling to 1.2k Hz. The electrodes were chosen for LFP analysis independently for each animal according to the probe position for the lateral septum (LS) and sharp wave oscillatory patterns for the hippocampus (HPC). We applied a notch filter to eliminate the power grid noise in the frequency ranges of 45-55 Hz and 145-155 Hz. To display the LFP data in spectrums, we interpolated the data in the aforementioned frequency ranges based on the data 10 Hz before and after, but we did not include it in the statistical analysis.

To identify the rapid-eye movement-like sleep state (REM-like sleep state) and the slow-wave sleep-like state (SWS-like sleep state), the electrode with the highest mean ripple power during the SWS-like sleep state was defined as the Ripple Channel. The Multi-taper Time-Frequency

spectrogram, created with the Ripple Channel and visualized by Neuroscope2, a built-in data viewer in CellExplorer (Petersen, Siegle, Steinmetz, Mahallati, & Buzsaki, 2021), was used to identify the different sleep states. REM-like sleep states were identified as epochs during which the instantaneous theta (3-6 Hz)/delta (0.2-1.2 Hz) power ratio was 1.4 times greater than the 1 hr average theta/delta ratio value. SWS-like sleep states were defined as epochs when the delta oscillation power was 1.4 times greater than the 1 hr average power of delta oscillation and when the theta/delta ratio was close to zero. Other periods were considered as transition sleep states and were not included in the analysis. The functional connectivity and the power of oscillatory components in the frequency domain between HPC and LS were analyzed with the MATLAB Fieldtrip toolbox (Oostenveld, Fries, Maris, & Schoffelen, 2011) from the REM-like sleep states.

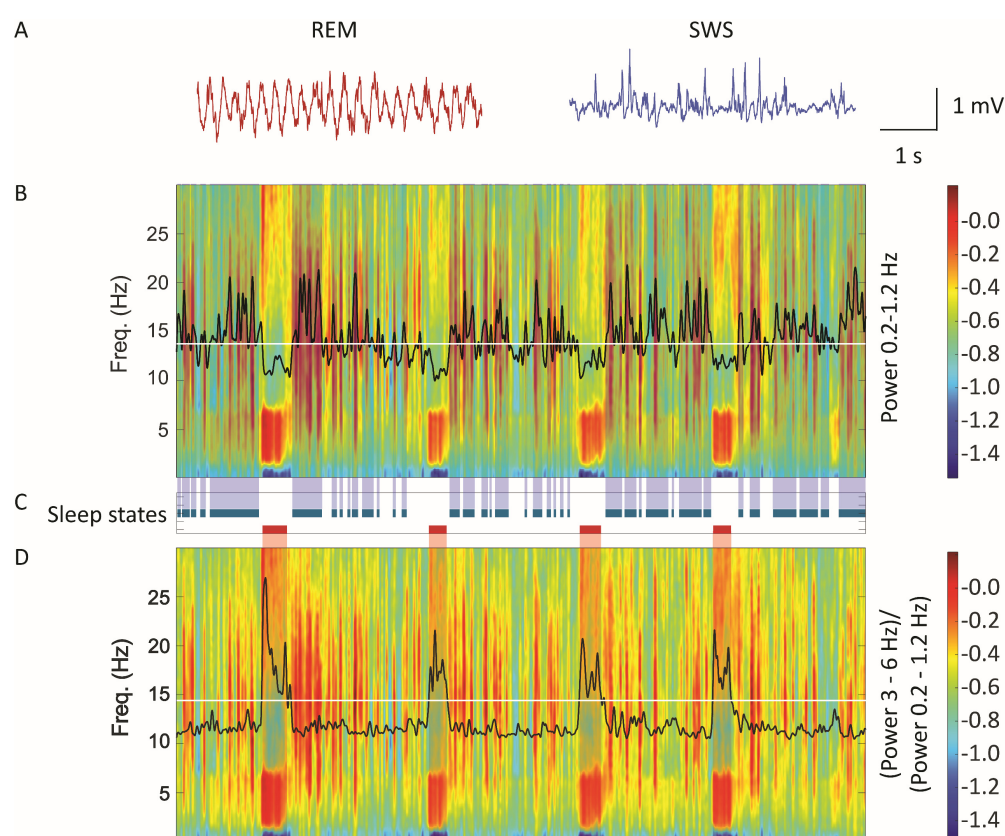


**Figure 11. Local Field Potential (LFP) analysis.** An exemplary spectrogram from the LFP recording of an individual animal. (A) Short representative excerpts of the SWS-like (blue trace) and REM-like (red trace) LFP are shown. (C) REM-like (red) and SWS-like sleep states (blue) were marked out with red (REM) and blue (SWS) shadows in the spectrogram. (B) Black lines in

the spectrograms represent instantaneous delta power. (D) Black lines in the spectrograms represent the instantaneous theta/delta (REM) ratio. White lines are placed at 1.4 x the average power.

### 11.2. Spike sorting and cell type classification.

Single-unit spike detection and sorting were performed with Klusta-suite software (<http://klusta.readthedocs.io>) and were manually curated with Phy 2.0 (<https://github.com/cortex-lab/phy>). Spikes were detected from the bandpass filtered raw signals (500 Hz-6000 Hz) as threshold-crossing deflections of the signal mean) of all electrodes (The parameters changed to fit different conditions of probes showed in Table 1). Spike features were extracted and assigned to single units, based on a principal component analysis in Klusta-suite. The isolation of units was curated with Phys2 by manual inspection of spike waveform consistency, autocorrelogram lags and sufficient distance between recordings sites. Only units with clear negative waveforms were included.

**Table 1. Spike detection parameters.**

Main parameters	Arc/Arg3.1 KO		HPC-cKO		LS-cKO	
	HPC	LS	HPC	LS	HPC	LS
Threshold strong factor	4.5	3.5	4.5	3.5	4.5	3.5
Threshold weak factor	3.4	2	3.5	2	3.5	3
Features	4	3	4	3	4	3

Single units in the hippocampus were classified into putative excitatory neurons and inhibitory interneurons (Sirota et al., 2008). The main parameters were used for classification listed in Table 1. Single units in the lateral septum were classified into medium-spiny neurons and fast-spiking neurons, a third group constituted unclassified neurons (Howe & Blair, 2021; Hagar G. Yamin et al., 2013). The classification was performed in CellExplorer (Petersen et al., 2021) based on the firing frequencies, spike through-to-peak latency, spike waveform asymmetry, and proportion of time associated with long interspike-intervals ( $ISIs > 2$  s) ( $PROP_{ISI > 2\text{ s}}$ )



(Schmitzer-Torbert & Redish, 2008). The main parameters were used for classification listed in Table 2 and 3.

**Table 2. Main parameters used for the unit classification in hippocampus.**

	Ab ratio	Firing rate (Hz)	Trough to peak ( $\mu$ s)	acg tau rise
Excitatory neurons	-0.45 $\pm$ 0.14	0.72 $\pm$ 0.43	0.60 $\pm$ 0.10	1.91 $\pm$ 1.57
Inhibitory neurons	0.07 $\pm$ 0.34	2.06 $\pm$ 1.83	0.38 $\pm$ 0.13	6.03 $\pm$ 5.53

Data presented as mean  $\pm$  SD.

**Table 3. Main parameters used for the unit classification in lateral septum.**

	Ab ratio	Firing rate (Hz)	Trough to peak ( $\mu$ s)	PROP <sub>ISI &gt; 2 s</sub>
Medium spiny neurons	-0.14 $\pm$ 0.14	0.55 $\pm$ 0.38	0.55 $\pm$ 0.07	>30%
Fast spiking neurons	-0.17 $\pm$ 0.15	3.57 $\pm$ 2.16	0.57 $\pm$ 0.09	< 29%

Data presented as mean  $\pm$  SD.

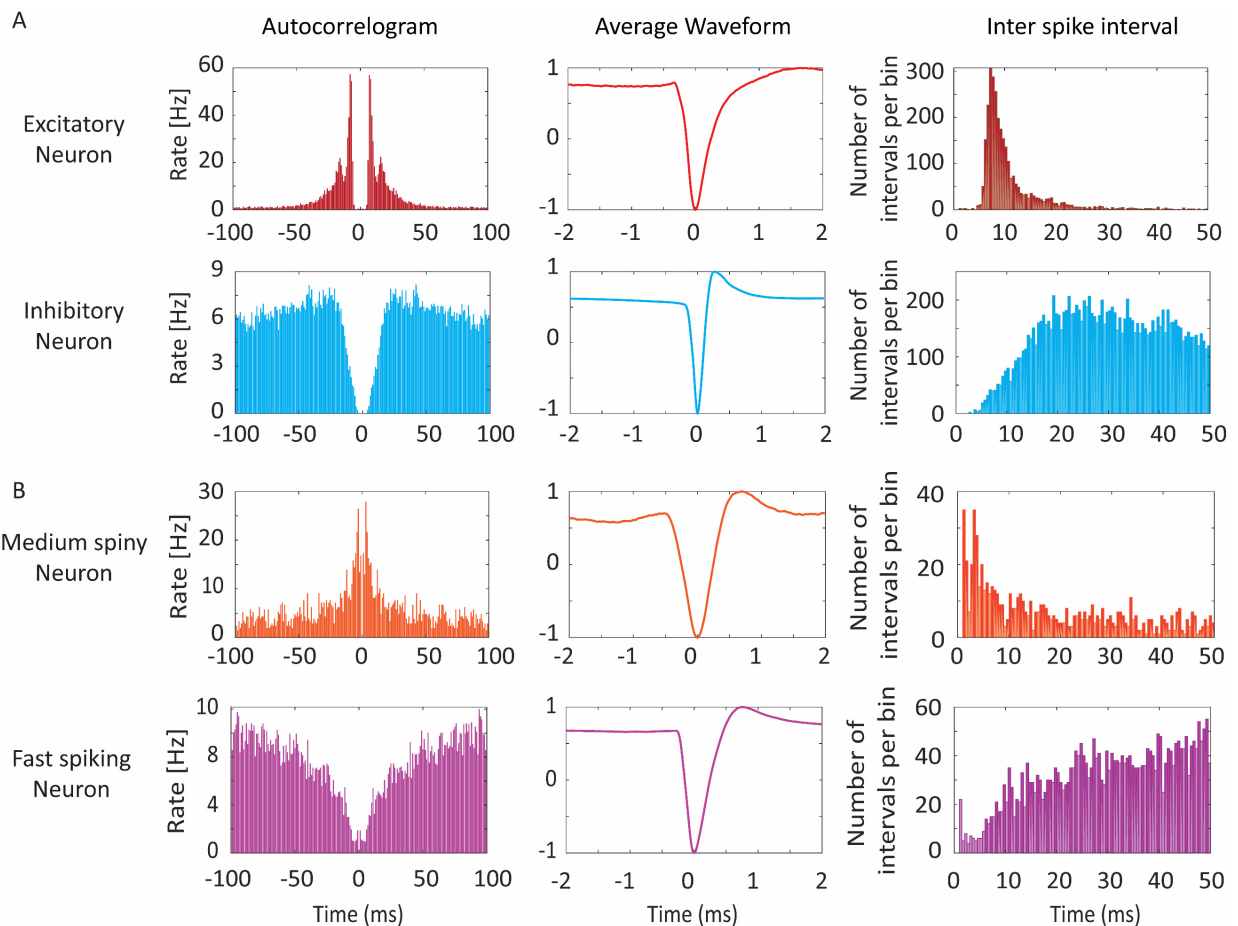


**Figure 82. Typical units in the Hippocampus and lateral septum .** (A) Examples of units in HPC that were classified as putative excitatory and inhibitory neurons. (B) Examples of units in the LS that were classified as medium-spiny and fast-spiking neurons.

## 12.Statistical analysis

For optical suppression fear condition test data, a Kruskal-Wallis test and Dunn's multiple comparison was applied between the control, stGtACR-Novel, and stGtACR-Condition groups. For cell counting data and in vivo local field potential recordings, the Mann-Whitney test was applied between groups. The Mann-Whitney test was applied between genotypes for the fear conditioning test in LS-cKO mice, SST-cKO mice, and PV-cKO mice. For the open field test, elevated plus maze test, forced swimming test, and tail suspension test in SST-cKO and PV-cKO mice, the Mann-Whitney test was applied between genotypes. For the acquisition of Morris water maze, cue test of water maze, and fear conditioning, a two-way ANOVA with a mixed-effects model was performed within subjects following time or trials, and a post hoc Bonferroni

test was used on comparisons between genotypes and groups. For the water maze probe test, a two-way ANOVA with a mixed-effects model and with a post hoc Bonferroni test was applied between genotypes and different zones/quadrants. In the optical suppression tone fear conditioning test, the Kruskal-Wallis test was applied between the control, stGtACR-Novel, and stGtACR-Condition groups during tone fear acquisition. In the optical suppression tone fear memory retrieval tests, a one-way ANOVA test with post hoc Bonferroni test was applied between the control, stGtACR-Novel, and stGtACR-Condition groups. The Mann-Whitney test was applied between genotypes for the tone fear conditioning and tone fear memory retrieval test in LS-cKO mice, SST-cKO mice, and PV-cKO mice. All statistics were done with GraphPad Prism 10.0, and  $p < 0.05$  was considered as significant. All graphs were generated with GraphPad Prism 10.0, Adobe Illustrator 2023, and Matlab R2021b (MathWorks). Values presented in line plots mean  $\pm$  S.E.M. The box plots showed the median (-), whiskers showed min to max, and all data points.

## **Appendix**



## 1. References

- Abraham, W. C., Jones, O. D., & Glanzman, D. L. (2019). Is plasticity of synapses the mechanism of long-term memory storage? *NPJ Sci Learn*, 4, 9. doi:10.1038/s41539-019-0048-y
- Abuse, S. (2014). Trauma-informed care in behavioral health services. *(No Title)*, 42.
- Adelhofer, N., & Beste, C. (2020). Pre-trial theta band activity in the ventromedial prefrontal cortex correlates with inhibition-related theta band activity in the right inferior frontal cortex. *Neuroimage*, 219, 117052. doi:10.1016/j.neuroimage.2020.117052
- Adler, G., & Gattaz, W. F. (1993). Pain perception threshold in major depression. *Biol Psychiatry*, 34(10), 687-689. doi:10.1016/0006-3223(93)90041-b
- Amemiya, S., & Redish, A. D. (2018). Hippocampal Theta-Gamma Coupling Reflects State-Dependent Information Processing in Decision Making. *Cell Reports*, 22(12), 3328-3338. doi:10.1016/j.celrep.2018.02.091
- Arnone, D., McIntosh, A. M., Ebmeier, K. P., Munafo, M. R., & Anderson, I. M. (2012). Magnetic resonance imaging studies in unipolar depression: systematic review and meta-regression analyses. *Eur Neuropsychopharmacol*, 22(1), 1-16. doi:10.1016/j.euroneuro.2011.05.003
- Ashley, J., Cordy, B., Lucia, D., Fradkin, L. G., Budnik, V., & Thomson, T. (2018). Retrovirus-like Gag Protein Arc1 Binds RNA and Traffics across Synaptic Boutons. *Cell*, 172(1-2), 262-274 e211. doi:10.1016/j.cell.2017.12.022
- Asok, A., Draper, A., Hoffman, A. F., Schulkin, J., Lupica, C. R., & Rosen, J. B. (2018). Optogenetic silencing of a corticotropin-releasing factor pathway from the central amygdala to the bed nucleus of the stria terminalis disrupts sustained fear. *Mol Psychiatry*, 23(4), 914-922. doi:10.1038/mp.2017.79
- Asok, A., Kandel, E. R., & Rayman, J. B. (2018). The Neurobiology of Fear Generalization. *Front Behav Neurosci*, 12, 329. doi:10.3389/fnbeh.2018.00329
- Association, A. (2000). Diagnostic and statistical manual of mental disorders (DSM-IV-TR), text revision. *(No Title)*.
- Baddeley, A. (2007). *Working Memory, Thought, and Action*.
- Baeg, E. H., Kim, Y. B., Jang, J., Kim, H. T., Mook-Jung, I., & Jung, M. W. (2001). Fast spiking and regular spiking neural correlates of fear conditioning in the medial prefrontal cortex of the rat. *Cereb Cortex*, 11(5), 441-451. doi:10.1093/cercor/11.5.441
- Bains, N., & Abdijadid, S. (2024). Major Depressive Disorder. In *StatPearls*. Treasure Island (FL).
- Bair, M. J., Robinson, R. L., Katon, W., & Kroenke, K. (2003). Depression and pain comorbidity: a literature review. *Arch Intern Med*, 163(20), 2433-2445. doi:10.1001/archinte.163.20.2433
- Baldi, E., & Bucherelli, C. (2015). Brain sites involved in fear memory reconsolidation and extinction of rodents. *Neurosci Biobehav Rev*, 53, 160-190. doi:10.1016/j.neubiorev.2015.04.003
- Banasr, M., Lepack, A., Fee, C., Duric, V., Maldonado-Aviles, J., DiLeone, R., . . . Sanacora, G. (2017). Characterization of GABAergic marker expression in the chronic unpredictable stress model of depression. *Chronic Stress (Thousand Oaks)*, 1. doi:10.1177/2470547017720459
- Banushi, B., & Polito, V. (2023). A Comprehensive Review of the Current Status of the Cellular Neurobiology of Psychedelics. *Biology (Basel)*, 12(11). doi:10.3390/biology12111380
- Bartos, M., Vida, I., & Jonas, P. (2007). Synaptic mechanisms of synchronized gamma oscillations in inhibitory interneuron networks. *Nat Rev Neurosci*, 8(1), 45-56. doi:10.1038/nrn2044
- Beba, F. (2023). *The role of Arc/Arg3.1 in SST-interneurons and their regulation of emotional behaviors and memory*. (Master). Universität zu Lübeck, Hamburg.
- Beique, J. C., Na, Y., Kuhl, D., Worley, P. F., & Hugarir, R. L. (2011). Arc-dependent synapse-specific homeostatic plasticity. *Proc Natl Acad Sci U S A*, 108(2), 816-821. doi:10.1073/pnas.1017914108
- Belleau, E. L., Treadway, M. T., & Pizzagalli, D. A. (2019). The Impact of Stress and Major Depressive Disorder on Hippocampal and Medial Prefrontal Cortex Morphology. *Biol Psychiatry*, 85(6), 443-453. doi:10.1016/j.biopsych.2018.09.031
- Belluscio, M. A., Mizuseki, K., Schmidt, R., Kempter, R., & Buzsáki, G. (2012). Cross-frequency phase-phase coupling between theta and gamma oscillations in the hippocampus. *Journal of Neuroscience*, 32(2), 423-435. doi:10.1523/JNEUROSCI.4122-11.2012
- Benchenane, K., Peyrache, A., Khamassi, M., Tierney, P. L., Gioanni, Y., Battaglia, F. P., & Wiener, S. I. (2010). Coherent Theta Oscillations and Reorganization of Spike Timing in the Hippocampal- Prefrontal Network upon Learning. *Neuron*, 66(6), 921-936. doi:10.1016/j.neuron.2010.05.013
- Bender, F., Gorbati, M., Cadavieco, M. C., Denisova, N., Gao, X., Holman, C., . . . Ponomarenko, A. (2015). Theta oscillations regulate the speed of locomotion via a hippocampus to lateral septum pathway. *Nature Communications*, 6. doi:10.1038/ncomms9521

- Berger, T. W., Alger, B., & Thompson, R. F. (1976). Neuronal substrate of classical conditioning in the hippocampus. *Science*, 192(4238), 483-485. doi:10.1126/science.1257783
- Berry, S. D., & Thompson, R. F. (1978). Prediction of learning rate from the hippocampal electroencephalogram. *Science*, 200(4347), 1298-1300. doi:10.1126/science.663612
- Besnard, A., Gao, Y., TaeWoo Kim, M., Twarkowski, H., Reed, A. K., Langberg, T., . . . Sahay, A. (2019). Dorsolateral septum somatostatin interneurons gate mobility to calibrate context-specific behavioral fear responses. *Nat Neurosci*, 22(3), 436-446. doi:10.1038/s41593-018-0330-y
- Besnard, A., Miller, S. M., & Sahay, A. (2020). Distinct Dorsal and Ventral Hippocampal CA3 Outputs Govern Contextual Fear Discrimination. *Cell Rep*, 30(7), 2360-2373 e2365. doi:10.1016/j.celrep.2020.01.055
- Besnard, A., & Sahay, A. (2016). Adult Hippocampal Neurogenesis, Fear Generalization, and Stress. *Neuropsychopharmacology*, 41(1), 24-44. doi:10.1038/npp.2015.167
- Besnard, A., & Sahay, A. (2021). Enhancing adult neurogenesis promotes contextual fear memory discrimination and activation of hippocampal-dorsolateral septal circuits. *Behav Brain Res*, 399, 112917. doi:10.1016/j.bbr.2020.112917
- Bian, X. L., Qin, C., Cai, C. Y., Zhou, Y., Tao, Y., Lin, Y. H., . . . Zhu, D. Y. (2019). Anterior Cingulate Cortex to Ventral Hippocampus Circuit Mediates Contextual Fear Generalization. *J Neurosci*, 39(29), 5728-5739. doi:10.1523/JNEUROSCI.2739-18.2019
- Bludau, A., Neumann, I. D., & Menon, R. (2023). HDAC1-mediated regulation of GABA signaling within the lateral septum facilitates long-lasting social fear extinction in male mice. *Transl Psychiatry*, 13(1), 10. doi:10.1038/s41398-023-02310-y
- Borderie, A., Caclin, A., Lachaux, J. P., Perrone-Bertolotti, M., Hoyer, R. S., Kahane, P., . . . Albouy, P. (2024). Cross-frequency coupling in cortico-hippocampal networks supports the maintenance of sequential auditory information in short-term memory. *PLoS Biol*, 22(3), e3002512. doi:10.1371/journal.pbio.3002512
- Boulle, F., Massart, R., Stragier, E., Paizanis, E., Zaidan, L., Marday, S., . . . Lanfumey, L. (2014). Hippocampal and behavioral dysfunctions in a mouse model of environmental stress: normalization by agomelatine. *Transl Psychiatry*, 4(11), e485. doi:10.1038/tp.2014.125
- Bramham, C. R., & Messaoudi, E. (2005). BDNF function in adult synaptic plasticity: the synaptic consolidation hypothesis. *Prog Neurobiol*, 76(2), 99-125. doi:10.1016/j.pneurobio.2005.06.003
- Brand, G., & Schaal, B. (2017). [Olfaction in depressive disorders: Issues and perspectives]. *Encephale*, 43(2), 176-182. doi:10.1016/j.encep.2016.04.008
- Bubl, E., Kern, E., Ebert, D., Bach, M., & Tebartz van Elst, L. (2010). Seeing gray when feeling blue? Depression can be measured in the eye of the diseased. *Biol Psychiatry*, 68(2), 205-208. doi:10.1016/j.biopsych.2010.02.009
- Bunting, K. M., Nalloor, R. I., & Vazdarjanova, A. (2015). Influence of Isoflurane on Immediate-Early Gene Expression. *Front Behav Neurosci*, 9, 363. doi:10.3389/fnbeh.2015.00363
- Burjanadze, M. A., Dashniani, M. G., Solomon, R. O., Beselia, G. V., Tsverava, L., Lagani, V., . . . Chighladze, M. R. (2022). Age-related changes in medial septal cholinergic and GABAergic projection neurons and hippocampal neurotransmitter receptors: relationship with memory impairment. *Exp Brain Res*, 240(5), 1589-1604. doi:10.1007/s00221-022-06354-2
- Butler, C. W., Wilson, Y. M., Gunnarsen, J. M., & Murphy, M. (2015). Tracking the fear memory engram: discrete populations of neurons within amygdala, hypothalamus, and lateral septum are specifically activated by auditory fear conditioning. *Learning & Memory*, 22(8), 370-384. doi:10.1101/lm.037663.114
- Buzsaki, G., Leung, L. W., & Vanderwolf, C. H. (1983). Cellular bases of hippocampal EEG in the behaving rat. *Brain Res*, 287(2), 139-171. doi:10.1016/0165-0173(83)90037-1
- Buzsaki, G., & Moser, E. I. (2013). Memory, navigation and theta rhythm in the hippocampal-entorhinal system. *Nat Neurosci*, 16(2), 130-138. doi:10.1038/nn.3304
- Byers, C. E., Barylko, B., Ross, J. A., Southworth, D. R., James, N. G., Taylor, C. A. t., . . . Albanesi, J. P. (2015). Enhancement of dynamin polymerization and GTPase activity by Arc/Arg3.1. *Biochim Biophys Acta*, 1850(6), 1310-1318. doi:10.1016/j.bbagen.2015.03.002
- Calandreau, L., Desgranges, B., Jaffard, R., & Desmedt, A. (2010). Switching from contextual to tone fear conditioning and vice versa: The key role of the glutamatergic hippocampal-lateral septal neurotransmission. *Learning and Memory*, 17(9), 440-443. doi:10.1101/lm.1859810
- Camina, E., & Güell, F. (2017). The Neuroanatomical, Neurophysiological and Psychological Basis of Memory: Current Models and Their Origins. *Front Pharmacol*, 8, 438. doi:10.3389/fphar.2017.00438
- Cannon, B., Mulroy, R., Otto, M. W., Rosenbaum, J. F., Fava, M., & Nierenberg, A. A. (1999). Dysfunctional attitudes and poor problem solving skills predict hopelessness in major depression. *J Affect Disord*, 55(1), 45-49. doi:10.1016/s0165-0327(98)00123-2

- Cardin, J. A., Carlen, M., Meletis, K., Knoblich, U., Zhang, F., Deisseroth, K., . . . Moore, C. I. (2009). Driving fast-spiking cells induces gamma rhythm and controls sensory responses. *Nature*, 459(7247), 663-667. doi:10.1038/nature08002
- Carus-Cadavieco, M., Gorbati, M., Ye, L., Van Der Veldt, S., Kosse, C., Börgers, C., . . . Korotkova, T. (2017). Gamma oscillations organize top-down signalling to hypothalamus and enable food seeking. doi:10.1038/nature21066
- Cassaday, H. J., Muir, C., Stevenson, C. W., Bonardi, C., Hock, R., & Waite, L. (2023). From safety to frustration: The neural substrates of inhibitory learning in aversive and appetitive conditioning procedures. *Neurobiol Learn Mem*, 202, 107757. doi:10.1016/j.nlm.2023.107757
- Cavdar, S., Onat, F. Y., Cakmak, Y. O., Yananli, H. R., Gulcebi, M., & Aker, R. (2008). The pathways connecting the hippocampal formation, the thalamic reuniens nucleus and the thalamic reticular nucleus in the rat. *J Anat*, 212(3), 249-256. doi:10.1111/j.1469-7580.2008.00858.x
- Cenquizca, L. A., & Swanson, L. W. (2007). Spatial organization of direct hippocampal field CA1 axonal projections to the rest of the cerebral cortex. *Brain Res Rev*, 56(1), 1-26. doi:10.1016/j.brainresrev.2007.05.002
- Chamberland, S., & Topolnik, L. (2012). Inhibitory control of hippocampal inhibitory neurons. *Front Neurosci*, 6, 165. doi:10.3389/fnins.2012.00165
- Chau, L. S., Prakapenka, A., Fleming, S. A., Davis, A. S., & Galvez, R. (2013). Elevated Arc/Arg 3.1 protein expression in the basolateral amygdala following auditory trace-cued fear conditioning. *Neurobiol Learn Mem*, 106, 127-133. doi:10.1016/j.nlm.2013.07.010
- Chee, S. S., Menard, J. L., & Dringenberg, H. C. (2015). The lateral septum as a regulator of hippocampal theta oscillations and defensive behavior in rats. *J Neurophysiol*, 113(6), 1831-1841. doi:10.1152/jn.00806.2014
- Chen, R. F., Cai, Y., Zhu, Z. H., Hou, W. L., Chen, P., Wang, J., . . . Hui, L. (2022). Sleep disorder as a clinical risk factor of major depression: associated with cognitive impairment. *Asian J Psychiatr*, 76, 103228. doi:10.1016/j.ajp.2022.103228
- Chen, S., Chen, F., Amin, N., Ren, Q., Ye, S., Hu, Z., . . . Fang, M. (2022). Defects of parvalbumin-positive interneurons in the ventral dentate gyrus region are implicated depression-like behavior in mice. *Brain Behav Immun*, 99, 27-42. doi:10.1016/j.bbi.2021.09.013
- Chen, S., Cheng, Y., Zhao, W., & Zhang, Y. (2023). Psychological pain in depressive disorder: A concept analysis. *J Clin Nurs*, 32(13-14), 4128-4143. doi:10.1111/jocn.16543
- Chen, Y. H., Wu, J. L., Hu, N. Y., Zhuang, J. P., Li, W. P., Zhang, S. R., . . . Gao, T. M. (2021). Distinct projections from the infralimbic cortex exert opposing effects in modulating anxiety and fear. *J Clin Invest*, 131(14). doi:10.1172/JCI145692
- Chen, Y. T., Arano, R., Guo, J., Saleem, U., Li, Y., & Xu, W. (2023). Inhibitory hippocampus-medial septum projection controls locomotion and exploratory behavior. *Front Synaptic Neurosci*, 15, 1042858. doi:10.3389/fnsyn.2023.1042858
- Chmielewski, W. X., Muckschel, M., Dippel, G., & Beste, C. (2016). Concurrent information affects response inhibition processes via the modulation of theta oscillations in cognitive control networks. *Brain Struct Funct*, 221(8), 3949-3961. doi:10.1007/s00429-015-1137-1
- Cho, K. K., Hoch, R., Lee, A. T., Patel, T., Rubenstein, J. L., & Sohal, V. S. (2015). Gamma rhythms link prefrontal interneuron dysfunction with cognitive inflexibility in Dlx5/6(+/-) mice. *Neuron*, 85(6), 1332-1343. doi:10.1016/j.neuron.2015.02.019
- Chotiner, J. K., Nielson, J., Farris, S., Lewandowski, G., Huang, F., Banos, K., . . . Steward, O. (2010). Assessment of the role of MAP kinase in mediating activity-dependent transcriptional activation of the immediate early gene Arc/Arg3.1 in the dentate gyrus in vivo. *Learn Mem*, 17(2), 117-129. doi:10.1101/lm.1585910
- Chowdhury, A., Luchetti, A., Fernandes, G., Filho, D. A., Kastellakis, G., Tzilivaki, A., . . . Silva, A. J. (2022). A locus coeruleus-dorsal CA1 dopaminergic circuit modulates memory linking. *Neuron*, 110(20), 3374-3388 e3378. doi:10.1016/j.neuron.2022.08.001
- Chowdhury, S., Shepherd, J. D., Okuno, H., Lyford, G., Petralia, R. S., Plath, N., . . . Worley, P. F. (2006). Arc/Arg3.1 interacts with the endocytic machinery to regulate AMPA receptor trafficking. *Neuron*, 52(3), 445-459. doi:10.1016/j.neuron.2006.08.033
- Ciocchi, S., Herry, C., Grenier, F., Wolff, S. B., Letzkus, J. J., Vlachos, I., . . . Luthi, A. (2010). Encoding of conditioned fear in central amygdala inhibitory circuits. *Nature*, 468(7321), 277-282. doi:10.1038/nature09559
- Ciocchi, S., Passecker, J., Malagon-Vina, H., Mikus, N., & Klausberger, T. (2015). Brain computation. Selective information routing by ventral hippocampal CA1 projection neurons. *Science*, 348(6234), 560-563. doi:10.1126/science.aaa3245
- Colgin, L. L. (2016). Rhythms of the hippocampal network. *Nat Rev Neurosci*, 17(4), 239-249. doi:10.1038/nrn.2016.21



- Colgin, L. L., Denninger, T., Fyhn, M., Hafting, T., Bonnevie, T., Jensen, O., . . . Moser, E. I. (2009). LETTERS Frequency of gamma oscillations routes flow of information in the hippocampus. doi:10.1038/nature08573
- Collins, P. Y., Patel, V., Joestl, S. S., March, D., Insel, T. R., Daar, A. S., . . . Stein, D. J. (2011). Grand challenges in global mental health. *Nature*, 475(7354), 27-30. doi:10.1038/475027a
- Commons, K. G., Cholanians, A. B., Babb, J. A., & Ehlinger, D. G. (2017). The Rodent Forced Swim Test Measures Stress-Coping Strategy, Not Depression-like Behavior. *ACS Chem Neurosci*, 8(5), 955-960. doi:10.1021/acschemneuro.7b00042
- Cravens, C. J., Vargas-Pinto, N., Christian, K. M., & Nakazawa, K. (2006). CA3 NMDA receptors are crucial for rapid and automatic representation of context memory. *Eur J Neurosci*, 24(6), 1771-1780. doi:10.1111/j.1460-9568.2006.05044.x
- Crick, F. (1984). Function of the thalamic reticular complex: the searchlight hypothesis. *Proc Natl Acad Sci U S A*, 81(14), 4586-4590. doi:10.1073/pnas.81.14.4586
- Cryan, J. F., Mombereau, C., & Vassout, A. (2005). The tail suspension test as a model for assessing antidepressant activity: review of pharmacological and genetic studies in mice. *Neurosci Biobehav Rev*, 29(4-5), 571-625. doi:10.1016/j.neubiorev.2005.03.009
- Cubelli, R., & Della Sala, S. (2020). Implicit memory. *Cortex*, 125, 345. doi:10.1016/j.cortex.2020.01.011
- Cui, Y., Yang, Y., Ni, Z., Dong, Y., Cai, G., Foncelle, A., . . . Hu, H. (2018). Astroglial Kir4.1 in the lateral habenula drives neuronal bursts in depression. *Nature*, 554(7692), 323-327. doi:10.1038/nature25752
- Cullen, P. K., Gilman, T. L., Winiecki, P., Riccio, D. C., & Jasnow, A. M. (2015). Activity of the anterior cingulate cortex and ventral hippocampus underlie increases in contextual fear generalization. *Neurobiol Learn Mem*, 124, 19-27. doi:10.1016/j.nlm.2015.07.001
- Cummings, K. A., & Clem, R. L. (2020). Prefrontal somatostatin interneurons encode fear memory. *Nat Neurosci*, 23(1), 61-74. doi:10.1038/s41593-019-0552-7
- Cummings, K. A., Lacagnina, A. F., & Clem, R. L. (2021). GABAergic microcircuitry of fear memory encoding. *Neurobiol Learn Mem*, 184, 107504. doi:10.1016/j.nlm.2021.107504
- Cutsuridis, V., & Taxis, J. (2013). Deciphering the role of CA1 inhibitory circuits in sharp wave-ripple complexes. *Front Syst Neurosci*, 7, 13. doi:10.3389/fnsys.2013.00013
- da Silva, B. M., Bast, T., & Morris, R. G. (2013). Spatial memory: behavioral determinants of persistence in the watermaze delayed matching-to-place task. *Learn Mem*, 21(1), 28-36. doi:10.1101/lm.032169.113
- Dashniani, M. G., Burjanadze, M. A., Chkhikvishvili, N. C., Solomon, R. O., Kandashvili, M., Naneishvili, T. L., . . . Chighladze, M. R. (2020). Modulation of spatial memory and expression of hippocampal neurotransmitter receptors by selective lesion of medial septal cholinergic and GABAergic neurons. *Exp Brain Res*, 238(10), 2385-2397. doi:10.1007/s00221-020-05889-6
- DaSilva, L. L., Wall, M. J., L. P. d. A., Wauters, S. C., Januario, Y. C., Muller, J., & Correa, S. A. (2016). Activity-Regulated Cytoskeleton-Associated Protein Controls AMPAR Endocytosis through a Direct Interaction with Clathrin-Adaptor Protein 2. *eNeuro*, 3(3). doi:10.1523/ENEURO.0144-15.2016
- Daume, J., Kaminski, J., Schjetnan, A. G. P., Salimpour, Y., Khan, U., Kyzar, M., . . . Rutishauser, U. (2024). Control of working memory by phase-amplitude coupling of human hippocampal neurons. *Nature*, 629(8011), 393-401. doi:10.1038/s41586-024-07309-z
- Davachi, L. (2006). Item, context and relational episodic encoding in humans. *Curr Opin Neurobiol*, 16(6), 693-700. doi:10.1016/j.conb.2006.10.012
- Davis, M., Walker, D. L., Miles, L., & Grillon, C. (2010). Phasic vs sustained fear in rats and humans: role of the extended amygdala in fear vs anxiety. *Neuropsychopharmacology*, 35(1), 105-135. doi:10.1038/npp.2009.109
- de Bartolomeis, A., Sarappa, C., Buonaguro, E. F., Marmo, F., Eramo, A., Tomasetti, C., & Iasevoli, F. (2013). Different effects of the NMDA receptor antagonists ketamine, MK-801, and memantine on postsynaptic density transcripts and their topography: role of Homer signaling, and implications for novel antipsychotic and pro-cognitive targets in psychosis. *Prog Neuropsychopharmacol Biol Psychiatry*, 46, 1-12. doi:10.1016/j.pnpbp.2013.06.010
- de Kloet, E. R., Joels, M., & Holsboer, F. (2005). Stress and the brain: from adaptation to disease. *Nat Rev Neurosci*, 6(6), 463-475. doi:10.1038/nrn1683
- de Leon Reyes, N. S., Sierra Diaz, P., Nogueira, R., Ruiz-Pino, A., Nomura, Y., de Solis, C. A., . . . Leroy, F. (2023). Corticotropin-releasing hormone signaling from prefrontal cortex to lateral septum suppresses interaction with familiar mice. *Cell*, 186(19), 4152-4171 e4131. doi:10.1016/j.cell.2023.08.010

- de, S. T. M. A., Gaiardo, R. B., & Cerutti, S. M. (2023). Inactivation of the dorsal CA1 hippocampus impairs the consolidation of discriminative avoidance memory by modulating the intrinsic and extrinsic hippocampal circuitry. *J Chem Neuroanat*, 128, 102209. doi:10.1016/j.jchemneu.2022.102209
- Debiec, J., & Ledoux, J. E. (2004). Disruption of reconsolidation but not consolidation of auditory fear conditioning by noradrenergic blockade in the amygdala. *Neuroscience*, 129(2), 267-272. doi:10.1016/j.neuroscience.2004.08.018
- Decarie-Spain, L., Liu, C. M., Lauer, L. T., Subramanian, K., Bashaw, A. G., Klug, M. E., . . . Kanoski, S. E. (2022). Ventral hippocampus-lateral septum circuitry promotes foraging-related memory. *Cell Rep*, 40(13), 111402. doi:10.1016/j.celrep.2022.111402
- Delorme, J., Wang, L., Kuhn, F. R., Kodoth, V., Ma, J., Martinez, J. D., . . . Aton, S. J. (2021). Sleep loss drives acetylcholine- and somatostatin interneuron-mediated gating of hippocampal activity to inhibit memory consolidation. *Proc Natl Acad Sci U S A*, 118(32). doi:10.1073/pnas.2019318118
- Deng, K., Yang, L., Xie, J., Tang, H., Wu, G. S., & Luo, H. R. (2019). Whole-brain mapping of projection from mouse lateral septal nucleus. *Biol Open*, 8(7). doi:10.1242/bio.043554
- Dew, I. T. Z., & Cabeza, R. (2011). The porous boundaries between explicit and implicit memory: behavioral and neural evidence. *Ann N Y Acad Sci*, 1224, 174-190. doi:10.1111/j.1749-6632.2010.05946.x
- Dickey, C. W., Verzhbivsky, I. A., Jiang, X., Rosen, B. Q., Kajfez, S., Stedelin, B., . . . Halgren, E. (2022). Widespread ripples synchronize human cortical activity during sleep, waking, and memory recall. *Proc Natl Acad Sci U S A*, 119(28), e2107797119. doi:10.1073/pnas.2107797119
- Dittgen, T., Nimmerjahn, A., Komai, S., Licznarski, P., Waters, J., Margrie, T. W., . . . Osten, P. (2004). Lentivirus-based genetic manipulations of cortical neurons and their optical and electrophysiological monitoring in vivo. *Proc Natl Acad Sci U S A*, 101(52), 18206-18211. doi:10.1073/pnas.0407976101
- Dixsaut, L., & Graff, J. (2021). The Medial Prefrontal Cortex and Fear Memory: Dynamics, Connectivity, and Engrams. *Int J Mol Sci*, 22(22). doi:10.3390/ijms222212113
- Dong, H. W., Petrovich, G. D., & Swanson, L. W. (2001). Topography of projections from amygdala to bed nuclei of the stria terminalis. *Brain Res Brain Res Rev*, 38(1-2), 192-246. doi:10.1016/s0165-0173(01)00079-0
- Dong, P., Wang, H., Shen, X. F., Jiang, P., Zhu, X. T., Li, Y., . . . Li, X. M. (2019). A novel cortico-intrathalamic circuit for flight behavior. *Nat Neurosci*, 22(6), 941-949. doi:10.1038/s41593-019-0391-6
- Douillard-Guilloux, G., Lewis, D., Seney, M. L., & Sibille, E. (2017). Decrease in somatostatin-positive cell density in the amygdala of females with major depression. *Depress Anxiety*, 34(1), 68-78. doi:10.1002/da.22549
- Drouet, J. B., Fauvelle, F., Maunoir-Regimbal, S., Fidler, N., Maury, R., Peinnequin, A., . . . Canini, F. (2015). Differences in prefrontal cortex GABA/glutamate ratio after acute restraint stress in rats are associated with specific behavioral and neurobiological patterns. *Neuroscience*, 285, 155-165. doi:10.1016/j.neuroscience.2014.10.058
- Dudai, Y. (2004). The neurobiology of consolidations, or, how stable is the engram? *Annu Rev Psychol*, 55, 51-86. doi:10.1146/annurev.psych.55.090902.142050
- Duman, R. S., Sanacora, G., & Krystal, J. H. (2019). Altered Connectivity in Depression: GABA and Glutamate Neurotransmitter Deficits and Reversal by Novel Treatments. *Neuron*, 102(1), 75-90. doi:10.1016/j.neuron.2019.03.013
- Dunsmoor, J. E., Otto, A. R., & Phelps, E. A. (2017). Stress promotes generalization of older but not recent threat memories. *Proc Natl Acad Sci U S A*, 114(34), 9218-9223. doi:10.1073/pnas.1704428114
- Dunsmoor, J. E., Prince, S. E., Murty, V. P., Kragel, P. A., & LaBar, K. S. (2011). Neurobehavioral mechanisms of human fear generalization. *Neuroimage*, 55(4), 1878-1888. doi:10.1016/j.neuroimage.2011.01.041
- Duvarci, S., Bauer, E. P., & Pare, D. (2009). The bed nucleus of the stria terminalis mediates inter-individual variations in anxiety and fear. *J Neurosci*, 29(33), 10357-10361. doi:10.1523/JNEUROSCI.2119-09.2009
- Dyrvig, M., Hansen, H. H., Christiansen, S. H., Woldbye, D. P., Mikkelsen, J. D., & Lichota, J. (2012). Epigenetic regulation of Arc and c-Fos in the hippocampus after acute electroconvulsive stimulation in the rat. *Brain Res Bull*, 88(5), 507-513. doi:10.1016/j.brainresbull.2012.05.004
- Eichenbaum, H. (2016). Still searching for the engram. *Learn Behav*, 44(3), 209-222. doi:10.3758/s13420-016-0218-1
- Eichenbaum, H., & Cohen, N. J. (2004). *From Conditioning to Conscious Recollection: Memory Systems of the Brain*. Oxford University Press.
- Eid, R. S., Gobinath, A. R., & Galea, L. A. M. (2019). Sex differences in depression: Insights from clinical and preclinical studies. *Prog Neurobiol*, 176, 86-102. doi:10.1016/j.pneurobio.2019.01.006
- El-Boustani, S., Ip, J. P. K., Breton-Provencher, V., Knott, G. W., Okuno, H., Bito, H., & Sur, M. (2018). Locally coordinated synaptic plasticity of visual cortex neurons in vivo. *Science*, 360(6395), 1349-1354. doi:10.1126/science.aao0862

- Elizalde, N., Pastor, P. M., Garcia-Garcia, A. L., Serres, F., Venzala, E., Huarte, J., . . . Tordera, R. M. (2010). Regulation of markers of synaptic function in mouse models of depression: chronic mild stress and decreased expression of VGLUT1. *J Neurochem*, 114(5), 1302-1314. doi:10.1111/j.1471-4159.2010.06854.x
- Eriksen, M. S., & Bramham, C. R. (2022). Molecular physiology of Arc/Arg3.1: The oligomeric state hypothesis of synaptic plasticity. *Acta Physiol (Oxf)*, 236(3), e13886. doi:10.1111/apha.13886
- Eriksson, T. M., Delagrange, P., Spedding, M., Popoli, M., Mathe, A. A., Ogren, S. O., & Svenningsson, P. (2012). Emotional memory impairments in a genetic rat model of depression: involvement of 5-HT/MEK/Arc signaling in restoration. *Mol Psychiatry*, 17(2), 173-184. doi:10.1038/mp.2010.131
- Espinosa, N., Alonso, A., Caneo, M., Moran, C., & Fuentealba, P. (2022). Optogenetic Suppression of Lateral Septum Somatostatin Neurons Enhances Hippocampus Cholinergic Theta Oscillations and Local Synchrony. *Brain Sci*, 13(1). doi:10.3390/brainsci13010001
- Fanselow, M. S., & Dong, H. W. (2010). Are the dorsal and ventral hippocampus functionally distinct structures? *Neuron*, 65(1), 7-19. doi:10.1016/j.neuron.2009.11.031
- Fell, J., & Axmacher, N. (2011). The role of phase synchronization in memory processes. *Nat Rev Neurosci*, 12(2), 105-118. doi:10.1038/nrn2979
- Fell, J., Klaver, P., Elfadil, H., Schaller, C., Elger, C. E., & Fernandez, G. (2003). Rhinal-hippocampal theta coherence during declarative memory formation: interaction with gamma synchronization? *Eur J Neurosci*, 17(5), 1082-1088. doi:10.1046/j.1460-9568.2003.02522.x
- Fell, J., Klaver, P., Lehnertz, K., Grunwald, T., Schaller, C., Elger, C. E., & Fernandez, G. (2001). Human memory formation is accompanied by rhinal-hippocampal coupling and decoupling. *Nat Neurosci*, 4(12), 1259-1264. doi:10.1038/nn759
- Fernandez-Ruiz, A., Oliva, A., Soula, M., Rocha-Almeida, F., Nagy, G. A., Martin-Vazquez, G., & Buzsaki, G. (2021). Gamma rhythm communication between entorhinal cortex and dentate gyrus neuronal assemblies. *Science*, 372(6537). doi:10.1126/science.abf3119
- Ferrara, N. C., Cullen, P. K., Pullins, S. P., Rotondo, E. K., & Helmstetter, F. J. (2017). Input from the medial geniculate nucleus modulates amygdala encoding of fear memory discrimination. *Learn Mem*, 24(9), 414-421. doi:10.1101/lm.044131.116
- Ferro, M. A. (2016). Major depressive disorder, suicidal behaviour, bipolar disorder, and generalised anxiety disorder among emerging adults with and without chronic health conditions. *Epidemiol Psychiatr Sci*, 25(5), 462-474. doi:10.1017/S2045796015000700
- Fitzgerald, P. J. (2013). Gray colored glasses: is major depression partially a sensory perceptual disorder? *J Affect Disord*, 151(2), 418-422. doi:10.1016/j.jad.2013.06.045
- Fogaca, M. V., Wu, M., Li, C., Li, X. Y., Picciotto, M. R., & Duman, R. S. (2021). Inhibition of GABA interneurons in the mPFC is sufficient and necessary for rapid antidepressant responses. *Mol Psychiatry*, 26(7), 3277-3291. doi:10.1038/s41380-020-00916-y
- Foilib, A. R., Flyer-Adams, J. G., Maier, S. F., & Christianson, J. P. (2016). Posterior insular cortex is necessary for conditioned inhibition of fear. *Neurobiol Learn Mem*, 134 Pt B(Pt B), 317-327. doi:10.1016/j.nlm.2016.08.004
- Fosnaugh, J. S., Bhat, R. V., Yamagata, K., Worley, P. F., & Baraban, J. M. (1995). Activation of arc, a putative "effector" immediate early gene, by cocaine in rat brain. *J Neurochem*, 64(5), 2377-2380. doi:10.1046/j.1471-4159.1995.64052377.x
- Frankland, P. W., & Bontempi, B. (2005). The organization of recent and remote memories. *Nat Rev Neurosci*, 6(2), 119-130. doi:10.1038/nrn1607
- Frankland, P. W., Bontempi, B., Talton, L. E., Kaczmarek, L., & Silva, A. J. (2004). The Involvement of the Anterior Cingulate Cortex in Remote Contextual Fear Memory. *Science*, 304(5672), 881-883. doi:10.1126/science.1094804
- Freedman, M. (1994). Frontal and parietal lobe dysfunction in depression: delayed alternation and tactile learning deficits. *Neuropsychologia*, 32(8), 1015-1025. doi:10.1016/0028-3932(94)90050-7
- Freund, T. F., & Antal, M. (1988). GABA-containing neurons in the septum control inhibitory interneurons in the hippocampus. *Nature*, 336(6195), 170-173. doi:10.1038/336170a0
- Fries, P. (2009). Neuronal gamma-band synchronization as a fundamental process in cortical computation. *Annu Rev Neurosci*, 32, 209-224. doi:10.1146/annurev.neuro.051508.135603
- Fries, P. (2015). Rhythms for Cognition: Communication through Coherence. *Neuron*, 88(1), 220-235. doi:10.1016/j.neuron.2015.09.034
- Fries, P., Nikolic, D., & Singer, W. (2007). The gamma cycle. *Trends Neurosci*, 30(7), 309-316. doi:10.1016/j.tins.2007.05.005

- Frodl, T., Jager, M., Smajstrlova, I., Born, C., Bottlender, R., Palladino, T., . . . Meisenzahl, E. M. (2008). Effect of hippocampal and amygdala volumes on clinical outcomes in major depression: a 3-year prospective magnetic resonance imaging study. *J Psychiatry Neurosci*, 33(5), 423-430. Retrieved from <https://www.ncbi.nlm.nih.gov/pubmed/18787661>
- Fuchs, T., Jefferson, S. J., Hooper, A., Yee, P. H., Maguire, J., & Luscher, B. (2017). Disinhibition of somatostatin-positive GABAergic interneurons results in an anxiolytic and antidepressant-like brain state. *Mol Psychiatry*, 22(6), 920-930. doi:10.1038/mp.2016.188
- Fuentes, A. (2017). *The International Encyclopedia of Primatology, 3 Volume Set*: John Wiley & Sons.
- Fujisawa, S., & Buzsaki, G. (2011). A 4 Hz oscillation adaptively synchronizes prefrontal, VTA, and hippocampal activities. *Neuron*, 72(1), 153-165. doi:10.1016/j.neuron.2011.08.018
- Fukazawa, Y., Saitoh, Y., Ozawa, F., Ohta, Y., Mizuno, K., & Inokuchi, K. (2003). Hippocampal LTP is accompanied by enhanced F-actin content within the dendritic spine that is essential for late LTP maintenance in vivo. *Neuron*, 38(3), 447-460. doi:10.1016/s0896-6273(03)00206-x
- Gao, L., Sommerlade, L., Coffman, B., Zhang, T., Stephen, J. M., Li, D., . . . Schelter, B. (2015). Granger causal time-dependent source connectivity in the somatosensory network. *Sci Rep*, 5, 10399. doi:10.1038/srep10399
- Gao, X. (2016). *Dependence of learning and memory consolidation on spatiotemporal expression of Arc/Arg3.1 in hippocampal-cortical networks*. (PhD Dissertation). University Hamburg, Hamburg, Germany. Retrieved from <https://ediss.sub.uni-hamburg.de/handle/ediss/6958>
- Gao, X., Castro-Gomez, S., Grendel, J., Graf, S., Süssens, U., Binkle, L., . . . Ohana, O. (2018). Arc/Arg3.1 mediates a critical period for spatial learning and hippocampal networks. doi:10.1073/pnas.1810125115
- Gao, X., Grendel, J., Muhia, M., Castro-Gomez, S., Süssens, U., Isbrandt, D., . . . Ohana, O. (2019). Disturbed Prefrontal Cortex Activity in the Absence of Schizophrenia-Like Behavioral Dysfunction in Arc/Arg3.1 Deficient Mice. *J Neurosci*, 39(41), 8149-8163. doi:10.1523/JNEUROSCI.0623-19.2019
- Garcia, R., & Jaffard, R. (1992). The hippocampo-septal projection in mice: long-term potentiation in the lateral septum. *Neuroreport*, 3(2), 193-196. doi:10.1097/00001756-199202000-00018
- Garcia, R., & Jaffard, R. (2006). Changes in Synaptic Excitability in the Lateral Septum Associated with Contextual and Auditory Fear Conditioning in Mice. *European Journal of Neuroscience*, 8(4), 809-815. doi:10.1111/j.1460-9568.1996.tb01266.x
- Garcia, R., Vouimba, R. M., & Jaffard, R. (1997). Contextual Conditioned Fear Blocks the Induction But Not the Maintenance of Lateral Septal LTP in Behaving Mice. *Journal of Neurophysiology*, 78(1), 76-81. doi:10.1152/jn.1997.78.1.76
- Giachero, M., Calfa, G. D., & Molina, V. A. (2013). Hippocampal structural plasticity accompanies the resulting contextual fear memory following stress and fear conditioning. *Learn Mem*, 20(11), 611-616. doi:10.1101/lm.031724.113
- Giachero, M., Calfa, G. D., & Molina, V. A. (2015). Hippocampal dendritic spines remodeling and fear memory are modulated by GABAergic signaling within the basolateral amygdala complex. *Hippocampus*, 25(5), 545-555. doi:10.1002/hipo.22409
- Gilmartin, M. R., & McEchron, M. D. (2005). Single neurons in the medial prefrontal cortex of the rat exhibit tonic and phasic coding during trace fear conditioning. *Behav Neurosci*, 119(6), 1496-1510. doi:10.1037/0735-7044.119.6.1496
- Giorgi, C., & Marinelli, S. (2021). Roles and Transcriptional Responses of Inhibitory Neurons in Learning and Memory. *Front Mol Neurosci*, 14, 689952. doi:10.3389/fnmol.2021.689952
- Giorgi, C., Yeo, G. W., Stone, M. E., Katz, D. B., Burge, C., Turrigiano, G., & Moore, M. J. (2007). The EJC factor eIF4AIII modulates synaptic strength and neuronal protein expression. *Cell*, 130(1), 179-191. doi:10.1016/j.cell.2007.05.028
- Girardeau, G., & Lopes-Dos-Santos, V. (2021). Brain neural patterns and the memory function of sleep. *Science*, 374(6567), 560-564. doi:10.1126/science.abi8370
- Givens, B. S., & Olton, D. S. (1990). Cholinergic and GABAergic modulation of medial septal area: effect on working memory. *Behav Neurosci*, 104(6), 849-855. doi:10.1037//0735-7044.104.6.849
- Goh, W. D., & Lu, S. H. (2012). Testing the myth of the encoding-retrieval match. *Mem Cognit*, 40(1), 28-39. doi:10.3758/s13421-011-0133-9
- Goldsmith, S. K., Pellmar, T. C., Kleinman, A. M., & Bunney, W. E. (2002). Reducing Suicide: A National Imperative. In S. K. Goldsmith, T. C. Pellmar, A. M. Kleinman, & W. E. Bunney (Eds.), *Reducing Suicide: A National Imperative*. Washington (DC).
- Gómez, M. S. C. (2016). *Developmental and adult expression of Arc/Arg3.1 in corticolimbic structures determines memory and emotional control*. (PhD). Universität Hamburg, Hamburg.
- Goodenough, J., McGuire, B., & Jakob, E. (2009). *Perspectives on animal behavior*: John Wiley & Sons.

- Goto, A. (2022). Synaptic plasticity during systems memory consolidation. *Neurosci Res*, 183, 1-6. doi:10.1016/j.neures.2022.05.008
- Gray, C. M., Konig, P., Engel, A. K., & Singer, W. (1989). Oscillatory responses in cat visual cortex exhibit inter-columnar synchronization which reflects global stimulus properties. *Nature*, 338(6213), 334-337. doi:10.1038/338334a0
- Gray, J. A. (1987). *The psychology of fear and stress* (Vol. 5): CUP Archive.
- Griffin, A. L., Asaka, Y., Darling, R. D., & Berry, S. D. (2004). Theta-contingent trial presentation accelerates learning rate and enhances hippocampal plasticity during trace eyeblink conditioning. *Behav Neurosci*, 118(2), 403-411. doi:10.1037/0735-7044.118.2.403
- Griffin, A. L., Owens, C. B., Peters, G. J., Adelman, P. C., & Cline, K. M. (2012). Spatial representations in dorsal hippocampal neurons during a tactile-visual conditional discrimination task. *Hippocampus*, 22(2), 299-308. doi:10.1002/hipo.20898
- Grillon, C., & Morgan, C. A., 3rd. (1999). Fear-potentiated startle conditioning to explicit and contextual cues in Gulf War veterans with posttraumatic stress disorder. *J Abnorm Psychol*, 108(1), 134-142. doi:10.1037//0021-843x.108.1.134
- Gross, C. T., & Canteras, N. S. (2012). The many paths to fear. *Nat Rev Neurosci*, 13(9), 651-658. doi:10.1038/nrn3301
- Gu, Z., & Yakel, J. L. (2022). Cholinergic Regulation of Hippocampal Theta Rhythm. *Biomedicines*, 10(4). doi:10.3390/biomedicines10040745
- Guilloux, J. P., Douillard-Guilloux, G., Kota, R., Wang, X., Gardier, A. M., Martinowich, K., . . . Sibille, E. (2012). Molecular evidence for BDNF- and GABA-related dysfunctions in the amygdala of female subjects with major depression. *Mol Psychiatry*, 17(11), 1130-1142. doi:10.1038/mp.2011.113
- Gusev, P. A., & Gubin, A. N. (2010). Arc/Arg3.1 mRNA global expression patterns elicited by memory recall in cerebral cortex differ for remote versus recent spatial memories. *Front Integr Neurosci*, 4, 15. doi:10.3389/fnint.2010.00015
- Guzowski, J. F., Lyford, G. L., Stevenson, G. D., Houston, F. P., McGaugh, J. L., Worley, P. F., & Barnes, C. A. (2000). Inhibition of activity-dependent arc protein expression in the rat hippocampus impairs the maintenance of long-term potentiation and the consolidation of long-term memory. *J Neurosci*, 20(11), 3993-4001. doi:10.1523/JNEUROSCI.20-11-03993.2000
- Hains, A. B., Vu, M. A., Maciejewski, P. K., van Dyck, C. H., Gottron, M., & Arnsten, A. F. (2009). Inhibition of protein kinase C signaling protects prefrontal cortex dendritic spines and cognition from the effects of chronic stress. *Proc Natl Acad Sci U S A*, 106(42), 17957-17962. doi:10.1073/pnas.0908563106
- Hajszan, T., Dow, A., Warner-Schmidt, J. L., Szigeti-Buck, K., Sallam, N. L., Parducz, A., . . . Duman, R. S. (2009). Remodeling of hippocampal spine synapses in the rat learned helplessness model of depression. *Biol Psychiatry*, 65(5), 392-400. doi:10.1016/j.biopsych.2008.09.031
- Halassa, M. M., & Acsady, L. (2016). Thalamic Inhibition: Diverse Sources, Diverse Scales. *Trends Neurosci*, 39(10), 680-693. doi:10.1016/j.tins.2016.08.001
- Halassa, M. M., Chen, Z., Wimmer, R. D., Brunetti, P. M., Zhao, S., Zikopoulos, B., . . . Wilson, M. A. (2014). State-dependent architecture of thalamic reticular subnetworks. *Cell*, 158(4), 808-821. doi:10.1016/j.cell.2014.06.025
- Hampton, R. R., Engelberg, J. W. M., & Brady, R. J. (2020). Explicit memory and cognition in monkeys. *Neuropsychologia*, 138, 107326. doi:10.1016/j.neuropsychologia.2019.107326
- Han, C., & Pae, C. U. (2015). Pain and depression: a neurobiological perspective of their relationship. *Psychiatry Investig*, 12(1), 1-8. doi:10.4306/pi.2015.12.1.1
- Harris, E. C., & Barraclough, B. (1997). Suicide as an outcome for mental disorders. A meta-analysis. *Br J Psychiatry*, 170, 205-228. doi:10.1192/bjp.170.3.205
- Hashimoto, M., Brito, S. I., Venner, A., Pasqualini, A. L., Yang, T. L., Allen, D., . . . Anthony, T. E. (2022). Lateral septum modulates cortical state to tune responsivity to threat stimuli. *Cell Rep*, 41(4), 111521. doi:10.1016/j.celrep.2022.111521
- Heckmann, J. G., & Lang, C. J. G. (2006). Neurological causes of taste disorders. *Adv Otorhinolaryngol*, 63, 255-264. doi:10.1159/000093764
- Heimrath, K., Brechmann, A., Blobel-Luer, R., Stadler, J., Budinger, E., & Zaehle, T. (2020). Transcranial direct current stimulation (tDCS) over the auditory cortex modulates GABA and glutamate: a 7 T MR-spectroscopy study. *Sci Rep*, 10(1), 20111. doi:10.1038/s41598-020-77111-0
- Hildyard, J. C. W., Rawson, F., Wells, D. J., & Piercy, R. J. (2020). Multiplex in situ hybridization within a single transcript: RNAscope reveals dystrophin mRNA dynamics. *PLoS ONE*, 15(9), e0239467. doi:10.1371/journal.pone.0239467

- Hintiryan, H., Bowman, I., Johnson, D. L., Korobkova, L., Zhu, M., Khanjani, N., . . . Dong, H. W. (2021). Connectivity characterization of the mouse basolateral amygdalar complex. *Nat Commun*, 12(1), 2859. doi:10.1038/s41467-021-22915-5
- Hippenmeyer, S., Vrieseling, E., Sigrist, M., Portmann, T., Laengle, C., Ladle, D. R., & Arber, S. (2005). A developmental switch in the response of DRG neurons to ETS transcription factor signaling. *PLoS Biol*, 3(5), e159. doi:10.1371/journal.pbio.0030159
- Hirabayashi, T., Takeuchi, D., Tamura, K., & Miyashita, Y. (2013). Functional microcircuit recruited during retrieval of object association memory in monkey perirhinal cortex. *Neuron*, 77(1), 192-203. doi:10.1016/j.neuron.2012.10.031
- Holloway, C. M., & McIntyre, C. K. (2011). Post-training disruption of Arc protein expression in the anterior cingulate cortex impairs long-term memory for inhibitory avoidance training. *Neurobiol Learn Mem*, 95(4), 425-432. doi:10.1016/j.nlm.2011.02.002
- Holschneider, D. P., Yang, J., Sadler, T. R., Nguyen, P. T., Givrad, T. K., & Maarek, J. M. (2006). Mapping cerebral blood flow changes during auditory-cued conditioned fear in the nontethered, nonrestrained rat. *Neuroimage*, 29(4), 1344-1358. doi:10.1016/j.neuroimage.2005.08.038
- Holtmaat, A., & Caroni, P. (2016). Functional and structural underpinnings of neuronal assembly formation in learning. *Nat Neurosci*, 19(12), 1553-1562. doi:10.1038/nn.4418
- Honore, E., Khlaifia, A., Bosson, A., & Lacaille, J. C. (2021). Hippocampal Somatostatin Interneurons, Long-Term Synaptic Plasticity and Memory. *Front Neural Circuits*, 15, 687558. doi:10.3389/fncir.2021.687558
- Hossaini, M., Jongen, J. L., Biesheuvel, K., Kuhl, D., & Holstege, J. C. (2010). Nociceptive stimulation induces expression of Arc/Arg3.1 in the spinal cord with a preference for neurons containing enkephalin. *Mol Pain*, 6, 43. doi:10.1186/1744-8069-6-43
- Houser, C. R., Vaughn, J. E., Barber, R. P., & Roberts, E. (1980). GABA neurons are the major cell type of the nucleus reticularis thalami. *Brain Res*, 200(2), 341-354. doi:10.1016/0006-8993(80)90925-7
- Howe, A. G., & Blair, H. T. (2021). Modulation of lateral septal and dorsomedial striatal neurons by hippocampal sharp - wave ripples, theta rhythm, and running speed. *Hippocampus*. doi:10.1002/hipo.23398
- Hu, S., Dai, G., Worrell, G. A., Dai, Q., & Liang, H. (2011). Causality analysis of neural connectivity: critical examination of existing methods and advances of new methods. *IEEE Trans Neural Netw*, 22(6), 829-844. doi:10.1109/TNN.2011.2123917
- Huang, F., Chotiner, J. K., & Steward, O. (2007). Actin polymerization and ERK phosphorylation are required for Arc/Arg3.1 mRNA targeting to activated synaptic sites on dendrites. *J Neurosci*, 27(34), 9054-9067. doi:10.1523/JNEUROSCI.2410-07.2007
- Ibarra, I. L., Ratnu, V. S., Gordillo, L., Hwang, I. Y., Mariani, L., Weinand, K., . . . Noh, K. M. (2022). Comparative chromatin accessibility upon BDNF stimulation delineates neuronal regulatory elements. *Mol Syst Biol*, 18(8), e10473. doi:10.15252/msb.202110473
- Igarashi, K. M. (2015). Plasticity in oscillatory coupling between hippocampus and cortex. *Curr Opin Neurobiol*, 35, 163-168. doi:10.1016/j.conb.2015.09.005
- Igarashi, K. M., Lu, L., Colgin, L. L., Moser, M.-B., & Moser, E. I. (2014). Coordination of entorhinal-hippocampal ensemble activity during associative learning. *Nature*, 510(7503), 143-147. doi:10.1038/nature13162
- Imbrosci, B., Nitzan, N., McKenzie, S., Donoso, J. R., Swaminathan, A., Bohm, C., . . . Schmitz, D. (2021). Subiculum as a generator of sharp wave-ripples in the rodent hippocampus. *Cell Rep*, 35(3), 109021. doi:10.1016/j.celrep.2021.109021
- Inberg, S., Elkobi, A., Edri, E., & Rosenblum, K. (2013). Taste familiarity is inversely correlated with Arc/Arg3.1 hemispheric lateralization. *J Neurosci*, 33(28), 11734-11743. doi:10.1523/JNEUROSCI.0801-13.2013
- Inberg, S., Jacob, E., Elkobi, A., Edry, E., Rappaport, A., Simpson, T. I., . . . Rosenblum, K. (2016). Fluid consumption and taste novelty determines transcription temporal dynamics in the gustatory cortex. *Mol Brain*, 9, 13. doi:10.1186/s13041-016-0188-4
- Institute of Health Metrics and Evaluation (2023). *Global Health Data Exchange (GHDx)*. Retrieved from: <https://vizhub.healthdata.org/gbd-results/>
- Izquierdo, I., Furini, C. R., & Myskiw, J. C. (2016). Fear Memory. *Physiol Rev*, 96(2), 695-750. doi:10.1152/physrev.00018.2015
- Jacobson, L. H., Vlachou, S., Slaterry, D. A., Li, X., & Cryan, J. F. (2018). The Gamma-Aminobutyric Acid B Receptor in Depression and Reward. *Biol Psychiatry*, 83(11), 963-976. doi:10.1016/j.biopsych.2018.02.006
- Jakkamsetti, V., Tsai, N. P., Gross, C., Molinaro, G., Collins, K. A., Nicoletti, F., . . . Huber, K. M. (2013). Experience-induced Arc/Arg3.1 primes CA1 pyramidal neurons for metabotropic glutamate receptor-dependent long-term synaptic depression. *Neuron*, 80(1), 72-79. doi:10.1016/j.neuron.2013.07.020
- Jawabri, K. H., & Cascella, M. (2024). Physiology, Explicit Memory. In *StatPearls*. Treasure Island (FL).



- Ji, M. H., Zhang, L., Mao, M. J., Zhang, H., Yang, J. J., & Qiu, L. L. (2020). Overinhibition mediated by parvalbumin interneurons might contribute to depression-like behavior and working memory impairment induced by lipopolysaccharide challenge. *Behav Brain Res*, 383, 112509. doi:10.1016/j.bbr.2020.112509
- Jia, X., & Kohn, A. (2011). Gamma rhythms in the brain. *PLoS Biol*, 9(4), e1001045. doi:10.1371/journal.pbio.1001045
- Jimenez, J. C., Su, K., Goldberg, A. R., Luna, V. M., Biane, J. S., Ordek, G., . . . Kheirbek, M. A. (2018). Anxiety Cells in a Hippocampal-Hypothalamic Circuit. *Neuron*, 97(3), 670-683 e676. doi:10.1016/j.neuron.2018.01.016
- Jones, M. W., Errington, M. L., French, P. J., Fine, A., Bliss, T. V. P., Garell, S., . . . Davis, S. (2001). A requirement for the immediate early gene Zif268 in the expression of late LTP and long-term memories. *Nature Neuroscience*, 4(3), 289-296. doi:10.1038/85138
- Josselyn, S. A., Kohler, S., & Frankland, P. W. (2017). Heroes of the Engram. *J Neurosci*, 37(18), 4647-4657. doi:10.1523/JNEUROSCI.0056-17.2017
- Josselyn, S. A., & Tonegawa, S. (2020). Memory engrams: Recalling the past and imagining the future. *Science*, 367(6473). doi:10.1126/science.aaw4325
- Jovanovic, T., & Ressler, K. J. (2010). How the neurocircuitry and genetics of fear inhibition may inform our understanding of PTSD. *Am J Psychiatry*, 167(6), 648-662. doi:10.1176/appi.ajp.2009.09071074
- Julian Keil, H. K., Liam Doherty, Victor Hernandez-Urbina, Hamed Bahmani. (2023). Spatially organized flicker can evoke high-frequency responses above 100Hz in visual cortex. *Authorea*. doi:10.22541/au.168130633.37187628/v1
- Jutras, M. J., Fries, P., & Buffalo, E. A. (2009). Gamma-band synchronization in the macaque hippocampus and memory formation. *J Neurosci*, 29(40), 12521-12531. doi:10.1523/JNEUROSCI.0640-09.2009
- Kanes, S., Colquhoun, H., Gunduz-Bruce, H., Raines, S., Arnold, R., Schacterle, A., . . . Meltzer-Brody, S. (2017). Brexanolone (SAGE-547 injection) in post-partum depression: a randomised controlled trial. *Lancet*, 390(10093), 480-489. doi:10.1016/S0140-6736(17)31264-3
- Kang, K., & Bae, C. (2021). Memory Model for Morphological Semantics of Visual Stimuli Using Sparse Distributed Representation. *Applied Sciences*, 11(22). doi:10.3390/app112210786
- Karakas, S. (2020). A review of theta oscillation and its functional correlates. *Int J Psychophysiol*, 157, 82-99. doi:10.1016/j.jpsycho.2020.04.008
- Katsuki, F., Gerashchenko, D., & Brown, R. E. (2022). Alterations of sleep oscillations in Alzheimer's disease: A potential role for GABAergic neurons in the cortex, hippocampus, and thalamus. *Brain Res Bull*, 187, 181-198. doi:10.1016/j.brainresbull.2022.07.002
- Kawashima, T., Okuno, H., Nonaka, M., Adachi-Morishima, A., Kyo, N., Okamura, M., . . . Bito, H. (2009). Synaptic activity-responsive element in the Arc/Arg3.1 promoter essential for synapse-to-nucleus signaling in activated neurons. *Proc Natl Acad Sci U S A*, 106(1), 316-321. doi:10.1073/pnas.0806518106
- Keene, C. S., Bladon, J., McKenzie, S., Liu, C. D., O'Keefe, J., & Eichenbaum, H. (2016). Complementary Functional Organization of Neuronal Activity Patterns in the Perirhinal, Lateral Entorhinal, and Medial Entorhinal Cortices. *The Journal of Neuroscience*, 36(13), 3660-3675. doi:10.1523/jneurosci.4368-15.2016
- Kessler, R. C., Berglund, P., Borges, G., Nock, M., & Wang, P. S. (2005). Trends in suicide ideation, plans, gestures, and attempts in the United States, 1990-1992 to 2001-2003. *JAMA*, 293(20), 2487-2495. doi:10.1001/jama.293.20.2487
- Khakpai, F., Nasehi, M., Haeri-Rohani, A., Eidi, A., & Zarrindast, M. R. (2013). Septo-hippocampo-septal loop and memory formation. *Basic Clin Neurosci*, 4(1), 5-23. Retrieved from <https://www.ncbi.nlm.nih.gov/pubmed/25337323>
- Khakpai, F., Zarrindast, M. R., Nasehi, M., Haeri-Rohani, A., & Eidi, A. (2013). The role of glutamatergic pathway between septum and hippocampus in the memory formation. *EXCLI J*, 12, 41-51. Retrieved from <https://www.ncbi.nlm.nih.gov/pubmed/27231475>
- Khodagholy, D., Gelinas, J. N., & Buzsaki, G. (2017). Learning-enhanced coupling between ripple oscillations in association cortices and hippocampus. *Science*, 358(6361), 369-372. doi:10.1126/science.aan6203
- Kim, D., Jeong, H., Lee, J., Ghim, J. W., Her, E. S., Lee, S. H., & Jung, M. W. (2016). Distinct Roles of Parvalbumin- and Somatostatin-Expressing Interneurons in Working Memory. *Neuron*, 92(4), 902-915. doi:10.1016/j.neuron.2016.09.023
- Kim, H., Ahrlund-Richter, S., Wang, X., Deisseroth, K., & Carlen, M. (2016). Prefrontal Parvalbumin Neurons in Control of Attention. *Cell*, 164(1-2), 208-218. doi:10.1016/j.cell.2015.11.038
- Kim, W. B., & Cho, J. H. (2020). Encoding of contextual fear memory in hippocampal-amygdala circuit. *Nat Commun*, 11(1), 1382. doi:10.1038/s41467-020-15121-2

- Kitamura, T., Ogawa, S. K., Roy, D. S., Okuyama, T., Morrissey, M. D., Smith, L. M., . . . Tonegawa, S. (2017). Engrams and circuits crucial for systems consolidation of a memory. *Science*, 356(6333), 73-78. doi:10.1126/science.aam6808
- Kobayashi, H., Yamamoto, S., Maruo, T., & Murakami, F. (2005). Identification of a cis-acting element required for dendritic targeting of activity-regulated cytoskeleton-associated protein mRNA. *Eur J Neurosci*, 22(12), 2977-2984. doi:10.1111/j.1460-9568.2005.04508.x
- Komorowski, R. W., Manns, J. R., & Eichenbaum, H. (2009). Robust conjunctive item-place coding by hippocampal neurons parallels learning what happens where. *J Neurosci*, 29(31), 9918-9929. doi:10.1523/JNEUROSCI.1378-09.2009
- Korb, E., Wilkinson, C. L., Delgado, R. N., Lovero, K. L., & Finkbeiner, S. (2013). Arc in the nucleus regulates PML-dependent GluA1 transcription and homeostatic plasticity. *Nat Neurosci*, 16(7), 874-883. doi:10.1038/nn.3429
- Korotkova, T., Ponomarenko, A., Monaghan, C. K., Poulter, S. L., Cacucci, F., Wills, T., . . . Lever, C. (2018). Reconciling the different faces of hippocampal theta: The role of theta oscillations in cognitive, emotional and innate behaviors. *Neurosci Biobehav Rev*, 85, 65-80. doi:10.1016/j.neubiorev.2017.09.004
- Kosugi, K., Yoshida, K., Suzuki, T., Kobayashi, K., Yoshida, K., Mimura, M., & Tanaka, K. F. (2021). Activation of ventral CA1 hippocampal neurons projecting to the lateral septum during feeding. *Hippocampus*, 31(3), 294-304. doi:10.1002/hipo.23289
- Kourosh-Arami, M., Komaki, A., & Zarrindast, M. R. (2023). Dopamine as a Potential Target for Learning and Memory: Contributing to Related Neurological Disorders. *CNS Neurol Disord Drug Targets*, 22(4), 558-576. doi:10.2174/1871527321666220418115503
- Krebs-Kraft, D. L., Wheeler, M. G., & Parent, M. B. (2007). The memory-impairing effects of septal GABA receptor activation involve GABAergic septo-hippocampal projection neurons. *Learn Mem*, 14(12), 833-841. doi:10.1101/lm.809407
- Krishnan, V., & Nestler, E. J. (2008). The molecular neurobiology of depression. *Nature*, 455(7215), 894-902. doi:10.1038/nature07455
- Ku, S. P., Atucha, E., Alavi, N., Mulla-Osman, H., Kayumova, R., Yoshida, M., . . . Sauvage, M. M. (2024). Phase locking of hippocampal CA3 neurons to distal CA1 theta oscillations selectively predicts memory performance. *Cell Rep*, 43(6), 114276. doi:10.1016/j.celrep.2024.114276
- Kuku, A. H. A. (2020). *Investigating the GABAergic principal neurons that express Arc/Arg3.1 in the Lateral Septum*. (Master). University of Southern Denmark, Denmark.
- Kyriazi, P., Headley, D. B., & Paré, D. (2020). Different Multidimensional Representations across the Amygdalo-Prefrontal Network during an Approach-Avoidance Task. *Neuron*, 107(4), 717-730.e715. doi:10.1016/j.neuron.2020.05.039
- Lachaux, J. P., Rodriguez, E., Martinerie, J., & Varela, F. J. (1999). Measuring phase synchrony in brain signals. *Hum Brain Mapp*, 8(4), 194-208. doi:10.1002/(sici)1097-0193(1999)8:4<194::aid-hbm4>3.0.co;2-c
- Larsen, M. H., Olesen, M., Woldbye, D. P., Hay-Schmidt, A., Hansen, H. H., Ronn, L. C., & Mikkelsen, J. D. (2005). Regulation of activity-regulated cytoskeleton protein (Arc) mRNA after acute and chronic electroconvulsive stimulation in the rat. *Brain Res*, 1064(1-2), 161-165. doi:10.1016/j.brainres.2005.09.039
- Lee, I., & Lee, C. H. (2013). Contextual behavior and neural circuits. *Front Neural Circuits*, 7, 84. doi:10.3389/fncir.2013.00084
- Lee, J. H., Latchoumane, C. V., Park, J., Kim, J., Jeong, J., Lee, K. H., & Shin, H. S. (2019). The rostroventral part of the thalamic reticular nucleus modulates fear extinction. *Nat Commun*, 10(1), 4637. doi:10.1038/s41467-019-12496-9
- Lee, S., Hjerling-Leffler, J., Zagha, E., Fishell, G., & Rudy, B. (2010). The largest group of superficial neocortical GABAergic interneurons expresses ionotropic serotonin receptors. *J Neurosci*, 30(50), 16796-16808. doi:10.1523/JNEUROSCI.1869-10.2010
- Leem, Y. H., & Chang, H. (2017). Arc/Arg3.1 protein expression in dorsal hippocampal CA1, a candidate event as a biomarker for the effects of exercise on chronic stress-evoked behavioral abnormalities. *J Exerc Nutrition Biochem*, 21(4), 45-51. doi:10.20463/jenb.2017.0033
- Leranth, C., Deller, T., & Buzsáki, G. (1992). Intraseptal connections redefined: lack of a lateral septum to medial septum path. *Brain Research*, 583(1-2), 1-11. doi:10.1016/S0006-8993(10)80004-6
- Leroy, F., Park, J., Asok, A., Brann, D. H., Meira, T., Boyle, L. M., . . . Siegelbaum, S. A. (2018). A circuit from hippocampal CA2 to lateral septum disinhibits social aggression. *Nature*, 564(7735), 213-218. doi:10.1038/s41586-018-0772-0



- Leung, H. W., Foo, G., & VanDongen, A. (2022). Arc Regulates Transcription of Genes for Plasticity, Excitability and Alzheimer's Disease. *Biomedicines*, 10(8). doi:10.3390/biomedicines10081946
- Li, H. H., Liu, Y., Chen, H. S., Wang, J., Li, Y. K., Zhao, Y., . . . Chen, J. G. (2023). PDGF-BB-Dependent Neurogenesis Buffers Depressive-Like Behaviors by Inhibition of GABAergic Projection from Medial Septum to Dentate Gyrus. *Adv Sci (Weinh)*, 10(22), e2301110. doi:10.1002/adv.202301110
- Li, X. Y., Zhang, S. Y., Hong, Y. Z., Chen, Z. G., Long, Y., Yuan, D. H., . . . Hong, H. (2024). TGR5-mediated lateral hypothalamus-dCA3-dorsolateral septum circuit regulates depressive-like behavior in male mice. *Neuron*. doi:10.1016/j.neuron.2024.02.019
- Li, Y., Pehrson, A. L., Waller, J. A., Dale, E., Sanchez, C., & Gulinello, M. (2015). A critical evaluation of the activity-regulated cytoskeleton-associated protein (Arc/Arg3.1)'s putative role in regulating dendritic plasticity, cognitive processes, and mood in animal models of depression. *Front Neurosci*, 9, 279. doi:10.3389/fnins.2015.00279
- Link, W., Konietzko, U., Kauselmann, G., Krug, M., Schwanke, B., Frey, U., & Kuhl, D. (1995). Somatodendritic expression of an immediate early gene is regulated by synaptic activity. *Proc Natl Acad Sci U S A*, 92(12), 5734-5738. doi:10.1073/pnas.92.12.5734
- Linke, R., Braune, G., & Schwegler, H. (2000). Differential projection of the posterior paralaminar thalamic nuclei to the amygdaloid complex in the rat. *Exp Brain Res*, 134(4), 520-532. doi:10.1007/s002210000475
- Lisman, J., Buzsaki, G., Eichenbaum, H., Nadel, L., Ranganath, C., & Redish, A. D. (2017). Viewpoints: how the hippocampus contributes to memory, navigation and cognition. *Nat Neurosci*, 20(11), 1434-1447. doi:10.1038/nn.4661
- Lisman, J. E., & Otmakhova, N. A. (2001). Storage, recall, and novelty detection of sequences by the hippocampus: elaborating on the SOCRATIC model to account for normal and aberrant effects of dopamine. *Hippocampus*, 11(5), 551-568. doi:10.1002/hipo.1071
- Lissek, S., & Grillon, C. (2010). Overgeneralization of Conditioned Fear in the Anxiety Disorders. *Zeitschrift für Psychologie / Journal of Psychology*, 218(2), 146-148. doi:10.1027/0044-3409/a000022
- Lissek, S., Kaczkurkin, A. N., Rabin, S., Geraci, M., Pine, D. S., & Grillon, C. (2014). Generalized anxiety disorder is associated with overgeneralization of classically conditioned fear. *Biol Psychiatry*, 75(11), 909-915. doi:10.1016/j.biopsych.2013.07.025
- Lissek, S., Powers, A. S., McClure, E. B., Phelps, E. A., Woldehawariat, G., Grillon, C., & Pine, D. S. (2005). Classical fear conditioning in the anxiety disorders: a meta-analysis. *Behaviour Research and Therapy*, 43(11), 1391-1424. doi:10.1016/j.brat.2004.10.007
- Liu, P. F., Wang, Y., Xu, L., Xiang, A. F., Liu, M. Z., Zhu, Y. B., . . . Mu, D. (2022). Modulation of itch and pain signals processing in ventrobasal thalamus by thalamic reticular nucleus. *iScience*, 25(1), 103625. doi:10.1016/j.isci.2021.103625
- Liu, X., Ramirez, S., Pang, P. T., Puryear, C. B., Govindarajan, A., Deisseroth, K., & Tonegawa, S. (2012). Optogenetic stimulation of a hippocampal engram activates fear memory recall. *Nature*, 484(7394), 381-385. doi:10.1038/nature11028
- Liu, Y., Deng, S. L., Li, L. X., Zhou, Z. X., Lv, Q., Wang, Z. Y., . . . Chen, J. G. (2022). A circuit from dorsal hippocampal CA3 to paravox nucleus mediates chronic social defeat stress-induced deficits in preference for social novelty. *Sci Adv*, 8(8), eabe8828. doi:10.1126/sciadv.abe8828
- Lodge, D. J., Elam, H. B., Boley, A. M., & Donegan, J. J. (2023). Discrete hippocampal projections are differentially regulated by parvalbumin and somatostatin interneurons. *Nat Commun*, 14(1), 6653. doi:10.1038/s41467-023-42484-z
- Lonergan, M. E., Gafford, G. M., Jarome, T. J., & Helmstetter, F. J. (2010). Time-dependent expression of Arc and zif268 after acquisition of fear conditioning. *Neural Plast*, 2010, 139891. doi:10.1155/2010/139891
- Lovett-Barron, M., Kaifosh, P., Kheirbek, M. A., Danielson, N., Zaremba, J. D., Reardon, T. R., . . . Losonczy, A. (2014). Dendritic inhibition in the hippocampus supports fear learning. *Science*, 343(6173), 857-863. doi:10.1126/science.1247485
- Lovibond, P. F., & Shanks, D. R. (2002). The role of awareness in Pavlovian conditioning: Empirical evidence and theoretical implications. *Journal of Experimental Psychology: Animal Behavior Processes*, 28(1), 3-26. doi:10.1037/0097-7403.28.1.3
- Lucas, E. K., & Clem, R. L. (2018). GABAergic interneurons: The orchestra or the conductor in fear learning and memory? *Brain Res Bull*, 141, 13-19. doi:10.1016/j.brainresbull.2017.11.016
- Luscher, B., Shen, Q., & Sahir, N. (2011). The GABAergic deficit hypothesis of major depressive disorder. *Mol Psychiatry*, 16(4), 383-406. doi:10.1038/mp.2010.120
- Luscher, C., & Malenka, R. C. (2012). NMDA receptor-dependent long-term potentiation and long-term depression (LTP/LTD). *Cold Spring Harb Perspect Biol*, 4(6). doi:10.1101/cshperspect.a005710

- Lv, X. F., Xu, Y., Han, J. S., & Cui, C. L. (2011). Expression of activity-regulated cytoskeleton-associated protein (Arc/Arg3.1) in the nucleus accumbens is critical for the acquisition, expression and reinstatement of morphine-induced conditioned place preference. *Behav Brain Res*, 223(1), 182-191. doi:10.1016/j.bbr.2011.04.029
- Lyford, G. L., Yamagata, K., Kaufmann, W. E., Barnes, C. A., Sanders, L. K., Copeland, N. G., . . . Worley, P. F. (1995). Arc, a growth factor and activity-regulated gene, encodes a novel cytoskeleton-associated protein that is enriched in neuronal dendrites. *Neuron*, 14(2), 433-445. doi:10.1016/0896-6273(95)90299-6
- MacQueen, G. M., Yucel, K., Taylor, V. H., Macdonald, K., & Joffe, R. (2008). Posterior hippocampal volumes are associated with remission rates in patients with major depressive disorder. *Biol Psychiatry*, 64(10), 880-883. doi:10.1016/j.biopsych.2008.06.027
- Maddox, S. A., & Schafe, G. E. (2011). The activity-regulated cytoskeletal-associated protein (Arc/Arg3.1) is required for reconsolidation of a Pavlovian fear memory. *J Neurosci*, 31(19), 7073-7082. doi:10.1523/JNEUROSCI.1120-11.2011
- Magdaleno-Madrigal, V. M., Pantoja-Jimenez, C. R., Bazaldua, A., Fernandez-Mas, R., Almazan-Alvarado, S., Bolanos-Alejos, F., . . . Ramirez-Rodriguez, G. B. (2016). Acute deep brain stimulation in the thalamic reticular nucleus protects against acute stress and modulates initial events of adult hippocampal neurogenesis. *Behav Brain Res*, 314, 65-76. doi:10.1016/j.bbr.2016.07.022
- Mahn, M., Prigge, M., Ron, S., Levy, R., & Yizhar, O. (2016). Biophysical constraints of optogenetic inhibition at presynaptic terminals. *Nat Neurosci*, 19(4), 554-556. doi:10.1038/nn.4266
- Malik, R., Li, Y., Schamiloglu, S., & Sohal, V. S. (2022). Top-down control of hippocampal signal-to-noise by prefrontal long-range inhibition. *Cell*, 185(9), 1602-1617 e1617. doi:10.1016/j.cell.2022.04.001
- Malkki, H. A., Mertens, P. E., Lankelma, J. V., Vinck, M., van Schalkwijk, F. J., van Mourik-Donga, L. B., . . . Pennartz, C. M. (2016). Effects of Arc/Arg3.1 gene deletion on rhythmic synchronization of hippocampal CA1 neurons during locomotor activity and sleep. *Neurobiol Learn Mem*, 131, 155-165. doi:10.1016/j.nlm.2016.03.021
- Malkov, A., Shevkova, L., Latyshkova, A., & Kitchigina, V. (2022). Theta and gamma hippocampal-neocortical oscillations during the episodic-like memory test: Impairment in epileptogenic rats. *Exp Neurol*, 354, 114110. doi:10.1016/j.expneurol.2022.114110
- Maller, J. J., Daskalakis, Z. J., & Fitzgerald, P. B. (2007). Hippocampal volumetrics in depression: the importance of the posterior tail. *Hippocampus*, 17(11), 1023-1027. doi:10.1002/hipo.20339
- Manago, F., Mereu, M., Mastwal, S., Mastrogiacomo, R., Scheggia, D., Emanuele, M., . . . Papaleo, F. (2016). Genetic Disruption of Arc/Arg3.1 in Mice Causes Alterations in Dopamine and Neurobehavioral Phenotypes Related to Schizophrenia. *Cell Rep*, 16(8), 2116-2128. doi:10.1016/j.celrep.2016.07.044
- Manoach, D. S., & Stickgold, R. (2019). Abnormal Sleep Spindles, Memory Consolidation, and Schizophrenia. *Annu Rev Clin Psychol*, 15, 451-479. doi:10.1146/annurev-clinpsy-050718-095754
- Maren, S. (2001). Neurobiology of Pavlovian fear conditioning. *Annu Rev Neurosci*, 24, 897-931. doi:10.1146/annurev.neuro.24.1.897
- Maroun, M., Ioannides, P. J., Bergman, K. L., Kavushansky, A., Holmes, A., & Wellman, C. L. (2013). Fear extinction deficits following acute stress associate with increased spine density and dendritic retraction in basolateral amygdala neurons. *Eur J Neurosci*, 38(4), 2611-2620. doi:10.1111/ejn.12259
- Martins, I., & Tavares, I. (2017). Reticular Formation and Pain: The Past and the Future. *Front Neuroanat*, 11, 51. doi:10.3389/fnana.2017.00051
- McEchron, M. D., & Disterhoft, J. F. (1999). Hippocampal encoding of non-spatial trace conditioning. *Hippocampus*, 9(4), 385-396. doi:10.1002/(sici)1098-1063(1999)9:4<385::Aid-hipo5>3.0.Co;2-k
- McHugh, T. J., Jones, M. W., Quinn, J. J., Balthasar, N., Coppari, R., Elmquist, J. K., . . . Tonegawa, S. (2007). Dentate gyrus NMDA receptors mediate rapid pattern separation in the hippocampal network. *Science*, 317(5834), 94-99. doi:10.1126/science.1140263
- McKinnon, M. C., Yucel, K., Nazarov, A., & MacQueen, G. M. (2009). A meta-analysis examining clinical predictors of hippocampal volume in patients with major depressive disorder. *J Psychiatry Neurosci*, 34(1), 41-54. Retrieved from <https://www.ncbi.nlm.nih.gov/pubmed/19125212>
- Mee, S., Bunney, B. G., Bunney, W. E., Hetrick, W., Potkin, S. G., & Reist, C. (2011). Assessment of psychological pain in major depressive episodes. *J Psychiatr Res*, 45(11), 1504-1510. doi:10.1016/j.jpsychires.2011.06.011
- Melchior, M., Caspi, A., Milne, B. J., Danese, A., Poulton, R., & Moffitt, T. E. (2007). Work stress precipitates depression and anxiety in young, working women and men. *Psychol Med*, 37(8), 1119-1129. doi:10.1017/S0033291707000414

- Melleu, F. F., de Oliveira, A. R., Grego, K. F., Blanchard, D. C., & Canteras, N. S. (2022). Dissecting the brain's fear systems responding to snake threats. *Eur J Neurosci*, 56(6), 4788-4802. doi:10.1111/ejn.15794
- Messaoudi, E., Kanhema, T., Soule, J., Tiron, A., Dagey, G., da Silva, B., & Bramham, C. R. (2007). Sustained Arc/Arg3.1 synthesis controls long-term potentiation consolidation through regulation of local actin polymerization in the dentate gyrus in vivo. *J Neurosci*, 27(39), 10445-10455. doi:10.1523/JNEUROSCI.2883-07.2007
- Migo, E. M., Corbett, K., Graham, J., Smith, S., Tate, S., Moran, P. M., & Cassaday, H. J. (2006). A novel test of conditioned inhibition correlates with personality measures of schizotypy and reward sensitivity. *Behav Brain Res*, 168(2), 299-306. doi:10.1016/j.bbr.2005.11.021
- Mikkelsen, J. D., & Larsen, M. H. (2006). Effects of stress and adrenalectomy on activity-regulated cytoskeleton protein (Arc) gene expression. *Neurosci Lett*, 403(3), 239-243. doi:10.1016/j.neulet.2006.04.040
- Miller, N. E. (1948). Studies of fear as an acquirable drive fear as motivation and fear-reduction as reinforcement in the learning of new responses. *J Exp Psychol*, 38(1), 89-101. doi:10.1037/h0058455
- Minatohara, K., Akiyoshi, M., & Okuno, H. (2016). Role of Immediate-Early Genes in Synaptic Plasticity and Neuronal Ensembles Underlying the Memory Trace. *Frontiers in Molecular Neuroscience*, 8. doi:10.3389/fnmol.2015.00078
- Miranda, J. M., Cruz, E., Bessieres, B., & Alberini, C. M. (2022). Hippocampal parvalbumin interneurons play a critical role in memory development. *Cell Rep*, 41(7), 111643. doi:10.1016/j.celrep.2022.111643
- Mizunuma, M., Norimoto, H., Tao, K., Egawa, T., Hanaoka, K., Sakaguchi, T., . . . Ikegaya, Y. (2014). Unbalanced excitability underlies offline reactivation of behaviorally activated neurons. *Nat Neurosci*, 17(4), 503-505. doi:10.1038/nn.3674
- Moga, D. E., Calhoun, M. E., Chowdhury, A., Worley, P., Morrison, J. H., & Shapiro, M. L. (2004). Activity-regulated cytoskeletal-associated protein is localized to recently activated excitatory synapses. *Neuroscience*, 125(1), 7-11. doi:10.1016/j.neuroscience.2004.02.004
- Molteni, R., Calabrese, F., Chourbaji, S., Brandwein, C., Racagni, G., Gass, P., & Riva, M. A. (2010). Depression-prone mice with reduced glucocorticoid receptor expression display an altered stress-dependent regulation of brain-derived neurotrophic factor and activity-regulated cytoskeleton-associated protein. *J Psychopharmacol*, 24(4), 595-603. doi:10.1177/0269881108099815
- Mondragón-Rodríguez, S., Gu, N., Fasano, C., Peña-Ortega, F., & Williams, S. (2019). Functional Connectivity between Hippocampus and Lateral Septum is Affected in Very Young Alzheimer's Transgenic Mouse Model. *Neuroscience*, 401, 96-105. doi:10.1016/J.NEUROSCIENCE.2018.12.042
- Monmaur, P., Ayadi, K., & Breton, P. (1993). Hippocampal EEG responses induced by carbachol and atropine infusions into the septum and the hippocampus in the urethane-anaesthetized rat. *Brain Res*, 631(2), 317-324. doi:10.1016/0006-8993(93)91551-3
- Monsey, M. S., Boyle, L. M., Zhang, M. L., Nguyen, C. P., Kronman, H. G., Ota, K. T., . . . Schafe, G. E. (2014). Chronic corticosterone exposure persistently elevates the expression of memory-related genes in the lateral amygdala and enhances the consolidation of a Pavlovian fear memory. *PLoS ONE*, 9(3), e91530. doi:10.1371/journal.pone.0091530
- Montgomery, S. M., & Buzsaki, G. (2007). Gamma oscillations dynamically couple hippocampal CA3 and CA1 regions during memory task performance. *Proc Natl Acad Sci U S A*, 104(36), 14495-14500. doi:10.1073/pnas.0701826104
- Morales, C., Morici, J. F., Espinosa, N., Sacson, A., Lara-Vasquez, A., Garcia-Perez, M. A., . . . Fuentealba, P. (2021). Dentate Gyrus Somatostatin Cells are Required for Contextual Discrimination During Episodic Memory Encoding. *Cereb Cortex*, 31(2), 1046-1059. doi:10.1093/cercor/bhaa273
- Morey, R. A., Dunsmoor, J. E., Haswell, C. C., Brown, V. M., Vora, A., Weiner, J., . . . LaBar, K. S. (2015). Fear learning circuitry is biased toward generalization of fear associations in posttraumatic stress disorder. *Transl Psychiatry*, 5(12), e700. doi:10.1038/tp.2015.196
- Morris, R. G., Garrud, P., Rawlins, J. N., & O'Keefe, J. (1982). Place navigation impaired in rats with hippocampal lesions. *Nature*, 297(5868), 681-683. doi:10.1038/297681a0
- Mowrer, O. H. (1956). Two-factor learning theory reconsidered, with special reference to secondary reinforcement and the concept of habit. *Psychol Rev*, 63(2), 114-128. doi:10.1037/h0040613
- Mowrer, O. H. (1960). *Learning theory and behavior*.
- Mulder, A. B., Nordquist, R. E., Orgut, O., & Pennartz, C. M. (2003). Learning-related changes in response patterns of prefrontal neurons during instrumental conditioning. *Behav Brain Res*, 146(1-2), 77-88. doi:10.1016/j.bbr.2003.09.016
- Muller, C., & Remy, S. (2018). Septo-hippocampal interaction. *Cell Tissue Res*, 373(3), 565-575. doi:10.1007/s00441-017-2745-2

- Murrough, J. W., Abdallah, C. G., Anticevic, A., Collins, K. A., Geha, P., Averill, L. A., . . . Charney, D. S. (2016). Reduced global functional connectivity of the medial prefrontal cortex in major depressive disorder. *Hum Brain Mapp*, 37(9), 3214-3223. doi:10.1002/hbm.23235
- Muzio, L., Brambilla, V., Calcaterra, L., D'Adamo, P., Martino, G., & Benedetti, F. (2016). Increased neuroplasticity and hippocampal microglia activation in a mice model of rapid antidepressant treatment. *Behav Brain Res*, 311, 392-402. doi:10.1016/j.bbr.2016.05.063
- Nader, K. (2003). Memory traces unbound. *Trends Neurosci*, 26(2), 65-72. doi:10.1016/S0166-2236(02)00042-5
- Nair, R. R., Patil, S., Tiron, A., Kanhema, T., Panja, D., Schiro, L., . . . Bramham, C. R. (2017). Dynamic Arc SUMOylation and Selective Interaction with F-Actin-Binding Protein Drebrin A in LTP Consolidation In Vivo. *Front Synaptic Neurosci*, 9, 8. doi:10.3389/fnsyn.2017.00008
- Nairne, J. S. (2005). The Functionalist Agenda in Memory Research. In *Experimental cognitive psychology and its applications*. (pp. 115-126).
- Negoias, S., Croy, I., Gerber, J., Puschmann, S., Petrowski, K., Joraschky, P., & Hummel, T. (2010). Reduced olfactory bulb volume and olfactory sensitivity in patients with acute major depression. *Neuroscience*, 169(1), 415-421. doi:10.1016/j.neuroscience.2010.05.012
- Nestler, E. J., Barrot, M., DiLeone, R. J., Eisch, A. J., Gold, S. J., & Monteggia, L. M. (2002). Neurobiology of depression. *Neuron*, 34(1), 13-25. doi:10.1016/S0896-6273(02)00653-0
- Neves, L., Lobao-Soares, B., Araujo, A. P. C., Furtunato, A. M. B., Paiva, I., Souza, N., . . . Belchior, H. (2022). Theta and gamma oscillations in the rat hippocampus support the discrimination of object displacement in a recognition memory task. *Front Behav Neurosci*, 16, 970083. doi:10.3389/fnbeh.2022.970083
- Nifosi, F., Toffanin, T., Follador, H., Zonta, F., Padovan, G., Pigato, G., . . . Perini, G. I. (2010). Reduced right posterior hippocampal volume in women with recurrent familial pure depressive disorder. *Psychiatry Res*, 184(1), 23-28. doi:10.1016/j.psychres.2010.05.012
- Nikolaenko, O., Patil, S., Eriksen, M. S., & Bramham, C. R. (2018). Arc protein: a flexible hub for synaptic plasticity and cognition. *Semin Cell Dev Biol*, 77, 33-42. doi:10.1016/j.semcdb.2017.09.006
- Norman, Y., Yeagle, E. M., Khuvis, S., Harel, M., Mehta, A. D., & Malach, R. (2019). Hippocampal sharp-wave ripples linked to visual episodic recollection in humans. *Science*, 365(6454). doi:10.1126/science.aax1030
- Nyhus, E., & Curran, T. (2010). Functional role of gamma and theta oscillations in episodic memory. In *Neuroscience and Biobehavioral Reviews* (Vol. 34, pp. 1023-1035).
- Okuno, H., Akashi, K., Ishii, Y., Yagishita-Kyo, N., Suzuki, K., Nonaka, M., . . . Bito, H. (2012). Inverse synaptic tagging of inactive synapses via dynamic interaction of Arc/Arg3.1 with CaMKII $\beta$ . *Cell*, 149(4), 886-898. doi:10.1016/j.cell.2012.02.062
- Okuno, H., Minatohara, K., & Bito, H. (2018). Inverse synaptic tagging: An inactive synapse-specific mechanism to capture activity-induced Arc/arg3.1 and to locally regulate spatial distribution of synaptic weights. *Semin Cell Dev Biol*, 77, 43-50. doi:10.1016/j.semcdb.2017.09.025
- Onoue, K., Nakayama, D., Ikegaya, Y., Matsuki, N., & Nomura, H. (2014). Fear extinction requires Arc/Arg3.1 expression in the basolateral amygdala. *Mol Brain*, 7, 30. doi:10.1186/1756-6606-7-30
- Ons, S., Marti, O., & Armario, A. (2004). Stress-induced activation of the immediate early gene Arc (activity-regulated cytoskeleton-associated protein) is restricted to telencephalic areas in the rat brain: relationship to c-fos mRNA. *J Neurochem*, 89(5), 1111-1118. doi:10.1111/j.1471-4159.2004.02396.x
- Ons, S., Rotllant, D., Marin-Blasco, I. J., & Armario, A. (2010). Immediate-early gene response to repeated immobilization: Fos protein and arc mRNA levels appear to be less sensitive than c-fos mRNA to adaptation. *Eur J Neurosci*, 31(11), 2043-2052. doi:10.1111/j.1460-9568.2010.07242.x
- Oostenveld, R., Fries, P., Maris, E., & Schoffelen, J. M. (2011). FieldTrip: Open source software for advanced analysis of MEG, EEG, and invasive electrophysiological data. *Comput Intell Neurosci*, 2011, 156869. doi:10.1155/2011/156869
- Opalka, A. N., & Wang, D. V. (2020). Hippocampal efferents to retrosplenial cortex and lateral septum are required for memory acquisition. *Learning and Memory*, 27(8), 310-318. doi:10.1101/LM.051797.120
- Orgy Buzs, G. (2015). Hippocampal Sharp Wave-Ripple: A Cognitive Biomarker for Episodic Memory and Planning. doi:10.1002/hipo.22488
- Osipova, D., Takashima, A., Oostenveld, R., Fernandez, G., Maris, E., & Jensen, O. (2006). Theta and gamma oscillations predict encoding and retrieval of declarative memory. *J Neurosci*, 26(28), 7523-7531. doi:10.1523/JNEUROSCI.1948-06.2006
- Panja, D., Kenney, J. W., D'Andrea, L., Zalfa, F., Vedeler, A., Wibbrand, K., . . . Bramham, C. R. (2014). Two-stage translational control of dentate gyrus LTP consolidation is mediated by sustained BDNF-TrkB signaling to MNK. *Cell Rep*, 9(4), 1430-1445. doi:10.1016/j.celrep.2014.10.016
- Papaj, D. R., & Lewis, A. C. (2012). Insect learning: Ecology and evolutionary perspectives.

- Paquet, A., Calvet, B., Lacroix, A., & Girard, M. (2022). Sensory processing in depression: Assessment and intervention perspective. *Clin Psychol Psychother*, 29(5), 1567-1579. doi:10.1002/cpp.2785
- Pardhan, S., Lopez Sanchez, G. F., Bourne, R., Davis, A., Leveziel, N., Koyanagi, A., & Smith, L. (2021). Visual, hearing, and dual sensory impairment are associated with higher depression and anxiety in women. *Int J Geriatr Psychiatry*, 36(9), 1378-1385. doi:10.1002/gps.5534
- Park, A., Jacob, A. D., Hsiang, H. L., Frankland, P. W., Howland, J. G., & Josselyn, S. A. (2023). Formation and fate of an engram in the lateral amygdala supporting a rewarding memory in mice. *Neuropsychopharmacology*, 48(5), 724-733. doi:10.1038/s41386-022-01472-5
- Park, S., Jung, J. H., Karimi, S. A., Jacob, A. D., & Josselyn, S. A. (2022). Opto-extinction of a threat memory in mice. *Brain Res Bull*, 191, 61-68. doi:10.1016/j.brainresbull.2022.10.012
- Pastuzyn, E. D., Day, C. E., Kearns, R. B., Kyrke-Smith, M., Taibi, A. V., McCormick, J., . . . Shepherd, J. D. (2018). The Neuronal Gene Arc Encodes a Repurposed Retrotransposon Gag Protein that Mediates Intercellular RNA Transfer. *Cell*, 172(1-2), 275-288 e218. doi:10.1016/j.cell.2017.12.024
- Pearce, J. M. (2013). *Animal learning and cognition: an introduction*: Psychology press.
- Pedemonte, M., Barrenechea, C., Nunez, A., Gambini, J. P., & Garcia-Austt, E. (1998). Membrane and circuit properties of lateral septum neurons: relationships with hippocampal rhythms. *Brain Res*, 800(1), 145-153. doi:10.1016/s0006-8993(98)00517-4
- Peebles, C. L., Yoo, J., Thwin, M. T., Palop, J. J., Noebels, J. L., & Finkbeiner, S. (2010). Arc regulates spine morphology and maintains network stability in vivo. *Proc Natl Acad Sci U S A*, 107(42), 18173-18178. doi:10.1073/pnas.1006546107
- Pei, Q., Zetterstrom, T. S., Sprakes, M., Tordera, R., & Sharp, T. (2003). Antidepressant drug treatment induces Arc gene expression in the rat brain. *Neuroscience*, 121(4), 975-982. doi:10.1016/s0306-4522(03)00504-9
- Penrod, R. D., Kumar, J., Smith, L. N., McCalley, D., Nentwig, T. B., Hughes, B. W., . . . Cowan, C. W. (2019). Activity-regulated cytoskeleton-associated protein (Arc/Arg3.1) regulates anxiety- and novelty-related behaviors. *Genes Brain Behav*, 18(7), e12561. doi:10.1111/gbb.12561
- Perova, Z., Delevich, K., & Li, B. (2015). Depression of excitatory synapses onto parvalbumin interneurons in the medial prefrontal cortex in susceptibility to stress. *J Neurosci*, 35(7), 3201-3206. doi:10.1523/JNEUROSCI.2670-14.2015
- Petersen, P. C., Siegle, J. H., Steinmetz, N. A., Mahallati, S., & Buzsaki, G. (2021). CellExplorer: A framework for visualizing and characterizing single neurons. *Neuron*, 109(22), 3594-3608 e3592. doi:10.1016/j.neuron.2021.09.002
- Pham, C. T., MacIvor, D. M., Hug, B. A., Heusel, J. W., & Ley, T. J. (1996). Long-range disruption of gene expression by a selectable marker cassette. *Proc Natl Acad Sci U S A*, 93(23), 13090-13095. doi:10.1073/pnas.93.23.13090
- Pilkiw, M., Insel, N., Cui, Y., Finney, C., Morrissey, M. D., & Takehara-Nishiuchi, K. (2017). Phasic and tonic neuron ensemble codes for stimulus-environment conjunctions in the lateral entorhinal cortex. *eLife*, 6. doi:10.7554/eLife.28611
- Pinault, D. (2004). The thalamic reticular nucleus: structure, function and concept. *Brain Res Brain Res Rev*, 46(1), 1-31. doi:10.1016/j.brainresrev.2004.04.008
- Pintchovski, S. A., Peebles, C. L., Kim, H. J., Verdin, E., & Finkbeiner, S. (2009). The serum response factor and a putative novel transcription factor regulate expression of the immediate-early gene Arc/Arg3.1 in neurons. *J Neurosci*, 29(5), 1525-1537. doi:10.1523/JNEUROSCI.5575-08.2009
- Pitkanen, A., Pikkarainen, M., Nurminen, N., & Ylinen, A. (2000). Reciprocal connections between the amygdala and the hippocampal formation, perirhinal cortex, and postrhinal cortex in rat. A review. *Ann N Y Acad Sci*, 911, 369-391. doi:10.1111/j.1749-6632.2000.tb06738.x
- Pizzagalli, D. A. (2014). Depression, stress, and anhedonia: toward a synthesis and integrated model. *Annu Rev Clin Psychol*, 10, 393-423. doi:10.1146/annurev-clinpsy-050212-185606
- Plath, N., Ohana, O., Dammermann, B., Errington, M. L., Schmitz, D., Gross, C., . . . Kuhl, D. (2006). Arc/Arg3.1 is essential for the consolidation of synaptic plasticity and memories. *Neuron*, 52(3), 437-444. doi:10.1016/j.neuron.2006.08.024
- Ploski, J. E., Pierre, V. J., Smucny, J., Park, K., Monsey, M. S., Overeem, K. A., & Schafe, G. E. (2008). The activity-regulated cytoskeletal-associated protein (Arc/Arg3.1) is required for memory consolidation of pavlovian fear conditioning in the lateral amygdala. *J Neurosci*, 28(47), 12383-12395. doi:10.1523/JNEUROSCI.1662-08.2008
- Plotnik, R., Kouyoumdjian, H., & Austin, C. (1989). *Introduction to psychology*: Random House New York.

- Poirier, M., Nairne, J. S., Morin, C., Zimmermann, F. G. S., Koutmeridou, K., & Fowler, J. (2012). Memory as discrimination: A challenge to the encoding–retrieval match principle. *Journal of Experimental Psychology: Learning, Memory, and Cognition*, 38(1), 16-29. doi:10.1037/a0024956
- Pollak, D. D., Rey, C. E., & Monje, F. J. (2010). Rodent models in depression research: classical strategies and new directions. *Ann Med*, 42(4), 252-264. doi:10.3109/07853891003769957
- Pompili, M., Lester, D., Leenaars, A. A., Tatarelli, R., & Girardi, P. (2008). Psychache and suicide: a preliminary investigation. *Suicide Life Threat Behav*, 38(1), 116-121. doi:10.1521/suli.2008.38.1.116
- Pontrello, C. G., Sun, M. Y., Lin, A., Fiacco, T. A., DeFea, K. A., & Ethell, I. M. (2012). Cofilin under control of beta-arrestin-2 in NMDA-dependent dendritic spine plasticity, long-term depression (LTD), and learning. *Proc Natl Acad Sci U S A*, 109(7), E442-451. doi:10.1073/pnas.1118803109
- Powell, T. R., Fernandes, C., & Schalkwyk, L. C. (2012). Depression-Related Behavioral Tests. *Curr Protoc Mouse Biol*, 2(2), 119-127. doi:10.1002/9780470942390.mo110176
- Qiu, S., Hu, Y., Huang, Y., Gao, T., Wang, X., Wang, D., . . . Xu, C. (2024). Whole-brain spatial organization of hippocampal single-neuron projectomes. *Science*, 383(6682), eadj9198. doi:10.1126/science.adj9198
- Radley, J. J., Anderson, R. M., Hamilton, B. A., Alcock, J. A., & Romig-Martin, S. A. (2013). Chronic stress-induced alterations of dendritic spine subtypes predict functional decrements in an hypothalamo-pituitary-adrenal-inhibitory prefrontal circuit. *J Neurosci*, 33(36), 14379-14391. doi:10.1523/JNEUROSCI.0287-13.2013
- Ramanathan, K. R., Ressler, R. L., Jin, J., & Maren, S. (2018). Nucleus Reunians Is Required for Encoding and Retrieving Precise, Hippocampal-Dependent Contextual Fear Memories in Rats. *J Neurosci*, 38(46), 9925-9933. doi:10.1523/JNEUROSCI.1429-18.2018
- Ramirez-Gordillo, D., Bayer, K. U., & Restrepo, D. (2022). Hippocampal-prefrontal theta coupling develops as mice become proficient in associative odorant discrimination learning. *eNeuro*, 9(5). doi:10.1523/ENEURO.0259-22.2022
- Ramirez, S., Liu, X., Lin, P. A., Suh, J., Pignatelli, M., Redondo, R. L., . . . Tonegawa, S. (2013). Creating a false memory in the hippocampus. *Science*, 341(6144), 387-391. doi:10.1126/science.1239073
- Ramirez, S., Liu, X., MacDonald, C. J., Moffa, A., Zhou, J., Redondo, R. L., & Tonegawa, S. (2015). Activating positive memory engrams suppresses depression-like behaviour. *Nature*, 522(7556), 335-339. doi:10.1038/nature14514
- Raven, F., & Aton, S. J. (2021). The Engram's Dark Horse: How Interneurons Regulate State-Dependent Memory Processing and Plasticity. *Front Neural Circuits*, 15, 750541. doi:10.3389/fncir.2021.750541
- Reed Hunt, R. (2003). Two contributions of distinctive processing to accurate memory. *Journal of Memory and Language*, 48(4), 811-825. doi:10.1016/s0749-596x(03)00018-4
- Ren, L. Y., Meyer, M. A. A., Grayson, V. S., Gao, P., Guedea, A. L., & Radulovic, J. (2022). Stress-induced generalization of negative memories is mediated by an extended hippocampal circuit. *Neuropsychopharmacology*, 47(2), 516-523. doi:10.1038/s41386-021-01174-4
- Ressler, K. J., Berretta, S., Bolshakov, V. Y., Rosso, I. M., Meloni, E. G., Rauch, S. L., & Carlezon, W. A., Jr. (2022). Post-traumatic stress disorder: clinical and translational neuroscience from cells to circuits. *Nat Rev Neurol*, 18(5), 273-288. doi:10.1038/s41582-022-00635-8
- Risold, P. Y., & Swanson, L. W. (1997a). Chemoarchitecture of the rat lateral septal nucleus. *Brain Res Brain Res Rev*, 24(2-3), 91-113. doi:10.1016/s0165-0173(97)00008-8
- Risold, P. Y., & Swanson, L. W. (1997b). *Full-length review Connections of the rat lateral septal complex 1*. Retrieved from
- Ritov, G., & Richter-Levin, G. (2014). Water associated zero maze: a novel rat test for long term traumatic re-experiencing. *Front Behav Neurosci*, 8, 1. doi:10.3389/fnbeh.2014.00001
- Rizzi-Wise, C. A., & Wang, D. V. (2021). Putting Together Pieces of the Lateral Septum: Multifaceted Functions and Its Neural Pathways. *eNeuro*, 8(6). doi:10.1523/ENEURO.0315-21.2021
- Rock, P. L., Roiser, J. P., Riedel, W. J., & Blackwell, A. D. (2014). Cognitive impairment in depression: a systematic review and meta-analysis. *Psychol Med*, 44(10), 2029-2040. doi:10.1017/S0033291713002535
- Rodriguez, J. J., Davies, H. A., Silva, A. T., De Souza, I. E., Peddie, C. J., Colyer, F. M., . . . Stewart, M. G. (2005). Long-term potentiation in the rat dentate gyrus is associated with enhanced Arc/Arg3.1 protein expression in spines, dendrites and glia. *Eur J Neurosci*, 21(9), 2384-2396. doi:10.1111/j.1460-9568.2005.04068.x
- Rodriguez, L. A., Kim, S. H., Page, S. C., Nguyen, C. V., Pattie, E. A., Hallock, H. L., . . . Martinowich, K. (2023). The basolateral amygdala to lateral septum circuit is critical for regulating social novelty in mice. *Neuropsychopharmacology*, 48(3), 529-539. doi:10.1038/s41386-022-01487-y
- Rolls, E. T. (2013). The mechanisms for pattern completion and pattern separation in the hippocampus. *Front Syst Neurosci*, 7, 74. doi:10.3389/fnsys.2013.00074

- Roque, P. S., Thorn Perez, C., Hooshmandi, M., Wong, C., Eslamizade, M. J., Heshmati, S., . . . Khoutorsky, A. (2023). Parvalbumin interneuron loss mediates repeated anesthesia-induced memory deficits in mice. *J Clin Invest*, 133(2). doi:10.1172/JCI159344
- Rosenbaum, R. S., Gilboa, A., & Moscovitch, M. (2014). Case studies continue to illuminate the cognitive neuroscience of memory. *Ann N Y Acad Sci*, 1316, 105-133. doi:10.1111/nyas.12467
- Roy, D. S., Kitamura, T., Okuyama, T., Ogawa, S. K., Sun, C., Obata, Y., . . . Tonegawa, S. (2017). Distinct Neural Circuits for the Formation and Retrieval of Episodic Memories. *Cell*, 170(5), 1000-1012 e1019. doi:10.1016/j.cell.2017.07.013
- Rozeske, R. R., Valerio, S., Chaudun, F., & Herry, C. (2015). Prefrontal neuronal circuits of contextual fear conditioning. *Genes Brain Behav*, 14(1), 22-36. doi:10.1111/gbb.12181
- Rozov, A., Rannap, M., Lorenz, F., Nasretidinov, A., Draguhn, A., & Egorov, A. V. (2020). Processing of Hippocampal Network Activity in the Receiver Network of the Medial Entorhinal Cortex Layer V. *J Neurosci*, 40(44), 8413-8425. doi:10.1523/JNEUROSCI.0586-20.2020
- Rudy, B., Fishell, G., Lee, S., & Hjerling-Leffler, J. (2011). Three groups of interneurons account for nearly 100% of neocortical GABAergic neurons. *Dev Neurobiol*, 71(1), 45-61. doi:10.1002/dneu.20853
- Ruikes, T. R., Fiorilli, J., Lim, J., Huis In 't Veld, G., Bosman, C., & Pennartz, C. M. A. (2024). Theta phase-entrainment of single cell spiking in rat somatosensory barrel cortex and secondary visual cortex is enhanced during multisensory discrimination behavior. *eNeuro*. doi:10.1523/ENEURO.0180-23.2024
- Saleh, K., Carballedo, A., Lisiecka, D., Fagan, A. J., Connolly, G., Boyle, G., & Frodl, T. (2012). Impact of family history and depression on amygdala volume. *Psychiatry Res*, 203(1), 24-30. doi:10.1016/j.psychres.2011.10.004
- Salery, M., Dos Santos, M., Saint-Jour, E., Moumne, L., Pages, C., Kappes, V., . . . Vanhoutte, P. (2017). Activity-Regulated Cytoskeleton-Associated Protein Accumulates in the Nucleus in Response to Cocaine and Acts as a Brake on Chromatin Remodeling and Long-Term Behavioral Alterations. *Biol Psychiatry*, 81(7), 573-584. doi:10.1016/j.biopsych.2016.05.025
- Sandi, C., Davies, H. A., Cordero, M. I., Rodriguez, J. J., Popov, V. I., & Stewart, M. G. (2003). Rapid reversal of stress induced loss of synapses in CA3 of rat hippocampus following water maze training. *Eur J Neurosci*, 17(11), 2447-2456. doi:10.1046/j.1460-9568.2003.02675.x
- Sanford, C. A., Soden, M. E., Baird, M. A., Miller, S. M., Schulkin, J., Palmiter, R. D., . . . Zweifel, L. S. (2017). A Central Amygdala CRF Circuit Facilitates Learning about Weak Threats. *Neuron*, 93(1), 164-178. doi:10.1016/j.neuron.2016.11.034
- Sans-Dublanc, A., Razzauti, A., Desikan, S., Pascual, M., Monyer, H., & Sindreu, C. (2020). Septal GABAergic inputs to CA1 govern contextual memory retrieval. *Sci Adv*, 6(44). doi:10.1126/sciadv.aba5003
- Santini, M. A., Klein, A. B., El-Sayed, M., Ratner, C., Knudsen, G. M., Mikkelsen, J. D., & Aznar, S. (2011). Novelty-induced activity-regulated cytoskeletal-associated protein (Arc) expression in frontal cortex requires serotonin 2A receptor activation. *Neuroscience*, 190, 251-257. doi:10.1016/j.neuroscience.2011.05.048
- Sauseng, P., Griesmayr, B., Freunberger, R., & Klimesch, W. (2010). Control mechanisms in working memory: a possible function of EEG theta oscillations. *Neurosci Biobehav Rev*, 34(7), 1015-1022. doi:10.1016/j.neubiorev.2009.12.006
- Saylam, C., Ucerler, H., Kitis, O., Ozand, E., & Gonul, A. S. (2006). Reduced hippocampal volume in drug-free depressed patients. *Surg Radiol Anat*, 28(1), 82-87. doi:10.1007/s00276-005-0050-3
- Scacheri, P. C., Crabtree, J. S., Novotny, E. A., Garrett-Beal, L., Chen, A., Edgemon, K. A., . . . Collins, F. S. (2001). Bidirectional transcriptional activity of PGK-neomycin and unexpected embryonic lethality in heterozygote chimeric knockout mice. *Genesis*, 30(4), 259-263. doi:10.1002/gene.1072
- Schacter, D. L. (1987). Implicit memory: History and current status. *Journal of Experimental Psychology: Learning, Memory, and Cognition*, 13(3), 501-518. doi:10.1037/0278-7393.13.3.501
- Schermuly, I., Wolf, D., Lieb, K., Stoeter, P., & Fellgiebel, A. (2011). State dependent posterior hippocampal volume increases in patients with major depressive disorder. *J Affect Disord*, 135(1-3), 405-409. doi:10.1016/j.jad.2011.07.017
- Schmid, L. C., Mittag, M., Poll, S., Steffen, J., Wagner, J., Geis, H. R., . . . Fuhrmann, M. (2016). Dysfunction of Somatostatin-Positive Interneurons Associated with Memory Deficits in an Alzheimer's Disease Model. *Neuron*, 92(1), 114-125. doi:10.1016/j.neuron.2016.08.034
- Schmitzer-Torbert, N. C., & Redish, A. D. (2008). Task-dependent encoding of space and events by striatal neurons is dependent on neural subtype. *Neuroscience*, 153(2), 349-360. doi:10.1016/j.neuroscience.2008.01.081
- Schwenzer, M., Zattarin, E., Grozinger, M., & Mathiak, K. (2012). Impaired pitch identification as a potential marker for depression. *BMC Psychiatry*, 12, 32. doi:10.1186/1471-244X-12-32

- Scoville, W. B., & Milner, B. (1957). Loss of recent memory after bilateral hippocampal lesions. *J Neurol Neurosurg Psychiatry*, 20(1), 11-21. doi:10.1136/jnnp.20.1.11
- Seager, M. A., Johnson, L. D., Chabot, E. S., Asaka, Y., & Berry, S. D. (2002). Oscillatory brain states and learning: Impact of hippocampal theta-contingent training. *Proc Natl Acad Sci U S A*, 99(3), 1616-1620. doi:10.1073/pnas.032662099
- Segal, M., Disterhoft, J. F., & Olds, J. (1972). Hippocampal unit activity during classical aversive and appetitive conditioning. *Science*, 175(4023), 792-794. doi:10.1126/science.175.4023.792
- Seney, M. L., Tripp, A., McCune, S., Lewis, D. A., & Sibille, E. (2015). Laminar and cellular analyses of reduced somatostatin gene expression in the subgenual anterior cingulate cortex in major depression. *Neurobiol Dis*, 73, 213-219. doi:10.1016/j.nbd.2014.10.005
- Sengün, T. (2021). *Characterizing the neural subtypes that express Arg3.1/Arc in the Hippocampus and Cortex*. (Bachelor). University of Hamburg, Hamburg.
- Sengupta, A., Yau, J. O. Y., Jean-Richard-Dit-Bressel, P., Liu, Y., Millan, E. Z., Power, J. M., & McNally, G. P. (2018). Basolateral Amygdala Neurons Maintain Aversive Emotional Salience. *J Neurosci*, 38(12), 3001-3012. doi:10.1523/JNEUROSCI.2460-17.2017
- Serra, M. P., Poddighe, L., Boi, M., Sanna, F., Piludu, M. A., Sanna, F., . . . Quartu, M. (2018). Effect of Acute Stress on the Expression of BDNF, trkB, and PSA-NCAM in the Hippocampus of the Roman Rats: A Genetic Model of Vulnerability/Resistance to Stress-Induced Depression. *Int J Mol Sci*, 19(12). doi:10.3390/ijms19123745
- Sheehan, T. P., Chambers, R. A., & Russell, D. S. (2004). Regulation of affect by the lateral septum: Implications for neuropsychiatry. In *Brain Research Reviews* (Vol. 46, pp. 71-117).
- Sheets, E. S., & Craighead, W. E. (2014). Comparing chronic interpersonal and noninterpersonal stress domains as predictors of depression recurrence in emerging adults. *Behav Res Ther*, 63, 36-42. doi:10.1016/j.brat.2014.09.001
- Shneidman, E. S. (1993). Suicide as psychache. *J Nerv Ment Dis*, 181(3), 145-147. doi:10.1097/00005053-199303000-00001
- Singh, S., & Topolnik, L. (2023). Inhibitory circuits in fear memory and fear-related disorders. *Front Neural Circuits*, 17, 1122314. doi:10.3389/fncir.2023.1122314
- Sirgy, M. J. (2019). Positive balance: a hierarchical perspective of positive mental health. *Qual Life Res*, 28(7), 1921-1930. doi:10.1007/s11136-019-02145-5
- Sirota, A., Montgomery, S., Fujisawa, S., Isomura, Y., Zugaro, M., & Buzsáki, G. (2008). Entrainment of Neocortical Neurons and Gamma Oscillations by the Hippocampal Theta Rhythm. *Neuron*, 60(4), 683-697. doi:10.1016/j.neuron.2008.09.014
- Siwani, S., Franca, A. S. C., Mikulovic, S., Reis, A., Hilscher, M. M., Edwards, S. J., . . . Kullander, K. (2018). OLMalpha2 Cells Bidirectionally Modulate Learning. *Neuron*, 99(2), 404-412 e403. doi:10.1016/j.neuron.2018.06.022
- Smith-Hicks, C., Xiao, B., Deng, R., Ji, Y., Zhao, X., Shepherd, J. D., . . . Linden, D. J. (2010). SRF binding to SRE 6.9 in the Arc promoter is essential for LTD in cultured Purkinje cells. *Nat Neurosci*, 13(9), 1082-1089. doi:10.1038/nn.2611
- Solari, N., & Hangya, B. (2018). Cholinergic modulation of spatial learning, memory and navigation. *Eur J Neurosci*, 48(5), 2199-2230. doi:10.1111/ejn.14089
- Sossin, W. S. (2018). Memory Synapses Are Defined by Distinct Molecular Complexes: A Proposal. *Front Synaptic Neurosci*, 10, 5. doi:10.3389/fnsyn.2018.00005
- Sotres-Bayon, F., Sierra-Mercado, D., Pardilla-Delgado, E., & Quirk, G. J. (2012). Gating of fear in prelimbic cortex by hippocampal and amygdala inputs. *Neuron*, 76(4), 804-812. doi:10.1016/j.neuron.2012.09.028
- Soumier, A., & Sibille, E. (2014). Opposing effects of acute versus chronic blockade of frontal cortex somatostatin-positive inhibitory neurons on behavioral emotionality in mice. *Neuropsychopharmacology*, 39(9), 2252-2262. doi:10.1038/npp.2014.76
- Spencer, J. P. (2008). Food for thought: the role of dietary flavonoids in enhancing human memory, learning and neuro-cognitive performance. *Proc Nutr Soc*, 67(2), 238-252. doi:10.1017/S0029665108007088
- Speranza, L., di Porzio, U., Viggiano, D., de Donato, A., & Volpicelli, F. (2021). Dopamine: The Neuromodulator of Long-Term Synaptic Plasticity, Reward and Movement Control. *Cells*, 10(4). doi:10.3390/cells10040735
- Squire, L. R. (1992). Declarative and nondeclarative memory: multiple brain systems supporting learning and memory. *J Cogn Neurosci*, 4(3), 232-243. doi:10.1162/jocn.1992.4.3.232
- Squire, L. R. (2009). Memory and brain systems: 1969-2009. *J Neurosci*, 29(41), 12711-12716. doi:10.1523/JNEUROSCI.3575-09.2009



- Squire, L. R., & Dede, A. J. (2015). Conscious and unconscious memory systems. *Cold Spring Harb Perspect Biol*, 7(3), a021667. doi:10.1101/cshperspect.a021667
- Squire, L. R., Genzel, L., Wixted, J. T., & Morris, R. G. (2015). Memory consolidation. *Cold Spring Harb Perspect Biol*, 7(8), a021766. doi:10.1101/cshperspect.a021766
- Squire, L. R., Stark, C. E., & Clark, R. E. (2004). The medial temporal lobe. *Annu Rev Neurosci*, 27, 279-306. doi:10.1146/annurev.neuro.27.070203.144130
- Squire, L. R., & Wixted, J. T. (2011). The cognitive neuroscience of human memory since H.M. *Annu Rev Neurosci*, 34, 259-288. doi:10.1146/annurev-neuro-061010-113720
- Squire, L. R., & Zola-Morgan, S. (1991). The medial temporal lobe memory system. *Science*, 253(5026), 1380-1386. doi:10.1126/science.1896849
- Staresina, B. P., Bergmann, T. O., Bonnefond, M., van der Meij, R., Jensen, O., Deuker, L., . . . Fell, J. (2015). Hierarchical nesting of slow oscillations, spindles and ripples in the human hippocampus during sleep. *Nat Neurosci*, 18(11), 1679-1686. doi:10.1038/nn.4119
- Staresina, B. P., Duncan, K. D., & Davachi, L. (2011). Perirhinal and parahippocampal cortices differentially contribute to later recollection of object- and scene-related event details. *J Neurosci*, 31(24), 8739-8747. doi:10.1523/JNEUROSCI.4978-10.2011
- Stegemann, A., Liu, S., Retana Romero, O. A., Oswald, M. J., Han, Y., Beretta, C. A., . . . Kuner, R. (2023). Prefrontal engrams of long-term fear memory perpetuate pain perception. *Nat Neurosci*, 26(5), 820-829. doi:10.1038/s41593-023-01291-x
- Steru, L., Chermat, R., Thierry, B., & Simon, P. (1985). The tail suspension test: a new method for screening antidepressants in mice. *Psychopharmacology (Berl)*, 85(3), 367-370. doi:10.1007/BF00428203
- Steward, O., Wallace, C. S., Lyford, G. L., & Worley, P. F. (1998). Synaptic activation causes the mRNA for the IEG Arc to localize selectively near activated postsynaptic sites on dendrites. *Neuron*, 21(4), 741-751. doi:10.1016/s0896-6273(00)80591-7
- Stokes, P. A., & Purdon, P. L. (2017). A study of problems encountered in Granger causality analysis from a neuroscience perspective. *Proc Natl Acad Sci U S A*, 114(34), E7063-E7072. doi:10.1073/pnas.1704663114
- Stujenske, J. M., Likhtik, E., Topiwala, M. A., & Gordon, J. A. (2014). Fear and Safety Engage Competing Patterns of Theta-Gamma Coupling in the Basolateral Amygdala. *Neuron*, 83(4), 919-933. doi:10.1016/j.neuron.2014.07.026
- Sweeney, P., & Yang, Y. (2015). An excitatory ventral hippocampus to lateral septum circuit that suppresses feeding. *Nature Communications*, 6. doi:10.1038/ncomms10188
- Takata, N., Yoshida, K., Komaki, Y., Xu, M., Sakai, Y., Hikishima, K., . . . Tanaka, K. F. (2015). Optogenetic activation of CA1 pyramidal neurons at the dorsal and ventral hippocampus evokes distinct brain-wide responses revealed by mouse fMRI. *PLoS ONE*, 10(3), e0121417. doi:10.1371/journal.pone.0121417
- Takenouchi, K., Nishijo, H., Uwano, T., Tamura, R., Takigawa, M., & Ono, T. (1999). Emotional and behavioral correlates of the anterior cingulate cortex during associative learning in rats. *Neuroscience*, 93(4), 1271-1287. doi:10.1016/s0306-4522(99)00216-x
- Tamura, M., Spellman, T. J., Rosen, A. M., Gogos, J. A., & Gordon, J. A. (2017). Hippocampal-prefrontal theta-gamma coupling during performance of a spatial working memory task. *Nature Communications*, 8(1). doi:10.1038/s41467-017-02108-9
- Taniguchi, H., He, M., Wu, P., Kim, S., Paik, R., Sugino, K., . . . Huang, Z. J. (2011). A resource of Cre driver lines for genetic targeting of GABAergic neurons in cerebral cortex. *Neuron*, 71(6), 995-1013. doi:10.1016/j.neuron.2011.07.026
- Tao, S., Wang, Y., Peng, J., Zhao, Y., He, X., Yu, X., . . . Xu, F. (2021). Whole-Brain Mapping the Direct Inputs of Dorsal and Ventral CA1 Projection Neurons. *Front Neural Circuits*, 15, 643230. doi:10.3389/fncir.2021.643230
- Tata, D. A., Marciano, V. A., & Anderson, B. J. (2006). Synapse loss from chronically elevated glucocorticoids: relationship to neuropil volume and cell number in hippocampal area CA3. *J Comp Neurol*, 498(3), 363-374. doi:10.1002/cne.21071
- Tendolkar, I., van Beek, M., van Oostrom, I., Mulder, M., Janzing, J., Voshaar, R. O., & van Eijndhoven, P. (2013). Electroconvulsive therapy increases hippocampal and amygdala volume in therapy refractory depression: a longitudinal pilot study. *Psychiatry Res*, 214(3), 197-203. doi:10.1016/j.psychres.2013.09.004
- Tervo, D. G., Hwang, B. Y., Viswanathan, S., Gaj, T., Lavzin, M., Ritola, K. D., . . . Karpova, A. Y. (2016). A Designer AAV Variant Permits Efficient Retrograde Access to Projection Neurons. *Neuron*, 92(2), 372-382. doi:10.1016/j.neuron.2016.09.021
- Teyler, T. J., & DiScenna, P. (1986). The hippocampal memory indexing theory. *Behav Neurosci*, 100(2), 147-154. doi:10.1037//0735-7044.100.2.147

- Tingley, D., & Buzsáki, G. (2018). Transformation of a Spatial Map across the Hippocampal-Lateral Septal Circuit. *Neuron*, 98(6), 1229-1242. doi:10.1016/j.neuron
- Tingley, D., & Buzsáki, G. (2020). Routing of Hippocampal Ripples to Subcortical Structures via the Lateral Septum. *Neuron*, 105(1), 138-149.e135. doi:10.1016/j.neuron.2019.10.012
- Tonegawa, S., Morrissey, M. D., & Kitamura, T. (2018). The role of engram cells in the systems consolidation of memory. *Nat Rev Neurosci*, 19(8), 485-498. doi:10.1038/s41583-018-0031-2
- Topolnik, L., & Tamboli, S. (2022). The role of inhibitory circuits in hippocampal memory processing. *Nat Rev Neurosci*, 23(8), 476-492. doi:10.1038/s41583-022-00599-0
- Tort, A. B. L., Komorowski, R. W., Manns, J. R., Kopell, N. J., & Eichenbaum, H. (2009a). Theta-gamma coupling increases during the learning of item-context associations. *Proceedings of the National Academy of Sciences of the United States of America*, 106(49), 20942-20947. doi:10.1073/pnas.0911331106
- Tort, A. B. L., Komorowski, R. W., Manns, J. R., Kopell, N. J., & Eichenbaum, H. (2009b). *Theta-gamma coupling increases during the learning of item-context associations*. Retrieved from [www.pnas.org/cgi/doi/10.1073/pnas.0911331106](http://www.pnas.org/cgi/doi/10.1073/pnas.0911331106)
- Torta, R. G., & Munari, J. (2010). Symptom cluster: Depression and pain. *Surg Oncol*, 19(3), 155-159. doi:10.1016/j.suronc.2009.11.007
- Tovote, P., Fadok, J. P., & Luthi, A. (2015). Neuronal circuits for fear and anxiety. *Nat Rev Neurosci*, 16(6), 317-331. doi:10.1038/nrn3945
- Travis, S., Coupland, N. J., Silversone, P. H., Huang, Y., Fujiwara, E., Carter, R., . . . Malykhin, N. V. (2015). Dentate gyrus volume and memory performance in major depressive disorder. *J Affect Disord*, 172, 159-164. doi:10.1016/j.jad.2014.09.048
- Tripp, A., Kota, R. S., Lewis, D. A., & Sibille, E. (2011). Reduced somatostatin in subgenual anterior cingulate cortex in major depression. *Neurobiol Dis*, 42(1), 116-124. doi:10.1016/j.nbd.2011.01.014
- Trneckova, L., Rotllant, D., Klenerova, V., Hynie, S., & Armario, A. (2007). Dynamics of immediate early gene and neuropeptide gene response to prolonged immobilization stress: evidence against a critical role of the termination of exposure to the stressor. *J Neurochem*, 100(4), 905-914. doi:10.1111/j.1471-4159.2006.04278.x
- Tsanov, M. (2018). Differential and complementary roles of medial and lateral septum in the orchestration of limbic oscillations and signal integration. *European Journal of Neuroscience*, 48(8), 2783-2794. doi:10.1111/ejn.13746
- Tse, D., Takeuchi, T., Kakeyama, M., Kajii, Y., Okuno, H., Tohyama, C., . . . Morris, R. G. M. (2011). Schema-Dependent Gene Activation and Memory Encoding in Neocortex. *Science*, 333(6044), 891-895. doi:10.1126/science.1205274
- Tzilivaki, A., Kastellakis, G., Schmitz, D., & Poirazi, P. (2022). GABAergic Interneurons with Nonlinear Dendrites: From Neuronal Computations to Memory Engrams. *Neuroscience*, 489, 34-43. doi:10.1016/j.neuroscience.2021.11.033
- Tzilivaki, A., Tukker, J. J., Maier, N., Poirazi, P., Sammons, R. P., & Schmitz, D. (2023). Hippocampal GABAergic interneurons and memory. *Neuron*, 111(20), 3154-3175. doi:10.1016/j.neuron.2023.06.016
- Tzingounis, A. V., & Nicoll, R. A. (2006). Arc/Arg3.1: linking gene expression to synaptic plasticity and memory. *Neuron*, 52(3), 403-407. doi:10.1016/j.neuron.2006.10.016
- Ullman, M. T. (2004). Contributions of memory circuits to language: the declarative/procedural model. *Cognition*, 92(1-2), 231-270. doi:10.1016/j.cognition.2003.10.008
- van der Veldt, S., Etter, G., Mosser, C. A., Manseau, F., & Williams, S. (2021). Conjunctive spatial and self-motion codes are topographically organized in the GABAergic cells of the lateral septum. *PLoS Biol*, 19(8), e3001383. doi:10.1371/journal.pbio.3001383
- van Groen, T., & Wyss, J. M. (1990). Extrinsic projections from area CA1 of the rat hippocampus: olfactory, cortical, subcortical, and bilateral hippocampal formation projections. *J Comp Neurol*, 302(3), 515-528. doi:10.1002/cne.903020308
- Vantomme, G., Osorio-Forero, A., Lüthi, A., & Fernandez, L. M. J. (2019). Regulation of local sleep by the thalamic reticular nucleus. In *Frontiers in Neuroscience* (Vol. 13): Frontiers Media S.A.
- Vazdarjanova, A., Ramirez-Amaya, V., Insel, N., Plummer, T. K., Rosi, S., Chowdhury, S., . . . Barnes, C. A. (2006). Spatial exploration induces ARC, a plasticity-related immediate-early gene, only in calcium/calmodulin-dependent protein kinase II-positive principal excitatory and inhibitory neurons of the rat forebrain. *J Comp Neurol*, 498(3), 317-329. doi:10.1002/cne.21003
- Veres, J. M., Andrasi, T., Nagy-Pal, P., & Hajos, N. (2023). CaMKIIalpha Promoter-Controlled Circuit Manipulations Target Both Pyramidal Cells and Inhibitory Interneurons in Cortical Networks. *eNeuro*, 10(4). doi:10.1523/ENEURO.0070-23.2023

- Vestergaard-Poulsen, P., Wegener, G., Hansen, B., Bjarkam, C. R., Blackband, S. J., Nielsen, N. C., & Jespersen, S. N. (2011). Diffusion-weighted MRI and quantitative biophysical modeling of hippocampal neurite loss in chronic stress. *PLoS ONE*, 6(7), e20653. doi:10.1371/journal.pone.0020653
- Viellard, J. M. A., Melleu, F. F., Tamais, A. M., de Almeida, A. P., Zerbini, C., Ikebara, J. M., . . . Canteras, N. S. (2024). A subiculum-hypothalamic pathway functions in dynamic threat detection and memory updating. *Curr Biol*. doi:10.1016/j.cub.2024.05.006
- Vivekananda, U., Bush, D., Bisby, J. A., Baxendale, S., Rodionov, R., Diehl, B., . . . Burgess, N. (2021). Theta power and theta-gamma coupling support long-term spatial memory retrieval. *Hippocampus*, 31(2), 213-220. doi:10.1002/hipo.23284
- Vu, T., Gugustea, R., & Leung, L. S. (2020). Long-term potentiation of the nucleus reuniens and entorhinal cortex to CA1 distal dendritic synapses in mice. *Brain Struct Funct*, 225(6), 1817-1838. doi:10.1007/s00429-020-02095-6
- Walczyk-Mooradally, A., Holborn, J., Singh, K., Tyler, M., Patnaik, D., Wesseling, H., . . . Lalonde, J. (2021). Phosphorylation-dependent control of Activity-regulated cytoskeleton-associated protein (Arc) protein by TNK1. *J Neurochem*, 158(5), 1058-1073. doi:10.1111/jnc.15440
- Wall, M. J., & Correa, S. A. L. (2018). The mechanistic link between Arc/Arg3.1 expression and AMPA receptor endocytosis. *Semin Cell Dev Biol*, 77, 17-24. doi:10.1016/j.semcdb.2017.09.005
- Waltereit, R., Dammermann, B., Wulff, P., Scafidi, J., Staubli, U., Kauselmann, G., . . . Kuhl, D. (2001). Arg3.1/Arc mRNA induction by Ca<sup>2+</sup> and cAMP requires protein kinase A and mitogen-activated protein kinase/extracellular regulated kinase activation. *J Neurosci*, 21(15), 5484-5493. doi:10.1523/JNEUROSCI.21-15-05484.2001
- Wang, C., Furlong, T. M., Stratton, P. G., Lee, C. C. Y., Xu, L., Merlin, S., . . . Sah, P. (2021). Hippocampus-Prefrontal Coupling Regulates Recognition Memory for Novelty Discrimination. *J Neurosci*, 41(46), 9617-9632. doi:10.1523/JNEUROSCI.1202-21.2021
- Wang, D., Pan, X., Zhou, Y., Wu, Z., Ren, K., Liu, H., . . . Yang, C. (2023). Lateral septum-lateral hypothalamus circuit dysfunction in comorbid pain and anxiety. *Mol Psychiatry*, 28(3), 1090-1100. doi:10.1038/s41380-022-01922-y
- Wang, F., Flanagan, J., Su, N., Wang, L. C., Bui, S., Nielson, A., . . . Luo, Y. (2012). RNAscope: a novel in situ RNA analysis platform for formalin-fixed, paraffin-embedded tissues. *J Mol Diagn*, 14(1), 22-29. doi:10.1016/j.jmoldx.2011.08.002
- Wang, H., Tan, Y. Z., Mu, R. H., Tang, S. S., Liu, X., Xing, S. Y., . . . Hong, H. (2021). Takeda G Protein-Coupled Receptor 5 Modulates Depression-like Behaviors via Hippocampal CA3 Pyramidal Neurons Afferent to Dorsolateral Septum. *Biol Psychiatry*, 89(11), 1084-1095. doi:10.1016/j.biopsych.2020.11.018
- Wang, K. H., Majewska, A., Schummers, J., Farley, B., Hu, C., Sur, M., & Tonegawa, S. (2006). In vivo two-photon imaging reveals a role of arc in enhancing orientation specificity in visual cortex. *Cell*, 126(2), 389-402. doi:10.1016/j.cell.2006.06.038
- Wang, M., Li, P., Li, Z., da Silva, B. S., Zheng, W., Xiang, Z., . . . Guo, W. (2023). Lateral septum adenosine A2A receptors control stress-induced depressive-like behaviors via signaling to the hypothalamus and habenula. *Nature Communications*, 14(1), 1880-1880. doi:10.1038/s41467-023-37601-x
- Wang, S. H., Teixeira, C. M., Wheeler, A. L., & Frankland, P. W. (2009). The precision of remote context memories does not require the hippocampus. *Nat Neurosci*, 12(3), 253-255. doi:10.1038/nn.2263
- Wang, X. Y., Xu, X., Chen, R., Jia, W. B., Xu, P. F., Liu, X. Q., . . . Zhang, Y. (2023). The thalamic reticular nucleus-lateral habenula circuit regulates depressive-like behaviors in chronic stress and chronic pain. *Cell Rep*, 42(10), 113170. doi:10.1016/j.celrep.2023.113170
- Wang, Y. J., Zan, G. Y., Xu, C., Li, X. P., Shu, X., Yao, S. Y., . . . Liu, J. G. (2023). The claustrum-prelimbic cortex circuit through dynorphin/kappa-opioid receptor signaling underlies depression-like behaviors associated with social stress etiology. *Nat Commun*, 14(1), 7903. doi:10.1038/s41467-023-43636-x
- Waung, M. W., Pfeiffer, B. E., Nosyreva, E. D., Ronesi, J. A., & Huber, K. M. (2008). Rapid translation of Arc/Arg3.1 selectively mediates mGluR-dependent LTD through persistent increases in AMPAR endocytosis rate. *Neuron*, 59(1), 84-97. doi:10.1016/j.neuron.2008.05.014
- Wee, C. L., Teo, S., Oey, N. E., Wright, G. D., VanDongen, H. M., & VanDongen, A. M. (2014). Nuclear Arc Interacts with the Histone Acetyltransferase Tip60 to Modify H4K12 Acetylation(1,2,3). *eNeuro*, 1(1). doi:10.1523/ENEURO.0019-14.2014
- Weinberger, N. M. (2011). The medial geniculate, not the amygdala, as the root of auditory fear conditioning. *Hear Res*, 274(1-2), 61-74. doi:10.1016/j.heares.2010.03.093
- Whittington, M. A., Traub, R. D., & Jefferys, J. G. (1995). Synchronized oscillations in interneuron networks driven by metabotropic glutamate receptor activation. *Nature*, 373(6515), 612-615. doi:10.1038/373612a0

- Wilkerson, J. R., Albanesi, J. P., & Huber, K. M. (2018). Roles for Arc in metabotropic glutamate receptor-dependent LTD and synapse elimination: Implications in health and disease. *Semin Cell Dev Biol*, 77, 51-62. doi:10.1016/j.semcdb.2017.09.035
- Wilson, M. A., & Fadel, J. R. (2017). Cholinergic regulation of fear learning and extinction. *J Neurosci Res*, 95(3), 836-852. doi:10.1002/jnr.23840
- Wiltgen, B. J., Zhou, M., Cai, Y., Balaji, J., Karlsson, M. G., Parivash, S. N., . . . Silva, A. J. (2010). The hippocampus plays a selective role in the retrieval of detailed contextual memories. *Curr Biol*, 20(15), 1336-1344. doi:10.1016/j.cub.2010.06.068
- Wirtshafter, H. S., & Wilson, M. A. (2021). Lateral septum as a nexus for mood, motivation, and movement. In *Neuroscience and Biobehavioral Reviews* (Vol. 126, pp. 544-559): Elsevier Ltd.
- Wohleb, E. S., Franklin, T., Iwata, M., & Duman, R. S. (2016). Integrating neuroimmune systems in the neurobiology of depression. *Nat Rev Neurosci*, 17(8), 497-511. doi:10.1038/nrn.2016.69
- Wurtman, R. J. (2005). Genes, stress, and depression. *Metabolism*, 54(5 Suppl 1), 16-19. doi:10.1016/j.metabol.2005.01.007
- Wynn, S. C., Townsend, C. D., & Nyhus, E. (2023). The role of theta and gamma oscillations in item memory, source memory, and memory confidence. *bioRxiv*. doi:10.1101/2023.10.18.562880
- Xi, K., Xiao, H., Huang, X., Yuan, Z., Liu, M., Mao, H., . . . Wu, S. (2023). Reversal of hyperactive higher-order thalamus attenuates defensiveness in a mouse model of PTSD. *Sci Adv*, 9(5), eade5987. doi:10.1126/sciadv.ade5987
- Xu, W., & Sudhof, T. C. (2013). A neural circuit for memory specificity and generalization. *Science*, 339(6125), 1290-1295. doi:10.1126/science.1229534
- Yager, L. M., Garcia, A. F., Wunsch, A. M., & Ferguson, S. M. (2015). The ins and outs of the striatum: role in drug addiction. *Neuroscience*, 301, 529-541. doi:10.1016/j.neuroscience.2015.06.033
- Yamada, K., Homma, C., Tanemura, K., Ikeda, T., Itohara, S., & Nagaoka, Y. (2011). Analyses of fear memory in Arc/Arg3.1-deficient mice: intact short-term memory and impaired long-term and remote memory. *World Journal of Neuroscience*, 01(01), 1-8. doi:10.4236/wjns.2011.11001
- Yamamoto, J., Suh, J., Takeuchi, D., & Tonegawa, S. (2014). Successful execution of working memory linked to synchronized high-frequency gamma oscillations. *Cell*, 157(4), 845-857. doi:10.1016/j.cell.2014.04.009
- Yamin, H. G., Stern, E. A., & Cohen, D. (2013). Parallel processing of environmental recognition and locomotion in the mouse striatum. *J Neurosci*, 33(2), 473-484. doi:10.1523/JNEUROSCI.4474-12.2013
- Yamin, H. G., Stern, E. A., & Cohen, D. (2013). Systems/Circuits Parallel Processing of Environmental Recognition and Locomotion in the Mouse Striatum. doi:10.1523/JNEUROSCI.4474-12.2013
- Yan, Y., Aierken, A., Wang, C., Jin, W., Quan, Z., Wang, Z., . . . Zhao, J. (2023). Neuronal Circuits Associated with Fear Memory: Potential Therapeutic Targets for Posttraumatic Stress Disorder. *Neuroscientist*, 29(3), 332-351. doi:10.1177/10738584211069977
- Yang, D. D., Kuan, C. Y., Whitmarsh, A. J., Rincon, M., Zheng, T. S., Davis, R. J., . . . Flavell, R. A. (1997). Absence of excitotoxicity-induced apoptosis in the hippocampus of mice lacking the Jnk3 gene. *Nature*, 389(6653), 865-870. doi:10.1038/39899
- Yang, X., Wen, Y., Zhang, Y., Gao, F., Yang, J., Yang, Z., & Yan, C. (2020). Dynamic Changes of Cytoskeleton-Related Proteins Within Reward-Related Brain Regions in Morphine-Associated Memory. *Front Neurosci*, 14, 626348. doi:10.3389/fnins.2020.626348
- Yang, X. Y., Ma, Z. L., Storm, D. R., Cao, H., & Zhang, Y. Q. (2021). Selective ablation of type 3 adenylyl cyclase in somatostatin-positive interneurons produces anxiety- and depression-like behaviors in mice. *World J Psychiatry*, 11(2), 35-49. doi:10.5498/wjp.v11.i2.35
- Yankelevitch-Yahav, R., Franko, M., Huly, A., & Doron, R. (2015). The forced swim test as a model of depressive-like behavior. *J Vis Exp*(97). doi:10.3791/52587
- Yau, J. O., & McNally, G. P. (2022). The activity of ventral tegmental area dopamine neurons during shock omission predicts safety learning. *Behav Neurosci*, 136(3), 276-284. doi:10.1037/bne0000506
- Yi, G. L., Zhu, M. Z., Cui, H. C., Yuan, X. R., Liu, P., Tang, J., . . . Zhu, X. H. (2022). A hippocampus dependent neural circuit loop underlying the generation of auditory mismatch negativity. *Neuropharmacology*, 206, 108947. doi:10.1016/j.neuropharm.2022.108947
- Yin, H., Pantazatos, S. P., Galfalvy, H., Huang, Y. Y., Rosoklija, G. B., Dwork, A. J., . . . Mann, J. J. (2016). A pilot integrative genomics study of GABA and glutamate neurotransmitter systems in suicide, suicidal behavior, and major depressive disorder. *Am J Med Genet B Neuropsychiatr Genet*, 171B(3), 414-426. doi:10.1002/ajmg.b.32423
- Ying, S. W., Futter, M., Rosenblum, K., Webber, M. J., Hunt, S. P., Bliss, T. V., & Bramham, C. R. (2002). Brain-derived neurotrophic factor induces long-term potentiation in intact adult hippocampus: requirement for

- ERK activation coupled to CREB and upregulation of Arc synthesis. *J Neurosci*, 22(5), 1532-1540. doi:10.1523/JNEUROSCI.22-05-01532.2002
- Yu, J., Naoi, T., & Sakaguchi, M. (2021). Fear generalization immediately after contextual fear memory consolidation in mice. *Biochem Biophys Res Commun*, 558, 102-106. doi:10.1016/j.bbrc.2021.04.072
- Yu, J. Y., Fang, P., Wang, C., Wang, X. X., Li, K., Gong, Q., . . . Wang, X. D. (2018). Dorsal CA1 interneurons contribute to acute stress-induced spatial memory deficits. *Neuropharmacology*, 135, 474-486. doi:10.1016/j.neuropharm.2018.04.002
- Yu, X. J., Xu, X. X., He, S., & He, J. (2009). Change detection by thalamic reticular neurons. *Nat Neurosci*, 12(9), 1165-1170. doi:10.1038/nn.2373
- Zhang, H., & Bramham, C. R. (2021). Arc/Arg3.1 function in long-term synaptic plasticity: Emerging mechanisms and unresolved issues. *Eur J Neurosci*, 54(8), 6696-6712. doi:10.1111/ejn.14958
- Zhang, Y., Fukushima, H., & Kida, S. (2011). Induction and requirement of gene expression in the anterior cingulate cortex and medial prefrontal cortex for the consolidation of inhibitory avoidance memory. *Mol Brain*, 4, 4. doi:10.1186/1756-6606-4-4
- Zhao, C., Eisinger, B., & Gammie, S. C. (2013). Characterization of GABAergic neurons in the mouse lateral septum: a double fluorescence in situ hybridization and immunohistochemical study using tyramide signal amplification. *PLoS ONE*, 8(8), e73750. doi:10.1371/journal.pone.0073750
- Zhou, W., Jin, Y., Meng, Q., Zhu, X., Bai, T., Tian, Y., . . . Zhang, Z. (2019). A neural circuit for comorbid depressive symptoms in chronic pain. *Nat Neurosci*, 22(10), 1649-1658. doi:10.1038/s41593-019-0468-2
- Zhu, H., Pleil, K. E., Urban, D. J., Moy, S. S., Kash, T. L., & Roth, B. L. (2014). Chemogenetic inactivation of ventral hippocampal glutamatergic neurons disrupts consolidation of contextual fear memory. *Neuropsychopharmacology*, 39(8), 1880-1892. doi:10.1038/npp.2014.35
- Zhu, L., Zhu, L., Huang, Y., Shi, W., & Yu, B. (2018). Memory reconsolidation and extinction of fear conditioning induced different Arc/Arg3.1 expression. *Neuroreport*, 29(12), 1036-1045. doi:10.1097/WNR.0000000000001069
- Zicho, K., Sos, K. E., Papp, P., Barth, A. M., Misak, E., Orosz, A., . . . Nyiri, G. (2023). Fear memory recall involves hippocampal somatostatin interneurons. *PLoS Biol*, 21(6), e3002154. doi:10.1371/journal.pbio.3002154

## 2. Statement of contribution

Prof. Dietmar Kuhl and former colleagues in our lab generated the Arc/Arg3.1<sup>flox/flox</sup> mice line. Xiaoyu Yang performed all the behavioral tests, immunohistochemical staining, *in vivo* LFP recordings, and data analysis. Dr. Abdurahman Kuku generated the analysis scripts in Matlab. Prof. Dietmar Kuhl and Dr. Ora Ohana generated the project concept and provided funding. Dr. Ora Ohana and Dr. Xiaoyan Gao performed initial experiments. Dr. Ora Ohana directed all experiments.

### 3. Curriculum vitae

#### Personal information

---

Front name: Xiaoyu  
 Surname: Yang  
 Date of birth: 07.04.1994  
 Gender: Female  
 Nationality: P.R.China

#### Education

---

**12.2019 - Present**

**Ph.D. in Neurobiology**

Institute for Molecular and Cellular Cognition (IMCC)

**Supervisors:**

Center for Molecular Neurobiology Hamburg (ZMNH)

Prof. Dietmar Kuhl and Dr. Ora Ohana

University Medical Center (UKE)

**Co-supervisor in the Department of  
Biology:**

University of Hamburg (UHH), Hamburg, Germany

Prof. Christian Lohr

---

**09.2016 - 06.2019**

**Master of Science in Neurobiology**

**Supervisors:**

Institute of Brain Science

Prof. Hong Cao and Prof. Yuqiu Zhang

Fudan University, Shanghai, China

---

**09.2012 - 06.2016**

**Bachelor of Engineering in Bioengineering**

School of Life Science

Shandong First Medical University, Shandong, China

## Acknowledgment / Danksagung

First, I would like to thank myself for deciding to dive into memory research, never giving up my curiosity, and continuously striving to learn new knowledge during the last four and a half years. I want to tell myself in the future: Xiaoyu. This is not the end of learning. This is the start. You don't need to be successful. Enjoy science and your lovely life.

Second, I would like to thank Prof. Dietmar Kuhl and Dr. Ora Ohana, who provided this opportunity for me to work and study at the Institute of Molecular and Cellular Cognition. Especially, I would like to thank Dr. Ora Ohana, the most creative scientist I have ever seen, who excellently supervised my projects and corrected this thesis. I was always surprised by the various ideas that came up from her brain, which inspired me with my research and gave me a lot of support when I felt confused with the complex results.

Third, I would like to thank my talented friends, Ms. Daniela Ballesteros, Mr. Abdurahman Kuku, and Dr. Marcel Klein, who supported me and helped me in my work and daily life. I am so unlucky the COVID pandemic started along with my life in Germany, but I am so lucky that I have such nice friends around me during that dark time.

Finally, I would like to thank our technician, Ms. Ute Süssens, who helped a lot during the experiment and her contributions to this project. Thanks, Dr. Ingke Braren from the Vector facility of UKE. Thanks, Dr. Antonio Virgilio Failla from the UKE Microscopy Imaging Facility (UMIF). Thanks, Dr. Xiaoyan Gao helped me a lot when I started my work here. I also would like to say thank you to all of my colleagues from Kuhl's lab who shared many happy moments together with me. They are Christina, Iris, Frederic, Guido, Darks, Uwe, Andrea, Timo. I would like to thank the Schaller Nikolich Foundation, which supported my study and research.

I would like to thank Ms. Miao Zhang and Mr. Jin Lou, who supported me with delicious Dim sums and love during my thesis writing periods. I would like to thank my parents who always support my decisions and give me a lot of love. I would like to thank my cute cats, CC and Deedee, who accompany me whenever I feel upset.



With the highest respect and gratitude, I would like to thank all the mice who participated in my project.